Lib
572
7/9/88

Indian J. Chem. Vol. 27A No. 7 pp. 561-652
July 1988
CODEN : IJOCAP ISSN : 0019-5103
27A(7) 561-652 (1988)

Indian Journal of
CHEMISTRY

SECTION A
(Inorganic, Physical, Theoretical & Analytical)

Published by
PUBLICATIONS & INFORMATION DIRECTORATE, CSIR, NEW DELHI
in association with
THE INDIAN NATIONAL SCIENCE ACADEMY, NEW DELHI

A RANGE OF HIGH PRECISION, HIGH QUALITY RECORDING INSTRUMENTS FOR THE DISCRIMINATING RESEARCH SCIENTIST

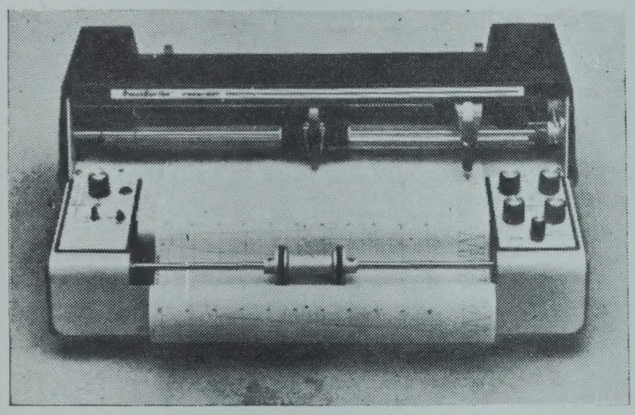

Series 5000 Strip Chart Recorder

The series 5000 Strip Chart Recorder and the series 2000 XY Recorder are well proven instruments incorporating State of the Art Circuitry. A wide range of models offer tremendous flexibility to the user. With over 5000 installations, these instruments are the preferred choice of discriminating users all over India.

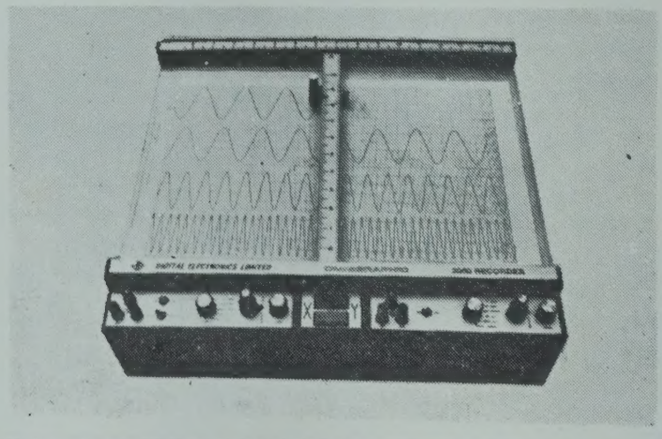

Series 2000 XY Recorder

DIGITAL
ELECTRONICS

In collaboration with Houston Instrument, U.S.A.

Digital Electronics Limited, 74/II 'C' Cross Road, Marol MIDC, Andheri (East), Bombay 400 093.
Phone : 6360225 Telex : 011 6891 DEL IN

INDIAN JOURNAL OF CHEMISTRY

Section A: Inorganic, Physical, Theoretical & Analytical Chemistry

Editorial Board

Prof. C.N.R. Rao
Director
Indian Institute of Science
Bangalore 560 012

Prof. R.P. Rastogi
Vice-Chancellor
Banaras Hindu University
Varanasi 221 005

Prof. A.R. Vasudeva Murthy
Department of Inorganic &
Physical Chemistry
Indian Institute of Science
Bangalore 560 012

Prof. J.C. Kuriacose
Department of Chemistry
Indian Institute of Technology
Madras 600 036

Prof. D.V.S. Jain
Department of Chemistry
Panjab University
Chandigarh 160 014

Prof. P. Natarajan
Department of Inorganic Chemistry
University of Madras
Madras 600 025

Prof. N.K. Ray
Department of Chemistry
University of Delhi
Delhi 110 007

Prof. A. Chakravorty
Department of Inorganic Chemistry
Indian Association for the
Cultivation of Science
Calcutta 700 032

Prof. S. Mitra
Tata Institute of Fundamental Research
Bombay 400 005

Dr K.N. Rao
Chemistry Division
Bhabha Atomic Research Centre
Trombay, Bombay 400 085

Prof. S.M. Khopkar
Department of Chemistry
Indian Institute of Technology
Powai, Bombay 400 076

Prof. P.T. Manoharan
Department of Chemistry
Indian Institute of Technology
Madras 600 036

Dr A.C. Dash
Department of Chemistry
Utkal University
Bhubaneswar 751 004

Shri S.P. Ambasta, Editor-in-Chief
(*Ex-officio*)

Editors

S.S. Saksena — B.C. Sharma — S. Sivakamasundari

Assistant Editor

S.K. Bhasin

Published by the Publications & Information Directorate (CSIR), Hillside Road, New Delhi 110 012

Editor-in-Chief: S.P. Ambasta

Copyright, 1988, by the Council of Scientific & Industrial Research, New Delhi 110 012

The Indian Journal of Chemistry is issued monthly in two sections: A and B. Communications regarding contributions for publication in the journal should be addressed to the Editor, Indian Journal of Chemistry, Publications & Information Directorate, Hillside Road, New Delhi 110 012.

Correspondence regarding subscriptions and advertisements should be addressed to the Sales & Distribution Officer, Publications & Information Directorate, hillside Road, New Delhi 110 012.

The Publications & Information Directorate (CSIR) assumes no responsibility for the statements and opinions advanced by contributors. The Editorial Board in its work of examining papers received for publication is assisted, in an honorary capacity by a large number of distinguished scientists, working in various parts of India.

Annual Subscription: Rs. 300.00 £ 70.00 $ 100.00; 50% discount admissible to research workers and students and 25% discount to non-research individuals on annual subscription.

Single Copy: Rs. 30.00 £ 7.00 $ 10.00

Payments in respect of subscriptions and advertisements may be sent by cheque, bank draft, money order or postal order marked payable to Publications & Information Directorate, Hillside Road, New Delhi 110 012.

Claims for missing numbers will be allowed only if received within 3 months of the date of issue of the journal plus the time normally required for postal delivery of the journal and the claim.

AUTHOR INDEX

Agarwala Umesh 609
Arbad B R 601

Bajpai U D N 635
Banerji Kalyan K 581
Bathla Harindar K 606
Behera G B 561
Bhat J Ishwara 597

Darwish N A 645
Das S 574
De G S 577
De Kuntala 637
Dutta R L 637

El-Ansary A L 645

Ganorkar M C 617
Goyal M R 584
Gupta Anita 581
Gupta Minu 609
Gupta Mool C 626
Gupta Y K 584
Guraya P S 629

Hazra D K 574
Hingorani S 635

Idriss K A 622

Jahagirdar D V 601
Jain A 635
Jauhar S P 629

Kalra K C 569
Kandlikar Sushama 632
Katyal Parveen 569
Khairy E M 645
Kharwadkar R M 601
Krishnakutty K 648

Lingaiah P 613

Mahadevappa D S 589
Mahajan Vijay G 626
Majumdar S K 650
Mathur Sandhya 581
Mishra B K 561
Mitra Mustofy H G 577
Mittal R K 584

Naidu H M K 589
Nandi Debasis 574
Narula S P 629
Nema S K 635
Nigam R K 569

Parmar Swarn S 606
Paria P K 650
Pati Subas C 593

Sahadev 643
Sahay A K 561
Saleh Magda S 622
Saluja Harveen K 606
Sannigrahi A B 652
Sarangi Chintamani 593
Sarkar A 650
Saroja P 632
Sadaira H 622
Seleim M M 622
Seth Jyoti 609
Shah D O 561
Sharada N Nalanda 617
Sharma R K 643
Sherif O E 645
Shukla P R 640
Sindhwani S K 643
Singh Kehar 565
Srivastava S K 640
Swamy S J 613

Thankarajan N 648
Thimme Gowda B 597
Thokdar T K 650
Tiwari A K 565
Tiwari H P 635

Venkat Narayana G 613

Yamuna B 589

Indian Journal of Chemistry

Sect. A: Inorganic, Physical, Theoretical & Analytical

VOL. 27A NUMBER 7 JULY 1988

CONTENTS

Studies on Cyanine Dyes: Evaluation of Area/Molecule, Surface Potential & Rate Constants for $KMnO_4$ Oxidation in Two Dimensions 561
A K Sahay, B K Mishra, G B Behera* & D O Shah

Hydrodynamic & Electroosmotic Permeation Studies on Cholesterol Liquid Membrane. 565
Kehar Singh* & A K Tiwari

Formation of Anodic Oxidation films on Tantalum in Presence of Ultraviolet Radiations & Heat Treatment of Anodic Tantalum Oxide Films 569
R K Nigam*, K C Kalra & Parveen Katyal

Conductances of Tetraalkylammonium Bromides in 1,2-Dimethoxyethane at 25°C: Analysis of Data by Fuoss-Kraus Theory 574
Debasis Nandi, S Das & D K Hazra*

Substitution of Aquo Ligands from Hydroxopentaaquochromium(III) Ion by ethylenediaminetetraacetic Acid—A Kinetic Approach 577
H G Mitra Mustofy & G S De*

Separation of Polar & Steric Effects in Oxidation of *ortho*-Substituted Benzyl Alcohols by Acid Permanganate 581
Sandhya Mathur, Anita Gupta & Kalyan K Banerji*

Kinetics & Mechanism of Oxidation of Hyponitrous Acid by Chloramine-T in Aqueous Perchloric Acid 584
M R Goyal, R K Mittal & Y K Gupta*

Kinetics & Mechanism of Oxidation of α-Amino Acids by Bromamine-T in Sulphuric Acid Medium 589
B Yamuna, H M K Naidu & D S Mahadevappa*

Mechanism of Self-decomposition of Trichloroisocyanuric Acid in Acid Medium: A Kinetic Study 593
Subas C Pati* & Chintamani Sarangi

Effect of Metal Complexation on Kinetics & Mechanisms of Oxidation of Zn(II)-bound Thiosemicarbazide (TSC) by Chloramine-B (CAB) & Bromamine-B (BAB) in Aqueous Medium & by dichloramine-B (DCB) in Aqueous Methanol 597
B Thimme Gowda* & J Ishwara Bhat

Dependence of Hammett Constant Rho on Dielectric Constant & Water Activity in Mixed Aqueous Solvents. 601
D V Jahagirdar*, B R Arbad & R M Kharwadkar

A Structural Reinvestigation of the Reported Anhydride from *o*-$HO_2As(C_6H_4CO_2H)_2$: Novel Spirobicyclic & Tricyclic Acyloxy(carboxy)arsorane Structures . . . 606
Swarn S Parmar*, Harveen K Saluja & Harindar K Bathla

Continued overleaf

Chlorothionitrene Complexes of Molybdenum: Part I—Synthesis, Characterization & Reactivity of Mo(VI) Complexes 609
Jyoti Seth, Minu Gupta & Umesh Agarwala*

Ternary Complexes of Copper(II) with Malonic Acid & O,O; O,N & N,N Donor Ligands. 613
G Venkat Narayana, S J Swamy & P Lingaiah*

Synthesis & Structural Studies of Oxovanadium(IV), Manganese(II), Iron(II), Cobalt(II), Nickel(II) & Copper(II) Complexes with New Tridentate Schiff Bases having ONO & ONN Donor Systems 617
(Miss) N Nalanda Sharada & M C Ganorkar*

Molecular Complex Formation of Thiosalicylic Acid with *n*-Propanol 622
M M Seleim, Magda S Saleh, H Sedaira & K A Idriss*

Notes

Statistical Entropy of Adsorption of *n*-Alkanes 626
Mool C Gupta* & Vijay G Mahajan

Physico-chemical Studies in Mixed Solvents: Part III—Conductances of Lithium, Sodium & Potassium Perchlorates in Diethylformamide-Water Mixtures. 629
S P Jauhar*, P S Guraya & S P Narula

Kinetics of Ru(III)-catalysed & Uncatalysed Oxidation of Chloroacetic Acids by N-Bromosuccinimide in Aqueous Solution 632
P Saroja & Sushama Kandlikar*

Polyesters of Dimer Acid & Ethylene Glycol 635
U D N Bajpai*, S Hingorani, A Jain, H P Tiwari & S K Nema

Transition Metal Complexes of Hydrazones 637
R L Dutta* & Kuntala De

Synthesis & Characterisation of Some Bimetallic Derivatives of Dioxouranium(VI) Dialkyldithiophosphates $[UO_2(dtp)_2]$ 640
(Mrs) P R Shukla* & S K Srivastava

Potentiometric Studies on Some Bivalent Metal Complexes of 2-Hydroxy-1-naphthaldehyde Monosemicarbazone (HNAS). 643
Sahadev, R K Sharma & S K Sindhwani*

Stability Constants of Cobalt(II) Complexes with Some Thiols 645
E M Khairy, N A Darwish, A L El-Ansary* & O E Sherif

Phthalhydrazidylazoacetylacetone as a Chemiluminescent Complexometric Indicator. 648
K Krishnakutty & N Thankarajan*

Extractive Photometric Determination of Palladium(II) with 4-Nitrosoresorcinol in Presence of Pyridine & Some of Its Methyl Substituted Derivatives 650
A Sarkar, T K Thokdar, P K Paria* & S K Majumdar

Book Reviews

Applied Quantum Chemistry (Authors: G Naray-Szabo, P R Surjan & J G Angyan). 652
A B Sannigrahi

Authors for correspondence are indicated by (*)

Indian Journal of Chemistry
Vol. 27A, July 1988, pp. 561-564

Studies on Cyanine Dyes: Evaluation of Area/Molecule, Surface Potential & Rate Constants for $KMnO_4$ Oxidation in Two Dimensions

A K SAHAY, B K MISHRA & G B BEHERA*
Centre of Studies in Surface Science & Technology, Department of Chemistry, Sambalpur University, Jyoti Vihar, Burla 768 019
and
D O SHAH
Department of Chemical Engineering & Anaesthesiology, University of Florida, Gainsville, FL 326 11

Received 24 *February* 1987, *revised* 7 *September* 1987; *accepted* 11 *November* 1987

The limiting area/molecule and change in surface potential (ΔV) values of some synthesised surface active cyanine dyes (**1 a-e**) have been obtained. The results have been interpreted in terms of possible orientation of the molecules at the air/water interface. In all cases aggregate formation has been related to a phase transition in the surface pressure—area isotherm. The rate constants for acidified $KMnO_4$ oxidation of these compounds in fully compressed state have been determined from change in ΔV values with time.

The phenomenon of dye aggregation is of practical and theoretical interest because of photophysical behaviour and distinctive spectral features of the aggregates[1]. Vaidyanathan *et al.*[2] studied the *J*-aggregation of amphipathic oxacyanine and its thiacyanine analogue spectroscopically and observed more extensive aggregation of thiacyanine. Herz[3] also proposed *H*-aggregates of cyanine dyes. Two dimensional arrangement of chromophores in *J*-aggregates of long chain merocyanine dyes have been reported by Nakahara *et al.*[4], who used benzothiazole and rhodanine units as the electron donating groups and observed that these groups form good condensed monolayer and are favourable for formation of *J*-aggregates in mixed films. The properties of dye aggregates in monolayer has largely been obtained by transferring it to a solid surface. However, the extent of work relating to surface studies and nature of aggregation of cyanine dyes appear meagre.

In the present study we have determined area/molecule, surface potential and rate constant for acidified $KMnO_4$ oxidation in two dimensions on monolayers obtained from the surface active cyanine dyes (**1a-e**).

Materials and Methods

Melting points were determined in capillaries in "Yorco" model YS-1-536 and are uncorrected. The IR spectra were recorded in KBr on a Perkin-Elmer 398 spectrophotometer.

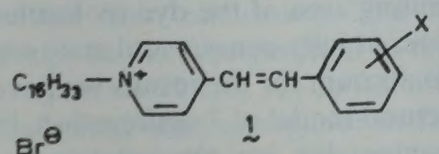

1

X = p-OH (a)
= p-OCH_3 (b)
= p-Cl (c)
= o-OH (d)
= p-$OC_{16}H_{33}$ (e)

Commercially available cetyl bromide and aromatic aldehydes were used as such. γ-Picoline was distilled just before use. Ether refers to diethyl ether.

1-*Cetyl*-4-*methylpyridinium bromide*

A mixture of γ-picoline (0.02 ml, 1.86 g) and cetyl bromide (0.02 ml, 6.1 g) was heated in a sealed tube in an oil bath for 6 hr at 110°. The resulting salt was washed with ether-acetone (4:1) and recrystallised twice from absolute ethanol, m.p. 58°, yield 60%; IR: 3500-3300, 1610 and 810 cm^{-1} (found: C, 65.2; H, 10.3; N, 3.4. $C_{22}H_{40}NBr$ requires C, 65.4; H, 10.5; N, 3.5%).

Cetyl ether of p-hydroxybenzaldehyde

To sodium ethoxide prepared from sodium metal and absolute ethanol (40 ml), *p*-hydroxybenzaldehyde (10 mmol) was added slowly with shaking followed by cetyl bromide (10 mmol) dropwise and the solution was refluxed in an oil-bath for 15 hr. The solid obtained on concentration and cooling was filtered and dried in air. The excess sodium salt was removed by suspending the compound in water. *p*-Cetyloxybenzaldehyde was washed with ether twice and recrystallised from acetonitrile, m.p. 42°, yield 35% (Found: C, 79.5; H, 10.8. $C_{23}H_{38}O$ requires C, 79.8; H, 10.9%) IR: 2920, 1700, 1600 and 840 cm^{-1}.

1-*Cetyl*-4-(*p-methoxystyryl*)*pyridinium bromide*

To a solution of 4-methylpyridinium bromide

(0.01 mol, 3.98 g) in hot absolute ethanol (25 ml) were added 2-3 drops of piperidine followed by anisaldehyde (0.01 mol, 1.36 g) and the reaction mixture was refluxed for 8 hr. The resultant product was filtered, washed with ether and recrystallised from methanol; m.p. 215°, yield 40%; IR: 3500-3300, 2800-2815, 1600, 1155, 850 cm^{-1} (Found: C, 69.7; H, 8.8; N, 2.6. $C_{30}H_{46}NOBr$ requires C, 69.8; H, 8.9 and N, 2.7%).

1-Cetyl-4-(X-substituted)styrylpyridinium bromides [where X = *p*-OH (**1a**), *o*-OH (**1d**), *p*-Cl (**1c**), *p*-$OC_{16}H_{33}$ (**1e**)] were prepared by a similar method. All these derivatives analysed satisfactorily and their IR spectra were comparable with their structures (Table 1).

Table 1—Analytical Data of 1-Cetyl-4-(X-substituted)styryl Pyridinium Bromide

Compound	m.p. °C	Mol. formula	Found (Calc.) (%)		
			C	H	N
1a	223	$C_{30}H_{46}NOBr$	69.6 (69.8	8.8 8.9	2.6 2.7)
1b	195	$C_{29}H_{44}NOBr$	69.2 (69.3	8.7 8.8	2.5 2.8)
1c	244	$C_{29}H_{43}NBrCl$	66.6 (66.9	8.2 8.3	2.6 2.7)
1d	179	$C_{29}H_{44}NOBr$	69.2 (69.3	8.5 8.8	2.6 2.8)
1e	159	$C_{45}H_{76}NOBr$	74.3 (74.4	10.3 10.5	1.6 1.9)

Surface pressure measurement

All measurements were carried out on a $25 \times 12 \times 2$ cm^3 periplex Langmuir trough with a motor driven glass plate barrier. Surface pressure data were recorded with a transducer attached to Wilhelmy plate. the output of the transducer was read as transducer read out and recorded on a x-y recorder to generate a surface pressure-area isotherm. The condition of water or sulphuric acid surface prior to spreading the dye sample was monitored by measuring stearic acid force-area curve. This was comparable with published isotherm[5]. Solution of the compounds were prepared in chloroform-hexane-methanol (1:3:1) mixture and the solution (0.02.ml) was spread on the subsolution using an Agla microsyringe.

Surface potential measurement

The surface potential of the monolayer was measured using an Ag-AgCl electrode and an ionizing electrode. This consisted of a metal rod with its tip 1-2 mm above the liquid surface and with polonium deposited on the tip to make the air gap ionizing. The electrodes were connected to an electrometer the output of which drove an x-y recorder to generate ΔV-area curves.

Results and Discussion

Oxidation with $KMnO_4$

Potassium permanganate solution (1 ml) was injected into the water subsolution. The solution was made homogeneous by rolling a magnet and the change in ΔV with time was recorded on the x-y recorder. Since the surface potential values change with time the rate constants were evaluated from such changes (Table 2). The observation that the compounds are oxidised by $KMnO_4$ indicates that double bonds are in contact with water.

Table 2—Area/Molecule, Surface Potential, Rate Constant for $KMnO_4$ Oxidation and Surface Dipole Moment of Cyanine Dyes

Compound	Area/ molecule in $Å^2$	Δv in mv	$\Delta v/n \times 10^{13}$	$10^4 k$ (sec^{-1})	μ
1a	115	650	74.75	FAST	5.95
1b	60	740	44.4	46.6	3.53
1c	60	730	43.8	89.03	3.48
1d	85	750	63.75	47.2	5.07
1e	90	760	68.4	57	5.44

Surface dipole moment

Surface potential (ΔV) is related to the resultant vertical component of the dipoles of the molecule by the equation: $\Delta V = Kn\mu^6$ where K is a constant ($= 4\pi$), n is the number of molecules per cm^2. The surface dipole moment values for the dyes **1b** and **1c** are approximately same indicating a similar type of orientation on the surface. With additional hydrophilic group like −OH as in the dyes **1a** and **1d**, the dipole moment values indicate additional interactions like H-bonding. In compound **1a** there is a lesser possibility of H-bond formation due to steric hindrance. This has been reflected in its low value of surface dipole moment as compared to that of the dye **1e**.

Area/molecule

Figure 1 represents the surface pressure-area/molecule isotherm of the dye **1a**. The phase transition in Fig. 1 reflects the formation of a condensed monolayer. The limiting area of the dye molecules and their $\Delta V/n$ values at fully compressed state are given in Table 2. To account for the results we have adopted an architectural model of *L*-aggregation. In this model the cyanine dye has the cetyl group oriented towards air and the hydrophilic styryl unit

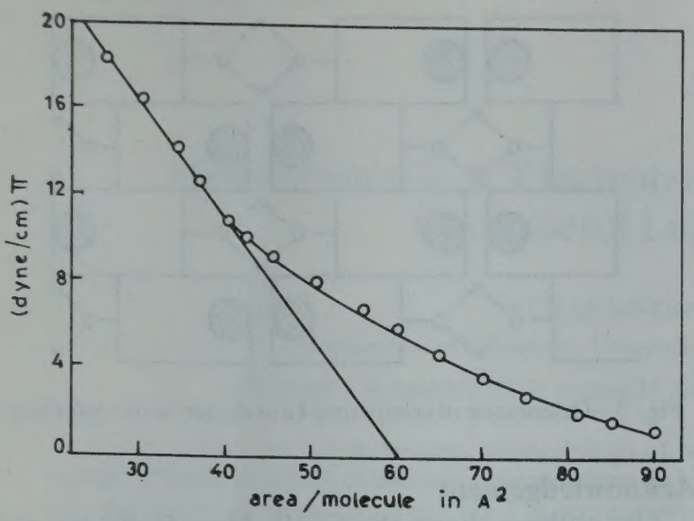

Fig. 1—π (in dyne/cm)-area/molecule for 1-cetyl-4-(*p*-methoxy styryl)pyridinium bromide (**1b**).

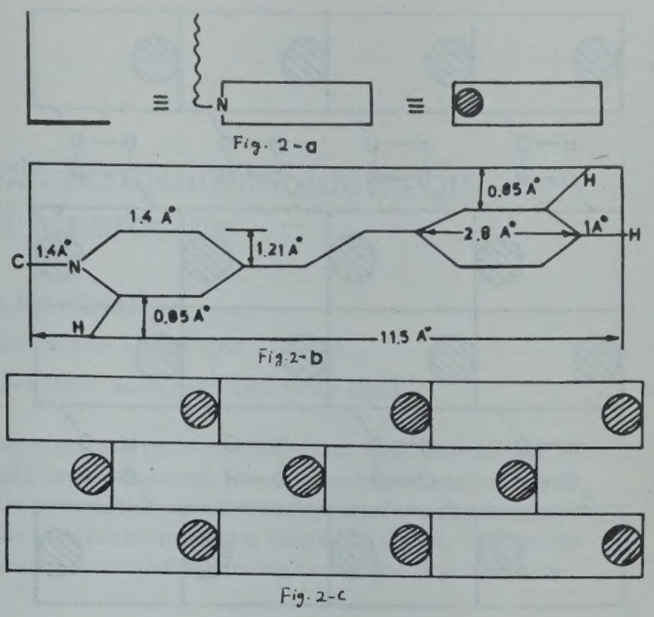

Fig. 2—(a) Schematic representation of the dye, (b) Representation of bond distances in the molecule, and (c) Orientation of parent cyanine dye in the monolayer.

lies flat on the water surface. In flat-on position the styryl unit covers an area of 60 Å^2 which has been calculated as follows. For the parent cyanine dye (with no substituents in the styryl moiety) the compound can be schematically represented as inFig. 2a. In fully compressed state the molecules may be arranged as bricks in a floor (of Fig. 2c) having the cetyl unit as big nails on each brick. The area of the head group has been calculated by considering (i) the molecule to be completely planar, (ii) the bond lengths of N − C, N = C, C − C and C = C to be 1.4 Å, (iii) C − H bond length to be 1 Å, and (iv) all the bond angles to be 120° (ref. 7). By adding all the bond lengths, the length of the styryl group has been calculated to be 11.5 Å.

The length of the polyene chain has also been calculated from the λ_{max} value of the compound employing free electron model as defined by Eq. (1)[8]

$$L = 5.507 \times 10^{-2}(2N+1) - 2 \quad \ldots (1)$$

where L = length of the polyene chain and N = number of double bonds.

In the parent molecule $N = 5$ and $\lambda_{max} = 475$ nm. The molecular length has been calculated to be 11.8 Å. Both the values agree quite well. Hence the additive method gives an approximate idea about the size of the head group. The other arm of the rectangle has been calculated by additive method and found to have a value of 5.52 Å (Fig. 2b). Thus the area of the rectangle is calculated to be 59.78 ≃ 60 Å^2. In the case of compounds **1b** and **1e** the limiting area per molecule in their fully compressed state is found to be 60 Å^2 which is interestingly found to be the same as that from calculation. The $-OCH_3$ and $-Cl$ groups at the *para*-position in the styryl unit (as in compounds **1b** and **1c**) do not affect the area of the head group. The aggregation in this case is schematically shown in Fig. 2c. The limiting area of the molecules for **1e** is found to be 90 Å^2. The cetyl groups at both the ends of the styryl unit force the compound to float in flat-on position. Vaidyanathan *et al.*[2] have shown that the free space between the hydrocarbon substituents extending upward from the chromophore to be sufficiently large to accommodate an additional alkyl chian. Thus it appears reasonable that in aggregated state the additional cetyl chain lies above the water surface when the spatial requirements in that region are met. This is reflected in an increase in area by 30 Å^2/molecule. For an additional cetyl group Shah *et al.*[9] have observed an increase of 20 Å^2 in the area of the molecule in its fully condensed state. But in this case the increase of 30 Å^2 may also include a molecular spacing due to arrangement of molecules (Fig. 3).

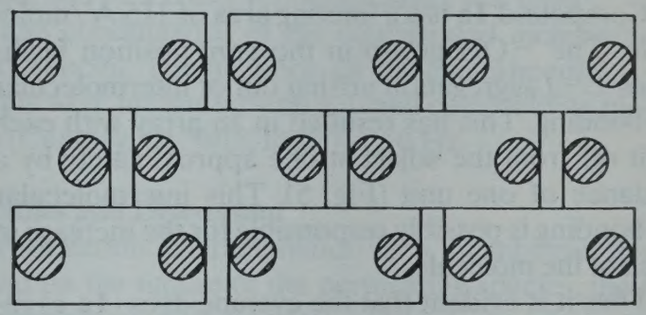

Fig. 3—Orientation of compound **1e** at the air/water interface.

Compound **1d** has a limiting area of 85 Å^2/molecule. This increase in area by 25 Å^2/molecule is due to the H-bonding in the $L-L$ aggregation. This H-bonding imposes the requirement that the dye molecules be organised into a two dimensional array with each unit off set from the adjacent one by a dis-

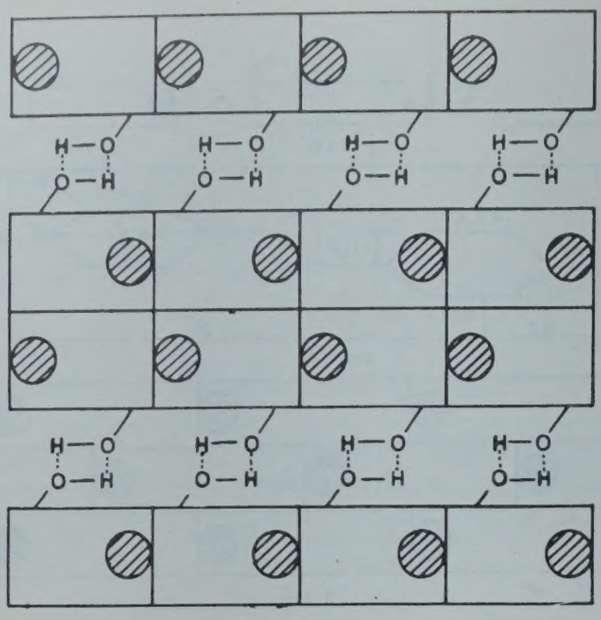

Fig. 4—Orientation of compound **1d** at the air/water interface.

tance of half a unit because the −OH group is in the *ortho* position (Fig. 4).

Compound **1a** has a limiting area of 115 Å^2/molecule. The −OH group in the *para*-position facilitates *L*−*J* aggregation arising out of intermolecular H-bonding. This has resulted in an array with each unit off from the adjacent one approximately by a distance of one unit (Fig. 5). This intermolecular H-bonding is possibly responsible for the increase in area of the molecule.

Thus it is evident that the cyanine dyes (**1a-e**) remain in L-aggregate in monolayer on a water subsolution and are expected to have similar kind of orientation in a monomolecular film on a solid surface. This information may provide the basis for studies in such dyes.

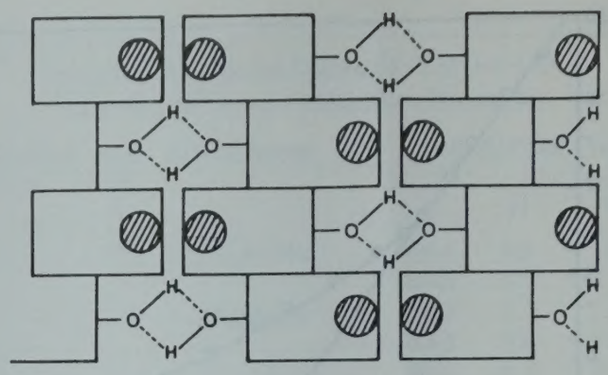

Fig. 5—Orientation of compound **1a** at the air/water inferface.

Acknowledgement

The authors thank the CSIR, New Delhi for the award of a junior research fellowship to one of them (AKS) and to the UGC, New Delhi for the award of Indo-US visitorship to GB. Grateful thanks are due to the University of Florida, Gainsville for providing facilities to carry out a part of this work.

References

1 Sturner D M in *Spectroscopy in heterocyclic chemistry*, edited by A Weisenberg & E C Taylor (Wiley, New York) 1977, p 540.
2 Vaidyanathan S, Patterson L K, Mobius D & Gruniger H R, *J phys Chem*, **89** (1985) 491.
3 Herz A H, *Photogr Sci Eng*, **18** (1974) 323.
4 Nakahara H & Fukuda K, *J phys Chem*, **90** (1986) 6144.
5 Feher I A, Collins F D & Healy T W, *Aust J Chem*, **30** (1977) 511.
6 *Insoluble monolayers at the liquid-gas interface*, edited by G L Gaines Jr, (Interscience, New York).
7 Smith D M, in *Comprehensive organic chemistry*, edited by P G Sammes (Pergamon, New York) 1978.
8 Rastogi R P & Srivastava V K in *An introduction of quantum mechanics of chemical systems* (Oxford & IBH, New Delhi) 1986, p 49.

Indian Journal of Chemistry
Vol. 27A, July 1988, pp. 565-568

Hydrodynamic & Electroosmotic Permeation Studies on Cholesterol Liquid Membrane

KEHAR SINGH* & A K TIWARI
Department of Chemistry, University of Gorakhpur, Gorakhpur 273 009

Received 7 *September* 1987; *revised* 25 *November* 1987; *accepted* 9 *December* 1987

Hydrodynamic and electroosmotic permeabilities of cellulose acetate supported cholesterol liquid membrane, in sodium chloride solutions of different concentrations and *p*H have been measured. The permeabilities exhibit significant alteration with composition and *p*H. The permeability data in conjunction with membrane conductance data have been used for the determination of electrical characteristics of the membrane-permeant interfacial region. The results have also been examined in the light of electrochemical characteristics derived earlier using membrane potential data.

Cholesterol is an effective surfactant of biological significance[1]. Liquid membranes are generally generated by allowing the dispersions of liquid membrane forming moieties to interact with some suitable substrates such as cellulose acetate[2,3]. Formation of liquid membranes can be detected by different methods[2], including resistivity measurements[4]. For electrochemical characterization, membrane potential studies have also been carried out[5]. Presently we have measured the hydrodynamic and electroosmotic permeabilities of cellulose acetate supported cholesterol liquid membrane with the object of dimensional characterization and determination of character of electrified membrane-permeant interface[6]. The results of these studies have been correlated with the conclusions earlier drawn using membrane potential measurements.

Materials and Methods

Cellulose acetate membrane was prepared as reported elsewhere[6]. An all glass experimental setup[7] was used for the purpose of present investigation. A piece of cellulose acetate was fixed in the cell and equilibrated with the experimental solution. The effective cross sectional area of the membrane used in the present study was 1.60 cm^2 and its thickness was 1.9×10^{-2} cm.

Liquid membrane was generated as reported earlier[5]. The cellulose acetate was allowed to equilibrate with cholesterol dispersions of different concentrations, and liquid membrane formation was followed by resistivity measurements[4]. Minimum cholesterol concentration needed for the formation of liquid membrane was found to be 10 nmol.

Hydrodynamic and electroosmotic permeabilities were measured as described elsewhere[7]. For the estimation of electroosmotic permeability, a known potential difference was imposed across the membrane with the help of an electronically operated power supply using Ag/AgCl electrode system. For membrane potential measurements experimental setup and procedure reported earlier was used[8].

The conductance of the equilibrated membrane and specific conductance of the experimental liquids were measured with a digital conductivity meter (Century, CC 601, India) at 50 Hz.

Results and Discussion

Permeation characteristics of a membrane depend on the nature of the permeating species, their concentration and *p*H of the solution, in addition to the nature of the membrane material and the extent of openness the membrane is endowed with. The experimental results indicate that the hydrodynamically and electrically driven volumetric fluxes exhibit significant alteration with composition and *p*H. For a quantitative comparison, these data were examined using linear phenomenological equation (1),

$$J_v = L_{11}\left(\frac{\Delta P}{T}\right) + L_{12}\left(\frac{\Delta \phi}{T}\right) \quad \ldots (1)$$

derived using non-equilibrium thermodynamic principles[9,10]. The phenomenological coefficients L_{11} and L_{12} obtained from the slopes of the plots of $(J_v)_{\Delta\phi=0}$ versus ΔP and $(J_v)_{\Delta P=0}$ versus $\Delta\phi$ are summarized in Tables 1 and 2 respectively.

For the purpose of explaining these results, dimensional characterization of the membranes with the without cholesterol under different experimental conditions is essential. It has been shown elsewhere[11] that average membrane pore radius is given by Eq. (2)

$$r = \frac{8\eta L_{11}\kappa}{(I/\Delta\phi)_{\Delta P=0}} \quad \ldots (2)$$

Table 1—Phenomenological Coefficients and Membrane Parameters

Conc. of NaCl (mol dm^{-3})	$L_{11} \times 10^7$ (cm^5 s^{-1} dyne^{-1})		$L_{12} \times 10^4$ (cm^3 s^{-1}m V^{-1})	
	A	B	A	B
0.15	1.57	1.76	2.01	2.64
0.30	2.35	2.36	1.85	2.68
0.45	2.21	2.32	0.60	1.50
0.60	2.14	2.53	0.20	0.61

(A) With cholesterol; and (B) without cholesterol.

Table 2—Phenomenological Coefficients and Membrane Parameters

[Conc. of sodium chloride solution = 0.15 mol dm^{-3}]

*p*H	$L_{11} \times 10^7$ (cm^5 s^{-1} dyne^{-1})		$L_{12} \times 10^4$ (cm^3 s^{-1} V^{-1})	
	A	B	A	B
7.0	1.50	1.54	2.01	2.64
4.0	1.87	1.94	2.91	3.21
3.0	1.88	2.50	3.93	6.30
2.0	2.04	2.53	4.28	7.83

(A) With cholesterol; and (B) without cholesterol.

Table 3—Membrane Conductance, Pore Radius and Double Layer Thickness at Different Sodium Chloride Concentrations

Conc. of NaCl (mol dm^{-3})	$(I/\Delta\phi)_{\Delta P=0} \times 10^3$ (ohm^{-1})		$r \times 10^5$ (cm)		$\delta \times 10^9$ (cm)
	A	A	A	B	
0.15	2.30	3.07	4.030	4.080	76.74
0.30	3.90	4.30	5.043	5.053	54.31
0.45	5.60	6.40	4.890	5.010	44.45
0.60	7.70	8.80	4.812	5.232	38.49

(A) With cholesterol; and (B) without cholesterol.

Table 4—Membrane Conductance, Pore Radius and Double Layer Thickness at Different *p*H

*p*H	$(I/\Delta\phi)_{\Delta P=0} \times 10^3$ (ohm^{-1})		$r \times 10^5$ (cm)		$\delta \times 10^9$ (cm)
	A	B	A	B	
7.0	5.35	5.82	4.030	4.080	76.74
4.0	6.36	7.02	4.503	4.584	76.78
3.0	6.49	7.76	4.518	5.202	76.77
2.0	8.22	8.40	4.698	5.232	75.18

(A) With cholesterol; and (B) without cholesterol.

where $(I/\Delta\phi)_{\Delta P=0}$ represents membrane conductance, κ and η denote the specific conductance and coefficient of viscosity of the permeant, respectively. Membrane conductance values derived using current versus potential data alongwith average pore radius values obtained using Eq. (2) are given in Tables 3 and 4.

The results given in Table 1 show that membrane permeability depends on composition and it increases initially with increase in sodium chloride concentration and tends to become practically independent of concentration within the range of investigation. The permeability behaviour is consistent with the average pore radius values given in Table 3. There is a significant enhancement in membrane permeability with decrease in *p*H (Table 2). It appears that cellulose acetate undergoes deswelling when equilibrated with sodium chloride solution of progressively lowered *p*H. This is also borne out by the average pore radius values (Table 4). When cellulose acetate is equilibrated with sodium chloride solution, its *p*H may change as a result of H^+ ion uptake. Our earlier results[6] have shown that H^+ ion uptake is enhanced with decrease in *p*H of the solution. Cellulose acetate contains low concentration of carboxylic groups. It, therefore, appears that there is progressive suppression of dissociation of cellulose acetate with decrease in *p*H. Swelling of cellulose acetate occurs presumably due to solvation of the ionogenic groups. The concentration of these ionogenic groups as already argued decreases with decrease in *p*H due to suppression of dissociation. Water uptake thus declines with decrease in *p*H, i.e. deswelling of cellulose acetate is expected as the *p*H of the sodium chloride solution is lowered. This is consistent with the observed lowering of the average pore radius with increase in *p*H. The liquid membrane formation occurs due to the accumulation of cholesterol moieties on the cellulose acetate surface. Relatively lower permeability values are expected in this case. The experimental results included in Tables 1 and 2 lend credence to this expectation.

Because of low concentration of ionogenic groups cellulose acetate membranes with and without cholesterol exhibit very low selectivity. Volumetric flux driven by electrical field acting across these membranes may, therefore, be attributed to the existence of a space charge in the interfacial region generated as a result of preferential adsorption of ions by the membrane matrix and subsequent balance of their charge by an excess of oppositely charged ions diffusely dispersed in solution. The membrane solution interface is thus endowed with an electrical potential, i.e. the zeta-potential. The zeta-potential can be expressed in terms of the cross phenomenological coefficient L_{12} and membrane conductance

Table 5—Zeta-Potential at Different Concentrations and *p*H

Conc. of NaCl (mol dm^{-3}) (*p*H = 7.0)	(−ξ) mV		*p*H (0.15 *M* NaCl)	(−ξ) mV	
	A	B		A	B
0.15	4.007	5.322	7.0	4.012	5.259
0.30	3.664	2.988	4.0	5.815	6.393
0.45	1.485	2.988	3.0	7.861	12.568
0.60	0.398	1.194	2.0	8.532	15.610

(A) With cholesterol; and (B) without cholesterol.

Table 6—Fixed Charge Densities

[Mean conc. of NaCl solution used 0.15 mol dm^{-3}; $C_1 = 0.2$; $C_2 = 0.1$ mol dm^{-3}]

*p*H	$\phi\bar{X}$ (mol dm^{-3})	
	A	B
7.0	0.0869	0.1012
4.0	0.0896	0.1310
3.0	0.1068	0.1967
2.0	0.1068	0.2014

(A) With cholesterol; and (B) without cholesterol.

$\left(\frac{I}{\Delta\phi}\right)_{\Delta P=0}$ by Eq. (3)[12]. In Eq. (3)

$$\zeta = \frac{4\pi\eta\kappa}{\varepsilon(I/\Delta\phi)_{\Delta P=0}}\left(\frac{L_{12}}{T}\right) \times 9 \times 10^4 \text{ volts} \quad \ldots (3)$$

ε denotes dielectric constant of medium. The ζ-values estimated using Eq. (3) are summarized in Table 5 at different concentrations and *p*H of the sodium chloride solutions. The fixed charge density values derived earlier using membrane potential measurements are included in Table 6. Zeta-potential values across cellulose acetate membrane, with and without cholesterol decrease with increase in concentration, whereas the fixed charge density follows a reverse trend. Both these parameters indicate increased preferential adsorption with increase in concentration of sodium chloride solution. Accumulation of adsorbed species leads to compaction of the electrical double layer. The double layer thickness (δ)[13] may be estimated using Eq. (4)

$$\delta = \sqrt{\frac{RT\varepsilon_r\varepsilon_0}{2F^2C}} \quad \ldots (4)$$

Putting $R = 8.31 \times 10^3$ kg m^2 sec^2 K^{-1} k mol^{-1}, $F = 9.96 \times 10^7$ A sec k mol^{-1} and $\varepsilon_0 = 8.85 \times 10^{12}$ A^2 sec^4 m^3 kg^{-1}, at 30°C (= 303K), we get

$$\delta = 3.4 \times 10^{-11}\sqrt{\frac{\varepsilon_r}{C}} \quad \ldots (5)$$

The δ-values obtained using Eq. (5) are given in Tables 3 and 4. The double layer thickness is practically independent of *p*H of the sodium chloride solution, indicating that there is practically no change in the electrical nature of the membrane permeant interface with *p*H. It has already been inferred on the basis of the hydrodynamic permeability data that cellulose acetate undergoes deswelling with decrease in *p*H due to enhanced suppression of dissociation of carboxylic groups[16]. Due to this the electrical character of the membrane surface is predominantly determined by the preferential ionic accumulation. This is also supported by the fixed charge density values at different *p*H (Table 6). Fixed charge density, $\phi\bar{X}$, values were estimated earlier[14,15] using membrane potential data and Eq. (6)

$$\phi\bar{X} = \frac{2C \cdot P_s}{\sqrt{1-P_s^2}} \quad \ldots (6)$$

where P_s, which represents the permselectivity of the membrane, is given by Eq. (7)

$$P_s = \frac{\bar{t}_+ - t_+}{t_+ - (2t_+ - 1)\bar{t}_+} \quad \ldots (7)$$

In Eq. (7) t_+ denotes transport number of the cation and $\bar{t}_+$ represents transport number of the cation in the membrane phase. It may be estimated using Eq. (8)[5]

$$\bar{t}_+ = \frac{(\Delta\phi)_{I=0}}{2[(\Delta\phi)_{I=0}]_L}(1-2t_+) + 0.5 \quad \ldots (8)$$

where

$$[(\Delta\phi)_{I=0}]_L = \frac{(1-2t_+)RT}{F}\ln\frac{a_1}{a_2}$$

is the liquid junction potential and $(\Delta\phi)_{I=0}$ is the membrane potnetial.

Acknowledgement

One of us (AKT) is grateful to the CSIR, New Delhi for the award of a senior research fellowship.

References

1 Chapman D, *Introduction to lipids* (McGraw Hill, New York) 1969, pp. 10.

2 Srivastava R C & Jakhar R P S, *J phys Chem*, **85** (1981) 1457.

3 Srivastava R C & Yadav Saroj, *J non-equilib Thermodyn*, **4** (1979) 219.

4 Singh K, Ram Shabd & Srivastava V N, *Indian J Chem*, **20A** (1981) 391.

5 Singh K & Tiwari A K, *J Colloid Interface Sci*, **116** (1987) 42.

6 Singh K & Tiwari A K, *J membrane Sci*, **34** (1987) 155.

7 Singh K, Srivastava V N & Chand M, *J non-equilib Thermodyn*, **6** (1981) 101.

8 Singh K, Tiwari A K & Rai J P, *Indian J Chem*, **24A** (1985) 825.

9 Rastogi R P, Singh K, Ram Shabd & Upadhyaya B M, *J Colloid Interface Sci*, **2** (1981) 80.

10 Katchalsky A & Curran P F, *Non-equilibrium thermodynamics in biophysics* (Harvard University Press, Cambridge) 1965, pp. 159.

11 DeGroot S R, *Thermodynamics of irreversible processes* (North-Holland, Amsterdam) 1963, pp. 198.

12 Kruyt H R, *Colloid science* (Elsevier amsterdam), 1952, pp. 201.

13 Kotyk A & Jancek K, *Biomembranes*, Membrane transport, an *indisciplinary approach*, Vol. 9 (Plenum, New York) 1977, pp. 253.

14 Lakshminarayanaiah N, *J Membrane Sci*, **21** (1975) 175.

15 Kobatke Y & Kamo N, *Prog Polym Sci Japan*, **5** (1973) 257.

16 Lonsdale H K, *Desalination by reverse-osmosis* edited by U Merten (MIT Press, Cambridge) 1966, pp. 93.

Indian Journal of Chemistry
Vol. 27A, July 1988, pp. 569-573

Formation of Anodic Oxide Films on Tantalum in Presence of Ultraviolet Radiations & Heat Treatment of Anodic Tantalum Oxide Films

R K NIGAM*, K C KALRA & PARVEEN KATYAL
Department of Chemistry, Maharshi Dayanand University, Rohtak 124001

Received 14 *August* 1987; *revised and accepted* 26 *November* 1987

The data obtained during the growth of anodic oxide films on tantalum indicate higher values of rates of growth, constant *A* (of Guntherschulze-Betz equation) and Tafel slopes in the presence of UV radiations than those in the absence of radiations. However, the values of constant *B* (of Guntherschultze-Betz equation), half-jump distances and breakdown voltages are lower in the presence of UV light. Faster rate in the presence of UV is probably due to increased number of mobile ions per unit volume and decreased width of potential energy barrier. Stimulated ionic movements due to UV radiations cause breakdown of films at lower voltages. Heat treatment of the oxide films in air makes these more conducting. This effect depends on the time period and temperature of heat treatment but is independent of film thickness and nature of electrolyte. The conductivity patterns before and after heating show similar trends and are of two types: One is associated with high conductance and lower rate of change of capacitance with increase in temperature and the other is associated with low conductances and changes capacitance more rapidly with increase in temperature. The hypothetical break temperature is independent of the nature of electrolyte or treatment.

The growth kinetics, breakdown characteristics, current efficiencies, dielectric measurements and ion-mobility studies of aqueous anodic oxide films on tantalum have been reported recently by the authors[1-4]. Film formation on valve metals under UV radiations has also received much attention[5-11]. However, the data obtained and the views expressed are at variance.

The properties of anodic oxide films undergo change when heated in vacuum[13-17] but the effect of heating anodized tantalum in air has not received much attention and needs further probing. The trends in the conductivity profile during heat treatment also require investigation. In this paper are presented the results of ionic conduction study of anodic oxide films formed on tantalum at constant current density and very high-field strength in the presence and absence of UV radiations.

Materials and Methods

Tantalum specimens (16×10^{-4} m^2 in area) with small tags were cut from 99.9% Ta sheets and their surfaces prepared in the manner described earlier[1]. The specimens thus prepared were placed in glass cells containing aqueous electrolyte and were surrounded by platinum gauzes which served as cathodes. The assembly was then put in a photochemical reactor (Srinivasan-Griffin-Rayonet Type, Popular Traders, India) and anodic polarization was carried out at a particular current density using constant current generator (General Electronics, India) as reported earlier[1]. The temperature during these measurements was 305 ± 1 K.

The heating of the samples in air was done in a pre-calibrated silica tube furnace. The capacitances before and after heating the oxide films were measured at 1 kHz using an electrolytic capacitor bridge (BPL, India) in the respective aqueous electrolyte taking special care that the tags did not dip into the electrolyte. For studying conductivity profile the cell was kept in an ultracryostat (model MK 70, GDR) and the liquid used was 38% H_2SO_4. Such an arrangement allowed temperature variation from 248 to 298 K. The density of the tantalum oxide film was taken as 793 kg m^{-3} as reported by Young[18]. All the chemicals used were of AR (BDH) grade.

Results and Discussion

A. Formation of aqueous oxide films in presence and absence of UV radiations

Anodic oxide films were formed in 100 mol m^{-3} aqueous solution separately in citric, tartaric and acetic acids at various current densities (6.25, 12.50, 62.5 and 125 A m^{-2}). The plots of voltages of film formation (V) in aqueous citric acid versus time (t) for which charges were passed are shown in Fig. 1 and are linear up to a film formation voltage of 200 V and thereafter there was deviation from linearity. Similar trends were also observed in tartaric and acetic acids. The rates of formation (dV/dt) were lower in the absence of

Table 1 – Constants A & B, Tafel Slopes, Half-Jump Distances and Breakdown Voltages of Variously Formed Oxide Films in Presence and Absence of UV Radiations

Electrolyte	A $Am^{-2} \times 10^8$	B $mV^{-1} \times 10^8$	Tafel slope $Vm^{-1} \times 10^{-7}$	Half jump distance,nm	Breakdown voltage,V
Citric acid	16.11(0.41)*	3.01(3.77)	3.46(2.63)	0.158(0.199)	340(365)
Tartaric acid	38.10(3.40)	2.82(3.41)	3.52(2.38)	0.148(0.185)	350(375)
Acetic acid	0.82(0.07)	3.50(4.02)	2.67(1.89)	0.185(0.212)	420(460)

* Values in parentheses are for the systems in the absence of UV radiations.

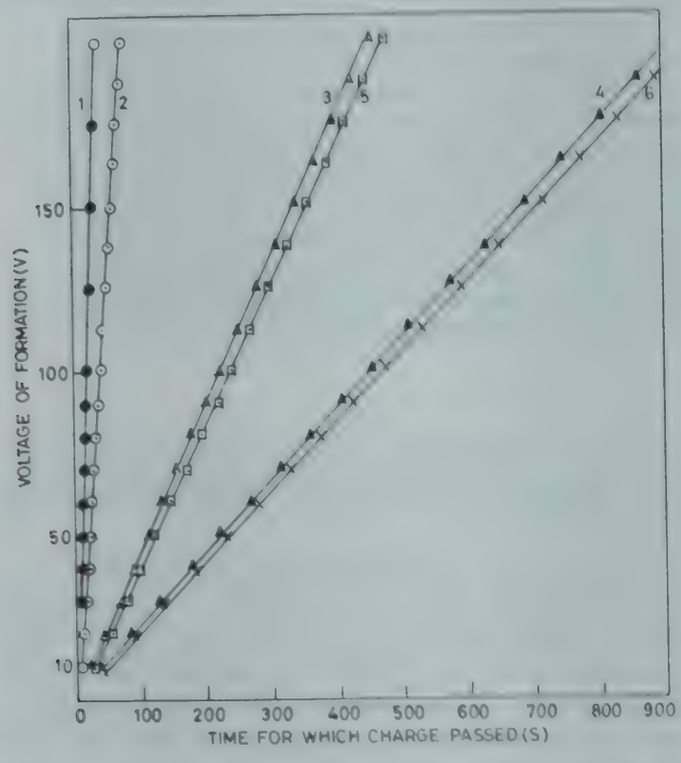

Fig. 1 – Variation of voltage of formation with time at different current densities for the films formed in citric acid [(1) 125.0 A m^{-2}; (2) 62.50; (3) 12.5 and (4) 6.25 in presence of UV radiations; (5) 12.5 A m^{-2} and (6) 6.25 in the absence of UV radiations]

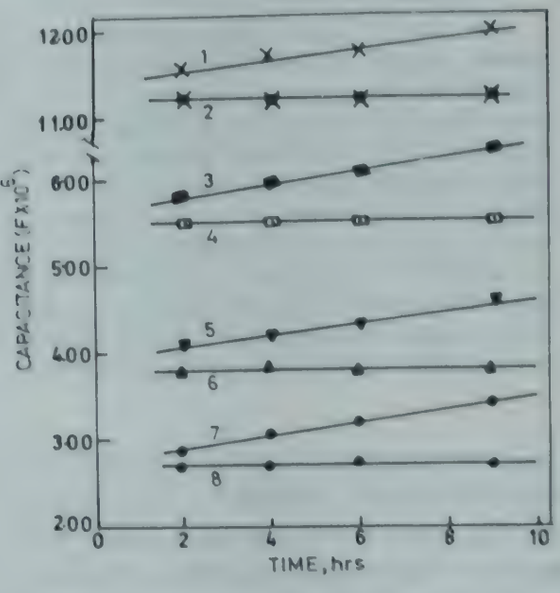

Fig. 2 – Variation of capacitance with time for the films formed upto different voltages in citric acid before and after heating [(1) Heated 25 V; (2) unheated 25 V; (3) heated 50 V; (4) unheated 50 V; (5) heated 75 V; (6) unheated 75 V; (7) heated 100 V; (8) unheated 100 V.

UV radiations than those observed in the presence of UV radiations (Fig. 1). The values of breakdown voltage (V_B) obtained in 100 mol m^{-3} citric, acetic and tartaric acids in the presence of UV radiations (Table 1) are lower than those obtained in their absence. The values of V_B (in the presence of UV radiations) decrease with increase in electrolyte concentrations (e.g. the values of V_B in 100 mol m^{-3} citric and acetic acids are 340 and 420 V while the corresponding values in 500 mol m^{-3} acids are 295 and 385 V). The plots of field strength (E) versus log (current density) in the case of citric, tartaric and acetic acids are linear. Thus, the dependence of field on current density in the presence of UV radiations can be represented by Guntherschultze-Betz equation,

$$i = A \exp BE \quad \ldots (1)$$

where A and B are constants. The values of constants A and B were evaluated both in the presence and absence of UV radiations and the results are presented in Table 1. The A-values are dependent on the nature of electrolyte and are higher in magnitude in the presence of UV radiations than those in their absence. Higher A-values indicate larger number of mobile ions per unit volume. The higher A-value in citric acid than that in acetic acid may be due to higher dissociation constant of citric acid (8.7×10^{-4}) than that of acetic acid (1.8×10^{-5}). The B-values show only small changes in different electrolytes; however, the B-values are lower in the presence of UV radiations. Using $B = qa/kT$ (ref. 19) (where q is the charge on Ta_2O_5 and can be taken as 5e, k is the Boltzmann constant, T is the temperature and a is the half-jump distance between lattice points), the values of a were calculated (Table 1). The results show that a-values are higher in the presence of UV radiations than those in their abs-

Table 2 – Capacitances of Films Formed at Formation Voltages of 25 and 50 V in Various Electrolytes Before and After Heating for 9 hr at 748 K

Electrolyte	Film formation voltage (V)	Capacitance ($F \times 10^6$)	
		Before heating	After heating
Citric acid	25	11.20	11.95
	50	5.50	6.30
Tartaric acid	25	10.40	11.05
	50	5.20	5.90
Acetic acid	25	10.90	11.55
	50	5.35	6.00
Sulphuric acid	25	11.00	11.70
	50	5.40	6.10

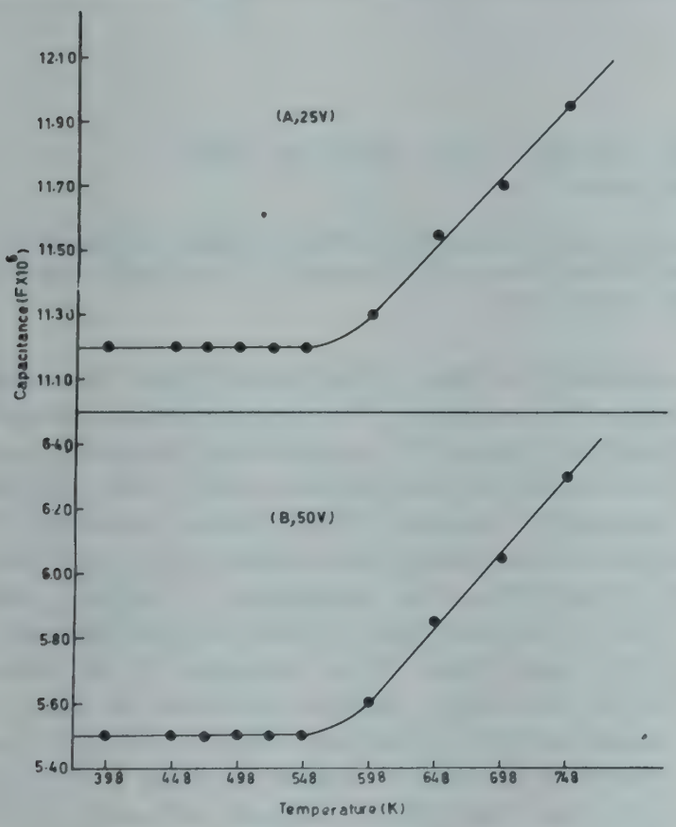

Fig. 3 – Variation of capacitance with temperature for the films formed upto film formation voltages of 25 and 50 V in citric acid.

ence. The Tafel slopes ($\partial E/\partial \ln i$) were calculated from the linear plots of field strength (E) versus log (current density) and the results are given in Table 1. The Tafel slopes for films formation induced by UV radiations are higher than those in their absence.

Irradiation with UV mainly produces an electronic photocurrent. Since the applied current is fixed, irradiation results in an enhanced rate of growth of oxide films as observed above. Hence irradiation should stimulate ionic conduction even in the presence of large ionic currents and, therefore, higher rates of growth of anodic films are observed for films grown in the presence of UV raditions at all current densities. It appears that in the presence of UV radiations there is an increase in the number of mobile ions per unit volume and this causes an increase in the rate of growth in the presence of UV radiations (Table 1). The faster growth rate in the presence of UV light may also be due to decrease in the width of the potential energy barrier and this is substantiated by the observed decrease in half-jump distances (a). Since the ionic movement is stimulated in the presence of UV radiations, the maximum film formation is reached at relatively lower voltages and this explains the observed lower breakdown voltages in the presence of UV radiations.

Heat treatment of anodic tantalum oxide films

Tantalum specimens were anodically polarised in 100 mol m^{-3} aqueous citric, tartaric, acetic and sulphuric acids (at a current density of 50 Am^{-2}) up to 25, 50, 75 and 100 V. These anodically oxidized samples after washing were separately heated in a tube furnace in the presence of air at a constant temperature for different intervals of time. The specimens were allowed to cool and taken out and their capacitances measured in the respective aqueous solutions at room temperature (303 ± 1 K). The plots of capacitance versus time of heating films formed up to different formation voltages (25, 50, 75 and 100 V in citric acid) at a fixed temperature (748 K) are shown in Fig. 2. The corresponding plots between capacitance after the same interval of time (equal to time of heating) at room temperature are also included in Fig. 2. The plots show that while there is no appreciable change in the values of capacitance with time at room temperature, the capacitance of each of the film increases with the duration of heating. Thus heat treatment makes the films more conducting. After 2 hr, the change in capacitance is more for a 25-V film and decreases as the voltage of film formation (i.e. thickness) increases. However, after longer time periods these differences disappear and films become equally conducting irrespective of film thickness. Similar trends were shown by the films formed in other acids. The capacitances, before and after heating for 9 hr, for the films formed in different electrolytes are given in Table 2. The results show that the variously formed films are affected by heat treatment to the same extent and hence the effect of heat treatment on oxide films is independent of the nature of the electrolyte.

The effect of temperature of heating was studied next by heating the oxide films formed at different

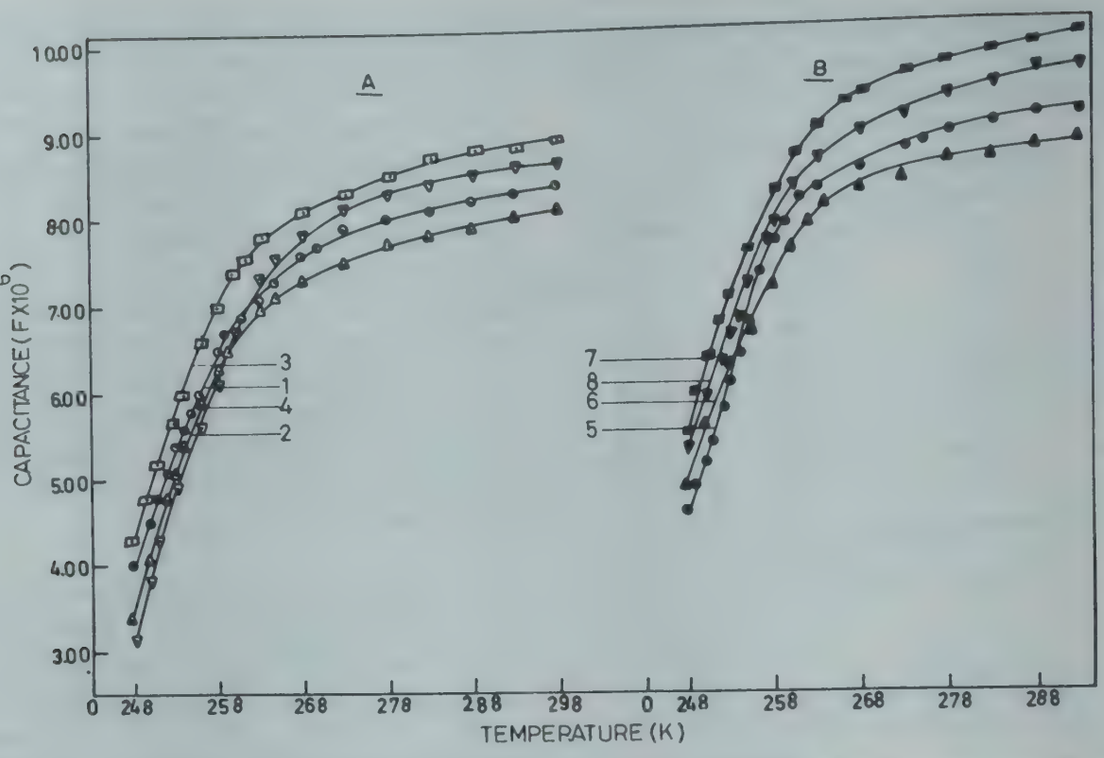

Fig. 4 – Variation of capacitance as a function of temperature for heated and unheated oxide films formed in various electrolytes. [(A) Unheated – (1) citric acid; (2) tartaric acid; (3) acetic acid; (4) sulphuric acid. (B) Heated – (5) citric acid; (6) tartaric acid; (7) acetic acid; (8) sulphuric acid]

temperatures upto 748 K for a fixed interval of time (9 hr). It was not possible to work beyond this temperature (748 K) as the films got damaged. The plots of capacitance versus temperature of heating for the oxide films formed in citric acid upto formation voltages 25 and 50 V are shown in Fig. 3 (A, B). The capacitances of the oxide films did not change when these were heated up to about 575 K. However, beyond this temperature, the capacitances increased almost linearly with rise in temperature of heating. Similar trends were shown by the films formed in other acids.

The conductivity profile across the Ta_2O_5 film was studied by measuring the capacitance of heated as well as unheated oxide samples as a function of temperature in 38% H_2SO_4 in the temperature range of 248 and 298 K. The plots of capacitance versus temeprature for films formed in citric, tartaric, acetic and sulphuric acids are shown in Fig. 4. The plots show the conductivity profile to be of two types: one which is associated with high conductance and smaller rate of change of capacitance with temperature; and the other associated with low conductance and higher rate of change of capacitance with temperature. The conductivity patterns for both heated and unheated samples show similar trends. Our results on conductivity profile do not agree with those of Smyth and Tripp[12]. This may be probably due to non-availability of data to Smyth and Tripp in a wide range of electrolytes. The hypothetical break temperature (obtained by extrapolating the linear portions of the capacitance-temperatur plot) was independent of nature of electrolyte or treatment. It appears than during heat treatment the conductivity results from the extraction of oxygen from Ta_2O_5 by Ta and hence causing oxygen deficiency in the oxide film. In the presence of air, when oxygen deficiency reaches oxide/air interface it renders oxygen to flow into the film. Oxygen flow maintains the oxide composition both at the Ta/Ta_2O_5 and Ta_2O_5/air interfaces and is not affected by the nature of the electrolyte.

Acknowledgement

One of the authors (PK) is thankful to the CSIR, New Delhi, for the award of a junior research fellowship.

References

1 Nigam R K, Kalra K C & Katyal P, *Indian J Chem*, **25A** (1986) 1080.
2 Nigam R K, Kalra K C & Katyal P, *Indian J Chem*, **26A** (1987) 17.
3 Nigam R K, Kalra K C & Katyal P, *Indian J Chem*, **26A** (1987) 819.
4 Nigam R K, Kalra K C & Katyal P, *Indian J Chem*, **27A** (1988) 198.
5 *Young L, Anodic oxide films* (Academic Press, London), 1961.

6 Venables J D & Brondy R M, *J appl Phys*, **30** (1959) 1110.
7 Rupprecht T, *Naturwissenschaften*, **47** (1960) 127.
8 Dekkar A J & Van Geel W C H, *Philips Res Rep*, **2** (1947) 313.
9 Vermilyea D A, *J appl Phys*, **26** (1955) 489.
10 Bray A R, Jacobs P W M & Young L, *J nuclear Materials*, **4** (1959) 356.
11 Nigam R K & Kapoor R, *Indian J Chem*, **16A** (1978) 283.
12 Smyth D M & Tripp T B, *J electrochem Soc*, **110** (1963) 1271.
13 Okubo K, *Kinzoku Hyoman Gijutsu*, **24** (1973) 74.
14 Kiselev I P, *Tr Kazan Aviats Inst*, **148** (1972) 17.
15 Vermilyea D A, *Acta Met*, **5** (1957) 113.
16 Dewald J F, *J phys Chem Solids*, **2** (1957) 55.
17 Nigam R K & Kapoor R, *Indian J Chem*, **15A** (1977) 954.
18 Young L, *Proc Roy Soc*, **A244** (1958) 41.
19 Cabrera N & Mott N F, *Rep Prog Phys*, **12** (1948) 163.

Indian Journal of Chemistry
Vol. 27A, July 1988, pp. 574-576

Conductances of Tetraalkylammonium Bromides in 1,2-Dimethoxyethane at 25°C: Analysis of Data by Fuoss-Kraus Theory

DEBASIS NANDI, S DAS & D K HAZRA*
Department of Chemistry, North Bengal University, Darjeeling 734430

Received 29 *June* 1987; *revised* 4 *November* 1987; *accepted* 23 *November* 1987

Precise equivalent conductances of Bu_4NBr, $Pent_4NBr$, Hex_4NBr and $Hept_4NBr$ have been measured in 1,2-dimethoxyethane (DME) at 25 ± 0.005°C in the concentration range of 5.0×10^{-2} to 1.0×10^{-4} mol dm^{-3}. The conductance data have been analyzed by the Fuoss-Kraus theory and the values of the ion-pair and triple-ion formation constants have been calculated. Analysis of the data indicates that the electrolytes are mainly associated in the form of ion-pairs ($K_p \approx 10^6 M^{-1}$). A small amount of triple-ions are also detected for these salts at $0.01 M < C < 0.05 M$, the maximum concentration limit where the data have been analysed.

1,2-Dimethoxyethane (DME) is a potential solvent now-a-days for use in non-aqueous batteries and its applications in organic syntheses and electrochemical studies[1] have been widely stressed. It is, therefore, imperative to study the transport properties of ions in this aprotic medium. The conductometric method is well known to give valuable information regarding ion-solvent interactions. Although a number of studies have been made in DME on alkali metal halides[2-4], literature provides no information on conductometric behaviour of tetraalkylammonium halides in DME. This led us to undertake the title investigation, the results of which are reported in this paper.

Materials and Methods

1,2-Dimethoxyethane (Fluka, purum) was shaken with $FeSO_4$ (AR, BDH) for 1-2 hr, decanted, distilled, the distilate refluxed for 12hr and redistilled over metallic sodium. The b.p. and density compared fairly well with the corresponding literature values[5] (b.p. 83.5°; d_0, 0.86261 gcm^{-3} at 25°C). The specific conductance of DME was 0.81×10^{-6} ohm^{-1}cm^{-1} at 25°C.

Tetraalkylammonium bromides were Fluka products. Tetrabutylammonium and tetrapentylammonium bromides were recrystallized from acetone-ether and dried *in vacuo* at 60° for two days. Tetrahexylammonium and tetraheptylammonium bromides were washed with ether and dried *in vacuo* at room temperature for two days.

Conductances were measured at 25°C ± 0.005°C employing a Pye-Unicam PW 9509 conductivity meter at a frequency of 2000Hz using a diptype cell of cell constant 0.731 cm^{-1}.

Densities were measured with an Ostwald-Sprengal type pycknometer of about 25 ml capacity. The dielectric constant of DME ($\varepsilon = 7.012$) was taken from the literature[6].

Results and Discussion

The log-log plots of Λ versus concentration for tetrabutyl-, tetrapentyl-, tetrahexyl- and tetraheptyl-ammonium bromides, given in Fig. 1, show a minimum in every case. The precise equivalent conductances of the tetrabutyl-, tetrapentyl-, tetrahexyl- and tetraheptyl-ammonium bromides are given in Table 1.

The conductance data have been analysed by the Fuoss-Kraus theory[7] for the triple-ion formation (Eq. 1)

$$\Lambda\, g(c)\, C^{1/2} = \frac{\Lambda_0}{K_p^{1/2}} + \frac{\Lambda_0^T K_T}{K_p^{1/2}} \left(1 - \frac{\Lambda}{\Lambda_0}\right) C \qquad \ldots (1)$$

where g(c) is a factor that incorporates all the interionic interaction terms; Λ_0 and Λ_0^T are the limiting equivalent conductances of R_4NBr and of two possible triple-ions $R_4N(Br)_2^-$ and $(R_4N)_2Br^+$ and K_p and K_T are the ion-pair and triple-ion formation constants respectively. The symmetrical approximation of the two possible formation constants of triple-ions equal to each other has been considered[4].

The term g(c) is given by Eq. (2)

$$g(c) = \frac{\exp\left[-\frac{\beta'}{\Lambda_0^{1/2}} (C\Lambda)^{1/2}\right]}{\left(1 - \frac{S}{\Lambda_0^{3/2}} (C\Lambda)^{1/2}\right)\left(1 - \frac{\Lambda}{\Lambda_0}\right)} \qquad \ldots (2)$$

Table 1—Equivalent Conductances of Tetraalkylammonium Bromides in 1,2-Dimethoxyethane at 25°C

10^4C (mol l^{-1})	Λ (ohm^{-1}cm^{2}mol^{-1})	10^4C (mol l^{-1})	Λ (ohm^{-1}cm^{2}mol^{-1})	10^4C (mol l^{-1})	Λ (ohm^{-1}cm^{2}mol^{-1})	10^4C (mol l^{-1})	Λ (ohm^{-1}cm^{2}mol^{-1})
Bu_4NBr		$Pent_4NBr$		Hex_4NBr		$Hept_4NBr$	
1.0102	11.401	29.9798	2.801	5.9989	2.916	19.9989	2.025
1.9976	7.011	49.9899	2.541	8.0019	2.487	22.0019	1.902
4.0028	4.799	70.0101	2.414	9.9989	2.141	24.9998	1.611
5.9879	3.817	99.9897	2.341	12.4999	1.976	30.0210	1.367
8.0201	3.375	129.9951	2.323	14.9879	1.793	35.0111	1.289
9.9989	3.161	169.9895	2.341	18.0019	1.677	39.9959	1.223
20.0091	2.369	199.9969	2.369	20.0109	1.580	64.9981	1.166
40.0011	2.021	219.9899	2.381	24.9985	1.462	99.9989	1.161
59.9969	1.933	289.2401	2.458	30.0017	1.379	150.0119	1.227
80.0019	1.901	300.0109	2.466	35.0105	1.337	199.9791	1.283
100.0101	1.919			39.9879	1.305	249.9986	1.379
149.9992	2.013			64.9987	1.244	300.0101	1.456
159.9891	2.044			99.8998	1.279	350.0091	1.514
250.0112	2.476			149.9899	1.333		
300.0091	2.691			250.0107	1.464		
				300.0105	1.513		
				499.9899	1.682		

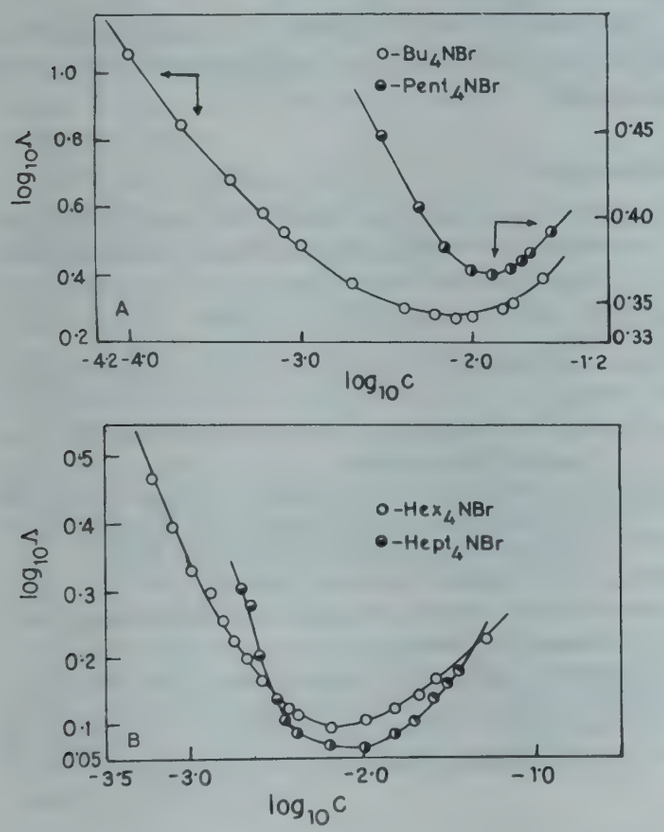

Fig. 1—Plot of $\log_{10}\Lambda$ versus $\log_{10} C$ for (A) Bu_4NBr and $Pent_4NBr$ and (B) Hex_4NBr and $Hept_4NBr$ in 1,2-DME at 25°C

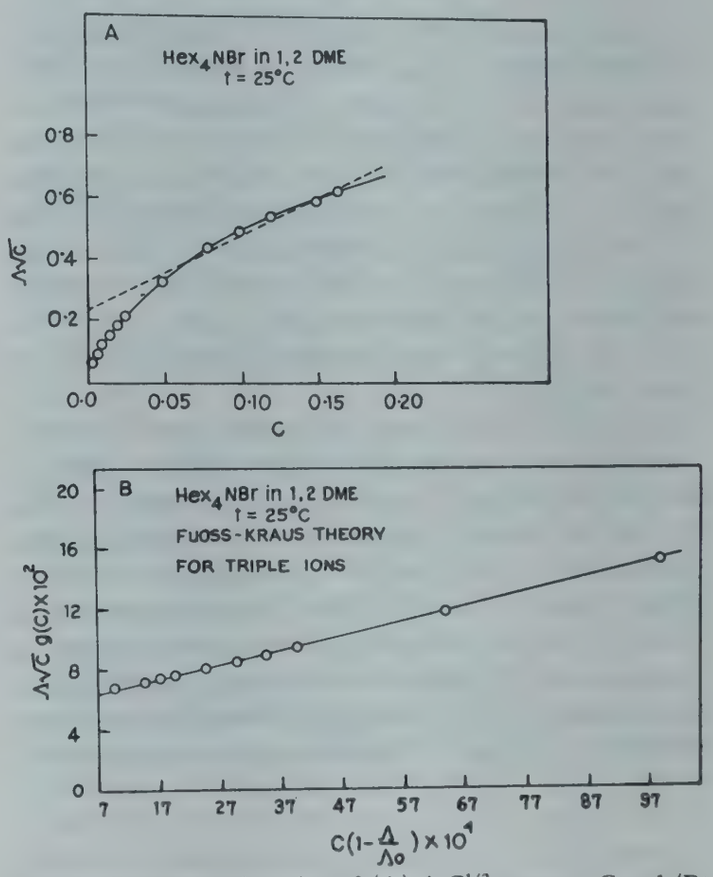

Fig. 2—Representative plot of (A) $\Lambda C^{1/2}$ versus C and (B) $\Lambda g(c) C^{1/2}$ versus $C(1-\Lambda/\Lambda_0)$ for Hex_4NBr in 1,2-DME at 25°C

where β' is the Debye-Huckel activity coefficient term and S the limiting Onsager coefficient. Neglecting Λ/Λ_0, $S/\Lambda_0^{3/2}(C/\Lambda)^{1/2}$ and assuming $f_\pm = 1$ lead to $g(c) = 1$ and we get

$$\Lambda(C)^{1/2} = \frac{\Lambda_0}{(K_p)^{1/2}} + \frac{\Lambda_0^T K_T}{(K_p)^{1/2}} \cdot C \qquad \ldots (3)$$

For the present data, it was found that Eq. (3) was inadequate, the data showing a downward curvature when plotted as $\Lambda C^{1/2}$ versus C (a representative plot for Hex_4NBr is shown in Fig. 2A). On the contrary Eq. (1) gives reasonably a linear plot (Fig. 2B).

Table 2—Ion-pair and Triple-ion Formation Constants of Electrolytes in DME at 25°C

Salt	Λ_0 ($ohm^{-1}cm^2mol^{-1}$)	$K_p \times 10^{-6}$ $(mol\ dm^{-3})^{-1}$	K_T $(mol\ dm^{-3})^{-1}$
Bu_4NBr	138.37	2.39	267.58
$Pent_4NBr$	132.76	1.12	192.01
Hex_4NBr	128.61	5.18	260.64
$Hept_4NBr$	125.93	4.74	230.74

Table 3—Values of Coefficients from Regression Analysis

Salt	r^2	Intercept	Slope
Bu_4NBr	0.968	8.95×10^{-2} (± 0.007)	15.96 (± 0.83)
$Pent_4NBr$	0.999	12.53×10^{-2} (± 0.002)	16.04 (± 0.11)
Hex_4NBr	0.996	5.65×10^{-2} (± 0.002)	9.82 (± 0.14)
$Hept_4NBr$	0.984	5.78×10^{-2} (± 0.005)	8.90 (± 0.34)

For evaluation of K_p and K_T values from Eq. (1), the average $\Lambda_0\eta_0$ values of the salts at 25°C were taken from the work of Krumgalz[8]. The viscosity (η_0) of 1,2-DME is 0.004129 poise. Therefore, from Walden's rule Λ_0 values of the electrolytes in 1,2-DME at 25°C were calculated (Table 2). Linear regression analysis of Eq. (1) gives coefficient (r^2), intercept and the slope (Table 3). From the above results and arbitrary position $\Lambda_0^T = 2/3\,\Lambda_0$, K_p and K_T values were calculated and are given in Table 2.

Table 2 shows that major portion of the electrolytes exists as ion-pairs with only a minor proportion as triple-ions (neglecting quadrupoles). The K_p and K_T values change in a zig-zag fashion with cationic size from Bu_4N^+ to $Hept_4N^+$ but decrease sharply for $Pent_4NBr$. This probably happens as a result of spherical interaction[9] (forming 'clathrate-like' structure around their hydrocarbon side chains) of the tetraalkylammonium ions with solvents in general. With the above values of K_p and K_T (Table 2), the ion-pair concentrations (c_p), of the electrloytes have been calculated[4] at a concentration of $c = 0.03\ M$ using the relation:

$$C_p = C(1 - \alpha - 3\alpha_T) \qquad \ldots (4)$$

where

$$\alpha = 1/(K_p^{1/2}\, C_p^{1/2})$$

and

$$\alpha_T = (K_T/K_p^{1/2})\, C^{1/2}$$

The values are: Bu_4NBr, 271.902×10^{-4}; $Pent_4NBr$, 270.112×10^{-4}; Hex_4NBr, 281.389×10^{-4} and $Hept_4NBr$, 282.688×10^{-4}.

The results indicate that a very small fraction of the electrolytes are present as triple-ions even at such a high concentration.

Acknowledgement

The authors are thankful to the UGC, New Delhi, for the award of a fellowship to one of them (DN).

References

1 Garst J F, in *Solute-solvent interactions*, edited by J F Coetzee & C D Ritchie (Marcel Dekker, New York) 1969, Chapter 8, p 541.
2 Onishi S, Faber H & Petrucci S, *J phys Chem*, **84** (1980) 2922.
3 Farber H, Irish D E & Petrucci S, *J phys Chem*, **87** (1983) 3515.
4 Maaser E H, Delsignore M, Newstein & Petrucci S, *J phys Chem*, **88** (1984) 5100.
5 Roy R N, Swensson E E, Lacross G & Kruegek O W, *Advances in chemistry series*, edited by W F Furter, (American Chemical Society, Washington DC) 1976.
6 Renard E & Justice J, *J solution Chem*, **3** (1974) 633.
7 Fuoss R M & Accascina F, *Electrolytic conductance*, (interscience, New York) 1959.
8 Krumgalz B S, *J chem Soc Faraday Trans I*, (1983) 571.
9 Yang-Wen W, in *Structure and transport processes in water and aqueous solutions*, edited by R A Horne (Wiley.Interscience, New York) 1971, Chapter 15.

Indian Journal of Chemistry
Vol. 27A, July 1988, pp. 577-580

Substitution of Aquo Ligands from Hydroxopentaaquochromium(III) Ion by Ethylenediaminetetraacetic Acid—A Kinetic Approach

H G MITRA MUSTOFY & G S DE*

Department of Chemistry, University of Burdwan, Burdwan 713104

Received 27 *July* 1987; *revised* 17 *September* 1987; *accepted* 4 *November* 1987

The kinetics of substitution of aquo ligands of hydroxopentaaquochromium(III) ion by EDTA in water-ethanol medium has been studied spectrophotometrically. The reaction rate is found to be *p*H dependent in the *p*H range of 4.4 to 5.2. The reaction rate is higher compared to the rates of water exchange process of the substrate complex. Activation parameters have been calculated. A low $\Delta H^{\ddagger}$ and a negative $\Delta S^{\ddagger}$ are suggestive of a mechanism involving the formation of ion-pair followed by associative interchange (I_a) process for the title reaction.

Anation reactions of hexaaquochromium(III) ion have been studied by many workers[1-6]. Significantly no single mechanistic conclusion has been drawn for such reactions. Hydroxopentaaquochromium(III) ion has not received similar attention. Interesting results are expected with this ion because of the presence of hydroxo group having both σ as well as π-bonding ability.

Ethylenediaminetetraacetic acid (EDTA) is a widely used chelating agent. Kinetics of reaction of EDTA with aquochromium(III) ion were first studied by Hamm[7] who observed that the rate of anation was independent of [EDTA]. Yamamto and Ohashi[8] made similar observation in the reaction between Cr(III) ion and EDTA catalysed by H_2O_2. On the otherhand Olson[9] reported that the reaction of $Cr(H_2O)_6^{3+}$ with EDTA involved reversible formation of an ion-pair followed by rate-determining anation. But Kimura *et al.*[10] while studying the reaction of EDTA with hexaaquochromium(III) ions in mixed solvents (*p*H range 3.5 to 4.6) suggested that the reaction is independent of [EDTA] and proceeded only through the dissociation of water molecules. The above facts prompted us to carry out the title reaction under a variety of conditions with a view to gaining information on the mechanism of the reaction.

Materials and Methods

$[Cr(H_2O)_6][ClO_4]_3$ was prepared bythe method of Moore and Basolo[11] using A R quality reagents. Hydroxopentaaquochromium(III) (complex-I) was prepared *in situ* from the hexaaquo complex by adjusting the *p*H to 5.0. The absorption spectrum of Complex-I exhibited λ_{max} at 430 (log ε 1.447) and 590 nm (log ε 1.255) quite different from those of hexaaquochromium(III) ion.

The product of the reaction between $Cr(H_2O)_5(OH)^{2+}$ and EDTA was prepared by mixing the two reactants in different molar ratios, viz. 1:1, 1:2, 1:3 and 1:30 thermostated at 45° for 72 hr. Absorption spectra of all the mixtures were similar exhibiting λ_{max} at 390 and 540 nm. The composition of the product in solution was determined by Jobs method of continuous variation. The metal-ligand ratio was found to be 1:1.

Complex-I and EDTA solution at *p*H 5.0 were mixed in 1:1 molar ratio, refluxed on water-bath for 10 hr, concentrated and the residue treated with acetone to get a solid mass. On drying violet coloured shining crystals were obtained. Elemental analyses of the isolated solid revealed the composition $Na[Cr(EDTA)(H_2O)]$ (complex-II). The absorption spectrum in solution of the isolated product was identical with that of the violet forms of the EDTA complex with chromium(III) ion studied by Hamm[7]. The author established the composition of the violet product as $H[Cr(EDTA)(H_2O)]$ in the *p*H range of 3-6 by spectrophotometric titration. In our case the reaction product $[Cr(EDTA)(OH)]^{2-}$ first formed got protonated to form the final product $[Cr(EDTA)(H_2O)]^{1-}$ in the *p*H range studied.

Kinetic experiments were carried out spectrophotometrically using a Hilger UVISPEK spectrophotometer. *p*H was adjusted by $NaOH/HClO_4$ using a Systronics digital *p*H meter. Ionic strength of the reaction medium was adjusted by adding $NaClO_4$. The course of the reaction was followed by measuring absorbances at 540 nm where a substantial difference existed in the spectra of the complexes-I and II. The [ligand] was always maintained high so that the pseudo-first order rate law could be applied. The pseudo-first order rate constants (k_{obs}) were determined graphically.

Results and Discussion

Effect of varying [complex-I] on rate constant

At [EDTA] = 0.05 mol dm^{-3}, ionic strength = 0.25 mol dm^{-3} and pH = 5.0, three sets of experiments were carried out at 35° at different [complex-I]. The k_{obs} values were 6.61×10^{-4}, 6.27×10^{-4} and 6.4×10^{-4} s^{-1} at [complex-I] = 0.0025, 0.003 and 0.0035 mol dm^{-3} respectively. Thus the rate showed first order dependence on [complex-I], i.e. d[complex-II]/$dt = k_{obs}$ [complex-I]

Effect of varying pH on rate constant

At fixed [complex-I] = 0.0025 mol dm^{-3}, [H_2EDTA^{2-}] = 0.025 mol dm^{-3} and ionic strength = 0.25 mol dm^{-3}, the values of k_{obs} at 35° were found to increase with increase in pH as shown in Fig. 1. The effect of pH variation on rate can be explained by considering the pK values of the ligand[12] and that of the aquo complex[13]. From the dissociation equilibria of EDTA it can be assumed that in the pH range of 4.4 to 5.2 the nature of the ligand remains almost unchanged and it exists mainly in the dinegative anionic form H_2EDTA^{2-}. So the increase in rate with the increase in pH should be due to the change in nature of the substrate complex. Considering the acid dissociation equilibrium (1) ($pK_1 = 3.8$ at 25°C)

$$Cr(H_2O)_6^{3+} \overset{K_1}{\rightleftharpoons} Cr(H_2O)_5(OH)^{2+} + H^+ \qquad \ldots(1)$$

it can be stated that at pH 3.8 the percentage of hexaaquo species and the hydroxopentaaquo species is approximately same at the experimental temperature. But increase in pH increases the percentage of the more reactive hydroxopentaaquo species. Enhanced reactivity of the hydroxopentaaquo species is due to well known labilising effect of the hydroxide ion adjacent to the water molecule by virtue of its lone pair of electron capable of exerting strong electromeric effect. Hydroxide ion is also a strong π-donor which facilitates the formation of very reactive hydroxo intermediate and hence increases the rate.

Effect of varying [EDTA] on rate constants

At fixed [complex-I] = 0.0025 mol dm^{-3}, ionic strength = 0.25 mol dm^{-3} and pH = 5.0, the [ligand] was varied in the range of 0.0125 to 0.05 mol dm^{-3} in 30% water-ethanol medium. The results of variation of [EDTA] on reaction rate at 25°, 31°, 35° and 40°C are summarised in Table 1. It is observed that the rate of reaction increases with the increase in [ligand] but at a high [ligand] the rate approaches a limiting value (Fig. 2), probably due to ion-pair formation. The limiting rate corresponds to completion of ion-pair formation. Scheme 1 can be proposed to explain the nature of variation of reaction rate with [ligand],

$$Cr(H_2O)_5(OH)^{2+} + H_2EDTA^{2-}$$

Complex-I

$$\overset{K_F}{\rightleftharpoons}_{\text{fast}} Cr(H_2O)_5(OH)^{2+} \ldots H_2EDTA^{2-}$$

ion-pair (IP)

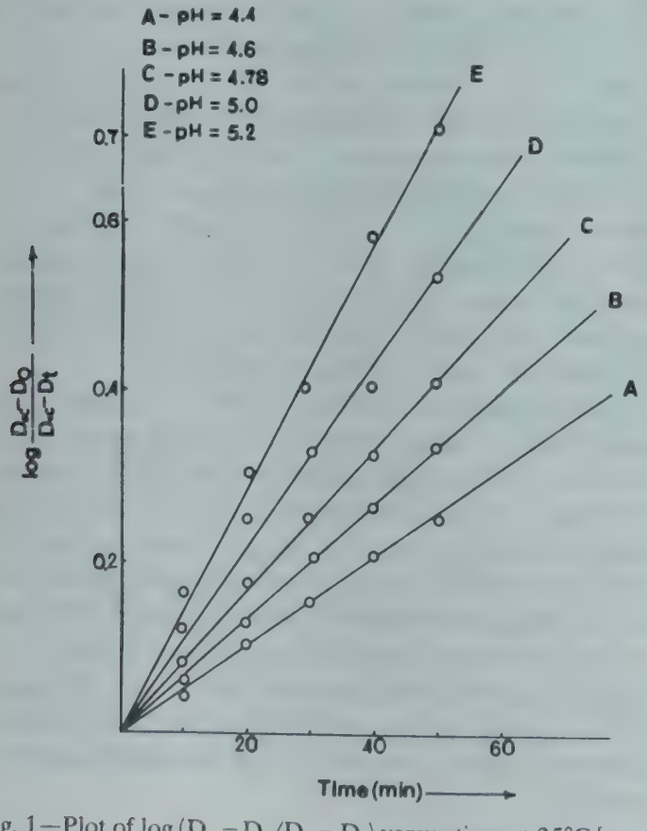

Fig. 1—Plot of log ($D_\alpha - D_0/D_\alpha - D_t$) versus time at 35°C [complex-I] = 0.0025 mol dm^{-3}, [H_2EDTA^{2-}] = 0.025 mol dm^{-3}, pH = (A) 4.4, (B) 4.6, (C) 4.78, (D) 5.0 and (E) 5.2.

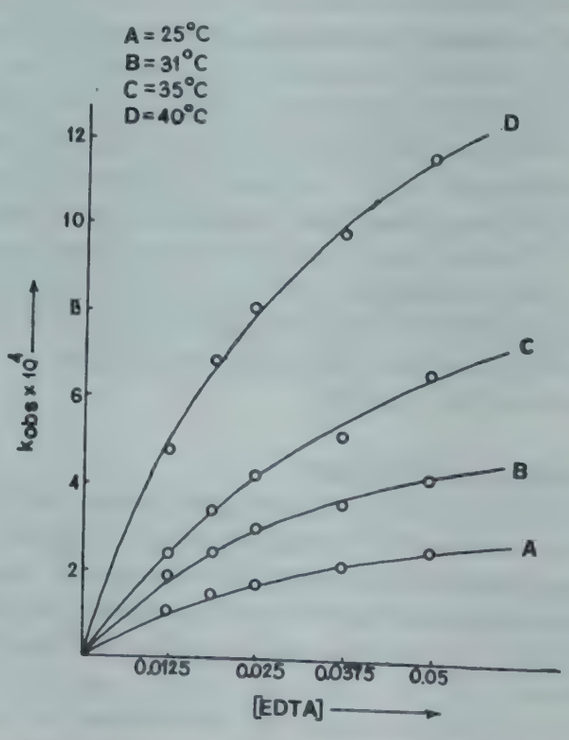

Fig. 2—Variaiton of k_{obs} with [H_2EDTA^{2-}] at different temperatures [complex-I] = 0.0025 mol dm^{-3}, pH = 5.0 (A) 25°C, (B) 31°C, (C) 35°C and (D) 40°C.

Table 1—Variation of Rate Constant with $[H_2EDTA^{2-}]$ at Different Temperatures

[pH = 5.0, and μ = 0.25 mol dm^{-3} ($NaClO_4$)]

$[H_2EDTA^{2-}]$ mol dm^{-3}	$k_{obs} \times 10^4$ (s^{-1})			
	25°	31°	35°	40°C
0.0125	1.07	1.89	2.95	4.78
0.019	1.46	2.44	3.42	6.80
0.025	1.72	3.10	4.13	8.05
0.0375	2.18	3.48	5.12	9.75
0.050	2.50	4.18	6.61	11.60

$$Cr(H_2O)_5(OH)^{2+} \ldots H_2EDTA^{2-}$$

I.P.

$$\xrightarrow[\text{slow}]{k_a} [Cr(H_2O)_4(OH)H_2EDTA] + H_2O$$

$$[Cr(H_2O)_4(OH)H_2EDTA] \xrightarrow[\text{steps and protonation of coordinated-OH}]{\text{series of fast}} [Cr(EDTA)(H_2O)]^{1-} + H_3O^+ + 3H_2O$$

Complex-II

Scheme 1

Based on Scheme 1 and considering the ion-pair equilibrium and rate-determining step, rate equation (2) for anation reaction can be obtained

$$\frac{d}{dt}[Cr(H_2O)(EDTA)^{1-}]$$

$$= \frac{k_a K_E [Cr(H_2O)_5(OH)^{2+}]_{total} [H_2EDTA^{2-}]}{1 + K_E [H_2EDTA]}$$

$$= k_{obs} [Cr(H_2O)_5(OH)^{2+}]_{total} \quad \ldots(2)$$

So,

$$k_{obs} = \frac{k_a K_E [H_2EDTA^{2-}]}{1 + K_E [H_2EDTA^{2-}]} \quad \ldots(3)$$

or

$$1/k_{obs} = 1/k_a + 1/k_a K_E [H_2EDTA^{2-}] \quad \ldots(4)$$

The plots of $1/k_{obs}$ versus $1/[H_2EDTA^{2-}]$ at different temperatures were linear with an intercept $= 1/k_a$ and slope $= 1/k_a K_E$. The k_a values thus obtained are presented in following discussion. K_E (ion-pair equilibrium constant) values are found to be almost constant (24-29) in the temperature range studied (25°-40°C).

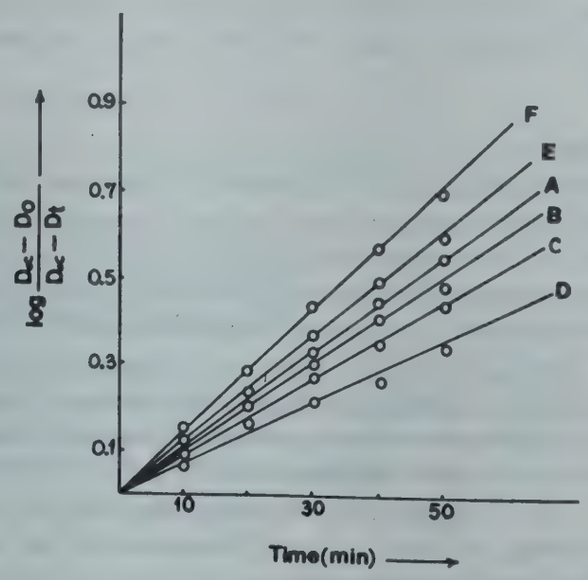

Fig. 3—Plot of log $(D_\alpha - D_0/D_\alpha - D_t)$ versus time at 35°C ([complex-I] = 0.0025 mol dm^{-3}, $[H_2EDTA]$ = 0.025 mol dm^{-3} pH = 5.0, [(A—D) perchlorate medium], [E.F nitrate medium]).

Effect of varying ionic strength on rate constant

At fixed [complex-I] = 0.0025 mol dm^{-3}, [ligand] = 0.025 mol dm^{-3}, pH = 5.0 and temperature = 35°C, the k_{obs} values were 4.1×10^{-4}, 3.9×10^{-4}, 3.5×10^{-4} and 2.7×10^{-4} s^{-1} for μ = 0.25, 0.75, 1.0 and 1.5 mol dm^{-3} respectively, i.e. increase in ionic strength (μ) by adding $NaClO_4$ decreases the rate of reaction. The results thus obtained can be supported by the theory of Bronsted, Bjerrum and Christiansen for the reaction between oppositely charged ions. But the rate of reaction increases with the increase of μ by adding $NaNO_3$ (Fig. 3). The k_{obs} values were 4.7×10^{-4} and 5.5×10^{-4} s^{-1} for μ = 0.25 and 0.5 mol dm^{-3}, respectively. This increase in rate in changing the anion from ClO_4^- to NO_3^- can be explained by the fact that nonsubstituting nitrate ion facilitates metal-water bond cleavage through specific attack on the coordinated water molecule. Consequently labilisation of water molecules catalyses the entry of the ligand and hence the increase in rate is observed in the presence of NO_3^-. This typical ionic strength effect has also been observed by different authors[14-16].

Effect of temperature on reaction rate

The reaction was studied at four different temperatures for different [ligand] to find out the effect of temperature on the rate constants for interchange process (k_a). The k_a values at 25°, 31°, 35° and 40°C are 4.00×10^{-4}, 7.10×10^{-4}, 11.11×10^{-4} and 18.86×10^{-4} s^{-1}, respectively. The values are considerably higher compared to the rates of isotopic water exchange process ($< 10.0 \times 10^{-5}$ s^{-1} at 25°C) of the same substrate complex[17]. Activation parameters were calculated from the linear Eyring plot of log k_a

versus 1/T and the values of $\Delta H^{\ddagger}$ and $\Delta S^{\ddagger}$ are found to be 74.8 kJ mol^{-1} and $-44.3\ JK^{-1}\ mol^{-1}$ respectively.

Mechanism

The dependence of reaction rate on the nature of ligand clearly indicates outer sphere association between the two oppositely charged reacting species. The ion-pair equilibrium constant values are high as is expected for the interaction between a bipositive cation $[Cr(H_2O)_5(OH)]^{2+}$ and a binegative anion $[H_2EDTA]^{2-}$. The high anation rate constant (compared to the rates of isotopic water exchange[17] and other substitution reactions by Cl^-, Br^-, SCN^-, NCS^- etc.)[18] suggest the associative character of the interchange process, i.e. bond formation by the incoming ligand plays a significant role in interchange step. The low values of $\Delta H^{\ddagger}$ (78.4 kJ mol^{-1}) also suggests ligand participation in the transition state. Further the activated complex formation through outer sphere association is stabilised by H-bonding between water molecule of the inner sphere complex and the negative end of the EDTA ion. This leads to the formation of a stable and compact activated state as is evidenced by the considerable negative $\Delta S^{\ddagger}$ value ($-44.33\ JK^{-1}\ mol^{-1}$). The above facts indicate that the reaction occurs through an associative interchange (I_a) process.

References

1 Hartley F R, *Aust J Chem*, **21** (1968) 2723.
2 Hamm R E, Johson R L, Perkins R H & Davis R E, *J Am chem Soc*, **80** (1958) 3369.
3 Banerjea D & Chatterjee C, *J inorg nucl Chem*, **31** (1969) 3845.
4 Banerjea D & Dutta Chaudhury S, *J inorg nucl Chem*, **30** (1968) 871.
5 Mandal J & De G S, *Indian J Chem*, **19A** (1980) 25.
6 Bhattacharya M & De G S, *Indian J Chem*, **20A** (1981) 780.
7 Hamm R E, *J Am chem Soc*, **75** (1953) 5670.
8 Yamamoto K & Ohishi K, *Bull chem soc Japan*, **49** (1976) 2433.
9 Olson M V, *Inorg Chem*, **12** (1973) 1416.
10 Kimura M & Shiral J, *J inorg nucl Chem*, **40** (1978) 1085.
11 Moore P & Basolo F, *Inorg Chem*, **4** (1965) 1671.
12 Martell A E & Smith R M, *Critical stability constants*, Vol. 1, 204.
13 Basolo F & Pearson R G, *Mechanism of inorganic reactions*, (Wiley Eastern, New Delhi) (1977) 32.
14 Brown P M & Harris G M, *Inorg Chem*, **3** (1964) 1334.
15 Van Eldik R, *Inorg chim Acta*, **44** (1980) L 197.
16 Ghosh M C & Banerjee P, *J chem Research(s)*, (1984) 271.
17 Thusius D, *Inorg Chem*, **10** (1971) 1106.
18 Espenson J H, *Inorg Chem*, **8** (1969) 1554.

Indian Journal of Chemistry
Vol. 27A, July 1988, pp. 581-583

Separation of Polar & Steric Effects in Oxidation of *ortho*-Substituted Benzyl Alcohols by Acid Permanganate

SANDHYA MATHUR, ANITA GUPTA & KALYAN K BANERJI*
Department of Chemistry, University of Jodhpur, Jodhpur 342 001

Received 1 *September* 1987; *revised and accepted* 9 *November* 1987

The kinetics of the oxidation of ten *ortho*-substituted benzyl alcohols by acid permanganate have been studied. The reaction is first order each with respect to [alcohol], [permanganate] and [H^+]. The correlation of the rates of oxidation with Charton's extended Hammett equation, involving inductive, resonance and steric parameters, is excellent. The polar reaction constants have negative values. The reaction is subject to steric acceleration by the *ortho*-substituents. The mechanistic aspects are discussed.

Correlation of rate and structure of *ortho*-substituted aromatic compounds is complicated because of the possible interaction of the substituent with the *ortho* site through polar effects, proximity effect, hydrogen bonding etc. Many attempts have been made to separate and analyse the contributions of various parameters to the *ortho*-effects[1-6]. Of these, Charton's treatment[4-6] is considered the best because of its wider applicability in explaining the nature of the *ortho*-effect.

Following our report[7] on the kinetics of the oxidation of *para*- and *meta*-substituted benzyl alcohols by permanganate ion in 1 : 4 (v/v) acetic acid-water in the presence of perchloric acid, we now report the kinetics of the oxidation of *ortho*-substituted benzyl alcohols. The rate data are correlated with various single parameter and multi parameter equations involving field, resonance and steric parameters.

Materials and Methods

o-Methylthio- and *o*-acetylamino-benzyl alcohols were prepared by the reported procedures[8,9]. The other alcohols were commercial products and were purified by recrystallization or distillation under reduced pressure.

Product analysis

To analyse the products, the alcohol (0.05 mol) and permanganate (0.005 mol), dissolved in 100 ml of 1 : 1 (v/v) acetic acid-water, in the presence of perchloric acid (0.2 mol dm^{-3}), were allowed to stand for nearly 12 hr and then treated overnight with an excess of 2,4-dinitrophenylhydrazine (2,4-DNP). The solid 2,4-DNP derivative obtained was recrystallized from ethanol and found to be identical (m.p. and mixture m.p.) with an authentic sample of the corresponding benzaldehyde 2,4-dinitrophenylhydrazone; yield 87-93%.

Kinetic measurements

The reactions were followed under pseudo-first order conditions, i.e. [alcohol] ≫ [permanganate]. The reactions were followed spectrophotometrically at 525 nm on a kinetic spectrophotometer (Photoelectric Instruments, Jodhpur). The solvent was 1 : 4 (v/v) acetic acid-water. Sodium fluoride (0.005 mol dm^{-3}) was added to each reaction mixture to suppress the reactions of Mn(III)/Mn(IV). The other experimental details have been described earlier[7].

Simple and multivariate linear regressions were carried out by the least squares method using a Workhorse II (HCL) microcomputer.

Results and Discussion

The oxidation of *ortho*-substituted benzyl alcohols by acid permanganate leads to the formation of the corresponding benzaldehydes. At the end of the reaction, the solutions were colourless indicating that MnO_4^- has been reduced to Mn^{2+}. The overall reaction may be represented by Eq (1).

$$5X\text{-}C_6H_4CH_2OH + 2MnO_4^- + 6H^+ \rightarrow 5X\text{-}C_6H_4CHO + 2Mn^{+2} + 8H_2O \quad \ldots (1)$$

The rate of oxidation of alcohols is first order each in [oxidant], [alcohol] and [H^+] (Table 1). Thus the experimental rate law has the form[7] (Eq 2).

$$-d[MnO_4^-]/dt = k[MnO_4^-][\text{alcohol}][H^+] \quad \ldots (2)$$

The oxidation of [α,α-$^2H_2$]benzyl alcohol is known to exhibit a primary kinetic isotope effect[7].

The values of specific rate constant, k, for the oxidation of alcohols were determined at different tem-

Table 1—Rate Constants for Oxidation of *o*-Bromobenzyl Alcohol by Acid Permanganate at 298 K

[Alcohol] (mol dm^{-3})	10^4 [MnO_4^-] (mol dm^{-3})	[H^+] (mol dm^{-3})	10^4 k_1 (s^{-1})
0.05	2.0	0.05	4.93
0.05	5.0	0.05	4.85
0.05	7.5	0.05	4.90
0.05	10.0	0.05	4.78
0.05	15.0	0.05	4.85
0.05	20.0	0.05	4.90
0.01	5.0	0.05	1.00
0.03	5.0	0.05	2.87
0.06	5.0	0.05	5.82
0.08	5.0	0.05	7.83
0.12	5.0	0.05	11.5
0.15	5.0	0.05	14.4
0.05	5.0	0.03*	3.00
0.05	5.0	0.08*	7.76
0.05	5.0	0.10*	9.62
0.05	5.0	0.15*	14.7
0.05	5.0	0.20*	19.7
0.05	5.0	0.25*	24.0
0.05	5.0	0.30*	29.3

*I = 0.50 mol dm^{-3}

peratures and the activation parameters were evaluated (Table 2). The average errors in the values of $\Delta H^{\ddagger}$, $\Delta S^{\ddagger}$ and $\Delta G^{\ddagger}$ (at 298 K) are $\pm$ 1.5 kJ mol^{-1}, $\pm$ 3 J mol^{-1} K^{-1}, and 1 kJ mol^{-1} respectively.

A linear isokinetic relationship between log k at 298 K and 318 K (r = 0.9912, slope = 0.9219) for the oxidation of benzyl alcohol and the ten *ortho*-substituted benzyl alcohols shows that all the compounds are oxidised by the same mechanism[10]. The value of isokinetic temperature is 1587 K. Current views do not attach much physical significance to isokinetic temperature[11]; however, an isokinetic relationship is a necessary condition for the validity of linear free energy relationships[12].

The rates at 298 K were analysed separately in terms of Taft's polar and steric parameter equations[1], but the results failed to yield signifiant correlations. Thus the observed reactivity of the *ortho*-substituted benzyl alcohols towards permanganate is not compatible with either the size of the substituents or their Taft's polar substituent parameters.

Since the single-substituent parameter equations did not yield satisfactory correlations, the rate data were analysed using Charton's method[5]. The rate constants were correlated with Eqs (3) and (4). In these equations σ_I, σ_R and V are inductive, resonance and steric substituent constants respectively and values used were those compiled by Aslam *et al*[6].

The result of the analysis of the rate data at 298 K in the terms of Eq. (3) is given in Eq. (5).

$$\log k_{ortho} = \alpha\sigma_I + \beta\sigma_R + h \quad \ldots (3)$$

$$\log k_{ortho} = \alpha\sigma_I + \beta\sigma_R + \phi V + h \quad \ldots (4)$$

$$\log k = -2.34\,\sigma_I - 1.51\,\sigma_R - 2.54 \quad \ldots (5)$$

$R = 0.8215$; $SD = 0.44$; $n = 11$.

In multivariate linear regression analysis using Eq. (3), the coefficient of correlation is poor and the standard deviation is high. The absence of significant correlation with Eq. (3) leads to the conclusion that electric effects alone are not sufficient to account for the *ortho*-substituent effect in this reaction.

The correlations with Eq. (4) were performed with the rate data obtained at 298 K, 303 K, 308 K, 313 K and 318 K and the results are presented in Table 3. The effect of *o*-NO_2 group is consistent with the orthogonal conformation.

The significance of the correlation was tested by means of an F-test[13]. The confidence level of the F-test was > 99.9%. The confidence leavels for the significance of the α, β, and ϕ terms were obtained by means of a Student's t-test[13]. The significance level of the t-test was > 99.9%, indicating the operation of significant field, resonance and steric effects. There was no significant correlation of the rates with σ_I and V, and with σ_R and V. The results show that this reaction belongs to the case 1 of the classification given by Charton[5].

The regression coefficients of σ_I and σ_R terms are negative indicating that electron-releasing groups accelerate the reaction and electron-withdrawing groups retard it, as was found for *meta*- and *para*-substituted benzyl alcohols[7]. The positive regression coefficient for the steric term indicates that the reaction is subject to steric acceleration by the *ortho* substituent.

The contribution of the resonance effect to the polar effect[5] was calculated using Eq. (6).

$$P_R = \frac{100 \times |\beta|}{|\alpha| \times |\beta|} \quad \ldots (6)$$

The contribution of the steric parameter[5] to the total effect of the substituent, P_s, was determined using Eq. (7).

$$P_s = \frac{|\phi| \times 100}{|\alpha| + |\beta| + |\phi|} \quad \ldots (7)$$

The values of P_R and P_s are also recorded in Table 3. The values of P_R indicate that the field effect is more

Table 2—Rate Constants and Activation Parameters for Oxidation of *ortho*-Substituted Benzyl Alcohols by Acid Permanganate

Substituent	$10^3 k$ ($dm^6 mol^{-2} s^{-1}$) at temp. (K)					$\Delta H^{\ddagger}$	$\Delta S^{\ddagger}$	$\Delta G^{\ddagger}$
	298	303	308	313	318	(kJ mol^{-1})	(J $mol^{-1} K^{-1}$)	(kJ mol^{-1})
H[a]	139	189	251	336	443	43.2	−116	77.3
NO_2	6.80	9.84	13.7	18.1	28.2	51.6	−113	85.2
Cl	138	170	262	320	438	43.7	−115	77.8
Br	194	268	330	517	600	43.2	−113	76.9
I	355	434	606	904	1080	43.9	−107	75.5
Me	2100	2570	3740	4200	5600	36.0	−118	71.1
OMe	815	1240	1700	2150	2600	41.7	−106	73.7
SMe	817	1050	1550	1830	2530	41.7	−107	73.4
NHCOMe	1200	1650	2210	2900	4010	44.2	−95	72.4
CF_3	167	245	305	400	540	42.0	−119	72.2
F	98.0	127	200	242	325	45.3	−112	78.6

[a]Data from ref. 7 except k at 298 K

Table 3—Temperature Dependence of Reaction Constants

Temp. (K)	α	β	ϕ	R	SD	P_R	P_s
298	−2.79	−1.82	1.54	0.9993	0.030	39.5	25.0
303	−2.75	−1.79	1.52	0.9991	0.034	39.4	25.1
308	−2.69	−1.83	1.43	0.9982	0.048	40.6	24.0
313	−2.63	−1.77	1.45	0.9984	0.042	40.2	24.8
318	−2.57	−1.72	1.37	0.9988	0.038	40.1	24.2

dominant than the resonance effect. The value of P_R is 50% for the *para* position by defination[4]. The observed value of P_R (40%) shows that the balance of the field and resonance effects is different for *ortho* and *para* positions, resonance effect being less pronounced in the former case. This may be due to the twisting away of the primary alcohol group from the plane of the benzene ring. The values of P_s show that the steric effect is considerable in the reaction. The magnitude of all the reaction constants decreases with increase in temperature indicating a decrease in the selectivity at higher temperature. The decrease is of similar order for all the three α, β, and ϕ reaction constants, reflected in almost constant values of P_R and P_s.

The reactivity of the *ortho*-substituted benzyl alcohols accords with the hydride-transfer mecahnism proposed earlier[7]. The large negative polar reaction constants support a transition state in which the positive charge is localized on the carbinol carbon atom. The steric acceleration of the rate by the *ortho*-substituents can be explained on the basis of high ground state energy level of the starting material. Since the crowding is relieved in the product aldehyde as well as in the transition state leading to it, the transition state energy of the crowded (*ortho*-substituted) and uncrowded alcohols, do not differ much and steric aceleration, therefore, results.

Acknowledgement

The financial support from the CSIR and UGC is gratefully acknowledged.

References

1 Taft R W, *Steric effects in organic chemistry* (John Wiley, New York), 1956, Ch. 13.
2 Pavelich W A & Taft R W, *J Am chem Soc*, **79** (1957) 5935.
3 Fujita T & Nishioka T, *Prog phys org Chem*, **13** (1976) 49.
4 Charton M, *Prog phys org Chem*, **8** (1971) 235.
5 Charton M, *J org Chem*, **40** (1975) 407.
6 Aslam M H, Burden A G, Chapman N B, Shorter J & Charton M, *J chem Soc Perkin Trans* 2, (1981) 500.
7 Banerji K K, *J chem Soc Perkin Trans* 2, (1973) 435.
8 Traynelis V J & Borgnaes D M, *J Org Chem*, **37** (1972) 3824.
9 Bhor J E, *Tetrahedron*, **20** (1964) 861.
10 Exner O, *Prog phys org Chem*, **10** (1973) 411.
11 Leffler J E, *J org Chem*, **31** (1966) 1535.
12 Leffler J E, *J org Chem*, **20** (1955) 1202.
13 Wine R L, *Statistics for scientists and engineers* (Prentice-Hall, New Delhi) 1966.

Indian Journal of Chemistry
Vol. 27A, July 1988, pp. 584-588

Kinetics & Mechanism of Oxidation of Hyponitrous Acid by Chloramine-T in Aqueous Perchloric Acid

M R GOYAL, R K MITTAL & Y K GUPTA*
Department of Chemistry, University of Rajasthan, Jaipur 302 004

Received 7 *July* 1987; *revised* 11 *September* 1987; *accepted* 16 *November* 1987

The redox reaction between hyponitrous acid and chloramine-T (CAT) occurs as follows:

$$4\,RNHCl + H_2N_2O_2 + 4\,H_2O \rightarrow 4\,RNH_2 + 2HNO_3 + 4HCl$$

The rate has second order dependence in [CAT] and complex dependence in $[H_2N_2O_2]$ and $[H^+]$. It has inverse dependence on *p*-toluenesulphonamide (PTS), one of the products. The mechanism and the rate law are found to be slightly different in the two acid ranges, viz. from 0.007-0.1 mol dm^{-3} and 0.75-2.0 mol dm^{-3} $HClO_4$. Dichloramine-T (DCT) is the reactive intermediate of CAT. Perhaps DCT exists in two forms, one of which is very reactive.

Essentially the title investigation was undertaken to know the solution chemistry of hyponitrous acid[1] about which not much is known. However, in addition to the information obtained in a recent investigation from our laboratory on its oxidation with Tl(III)[2] nothing tangible could be had. Nevertheless the title investigation has contributed to some extent to the already known chemistry of chloramine-T[3-5].

Most previous studies on CAT systems report the formation of a white turbidity at *p*H 3 to 4 and also in about 0.4 *M* aqueous acidic solutions. We found that the formation of white turbidity is a slow process and depends on [CAT] and [acid].

In redox systems of CAT, the initial reaction is fast which is followed by a slower one[6,7]. This has been attributed to the formation of dichloramine-T (DCT) formed by the slow disproportionation of CAT which reacts rapidly with reductant. Such a disproportionation reaction has been presently avoided by initiating the reaction by the addition of aqueous solution of CAT to the other reactants in the reaction mixture.

Materials and Methods

Sodium hyponitrite was prepared in 13% yield by electrolytic reduction[8] of nitrite; purity was from 70% to 96% as determined by precipitation method[9] and UV spectroscopy[10]. Solutions of $H_2N_2O_2$ were prepared whenever required in aqueous 0.5 *M* $HClO_4$ to which 0.1 mol % ethyl alchol was added to prevent its decomposition[10]. For all kinetic experiments the acid conditions were such (*p*H < 3) that the decomposition of $H_2N_2O_2$ was insignificant.

A stock solution of CAT (E Merck) was prepared by direct weighing and standardized iodometrically. Higuchi and coworkers[11] have mentioned the preparation of DCT without any details. We prepared it by adding an aqueous solution of $HClO_4$ to the CAT solution to render *p*H between 3 and 4. Oily droplets are first formed which settle to the bottom and white precipitate appears after sometime. Attempts to separate the oily liquid or extract it with a solvent, turned it into a white solid. The oxidizing capacity of these aqueous solutions or suspensions was reduced to half immediately if treated with a solution of $H_2N_2O_2$. The white solid reacted with $H_2N_2O_2$ only slowly. The white solid had all the properties of DCT as reported in literature.

All other chemicals were of AR (either E. Merck or BDH) grade. Doubly distilled conductivity water was used for preparing solutions.

The *p*H values were measured on a EC digital *p*H-meter and absorption spectra were recorded on a Perkin-Elmer spectrophotometer fitted with matched cells of 1 cm path lengths. Iodometric optical measurements were made on Spectronic 20.

Kinetic procedure

Reactions were initiated by the addition of CAT solution and the progress of reaction followed iodometrically. Initial rates[12] (v_0) were determined by the plane mirror method. Second order plots (1/[CAT] versus time) were also made with excess $H_2N_2O_2$. All the results were reproducible within ± 5%.

A few kinetic runs were also made with DCT to know the nature of this reaction and to ascertain whether it is a faster reaction than the disproportionation of CAT. The kinetics were followed by adding the aliquots from the reaction mixture to an acidified KI solution of known strength and measuring the ab-

Table 1—Variation of $[H_2N_2O_2]$ in Its Oxidation with CAT

$[CAT] = 2.0 \times 10^{-3}$ mol dm^{-3}, $[HClO_4] = 0.1$ mol dm^{-3}, temp. = 50°

$10^2 [H_2N_2O_2]$ (mol dm^{-3})	$10^7 (v_0)$ at [PTS] (mol dm^{-3})		
	0.0	0.01	0.015
0.01	6.3	—	—
0.02	8.5	—	—
0.05	10.2	6.85	5.75
0.08	11.5	7.8	7.0
0.10	11.5	8.3	7.8
0.20	—	10.2	9.6
0.30	11.5	11.5	11.0
0.40	11.5	11.5	11.3
0.50	11.5	11.5	11.5
0.75	11.5	—	—
1.0	11.5	11.5	11.5
1.5	11.5	11.5	—

Table 2—Variation of [*p*-Toluenesulphonamide] (PTS) in the Oxidation of $H_2N_2O_2$ with CAT

$[CAT] = 2.0 \times 10^{-3}$ mol dm^{-3}; $[HClO_4] = 0.1$ mol dm^{-3}; I = 0.5 mol dm^{-3}; temp. = 50°

10^2 [PTS] (mol dm^{-3})	$10^7 (v_0)$ (mol dm^{-3} s^{-1}) at $[H_2N_2O_2]$ (mol dm^{-3})			
	2.0×10^{-4}	1.0×10^{-3}	2.0×10^{-3}	5.0×10^{-3}
0	8.5	—	11	11.6
0.1	8.15	—	10.8	—
0.3	7.05	10	10.4	—
0.5	5.75	9.05	10.3	—
0.8	4.65	8.3	9.45	—
1.0	4.05	—	9.2	11.5
1.2	—	7.4	—	—
1.3	—	—	8.9	—
1.5	3.0	—	8.6	11.4

sorbance at 420 nm. The results were reproducible within ± 15%.

Disproportionation reaction of CAT

The rate of disproportionation of CAT was directly measured as follows. Preequilibrated aqueous solutions of CAT and $HClO_4$ were mixed, aliquots were taken out at predetermined time-intervals and added to an excess of $H_2N_2O_2$ solution followed immediately by the addition of aqueous solution of KI (0.1 mol dm^{-3}). The iodine liberated by the unconsumed CAT was titrated against standard thiosulphate.

Results

Stoichiometry

Various reaction mixtures containing excess CAT showed after 24 hr that four mol of CAT react with one mol of $H_2N_2O_2$ according to Eq. (1)

$$4RNHCl + H_2N_2O_2 + 4H_2O \rightarrow 4RNH_2 + 2HNO_2 + 4HCl \quad \ldots (1)$$

The same stoichiometry was found in 0.04 *M*, 0.1 *M* and 2.0 *M* $HClO_4$ solutions.

Hyponitrous acid dependence

$[H_2N_2O_2]$ was varied in the range of 1×10^{-4} to 1.5×10^{-2} mol dm^{-3} at two different [PTS]. The rate increases and becomes limiting with increase in $[H_2N_2O_2]$ (Table 1). These results seem to be in accord with the rate law,

$$-d[CAT]/dt = \frac{A[H_2N_2O_2]}{1 + B[H_2N_2O_2]}$$

CAT dependence

[CAT] was varied from $(0.5 \text{ to } 5.0) \times 10^{-3}$ mol dm^{-3} at 35°, 42.5° and 50°. A plot of initial rate (v_0) versus $[CAT]^2$ was linear passing through the origin. The pseudo-second order rate constants were found to be 0.3 dm^3 mol^{-1} s^{-1}, 0.18 dm^3 mol^{-1} s^{-1} and 0.12 dm^3 mol^{-1} s^{-1} at 50°, 42.5° and 35° respectively and at $[H^+] = 0.1$ mol dm^{-3}. If we divide the limiting rates of Table 1 by $[CAT]^2$, we get the pseudo-second order rate constant equal to 0.29 dm^3 mol^{-1} s^{-1} which is in good agreement with the value of 0.3 dm^3 mol^{-1} s^{-1} obtained in $H_2N_2O_2$ dependence.

Variation of p-toluenesulphonamide concentration

The rate decreases with increase in [PTS] (Table 2) and a plot of $(\text{rate})^{-1}$ versus [PTS] is linear with non-zero intercept. This dependence therefore is in accordance with the rate law

$$-d[CAT]\,dt = \frac{A}{(1 + B[PTS])}$$

Hydrogen ion dependence

This effect was studied by varying the concentration of $HClO_4$ first in the range of 0.007 mol dm^{-3} to 0.3 mol dm^{-3} and then extending it in a different set of experiments to 2.0 mol dm^{-3}. Table 3 gives the results of $[H^+]$ dependence at three different $[H_2N_2O_2]$. Several simple plots between suitable functions of rate and $[H^+]$ were tried to obtain a linear plot, but with no success. Thus $[H^+]$ dependence seems to be complex.

The rate increases at $[H^+] > 0.3$ mol dm^{-3} and hence a complete kinetic study of the reaction was made in 1.5 mol dm^{-3} $HClO_4$. The various rate dependences appear to be similar as found in the lower range of $[HClO_4]$, except that the rate has positive first order dependence in $[H^+]$ in this range (Table 4).

Table 3—Variation of $[HClO_4]$ in the Oxidation of $H_2N_2O_2$ with CAT

$[CAT] = 2.0 \times 10^{-3}$ mol dm^{-3}; $I = 0.5$ mol dm^{-3}; temp. = 50°

$[H^+]$ (mol dm^{-3})	10^7 (v_0) (mol dm^{-3} s^{-1}) at $[H_2N_2O_2]$ (mol dm^{-3})		
	5.0×10^{-4}	1.0×10^{-3}	1×10^{-2} mol dm^{-3}
0.3	6.5	8.0	8.3
0.2	7.0	9.2	9.6
0.1	10.5	12	12
0.075	—	14.5	—
0.05	20	24	24
0.03	38	48	47
0.01	90	115	109
0.007[a]	—	170	—

[a]In this reaction precision was not better than ± 15%.

Table 4—Initial Rate (v_0) in High $[H^+]$ of Reaction between CAT and $H_2N_2O_2$ at Different $[H^+]$ and [PTS]

$[CAT] = 2.0 \times 10^{-3}$ mol dm^{-3}; $[H_2N_2O_2] = 1.0 \times 10^{-3}$ mol dm^{-3}; $I = 2.0$ mol dm^{-3}; temp. = 50°C

$[HClO_4]$ (mol dm^{-3})	[PTS] (mol dm^{-3})	10^7 (v_0) (mol dm^{-3} s^{-1})
0.5	0.0	9.8
0.75	0.0	12.5
1.0	0.0	15
1.25	0.0	18.5
1.50	0.0	22
1.75	0.0	25
2.0	0.0	29.5
1.5	1.0	17.5
1.5	2.0	14.5
1.5	3.0	12.5
1.5	5.0	9.5
1.5	8.0	6.5

Effect of varying ionic strength

Variation in ionic strength in the range of 0.1 to 2.0 mol dm^{-3} ($NaNO_3$) had no effect on the rate.

Reaction of dichloramine-T with $H_2N_2O_2$

The results of this study are given in Table 5. The rate shows first order dependence each in [DCT] and $[H_2N_2O_2]$, and the second order rate constant at 0.1 mol dm^{-3} $HClO_4$ is 0.63 dm^3 mol^{-1} s^{-1} at 50°. The rate decreases with increase in $[H^+]$. A plot of the reciprocal of k_1 (pseudo-first order rate constant) versus $[H^+]$ is linear with a non-zero intercept. These results indicate a rate law,

$$-d[DCT]/dt = \frac{A[DCT][H_2N_2O_2]}{1 + B[H^+]}$$

The rate decreases with increase in [PTS], but no attempts have been made to obtain a quantitative relationship since solid DCT is not the true intermediate.

Discussion

The present system is somewhat unique in the sense that it has unusual rate dependences on [CAT] and $[H_2N_2O_2]$. [PTS] has inverse rate dependence which is controlled by the ratio $[H_2N_2O_2]$/[PTS]. $[H^+]$ has a complex rate dependence and it is this dependence which enables us to know more of solution chemistry of CAT.

Hyponitrous acid is a weak acid[13,14] with pK_1 and pK_2 of 7 and 11 respectively and hence it should exist as $H_2N_2O_2$ in the acid solutions employed in the present investigation. Thus $[H^+]$ dependence cannot be correlated with $H_2N_2O_2$.

Chloramine-T (RNHCl taken as RNNaCl) has a dissociation constant[3] of 2.8×10^{-5}. In the acid range employed, the predominant species of CAT would be RNHCl. This, however, can get protonated further to RNH_2Cl^+ as indicated by Rao and coworkers[15] but the value of protonation constant of 100 assumed by them, is not supported by our results. According to this value, RNH_2Cl^+ would be the predominent species in 0.1 mol dm^{-3} $HClO_4$. If this be so, the question arises what is the species in 1.0 mol dm^{-3} $HClO_4$ which has different reactivity pattern. It cannot be RNH_3Cl^{2+}. Thus, we believe that protonation constant of RNHCl is not large. The spectrophotometric work failed to yield any information on this point. In the acid range employed, three species, $RNCl^-$, RNHCl and RNH_2Cl^+ are likely to be significantly present via the equilibria (2) and (3).

$$RNHCl \overset{K_d}{\rightleftharpoons} RNCl^- + H^+ \quad \ldots (2)$$

$$RNHCl + H^+ \overset{K_p}{\rightleftharpoons} RNH_2Cl^+ \quad \ldots (3)$$

The order of two in [CAT], limiting rates at large $[H_2N_2O_2]$, inhibiting effect of [PTS], and inverse $[H^+]$ dependence of the rate in its lower range lead to the mechanism represented by Eqs (4-6).

$$RNHCl + RNCl^- \underset{k_2}{\overset{k_1}{\rightleftharpoons}} RNCl_2 + RNH^- \quad \ldots (4)$$

$$RNCl_2 + H_2N_2O_2 \overset{k_3}{\rightarrow} \text{Products} \quad \ldots (5)$$

$$RNH^- + H^+ \overset{K_A}{\rightleftharpoons} RNH_2 \quad \ldots (6)$$

Step (4) is a disproportionation reaction of CAT. Although in literature[4] the disproportionation is represented by Eq. (7),

$$2\,RNHCl \rightleftharpoons RNCl_2 + RNH_2 \quad \ldots (7)$$

Table 5—Pseudo-first Order Rate Constants (k) and Second Order Rate Constants (k_3) in Oxidation of $H_2N_2O_2$ by DCT ($I = 0.5$ mol dm^{-3}; temp. = 50°C)

10^4 [DCT] (mol dm^{-3})	10^4 [$H_2N_2O_2$] (mol dm^{-3})	[H^+] (mol dm^{-3})	10^3 k (s^{-1})	$k/[H_2N_2O_2] = k_3$
0.48	20	0.1	1.27	0.63
0.60	20	0.1	1.27	0.63
0.72	20	0.1	1.32	0.66
0.84	20	0.1	1.28	0.64
2.0	8	0.1	0.49	0.61
2.0	12	0.1	0.76	0.63
2.0	16	0.1	0.96	0.60
2.0	20	0.1	1.2	0.60
0.5	5.0	0.3	0.24	0.48
0.5	5.0	0.2	0.27	0.54
0.5	5.0	0.1	0.32	0.64
0.5	5.0	0.05	0.39	0.78
6.6	20	0.1	1.2	—
6.6	20	0.1	1.05[a]	—
6.6	20	0.1	0.69[b]	—
6.6	20	0.1	0.34[c]	—

[a]In the presence of 1.0×10^{-5} mol dm^{-3} PTS
[b]In the presence of 1.0×10^{-4} mol dm^{-3} PTS
[c]In the presence of 1.0×10^{-3} mol dm^{-3} PTS

a reaction between RNHCl and $RNCl^-$ seems to be more probable than that between two RNHCl, since $RNCl^-$ can accept a positive chlorine donated by RNHCl. Bishop and Jennings[16] have calculated the concentrations of various species of CAT at different *p*H values. [$RNCl^-$] increases about 7 times from *p*H 1 to 2. The rate in our system also increases about 8 times in the range of [H^+] from 0.1 to 0.01 mol dm^{-3}. Variation in [RNHCl] is not more than 15%. This shows that it is the $RNCl^-$ species in the lower acid range which controls the rate. The above mechanism leads to the rate law (8).

$$\frac{-d[CAT]}{dt} = \left(\frac{k_1 k_3 K_A [CAT]^2 [H^+][H_2N_2O_2]}{k_2[PTS] + k_3 K_A [H^+][H_2N_2O_2]} \right) \frac{K_d}{[H^+]} \quad \ldots (8)$$

Species RNH^- being an amide ion, would be largely protonated and RNH_2 would be significantly present since protonation constant of RNH^- is reported to be 2×10^{10} (ref. 17). At large [$H_2N_2O_2$] when the rate becomes limiting, or in the initial stages of the reaction when no PTS is present, rate law (8) reduces to (9).

$$-\frac{d[CAT]}{dt} = k_1 K_d [CAT]^2/[H^+] \quad \ldots (9)$$

A plot of rate versus $[H^+]^{-1}$ in the lower [H^+] range is linear passing through the origin. The value of $k_1 K_d$ from the slope is (0.03 ± 0.001) s^{-1} at 50°. A plot of (rate $[H^+]^{-1}$) versus ([PTS]/[$H_2N_2O_2$] [H^+]) (Fig. 1), from Eq. (8) is linear with a non-zero intercept from which $k_1 K_d$ is found to be (0.028 ± 0.001) s^{-1}. The two values of $k_1 K_d$ are almost similar. This value from CAT dependence was found to be 0.029 $(0.29 \times [H^+])$ s^{-1} at 0.1 mol dm^{-3} $HClO_4$ and 0.028 $(0.69 \times [H^+])$ at 0.04 mol dm^{-3} $HClO_4$. These values at the three temperatures, 50°, 42.5° and 35° when extrapolated in a plot of log $k_1 K_d$ versus 1/T, yield a value of 0.005 s^{-1} at 25° and *p*H = 1. This is quite comparable to the value of 0.0042 s^{-1} found by Higuchi and coworkers[17] in the direct disproportionation reaction at the same temperature and *p*H. This comparison is valid since [H^+] dependence in both the reactions is of the same type. Hence disproportionation step of CAT in the present redox system is the bottleneck of the reaction.

The mechanism at higher [acid] range is essentially the same (Eqs 4-6), but the species in the disproportionation reaction is slightly different. It is given below:

$$RNHCl + RNH_2Cl^+ \underset{k_2}{\overset{k_1}{\rightleftharpoons}} RNCl_2 + RNH_3^+ \quad \ldots (10)$$

$$RNCl_2 + H_2N_2O_2 \xrightarrow{k_3} \text{Products} \quad \ldots (5)$$

$$RNH_2 + H^+ \overset{K_P}{\rightleftharpoons} RNH_3^+ \quad \ldots (11)$$

The reaction between RNHCl and RNH_2Cl^+

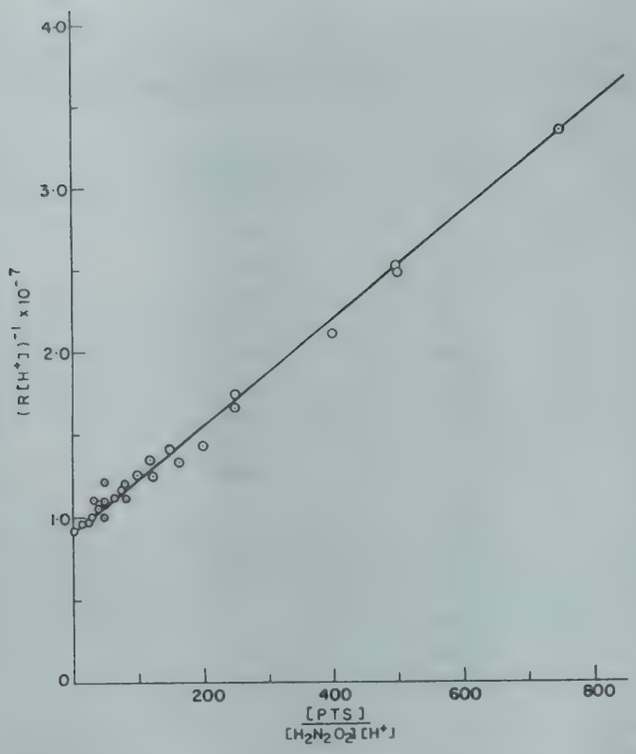

Fig. 1—A plot of $(R(H^+])^{-1}$ versus $[PTS]/[H_2N_2O_2]\ [H^+]$ ($[CAT] = 2.0 \times 10^{-3}$ mol dm^{-3}; $I = 0.5$ mol dm^{-3}; temp. = 50°C)

would be more favourable than that between two RNHCl for the same reason as given earlier. The above mechanism would lead to the rate law (12).

$$-\frac{d[CAT]}{dt} = \frac{k_1' k_3 K_P [CAT]^2 [H^+][H_2N_2O_2]}{k_2' K_P' [PTS][H^+] + k_3 [H_2N_2O_2]} \quad \ldots (12)$$

At high $[H_2N_2O_2]$, the rate law (12) reduces top (13).

$$-\frac{d[CAT]}{dt} = k_1' K_P [CAT]^2 [H^+] . \quad \ldots (13)$$

The value of $k_1' K_P$ from CAT dependence is (0.36 ± 0.02) dm^6 mol^{-2} s^{-1} at 50°. A limiting rate of 2.4×10^{-6} mol dm^{-3} s^{-1} at large $[H_2N_2O_2]$ yields a value of 0.40 dm^6 mol^{-2} s^{-1} for $k_1' K_P$. A plot of rate versus $[H^+]$ gives a value of (0.36 ± 0.02) dm^6 mol^{-2} s^{-1}. From Eq. (12), a plot of $(\text{rate}/[H^+])^{-1}$ versus $([PTS][H^+]/[H_2N_2O_2])$ is linear with an intercept giving $k_1' K_P$ equal to (0.39 ± 0.03) dm^6 mol^{-2} s^{-1} at 50°. Since K_d is 2.8×10^{-5} and K_P is not that small (about < 0.01 mol dm^{-3}), k_1 is much larger than k_1.

It would be difficult to verify the combined rate laws (8) and (12). However, the reduced forms of the two rate laws (9) and (13) can be combined to yield the rate law (14),

$$-d[CAT]/dt = \frac{k_1 K_d [CAT]^2}{[H^+]} + k_1' K_P [CAT]^2 [H^+] \quad \ldots (14)$$

For verification of rate law (14) a plot of $(\text{rate}[H^+])$ versus $[H^+]^2$ should be linear with non-zero intercept with the values of 0.025 s^{-1} and 0.36 dm^6 mol^{-2} s^{-1} for $k_1 K_d$ and $k_1' K_P$ respectively.

The two reactions, viz. reaction of DCT with $H_2N_2O_2$, and disproportionation of CAT, give only qualitative support to the main reaction.

References

1 Hughes M N, *Quart Rev*, **22** (1968) 1.
2 Goyal M R, Mittal R K & Gupta Y K, *Indian J Chem*, IC 5423.
3 Morris J C, Salazar J A & Wineman W A, *J Am chem Soc*, **70** (1948) 2036.
4 Soper F G, *J chem Soc*, **124** (1924) 1899.
5 Buchhloz J R & Powell R E, *J Am chem Soc*, **85** (1963) 509.
6 Agarwal M C & Mushran S P, *J phys Chem*, **75** (1971) 838.
7 Jha S, Sharma P D & Gupta Y K, *Inorg Chem*, **22** (1983) 1393.
8 Polydoropoulos C N, *Chem Ind*, (1963) 1686.
9 Polydoropoulos C N & Pipinis M, *Chim Chronica*, **28A** (1963) 107.
10 Polydoropoulos C N & Voliotes S D, *Anal Chim Acta*, **40** (1968) 170.
11 Higuchi T & Hussain A, *J chem Soc (B)*, (1967) 549.
12 Latshaw M, *J Am chem Soc*, **47** (1925) 793.
13 Polydoropoulos C N & Pipinis M, *Z physik Chem*, **40** (1964) 322.
14 Hughes M N & Stedman G, *J chem Soc*, (1963) 1239.
15 Narayanan S S & Rao V R S, *Radiochim Acta*, (1963) 211.
16 Bishop E & Jennings V J, *Talanta*, (1967) 549.
17 Higuchi T, Ikeda K & Hussain A, *J chem Soc (B)*, (1967) 546.

Indian Journal of Chemistry
Vol. 27A, July 1988, pp. 589-592

Kinetics & Mechanism of Oxidation of α-Amino Acids by Bromamine-T in Sulphuric Acid Medium

B YAMUNA, H M K NAIDU & D S MAHADEVAPPA*

Department of Post-graduate Studies & Research in Chemistry, University of Mysore, Manasagangothri, Mysore 570 006

Received 1 *December* 1986; *revised and accepted* 9 *November* 1987

Kinetics of oxidation of glycine, serine, alanine and leucine by bromamine-T (BAT) have been studied in sulphuric acid (0.05 to 0.15 mol dm^{-3}) at 35°C. The reaction shows a first order dependence each in $[oxidant]_0$, $[amino\ acid]_0$ and inverse first order in $[H^+]$. Added sulphate ions increase the rate while bisulphate ions retard the reaction. The rate of oxidation increases in the order: leucine > alanine > serine > glycine. The mechanism assumes the interaction of zwitterion of substrate with monobromamine-T in the rate-limiting step.

A survey of literature shows that only a few reactions of bioorganic compounds with organic haloamines have been studied from a kinetic point of view[1]. As a part of our broad project on the oxidation studies of amino acids in acid medium[2], we report the oxidation of leucine, alanine, serine and glycine by bromamine-T (BAT) in H_2SO_4 at 35°C.

Materials and Methods

Bromamine-T was prepared by literature method[3] and its aqueous solution was standardized by iodometry. Chromatographically pure α-amino acids, viz. leucine, alanine, serine and glycine were further assayed by the acetous-perchloric acid method[4]. All other reagents were of AR grade. Triply distilled water was used for preparing the solutions.

Requisite amounts of the amino acid, H_2SO_4, sodium perchlorate (to maintain ionic strength constant) and water (to keep total volume constant for all the runs) were taken in a pyrex tube and thermostated at 35°C. A measured amount of BAT also at the same temperature was rapidly added to the reaction mixture and the progress of the reaction was followed by iodometric estimation of unconsumed BAT present in a measured aliquot of the reaction mixture withdrawn at different time intervals.

In the stoichiometric runs reaction mixtures containing known excess of BAT over amino acids were kept at room temperature (27° ± 2°C) in the presence of 0.05-0.2 *M* H_2SO_4 for 24 hr. Estimation of unreacted BAT showed that the reaction followed the stoichiometries represented by Eqs (1) and (2):

$$R'CH(NH_2)COOH + 2\ RNBr^-Na^+ \rightarrow R'CN + 2\ RNH_2 + CO_2 + 2\ NaBr \quad \ldots (1)$$

$$R''CH(NH_2)COOH + 3\ RNBr^-Na^+ \rightarrow 3\ RNH_2 + R''CNO + CO_2 + 3\ NaBr \quad \ldots (2)$$

In Eqs (1) and (2) R′ = H for glycine, CH_2OH for serine and $(CH_3)_2CHCH_2$ for leucine; R″ = CH_3 for alanine; and R = *p*-$CH_3C_6H_4SO_2$.

The presence of *p*-toluenesulphonamide (RNH_2) among the reaction products was detected by paper chromatography. The nitriles formed (Eq. 1) were identified by their colour reaction with hydroxyl amine and ferric chloride[5]. The cyanate among the reaction products (Eq. 2) was detected by Werner's test[6].

Results

At fixed $[H_2SO_4]$ with [substrate] in excess, plots of log [BAT] versus time are linear indicating a first order dependence in $[BAT]_0$. The pseudo-first order rate constant (k') increases with increase in $[amino\ acid]_0$ and plots of log k' versus log $[amino\ acid]_0$ are linear with unit slopes, confirming the first order dependence in $[substrate]_0$ (Table 1).

The rate decreases with increase in gross $[H_2SO_4]$. The plots of log k' versus log $[H_2SO_4]$ are linear with negative fractional slopes (Table 2), but addition of sulphate ion in the form of Na_2SO_4 (0.1-0.2 mol dm^{-3}) at constant $[H^+] = 0.1$ mol dm^{-3} increases the rate. Plots of log k' versus log $[SO_4^{2-}]$ are linear with fractional slopes (~0.4). To study the effect of varying $[H^+]$ on the rate, sodium sulphate was added to keep $[SO_4^{2-}]$ at a high value (0.2 mol dm^{-3}) while varying $[H_2SO_4]$. The rate decreases and a plot of log k' versus log $[H^+]$ is linear with a slope of −1 indicating an inverse first order dependence of rate in $[H^+]$ in each case (Table 2).

Variation of ionic strength of the reaction mixture by adding sodium perchlorate or addition of

Table 1—Effect of Varying [Reactant] on Rate of Oxidation of Amino Acids at 35°C

$[H^+]$ & $[SO_4^{2-}] = 10.0 \times 10^{-2}$ mol dm^{-3} $\mu = 0.5$ mol dm^{-3}

$10^3[BAT]_0$ (mol dm^{-3})	$10^2[AA]$ (mol dm^{-3})	$10^4\,k'$(s^{-1})			
		Gly	Ser	Ala	Leu
2.0	3.0	1.44	4.10	4.61	5.15
3.0	3.0	1.44	4.09	4.61	5.12
4.0	3.0	1.44	4.09	4.60	5.12
5.0	3.0	1.42	4.09	4.61	5.10
3.0	2.0	—	2.69	3.07	3.45
3.0	2.5	1.20	3.33	3.84	4.22
3.0	3.0	1.44	4.09	4.61	5.12
3.0	4.0	1.87	5.18	4.89	6.65
3.0	5.0	2.35	6.65	7.68	8.52
3.0	8.0	—	—	11.99	—
3.0[a]	3.0	1.44	4.10	4.61	5.12
3.0[b]	3.0	1.42	4.09	4.60	5.10

(a) At ionic strength 1.0 mol dm^{-3}; and (b) in presence of excess PTS.

Table 2—Effect of Varying $[H_2SO_4]$ and $[H^+]$ on Rate of Oxidation of Amino Acids at 35°C

$[BAT] = 3.0 \times 10^{-3}$ mol dm^{-3}; $[AA] = 3.0 \times 10^{-2}$ mol dm^{-3}; $[SO_4^{2-}] = 0.2$ mol dm^{-3}; $\mu = 0.5$ mol dm^{-3}

$[H_2SO_4]_0 10^2$ (mol dm^{-3})*	$k' \times 10^4$ (s^{-1})†			
	Gly	Ser	Ala	Leu
5.0 (8.0)	2.21(2.34)	6.21(6.78)	7.23(7.23)	7.91(7.68)
7.5(10.0)	1.73(1.92)	4.80(5.37)	5.59(5.89)	6.05(6.39)
10.0(13.0)	1.44(1.44)	4.10(4.22)	4.61(4.61)	5.12(4.80)
12.5(15.0)	1.25(1.25)	3.58(3.65)	4.10(3.95)	4.35(4.10)
15.0(18.0)	1.14(1.04)	3.25(3.13)	3.62(3.33)	3.95(3.45)

*Values in parentheses to $[H^+] \times 10^2$ mol dm^{-3}.
†Values at the corresponding $[H^+]$

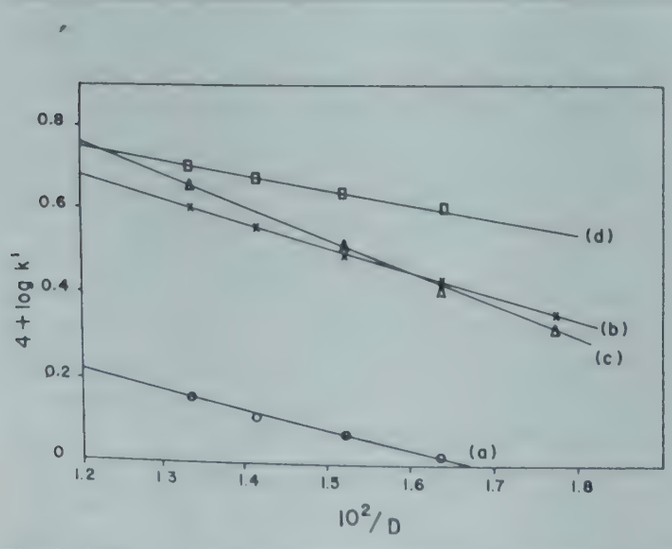

Fig. 1—Effect of varying dielectric constant of medium on the rate of oxidation of (a) glycine, (b) serine, (c) alanine and (d) leucine ([Amino acid] = 0.03 mol dm^{-3}; $[BAT]_0 = 0.003$ mol dm^{-3}; $[H_2SO_4] = 0.1$ mol dm^{-3}; $\mu = 0.5$ mol dm^{-3} mol dm^{-3}; temp. = 35°C)

Table 3—Thermodynamic Parameters for Oxidation of Amino Acids by BAT at 35°C

Parameters	Gly	Ser	Ala	Leu
E_a (kJ mol^{-1})	55.6	49.9	44.1	40.2
log A	6.1	5.6	4.7	4.04
$\Delta S^{\ddagger}$ (JK^{-1} mol^{-})	−132.3	−142.0	−159.7	−171.2
$\Delta H^{\ddagger}$ (kJ mol^{-1})	53.0	47.3	41.5	37.7
$\Delta G^{\ddagger}$ (kJ mol^{-1})	93.5	90.8	90.5	90.3

the reaction product RNH_2 has no significant effect on the rate.

The reaction rate decreases with increase in [methanol] in the reaction medium and the plots of log k' versus 1/D (where D is the dielectric constant of medium) are linear with negative slopes (Fig. 1). Blank experiments showed that methanol is not oxidized by BAT under the experimental conditions.

The reaction has been studied at different temperatures in the range 29 to 45°C and kinetic and activation parameters have been calculated (Table 3).

The solvent isotope studies in D_2O medium with gly as the probe show a decrease in rate and k'_{H_2O}/k'_{D_2O} is found to be 1.3.

Discussion

The dissociation of an amino acid depends upon the *p*H of the medium. In strongly acid medium, the reducing species may be either the cation (SH^+) or the zwitterion (S°). The inverse dependence on $[H^+]$ clearly points to the fact that the zwitterion (S°) is the reactive species in these investigations.

Bromamine-T, which is analogous to CAT is expected to have similar equilibria[7] in aqueous solutions. The possible oxidizing species in acidified BAT solutions are RNHBr, $RNBr_2$ and HOBr. If $RNBr_2$ were to be the reactive species, then the rate law predicts a second order dependence of rate on $[BAT]_0$, which is contrary to experimental observations. If HOBr is the active species, a first order retardation of rate by added *p*-toluenesulphonamide is expected. However, no such effect is noticed. It is therefore likely that the conjugate acid, RNHBr is the active oxidant species. Further, variation of the ionic strength of medium has no effect on the rate, indicating that neutral species are involved in the rate-determining step. Keeping these facts in view, Scheme 1 is proposed to account for the observed kinetics:

$$SH^+ \overset{K_1}{\rightleftharpoons} S^\circ + H^+ \quad \ldots\ldots\ldots \quad \text{(i) fast}$$

$$S^{\circ} + RNHBr \xrightarrow{k_2} X \quad \ldots\ldots\ldots \quad \text{(ii) slow and r.d.s}$$

$$X + n\,RNHBr \xrightarrow{k_3} \text{Products} \quad \ldots\ldots\ldots \quad \text{(iii) fast}$$

where $n = 1$ for gly, ser and leu and $n = 2$ for ala.

Scheme 1

Scheme 1 leads to rate law (3),

$$-\frac{d[BAT]}{dt} = \frac{K_1 k_2 [SH^+][RNHBr]}{[H^+]} \quad \ldots (3)$$

which is in agreement with experimental results. The proposed mechanism is supported by the moderate values of E_a and fairly high negative $\Delta S^{\ddagger}$ values indicate that the transition state is highly solvated and the near constancy of these values shows that the amino acids under investigation undergo oxidation by BAT by a similar mechanism. The linear plot of log k' versus 1/D supports the involvement of two dipoles in the rate-limiting step. Solvent isotope studies in D_2O medium show retardation of rate. It is well known that D_3O^+ is a stronger acid[8] than the hydronium ion and hence this observation supports the proposed mechanism.

The mechanism of oxidation envisages an electrophilic attack at the carboxyl group of substrate by Br^+, resulting in the formation of a N-bromo intermediate. Subsequent reactions are fast and decarboxylation and elimination of H^+ and Br^- are likely to be concerted. Further oxidation of nitrile by a third molecule of oxidant produces the cyanate.

The catalytic influence of sulphate ion at constant $[H^+]$, can be rationalised by Scheme 2:

$$RNHBr + SO_4^{2-} \underset{}{\overset{K_3}{\rightleftharpoons}} \underset{(X')}{RNHBr \ldots\ldots SO_4^{2-}} \ldots\ldots \text{(i) fast}$$

$$X' + S^{\circ} \xrightarrow{k_4} X'' \quad \ldots\ldots\ldots \quad \text{(ii) slow and r.l.s.}$$

$$X'' + n\,RNHBr \xrightarrow{k_5} \text{Products} \quad \ldots\ldots\ldots \quad \text{(iii) fast}$$

Scheme 2

Scheme (2) leads to rate law (4), which at constant $[H^+]$ can be transformed into Eq. (5):

$$\text{Rate} = \frac{k_4 K_3 [BAT]_t [SO_4^{2-}][SH^+]_0}{[H^+]\{1 + K_3[SO_4^{2-}]\}} \quad \ldots (4)$$

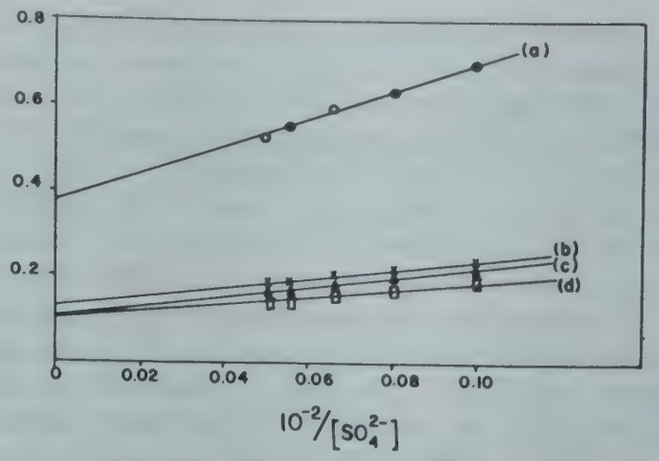

Fig. 2—Double reciprocal plots of k' versus $[SO_4^{2-}]$ for oxidation of (a) glycine, (b) serine, (c) alanine and (d) leucine by BAT ([Amino acid] = 0.03 mol dm^{-3}; [BAT] = 0.003 mol dm^{-3}; $[H^+]$ = 0.1 mol dm^{-3}; μ = 0.5 mol dm^{-3}; temp. = 35°C)

Table 4—Values of Formation Constant (K_3) and Decomposition Constant (k_4) of BAT-Sulphate Complex Formed during Oxidation of Amino Acids in H_2SO_4 Medium

Amino acids	K_3 ($dm^3\ mol^{-1}$)	$k_4 \times 10^4$ (sec^{-1})
Glycine	11.97	2.5
Serine	11.15	7.7
Alanine	9.43	9.1
Leucine	11.11	9.4

$$\frac{1}{k'} = \frac{1}{k_4 k_3 [SO_4^{2-}][SH^+]_0} + \frac{1}{k_4 [SH^+]_0} \quad \ldots (5)$$

From the double reciprocal plots (Fig. 2) of k' versus $[SO_4^{2-}]$ at constant $[H^+]$ and $[\text{amino acid}]_0$ values of formation constant (K_3) and the rate constant (k_4) have been calculated (Table 4). The decrease in rate by the addition of bisulphate ion is due to a mass law influence on the dissociation of H_2SO_4, as has been observed by Hardwick and Robertson[9] during their oxidation studies involving Ce(IV) ion in H_2SO_4.

Attempts to relate rates with the Taft substituent parameters σ^* and E_s through single parameter correlations[10] gave the following regression equations:

$$(\log k' - E_s) = -3.3\,\sigma^* + 0.6;\ (r = 0.9957) \quad \ldots (6)$$

$$\log k' = -0.42\,\sigma^* + 0.6;\ (r = 0.6000) \quad \ldots (7)$$

$$\log k' = -0.4\,E_s + 0.6;\ (r = 0.9414) \quad \ldots (8)$$

Although the correlation of k' with the individual parameter is poor, Eq. (6) shows that both steric and electronic effects play a role in determining the rates. The negative ρ-value indicates an electron deficient transition state, and electron releasing groups increase the rate.

The rates of oxidation of amino acids follow the sequence: leu > ala > ser > gly. The activation energy is the highest for the slowest reaction and vice versa, indicating that the reaction is enthalpy-controlled. The isokinetic temperature (β) is found to be 331K. The relationship is found to be genuine by the Exner criterion[11] by plotting log $k'_{40°}$ versus log $k'_{29°}$ from which β comes out to be 338K.

A comparison of oxidation of amino acids by chloramine-T[12] and BAT shows that the rates are higher with BAT. This may be attributed to the difference in electrophilicity of halonium cations Cl^+ and Br^+ which are generally the reactive species and/or to the moderate difference in van der waals radü of Cl and Br. A similar observation is made by Ruff and Kucsman[13] in their studies on the oxidation of dialkyl sulphides by BAT.

Acknowledgement

One of us (BY) gratefully acknowledges the award of a senior research fellowship by the UGC, New Delhi.

References

1 Kumar A, Bose A K & Mushran S P, *Mh Chem*, **106** (1975) 13; *J Indian chem Soc*, **53** (1976) 755.

2 (a) Gowda N M M & Mahadevappa D S, *Mh Chem*, **110** (1979) 157.

(b) Katgeri S N, Mahadevappa D S & Naidu H M K, *Bull Soc Chem*, Fr, **I-381** (1979) 9-10.

(c) Mahadevappa D S, Ahmed M S & Gowda N M M, *Indian J Chem*, **19A** (1980) 325.

3 Nair C G R & Indrasenan P, *Talanta*, **23** (1976) 239.

4 Vogel A I, *Quantitative organic analysis* (Longman & Green, London) 1958, 708.

5 Soloway S & Lipschitz A, *Analyt Chem*, **22** (1952) 898.

6 Werner E A, *J chem Soc*, **123** (1923) 2577.

7 Hardy F F & Johnston J P, *J chem Soc*, Perkin II (1973) 742.

8 Collins C J & Bowman N S, Ed, *Isotope effect in chemical reactions* (Van Nostrand-Reinhold, New York) 1970 pp 267.

9 Hardwick T J & Robertson E R, *Can J Chem*, **29** (1951) 828.

10 Gilliom R D, *Introduction to physical organic chemistry*, (Addison-Wesley, London) 1970, pp 264.

11 Exner O, *Colln Czech Chem Commun*, **29** (1964) 1094.

12 Gowda B T & Mahadevappa D S, *J chem Soc, Perkin* 2, (1983) 323 and references therein.

13 Ruff F & Kucsman A, *J chem Soc, Perkin* 2, (1982) 1075.

Indian Journal of Chemistry
Vol. 27A, July 1988, pp. 593-596

Mechanism of Self-decomposition of Trichloroisocyanuric Acid in Acid Medium: A Kinetic Study

SUBAS C PATI* & CHINTAMANI SARANGI
Department of Chemistry, Berhampur University, Berhampur 760 007

Received 31 *July* 1987; *revised* 16 *November* 1987; *accepted* 10 *December* 1987

Kinetics and mechanism of the self-decomposition of trichloroisocyanuric acid (TCCA) in aqueous acetic acid-perchloric acid medium has been studied in the presence as well as in the absence of Ru(III)-catalyst and chloride ion. The results show that the reaction has second order dependence on [TCCA]. The rate of the reaction decreases with increase in $[HClO_4]$. Increase in the percentage of acetic acid decreases the rate of decomposition. Addition of chloride ion as well as Ru(III)-catalyst into the reaction mixture accelerates the rate. The reaction has been carried out at four different temperatures and net activation parameters have also been evaluated. Based on the observed data a plausible mechanism has been suggested.

Studies on the decomposition and hydrolysis of trichloroisocyanuric acid (TCCA)[1] in aqueous medium are available in literature. However, no work seems to have been carried out on the self-decomposition of TCCA in acid medium, and hence the title investigation. Chloride ion and Ru(III) catalyst have been used in the present study separately with a view to determining the effect of each of these species on the reaction process.

Materials and Methods

All reagents used were of extra pure quality. Trichloroisocyanuric acid (TCCA) was of AR (Fluka) grade and was used as such. The estimation of TCCA was done iodometrically in acid medium in accordance with Eq. (1).

$$\underset{\text{(TCCA)}}{C_3O_3N_3(Cl)_3} + 6I^- + 3H^+ \rightarrow \underset{\text{(ICA)}}{C_3O_3N_3(H)_3} + 3I_2 + 3Cl^-$$

Perchloric acid (Merck, pro-analysis) was used to adjust $[H^+]$. Ruthenium(III) chloride (Johnson Mathey, London) solution was standardised[2] before use. All solutions were prepared in doubly distilled water. Acetic acid of high purity (Exlar, Glaxo) was used.

The progress of the reaction was monitored by withdrawing aliquots of the reaction mixture (5 ml each) at different time intervals, quenched by pouring into excess of acidified potassium iodide solution and the liberated iodine was titrated against standard thiosulphate solution using starch as an indicator. All kinetic runs were carried out in duplicate and the results are reproducible within ± 3%.

Results and Discussion

The disappearance of TCCA was second order as revealed by the linear plots of 1/[TCCA] versus time (Fig. 1). The second order dependence in [TCCA] was seen to be operative for different [TCCA], although the gradients of the plots of 1/[TCCA] versus time were different for different initial [TCCA] used. The rate constants (k_2) decreased at higher [TCCA] (Table 1) but the plot of $1/k_2$ versus $[TCCA]^2$ was linear.

The dependence of rate of decomposition on

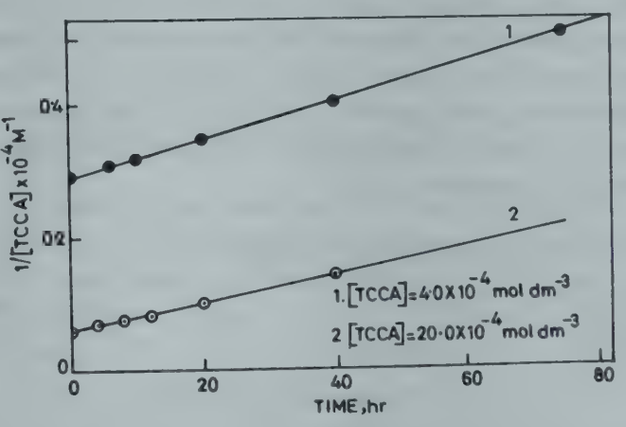

Fig. 1—Plot of 1/[TCCA] versus time, $([HClO_4] = 2.0 \times 10^{-2}$ mol dm^{-3}; HOAc = 20% aq. (v/v), temp. = 35°C; 1. $[TCCA] = 4.0 \times 10^{-4}$ mol dm^{-3}, 2. $[TCCA] = 20.0 \times 10^{-4}$ mol dm^{-3}.)

Table 1—Dependence of Rate Constant on [TCCA]
($[HClO_4] = 2.0 \times 10^{-2}$ mol dm^{-3}; solvent = 20% HOAc-80% H_2O (v/v); temp. = 35°C)

$10^3 \times$[TCCA] (mol dm^{-3})	$10^3 \times k_2$ (dm^3 mol^{-1} s^{-1})	$10^3 \times$[TCCA] (mol dm^{-3})	$10^3 \times k_2$ (dm^3 mol^{-1} s^{-1})
0.4	6.2	3.5	2.1
1.6	4.4	5.0	1.3
2.3	3.7		

acidity has been investigated using $HClO_4$ in a wide concentration range of 2.0×10^{-2} to 200×10^{-2} mol dm^{-3}. The k_2-values decreased with increase in $[HClO_4]$. Thus at $[TCCA] = 4.0 \times 10^{-4}$ mol dm^{-3} and $[H^+] = 2.0 \times 10^{-2}$, 10.0×10^{-2}, 20.0×10^{-2}, 50.0×10^{-2} and 200.0×10^{-2} mol dm^{-3}, the second order rate constants ($\times 10^3$) were 6.2, 4.2, 2.3, 1.0 and 0.3 dm^3 mol^{-1} s^{-1} respectively in 20% aq. HOAc and 35°C. The plots of log k_2 versus log $[H^+]$ were linear with a slope of -0.9, indicating that TCCA is more stable at higher acidity. However, to confirm the acidity effect, the reaction was carried out at two low [acid] using acetic acid-acetate buffer. The rates at *p*H 2.7 and 4.35 were 7.6×10^{-3} dm^3 mol^{-1} s^{-1}, and 300×10^{-3} dm^3 mol^{-1} s^{-1} respectively which are in consonance with the observed effect of acidity.

The role of solvent on the rate of decomposition has been investigated in water-HOAc mixtures having 10 to 90% HOAc (v/v). The rates (Table 2) decreased with increase in acetic acid content in the reaction medium up to water-acetic acid composition of 60% HOAc-40% H_2O (v/v). Thereafter there was a sharp fall in the rate constant with increase in acetic acid content. It appears that TCCA is quite stable in media containing higher percentage of acetic acid.

In order to determine the effect of added salt on the reaction rate, KCl was used in the reaction mixture. The k_2-values (Table 3) at different $[Cl^-]_{ad}$ indicate that added chloride ion accelerates the reaction rate. The results in Table 3 also reveal limiting dependence with increase in $[Cl^-]_{ad}$. The acceleration in the rate in the presence of added Cl^- may be due to the reaction (i-iii).

$$TCCA + H_2O \rightleftarrows DCCA + HOCl \quad \ldots (i)$$

$$HOCl + H^+ \rightleftarrows H_2OCl^+ \quad \ldots (ii)$$

$$H_2OCl^+ + Cl^- \rightleftarrows H_2O + Cl_2 \quad \ldots (iii)$$

The increasing and limiting dependence in $[Cl^-]$ may be due to the following fact: Addition of Cl^- generates molecular chlorine, which acts as an active oxidant species. The acceleration in the rate continues till the medium is saturated with molecular chlorine after which the rate approaches a limiting value. The linearity in the plot of $1/k_2[Cl^-]$ versus $1/[Cl^-]$ with finite intercept also confirms the limiting dependence.

The effect of ruthenium(III) catalyst on the rate of reaction has been studied. Increase in[Ru(III)] increases the rate of decomposition. The k_2-values given in Table 4 show a linear increase with limiting rate dependence. The plot of $1/k_2[Ru(III)]$ versus $1/[Ru(III)]$ is linear with a finite slope and an intercept in y-axis. The observed dependence of decomposition rate on [Ru(III)] can be explained via the formation of an outer sphere complex (see Scheme 1).

Table 2—Dependence on Solvent Composition

($[TCCA] = 4.0 \times 10^{-4}$ mol dm^{-3}; $[HClO_4] = 2.0 \times 10^{-2}$ mol dm^{-3}; temp. = 35°C)

% of (HOAc-H_2O)	$10^3 \times k_2$ (dm^3 $mol^{-1}s^{-1}$)	% of (HOAc-H_2O)	$10^3 \times k_2$ (dm^3 $mol^{-1}s^{-1}$)
10-90	8.2	50-50	3.2
20-80	6.2	60-40	2.0
30-70	5.0	70-30	0.5
40-60	4.4		

Table 3—Dependence on $[Cl^-]$

($[TCCA] = 4.0 \times 10^{-4}$ mol dm^{-3}; $[HClO_4 = 2.0 \times 10^{-2}$ mol dm^{-3}; solvent = 20% HOAc-80% H_2O (v/v); temp. = 35°C)

$10^2 \times [Cl^-]$ (mol dm^{-3})	$10^3 \times k_2$ (dm^3 mol^{-1} s^{-1})	$10^3 \times k^*_{2[Cl^-]}$ (dm^3 mol^{-1} s^{-1})
0	6.2	—
1.0	14.2	7.8
5.0	24.7	18.5
10.0	29.2	23.0
50.0	35.0	28.8

$^*k_{2[Cl^-]} = k_{2([Cl^-] = \text{finite})} - k_{2([Cl^-] = 0)}$

Table 4—Dependence on [Ru(III)]

($[TCCA] = 4.0 \times 10^{-4}$ mol dm^{-3}; $[HClO_4] = 2.0 \times 10^{-2}$ mol dm^{-3}; solvent = 20% HOAc-80% H_2O (v/v); temp. = 35°C)

$10^6 \times$ [Ru(III)] (mol dm^{-3})	$10^3 \times k_2$ (dm^3 mol^{-1} s^{-1})	$10^3 \times k^*_{2[Ru(III)]}$ (dm^3 mol^{-1} s^{-1})
0	6.2	—
1.53	10.5	4.3
3.06	15.0	8.8
15.30	30.2	24.0
30.60	43.4	37.2
75.00	51.3	45.1

$^*k_{2[Ru(III)]} = k_{2([Ru(III)] = \text{finite})} - k_{2([Ru(III)] = 0)}$

the reaction has been carried out at four different temperatures (35°, 40°, 45° and 50°C) and net activation parameters have been computed and the values are: $E_a = 52.0$ k J mol^{-1}; $\Delta H^{\neq} = 50.0$ k J mol^{-1} and $\Delta S^{\neq} = -126.0$ J K^{-1} mol^{-1} under the conditions: $[TCCA] = 4.0 \times 10^{-4}$ mol dm^{-3}; $[HClO_4] = 2.0 \times 10^{-2}$ mol dm^{-3} and solvent = 20% aq. HOAc.

Mechanism

Based on the observed results, a plausible mechanism given in Scheme 1 has been suggested.

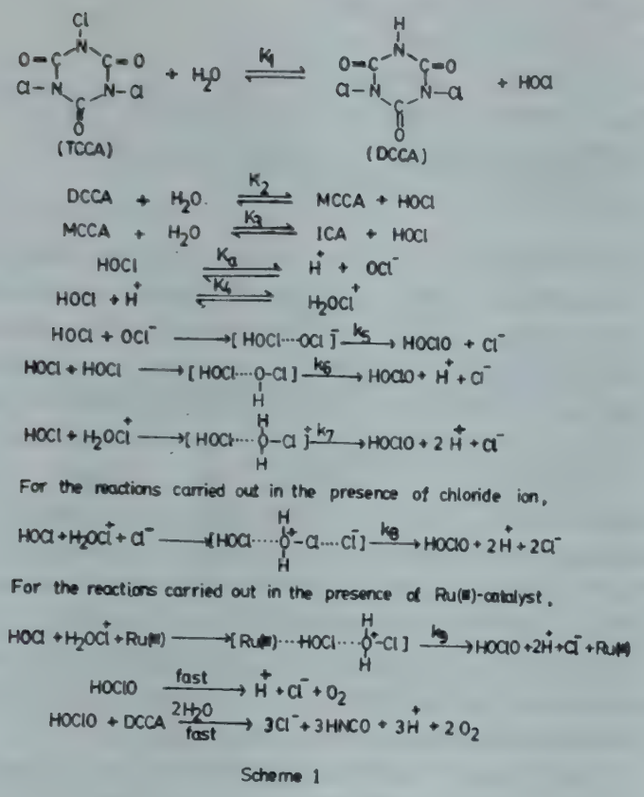

Scheme 1

In the absence of chloride ion and Ru(III)-catalyst, a general rate law (1) can be derived as follows:

$$\text{Rate} = -\frac{d[\text{TCCA}]_T}{dt}$$

$$= k_6[\text{HOCl}]^2 + k_7[\text{HOCl}][\text{H}_2\text{OCl}^+] \quad \ldots (1)$$

But $[\text{TCCA}]_T$

$$= [\text{TCCA}] + [\text{HOCl}] + [\text{H}_2\text{OCl}^+]$$

$$= [\text{TCCA}]\left(1 + \frac{K_1[\text{H}_2\text{O}]}{[\text{DCCA}]} + \frac{K_1K_4[\text{H}^+][\text{H}_2\text{O}]}{[\text{DCCA}]}\right)$$

$$= [\text{TCCA}]\left(\frac{[\text{DCCA}] + K_1[\text{H}_2\text{O}] + K_1K_4[\text{H}^+][\text{H}_2\text{O}]}{[\text{DCCA}]}\right)$$

$$= [\text{TCCA}]\left(\frac{[\text{DCCA}] + K_1 + K_1K_4[\text{H}^+]}{[\text{DCCA}]}\right)$$

(since $[\text{H}_2\text{O}]$ = constant).

Therefore,

$$[\text{TCCA}] = \frac{[\text{TCCA}]_T[\text{DCCA}]}{[\text{DCCA}] + K_1 + K_1K_4[\text{H}^+]} \quad \ldots (2)$$

Similarly,

$$[\text{HOCl}] = \frac{K_1[\text{TCCA}]_T}{[\text{DCCA}] + K_1 + K_1K_4[\text{H}^+]} \quad \ldots (3)$$

and

$$[\text{H}_2\text{OCl}^+] = \frac{K_1K_4[\text{H}^+][\text{TCCA}]_T}{[\text{DCCA}] + K_1 + K_1K_4[\text{H}^+]} \quad \ldots (4)$$

Substituting for $[\text{HOCl}]$ and $[\text{H}_2\text{OCl}^+]$ in Eq. (1), we get

Rate

$$= k_6\left\{\frac{K_1[\text{TCCA}]_T}{[\text{DCCA}] + K_1 + K_1K_4[\text{H}^+]}\right\}^2$$

$$+ \frac{k_7K_1^2K_4[\text{H}^+][\text{TCCA}]_T^2}{([\text{DCCA}] + K_1 + K_1K_4[\text{H}^+])^2}$$

$$= \frac{[\text{TCCA}]_T^2(k_6K_1^2 + k_7K_1^2K_4[\text{H}^+])}{([\text{DCCA}] + K_1 + K_1K_4[\text{H}^+])^2}$$

$$= \frac{[\text{TCCA}]_T^2(k_6K_1^2[\text{H}^+]^2 + k_7K_1^2K_4[\text{H}^+]^3)}{([\text{DCCA}][\text{H}^+] + K_1[\text{H}^+] + K_1K_4[\text{H}^+]^2)^2} \quad \ldots (5)$$

(multiplying the numerator and the denominator by $[\text{H}^+]^2$).

As a first approximation, neglecting $[\text{TCCA}]_T^2$ compared to those of $[\text{HOCl}]$ and $[\text{H}_2\text{OCl}^+]$., Eq. (5) reduces to Eq. (6).

Rate

$$= \frac{k_6K_1^2[\text{H}^+]^2 + k_7K_1^2K_4[\text{H}^+]^3}{([\text{DCCA}][\text{H}^+] + K_1[\text{H}^+] + K_1K_4[\text{H}^+]^2)^2} \quad \ldots (6)$$

Equation (6) explains the decrease in k_2 values at high [TCCA]. However, the magnitude of decrease in the rates could not be quantified with respect to [DCCA] as the sample of DCCA was not available. Making a reasonable assumption that at constant [TCCA], the small [DCCA] in the denominator can be neglected in comparison to the other terms, Eq. (6) reduces to

$$\text{Rate} = \frac{k_6[\text{H}^+]^2 + k_7K_4[\text{H}^+]^3}{([\text{H}^+] + K_4[\text{H}^+]^2)^2}$$

$$= \frac{k_6 + k_7[\text{H}^+]K_4}{(1 + K_4[\text{H}^+])^2} \quad \ldots (7)$$

Equation (7) holds good for $[\text{H}^+]$ in the range of 2.0×10^{-2} to 200×10^{-2}) mol dm^{-3} when OCl^- species is negligible formed.

At low acidity, e.g. $p\text{H} = 2.7$ and 4.35, when OCl^- species is predominant, the rate equation becomes

$$\text{Rate} = k_5[\text{HOCl}][\text{OCl}^-] \quad \ldots (8)$$

Table 5—Comparison of Calculated and Experimental k_2 Values

([TCCA] = 4.0×10^{-4} mol dm^{-3}; solvent = 20% HOAc-80% H_2O (v/v); temp. = 35°C)

$10^2 \times [H^+]$ (mol dm^{-3})	$10^3 \times k_2$ (dm^3 mol^{-1} s^{-1})	
	Obs.	Calc.
0.0045	300	292.5
0.2	7.6	8.3
2.0	6.2	7.3
5.0	5.1	5.6
10.0	4.2	4.1
20.0	2.3	2.5
50.0	1.0	1.0
200	0.3	0.3

But $[OCl^-] = K_a[HOCl]/[H^+]$.

Therefore, $[HOCl] = [H^+][OCl^-]/K_a$

Substituting for [HOCl] in Eq. (8), we get

$$\text{Rate} = = \frac{k_5[H^+][OCl^-]^2}{K_a} \quad \ldots (9)$$

In the presence of chloride ion, the observed accelerating and limiting dependence on rates with respect to the change in $[Cl^-]$ may be interpreted by incorporating a term, $k_8K_4[H^+][Cl^-]$ in the numerator and a term $k_4[H^+][Cl^-]$ in the denominator of Eq. (7). Hence the rate equation becomes,

$$\text{Rate} = \frac{k_6 + k_7K_4[H^+] + k_8K_4[H^+][Cl^-]}{(1 + K_4[H^+])^2 + K_4[H^+][Cl^-]} \quad \ldots (10)$$

For the reactions carried out in the presence of Ru(III) catalyst and in the absence of Cl^-, the reaction has also an accelerating and limiting dependence with increase in [Ru(III)]. Such an observation can be explained by incorporating an additional term like $k_9K_4[Ru(III)][H^+]$ in the numerator and a term like $K_4[H^+][Ru(III)]$ in the denominator in Eq. (10). Therefore the rate Eq. (10) can be written as;

$$\text{Rate} = \frac{k_6 + k_7K_4[H^+] + k_9K_4[H^+][Ru(III)]}{(1 + K_4[H^+])^2 + K_4[H^+][Ru(III)]} \quad \ldots (11)$$

Data treatment led to the following average kinetic values for various constants in 20% aq. HOAc (v/v) at 35°C.

$K_1 = 6.7 \times 10^{-4}$ mol dm^{-3};
$K_2 = 3.0 \times 10^{-4}$ mol dm^{-3};
$K_3 = 1.9 \times 10^{-4}$ mol dm^{-3};
$K_4 = 73$ dm^3 mol^{-1};
$K_a = 3.2 \times 10^{-8}$ mol dm^{-3};
$k_5 = 2.1 \times 10^{-4}$ dm^3 mol^{-1} s^{-1};
$k_6 = 3.4 \times 10^{-3}$ dm^3 mol^{-1} s^{-1};
$k_7 = 3.8 \times 10^{-2}$ dm^3 mol^{-1} s^{-1};
$k_8 = 0.25$ dm^6 mol^{-2} s^{-1} and
$k_9 = 1.22 \times 10^{-3}$ dm^6 mol^{-2} s^{-1}.

The calculated values of the second order rate constants are well in agreement with the experimental k_2-values (Table 5). We may mention here that the decomposition of HOCl in aqueous acid medium has been studied by Lister[3] in the presence of large excess of NaOCl. Lister has reported that the decomposition of HClO to oxygen (e.g. $HClO \rightarrow H^+ + Cl^- + 1/2\ O_2$) follows first order kinetics and their velocity constant is of the order of 10^{-4} min^{-1}. Lister[4] has also studied the decomposition of NaOCl in the absence and presence of metal ion catalyst. The postulated mechanism involves a slow bimolecular reaction of chlorite with more hypochlorite forming chlorate and chloride.

The present kinetic data along with the solvent effect and the average values of net activation parameters (under specified conditions) are compatible with the mechanism and transition state(s) of the decomposition study. The second and third hydrolysis constants of TCCA has been neglected in this report as $K_1K_2K_3 \ll K_1K_2 < K_1$. The final product of decomposition of TCCA has been reported[1] to be isocyanuric acid $(HNCO)_3$ and this work has been utilised for the purpose here.

In the present study (which can also be thought of as a disproportionation reaction of chlorine species produced by the hydrolysis of TCCA), the magnitude of the resolved constants i.e. k_5, k_6, k_7, k_8 and k_9 are apparently in the increasing order of electrophilicity of one of the hydrolysed species attacking the another hydrolysed species (viz. HOCl).

Acknowledgement

Our thanks to Prof. P S Radhakrishnamurti for some of his valuable suggestions and to the CSIR, New Delhi for award of a fellowship to CMS.

References

1 Osaka Pharmaceutical Association (Osaka, Jpn), *Osaka-fu-Yaku-Zasshi*, **30** (1979), 39.
2 Horiuchi, Yoshizo, Ichijyo & Osamu, *Chem Abstr*, **72** (1970) 50624.
3 Lister M W, *Can J Chem*, **30** (1952) 879.
4 Lister M W, *Can J Chem*, **34** (1956) 465, 479.

Indian Journal of Chemistry
Vol. 27A, July 1988, pp. 597-600

Effect of Metal Complexation on Kinetics & Mechanisms of Oxidation of Zn(II)-bound Thiosemicarbazide (TSC) by Chloramine-B (CAB) & Bromamine-B (BAB) in Aqueous Medium & by Dichloramine-B (DCB) in Aqueous Methanol

B THIMME GOWDA* & J ISHWARA BHAT†

Department of Post-Graduate Studies and Research in Chemistry, Mangalore University, Mangalagangothri 574 199, Mangalore

Received 21 *July* 1987; *revised* 24 *August*, *accepted* 1 *October* 1987

Title reactions show first order dependence in [oxidant], fractional order in [complex] and inverse fractional order in [H^+]. In comparison to pure TSC, the rate dependence of oxidation on [TSC] in the metal complex increases from zero to fractional order in the case of [BAB] and [DCB] oxidations. The effect is negligible in CAB oxidation. Addition of benzenesulphonamide, the reduced product of the oxidants has negligible effect on the rate in CAB and BAB oxidations, but the rate slightly increases in DCB reaction. The rates decrease slightly with increase in ionic strength of the medium in all the cases. Decrease in dielectric constant of the medium has little effect on the rate with CAB and BAB, but increases the rate considerably with DCB. Suitable mechanisms have been proposed and the rate laws derived. The coefficients of the rate limiting steps have been calculated.

N-Haloaromatic sulphonamides, viz. chloramine-T, chloramine-B, bromamine-B etc. have been extensively used for the assay of thiosemicarbazide (TSC) in the pure state and in its metal complexes[1]. However no reports are available on the mechanistic aspects of TSC and N-halosulphonamide reactions. We report herein the kinetics of oxidation of TSC in its zinc metal complex by chloramine-B (CAB) and bromamine-B(BAB) in aqueous media and dichloramine-B (DCB) in 25% (v/v) aqueous methanol.

Materials and Methods

CAB, BAB and DCB were prepared by literature methods and their purities were checked by IR and PMR spectra and by estimating the amount of active halogen present in them. Aqueous stock solutions (0.1 mol dm^{-3}) of CAB and BAB and DCB in methanol were prepared, standardised and stored in dark coloured bottles.

Thiosemicarbazide (TSC) (E. Merck) was recrystallized from water. The complex $Zn(TCS)_2SO_4$ was prepared by mixing concentrated aqueous solutions of TSC and zinc sulphate in the molar ratio 2:1 and recrystallised from water. Stock solution of the complex (0.02 mol dm^{-3}) in $HClO_4$ (0.03 mol dm^{-3}) was prepared. The ionic strength of the reaction medium was kept at 0.3 mol dm^{-3} with sodium perchlorate (E. Merck). All other reagents employed were of AR grade.

†Govinda Dasa College, Suratkal 574 158, Karnataka.

Kinetic measurements

The kinetic studies were made under pseudo-first order conditions. The other experimental details are as described elsewhere[2]. The reactions were monitored for at least two half-lives by iodometric method. The pseudo-first order rate constants (k_{obs}) were computed by the method of least squares and were reproducible within ± 3%.

Stoichiometry and product analysis

The stoichiometries of complex-CAB/BAB/DCB reactions were determined by allowing the reactions to go to completion at 303 K at different [complex]/[oxidant] ratios and [H^+] (0.02 to 0.2 mol dm^{-3}). The products, sulphate, cyanate and cyanogen bromide in the reaction mixtures were detected by standard tests. Further, CNBr and sulphate were quantitatively determined by iodometric and gravimetric methods respectively. The yields were 93 ± 3%. Benzenesulphonamide (BSA), the reduced product of the oxidants, was detected by TLC. The observed stoichiometries may be represented by Eqs (1) and (2) for the oxidation of TSC by CAB and BAB, respectively.

$$H_2NNHCSNH_2 + 6C_6H_4SO_2NClNa \text{ (or } 3C_6H_4SO_2NCl_2) + 5H_2O \rightarrow 6C_6H_4SO_2NH_2 \text{ (or } 3C_6H_4SO_2NH_2) + SO_4^{2-} + CNO^- + N_2 + 6Cl^- + 6Na^+ \text{ (or } 6H^+) + 3H^+ \quad \ldots (1)$$

$$H_2NNHCSNH_2 + 6C_6H_4SO_2NBrNa + 4H_2O \rightarrow 6C_6H_4SO_2NH_2 + SO_4^{2-} + CNBr + N_2 + 5Br^- + 6Na^+ + H^+ \quad \ldots (2)$$

Results

At constant [acid] with several fold excess of [complex] (5 to 20 times) over the [oxidant], the plots of $\log([\text{oxidant}]_0/[\text{oxidant}])$ versus time were linear for at least two half-lives, showing first order dependence in [oxidant]. At fixed $[\text{oxidant}]_0$ and $[\text{complex}]_0$ the rates decreased with increase in $[HClO_4]$ in all cases and the plots of log k_{obs} versus log $[H^+]$ (Table 1) were linear with varying slopes indicating inverse fractional order in $[H^+]$ (Table 2). At constant $[HClO_4]$ and [oxidant] the rates increased with increase in [complex] with fractional order dependence in [TSC] or [complex].

The rates decreased slightly with increase in ionic strength of the medium in all the cases. But the change in dielectric constant of the medium by increasing the methanol content of the medium increased the rate slightly in the case of CAB and BAB as oxidants. However, the effect was considerable with DCB as oxidant. Addition of reaction products and Cl^- (with CAB and DCB) or Br^- (0.01-0.1 mol dm^{-3}) (with BAB) had no effect on the rate. Addition of benzenesulphonamide (BSA) (0.0001 to 0.001 mol dm^{-3}) slightly increased the rate in the oxidations by CAB and DCB and had no effect in the oxidation by BAB.

The rates were measured at different temperatures (293-323 K) as a function of [complex] and the rate coefficients for the rate-limiting steps and activation parameters were calculated from the Arrhenius plots (log k versus $1/T$) and [log (k/T) versus $1/T$] for all the oxidants.

Discussion

Chloramine-B and bromamine-B are fairly strong electrolytes in aqueous solutions and furnish different reactive species, i.e. RNHX, $(RNH_2X)^+$, HOX, $(H_2OX)^+$ and RNX_2, depending upon the *p*H of the medium. Under the present experimental conditions ($[HClO_4] = 0.106$ mol dm^{-3}), the oxidants are likely to be in the protonated forms, $(RNH_2X)^+$ or $(H_2OX)^+$.

Mechanism of oxidation: (i) With chloramine-B

The first order dependence in [CAB], fractional order in [complex], inverse fractional order in $[H^+]$ and observed non-influence of the product (BSA, RNH_2) may be explained by two mechanisms (Schemes 1 and 2) (where S is TSC in the complex) as the plot of k_{obs} versus [S] was linear with finite intercept on the ordinate (Fig. 1). Further the double reciprocal plot of $1/k_{obs}$ versus $1/[S]$ was non-linear ruling out Michaelis-Menten type mechanism to account for the observed fractional order in [S].

$$(RNH_2Cl)^+ \underset{k_{-1}}{\overset{k_1}{\rightleftharpoons}} RNHCl + H^+, K_1 = \frac{k_1}{k_{-1}} \quad \text{(fast)}$$

$$RNHCl + H_2O \xrightarrow{k_2} RNH_2 + HOCl \quad \text{(slow)}$$

$$HOCl + S \rightarrow Y_1 \quad \text{(fast)}$$

$$Y_1 + 5HOCl \rightarrow \text{Products} \quad \text{(fast)}$$

Scheme 1

Table 1—Pseudo-first Order Rate Constants (k_{obs}) for Oxidation of Thiosemicarbazide (TSC) in $Zn(TSC)_2SO_4$ by Chloramine-B (CAB), Bromamine-B (BAB) and Dichloramine-B (DCB) at 303 K in Perchloric Acid Medium ($\mu = 0.3$ mol dm^{-3})

$10^4[\text{oxidant}]_0$ (mol dm^{-3})	$10^3[\text{complex}]_0$ (mol dm^{-3})	$10[H^+]$ (mol dm^{-3})	$10^4 k_{obs}$ (s^{-1})		
			CAB	BAB	DCB[a]
1.0	4.0	1.06	2.7	2.9	3.7
2.0	4.0	1.06	2.7	2.9	3.8
4.0	4.0	1.06	2.7	2.9	3.7
8.0	4.0	1.06	2.7	2.9	3.8
10.0	4.0	1.06	—	—	3.9
2.0b[1]	4.0	1.06	3.5	3.2	4.6
2.0b[2]	4.0	1.06	3.1	3.0	4.1
2.0b[3]	4.0	1.06	2.7	2.9	3.8
2.0b[4]	4.0	1.06	2.5	2.7	3.6
2.0c[1]	4.0	1.06	2.7	2.9	—
2.0c[2]	4.0	1.06	2.8	3.0	1.5
2.0c[3]	4.0	1.06	3.0	3.2	—
2.0c[4]	4.0	1.06	—	—	3.8
2.0c[5]	4.0	1.06	3.2	3.5	—
2.0c[6]	4.0	1.06	—	—	8.9
2.0c[7]	4.0	1.06	—	—	16.9

(a) 25% (v/v) methanol medium.
(b) μ(mol dm^{-3}) = 0.11 (1), 0.2 (2), 0.3 (3), 0.5 (4).
(c) % methanol = 0(1), 10(2), 20(3), 25(4), 40(5), 50(6), 80(7).

Table 2—Reaction Order Dependence in [oxidant], [S] and $[H^+]$ and Thermodynamic Parameters for Oxidation of $Zn(TSC)_2SO_4$ by CAB, BAB and DCB[a]

	CAB	BAB	DCB
Orders observed in			
[Oxidant]	1 (1)	1 (1)	1 (1)
[Complex]	0.2 (0.3)	0.3 (0)	0.5 (0)
$[H^+]$	−0.8 (−0.9)	−0.9 (−0.8)	−0.8 (−0.8)
Thermodynamic parameters			
log A	5.8 ± 0.1	7.4 ± 0.1	9.6 ± 0.3
Ea, (kJ mol^{-1})	44.8 ± 4.0	62.5 ± 2.4	62.6 ± 5.0
$\Delta S^{\ddagger}$ (JK^{-1})	−141.9 ± 6.0	−111.3 ± 5.0	−59.9 ± 4.1
$\Delta G^{\ddagger}$ (kJ mol^{-1})	85.2 ± 5.0	93.6 ± 4.0	78.2 ± 6.0

[a]Values in parentheses indicate parameters for the oxidation of TSC in the pure state.

Scheme 1 leads to rate law (3)

$$-\frac{d[CAB]}{dt}=\frac{K_1k_2[CAB][H_2O]}{k+[H^+]}, \text{ where } k=\frac{k_2[H_2O]}{k_{-1}} \quad \ldots (3)$$

$$(RNH_2Cl)^+ + S \xrightarrow{k_3} Y_2 \quad \text{(slow)}$$

$$Y_2 + 5(RNH_2Cl)^+ \rightarrow \text{Products} \quad \text{(fast)}$$

Scheme 2

The rate law corresponding to Scheme (2) is given by Eq. (4).

$$-\frac{d[CAB]}{dt}=k_3[CAB][S] \quad \ldots (4)$$

The combined rate law (5) accounts for the observed results, viz.

$$-\frac{d[CAB]}{dt}=\frac{K_1k_2[CAB][H_2O]}{k+[H^+]}+k_3[CAB][S] \quad \ldots (5)$$

or

$$k_{obs}=\frac{K_1k_2[H_2O]}{k+[H^+]}+k_3[S] \quad \ldots (6)$$

a linearity of the plot of k_{obs} versus [S] (Fig. 1). The slope of the plot of Fig. (1) gave the value of k_3 ($=0.014$ dm^3 mol^{-1} s^{-1}).

For the variation of $[H^+]$ at constant [S], the rate law (6) can be written as

$$k_{obs}=\frac{K_1k_2[H_2O]}{k+[H^+]}+k', \text{ where } k'=k_3[S]$$

or

$$(k_{obs}-k')=\frac{K_1k_2[H_2O]}{k+[H^+]} \quad \ldots (7)$$

or

$$\frac{1}{(k_{obs}-k')}=\frac{k}{(K_1k_2[H_2O]}+\frac{[H^+]}{K_1k_2[H_2O]}=\frac{1}{k_1}$$

$$+\frac{[H^+]}{K_1k_2[H_2O]} \quad \ldots (8)$$

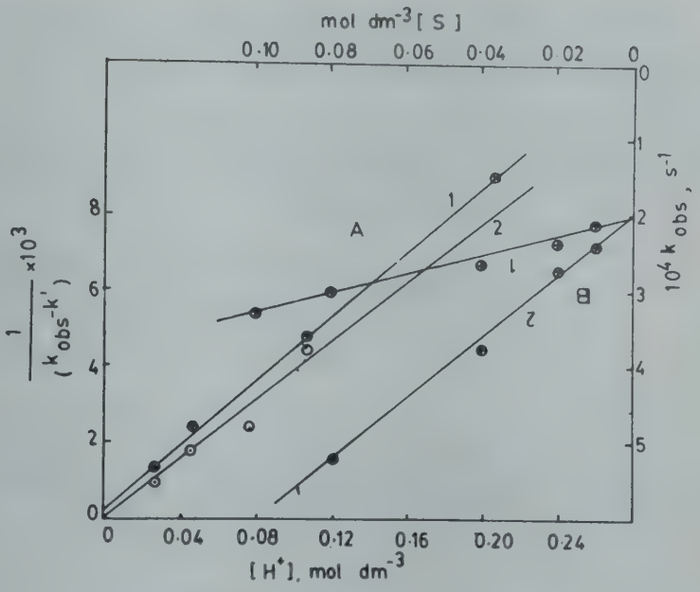

Fig. 1—(A) Plot of $1/(k_{obs}-k')$ versus $[H^+]$: {(1) $10^4[CAB]_0=2.0$ mol dm^{-3}, 10^3[complex]$_0=4.0$ mol dm^{-3}, temp = 303 K; $\mu=0.3$ mol dm^{-3}. (2) $10^4[DCB]_0=2.0$ mol dm^{-3}; 10^3[complex]$_0=4.0$ mol dm^{-3}, temp · 303 K; $\mu=0.3$ mol dm^{-3}; medium: 25% (v/v) aq. methanol}
(B) Plot of k_{obs} versus [S] {(1) $10^4[CAB]_0=2.0$ mol dm^{-3}; $10[H^+]=1.06$ mol dm^{-3}; temp = 303 K; $\mu=0.3$ mol dm^{-3}. (2) $10^4[DCB]_0=2.0$ mol dm^{-3}, $10[H^+]=1.06$ mol dm^{-3}, temp = 303 K; $\mu=0.3$ mol dm^{-3}; medium 25% (v/v) aq. methanol}

$$\frac{1}{(k_{obs}-k')}=a+b[H^+] \text{ where } a=\frac{1}{k_1} \text{ and}$$

$$b=\frac{1}{K_1k_2[H_2O]} \quad \ldots (9)$$

The rate law (9) predicts a linear plot of $1/(k_{obs}-k')$ versus $[H^+]$. Such a plot is shown in Fig. 1. The k_1 was calculated to be 0.005 s^{-1} from the intercept.

(ii) With bromamine-B

The observed results of first order dependence in [BAB], fractional order in [S] and inverse fractional order in $[H^+]$, and the negligible effect of the reaction products can be accounted by Michaelis-Menten type mechanism shown in Scheme 3.

$$SH^+ \overset{K_4}{\rightleftharpoons} S + H^+ \quad \text{(fast)}$$

$$S + RNH_2Br^+ \overset{K_5}{\rightleftharpoons} \underset{Z_1}{(RNH_2Br^+ \text{---} NH_2NHCSNH_2)} \quad \text{(fast)}$$

$$Z_1 \xrightarrow{k_6} Z_2 + RNH_3^+ + H^+ + Br^- \quad \text{(slow)}$$

$$Z_2 + 5RNH_2Br^+ \rightarrow \text{Products} \quad \text{(fast)}$$

Scheme 3

Applying steady state approximation to the intermediate Z_1, the rate laws (10-12) have been deduced.

$$-\frac{d[BAB]}{dt}=\frac{K_4K_5k_6[BAB]_0[SH^+]}{[H^+]+K_4K_5[SH^+]}$$

$$\text{where } [S]=\frac{K_4[SH^+]}{[H^+]} \qquad \ldots(10)$$

or

$$k_{obs}=\frac{K_4K_5k_6[SH^+]}{[H^+]+K_4K_5[SH^+]}=\frac{K_5k_6[S]}{1+K_5[S]} \qquad \ldots(11)$$

or

$$\frac{1}{k_{obs}}=\frac{[H^+]}{K_4K_5k_6[SH^+]}+\frac{1}{k_6}=\frac{1}{K_5k_6[S]}+\frac{1}{k_6} \qquad \ldots(12)$$

Rate law (12) predicts linearity between $1/k_{obs}$ and $[H^+]$ or $1/[S]$. The plots of $1/k_{obs}$ versus $1/[S]$ and $1/k_{obs}$ versus $[H^+]$ were linear in accord with rate law (12) (Fig. 2). The constants k_6 and K_5 were computed from the former plot ($k_6=4.16\times10^{-4}$ s^{-1}; $K_5=76.54$).

(iii) With dichloramine-B

In the case of DCB oxidation the rate slightly increased by the addition of BSA. The catalysis by BSA is probably due to the reaction first going through step (13).

$$(RNHCl_2)^+ + (RNH_3)^+ \rightleftharpoons 2(RNH_2Cl)^+ \qquad \ldots(13)$$

and then through reaction paths identical to those shown in Schemes 1 and 2 and the rate laws given by Eqs (3)-(9). Plot of k_{obs} versus [S] was linear with finite intercept on the ordinate (Fig. 1) in accordance with the combined rate law (6). Plot of $1/(k_{obs}-k')$ versus $[H^+]$ was also linear as predicted by rate law (9) (Fig. 1).

Activation parameters

Almost similar $\Delta G^{\ddagger}$ values for CAB and DCB oxidations may indicate the operation of similar mechanisms. The deviation with DCB is understandable as the reaction medium is different. The formation of more ordered activated complexes is evident from the negative $\Delta S^{\ddagger}$ values.

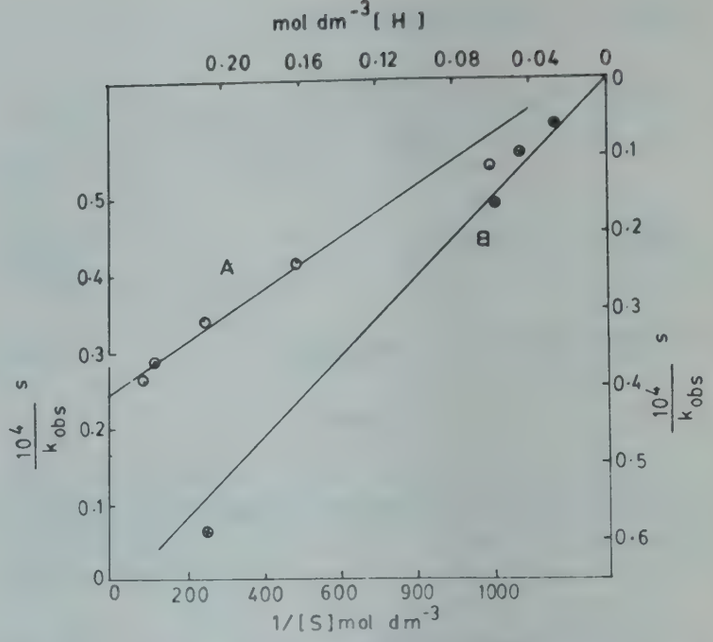

Fig. 2—(A) Plot of $1/k_{obs}$ versus $1/[S]$ ($10^4[BAB]_0=2.0$ mol dm^{-3}, $10[H^+]=1.06$ mol dm^{-3}, temp 303 K; $\mu=0.3$ mol dm^{-3})

(B) Plot of $1/k_{obs}$ versus $[H^+]$ {$10^4[BAB]_0=2.0$ mol dm^{-3}; $10^3[complex]_0=4.0$ mol dm^{-3}; temp = 303 K; $\mu=0.3$ mol dm^{-3}}

Observed increase in rate with decrease in dielectric constant of the medium in the case of DCB is in accordance with Amis-Jaffe equation[3].

The observed slight decrease in rate with increase in ionic strength of the medium is in conformity with Quinlan-Amis equation[4].

Comparison of kinetic data (Table 2) for the oxidation of TSC in the pure state[2] and that in bound state (as metal complex) reveals increase in the dependence of rate on [TSC] in the oxidation of zinc complex by BAB and DCB. But the effect is not significant in CAB oxidation.

References

1 Gowda B T & Mahadevappa D S, *Microchem J*, **28** (1983) 374.

2 Gowda B T & Bhat J I, *React Kinet Catal Lett*, **31** (1986) 461; *Tetrahedron*, **43** (1987) 2119; *Indian J Chem*, **25A** (1986) 1129 and 1149; **26A** (1987) 215 and *J Indian chem Soc*, **63** (1986) 665; **64** (1987) 150.

3 Amis E S, *Solvent effects on reaction rates and mechanisms*, (Academic Press, New York) 1966.

4 Quinlan J E & Amis E S, *J Am chem Soc*, **77** (1955) 4187.

Indian Journal of Chemistry
Vol. 27A, July 1988, pp. 601-605

Dependence of Hammett Constant Rho on Dielectric Constant & Water Activity in Mixed Aqueous Solvents

D V JAHAGIRDAR*, B R ARBAD & R M KHARWADKAR
Department of Chemistry, Marathwada University, Aurangabad 431 004

Received 3 *July* 1987; *revised* 31 *August* 1987; *accepted* 18 *September* 1987

pK values of several *m*- and *p*-substituted salicylic acids, anilinium and pyridinium ions have been determined in dioxane-water mixtures potentiometrically. The *pK* values for benzoic acids and phenols have been determined earlier. The consolidated data have been utilised to obtain values of Hammett constant (ρ). The magnitude of $\Delta\rho(=\rho_S-\rho_W)$ has been found to be almost equal for the five series in 10, 20, 40 and 60% dioxane-water mixtures. The variations of Δρ with the dielectric constant (D) of the solvent mixtures follow an empirical relationship ($\Delta\rho = 19.34\ 1/D - 0.201$). This relation is designated as Jahagirdar-Arbad-Kharwadkar (JAK) relation. The validity of this equation in different alcohol-water mixtures has been examined and its utility in predicting *pK* values of substituted compounds has been examined. It is observed that this equation is valid for solvent mixtures having mol fraction of water more than 0.5.

Linear free energy relationships have had a profound impact on the development of physical organic chemistry. The classification of substituent effects on reaction equilibria has led to many accepted concepts on bonding and electronic effects[1]. The most widely known attempt to systematize interpretation of acid-base data particularly for free energies and equilibrium constants is the Hammett equation[2,3]: $\log (K/K^\circ) = \rho\sigma$. The substituent constant σ depends primarily on the nature of the substituent and to a lesser degree on its position, and is assumed to be independent of temperature and solvent. The parameter ρ depends on a particular reaction series under consideration and also on solvent and temperature[4].

Earlier, the present authors[5] reported variation in ρ-values for benzoic acid and phenol series in different dioxane-water mixtures. Contrary to the usual belief that ρ should increase with the decrease in dielectric constant of the medium, in our investigations[5] in water-dioxane media ρ-values decreased after the mol fraction of dioxane reached 0.45, for the benzoic acid series[5]. The earlier study has now been extended to substituted salicyclic acids, pyridinium and anilinium ions. Thus the *pK* values have been determined for the dissociation of neutral species like phenols and benzoic acids as well as for the charged species like pyridinium and anilinium ions.

Materials and Methods

Substituted salicyclic acids and anilines were of AR grade (BDH) and pyridines (99.3% pure) were procured from Aldrich Chemicals, USA. Sodium hydroxide and sodium perchlorate were of AR grade and aqueous solution of sodium hydroxide was standardised with dried sodium carbonate (AR) via aqueous HCl. Potassium hydrogen phthalate and sodium tetraborate were recrystallised and dried by the standard procedure[6]. 1,4-Dioxane (AR) was purified as usual before use.

The *pK* values of all the compounds in water-dioxane mixtures were measured potentiometrically using an Elico digital *p*H meter model L1-100 fitted with glass SCE electrode assembly. When not in use, the glass electrode was kept immersed in a solvent mixture of identical composition to the one being studied. The accuracy of the *p*H measurement was ±0.01 *p*H unit. The *p*H meter was standardised against potassium hydrogen phthalate buffer (*N*/20 with a *p*H of 4.01 at 30°C) and sodium tetraborate (*p*H 9.11 at 30°C) and checked by titrating 0.025 *N* $HClO_4$ against standard NaOH. The *p*H meter readings were converted to $[H^+]$ from the analytical concentrations of $HClO_4$ and activity coefficients[7]. The *p*H meter readings in water-dioxane mixtures (20-80%) were converted into pa_{H^+} by making appropriate corrections proposed by Van Uitert and coworkers[8,9].

The Calvin-Bjerrum titration technique[10] was adopted for the determination of *pK* values of all the compounds. The experimental procedure involved potentiometric titrations of solutions of (i) free $HClO_4$ (10^{-2} *M*); and (ii) free $HClO_4$ (10^{-2} *M*) + organic acid (10^{-2} *M*) against standard sodium hydroxide (~0.2 *N*) solution. The ionic strength was maintained at ~0.1 *M* by the addition of sodium perchlorate solution. All titrations

were carried out at 30 ± 0.02°C under oxygen-free N_2 blanket. The titrating mixtures were well stirred for 1-2 min and the *p*H reading was noted after the stirring was stopped.

The values of $\bar{n}_A$ (proton-ligand formation number) at different *p*H values were obtained from the expression[11]

$$\bar{n}_A = \gamma - \frac{(v_2 - v_1)(N + E^\circ)}{(V^\circ + v_1)T^\circ_L}$$

where V° is the initial volume of the solution; E° and T°_L are the total concentrations of $HClO_4$ and organic compound, respectively; and v_1 and v_2 are the volumes of alkali of a given normality required during the (i) and (ii) titrations respectively, at a given *p*H; and γ is the number of replaceable hydrogen atoms in compound and N is the normality of NaOH.

$\bar{n}_A$ values at various *p*H were utilized to get *pK* values, initially by the half-integral method[11]. The accurate values of *pK* were determined further by the method of pointwise calculations[11]. The expression $\log \bar{n}_A/1 - \bar{n}_A = pK_1 - p\text{H}$ was used and the values of $\bar{n}_A$ selected were in the range 0.8 to 0.2. Two sets of measurements were taken for every compound and the magnitudes of $\bar{n}_A$ values at specific *p*H were compared. The average of the two was taken when the disagreement in the $\bar{n}_A$ value was in the third place of decimal. Whenever the disagreement was in the second place, a third set of experimental measurement was invariably carried out.

Results and Discussion

The *pK* values of the substituted and the parent compounds in different dioxane-water mixtures presented in Table 1. These correspond to the dissociation of $-COOH$ group in salicyclic acids, $-NH_3^+$ in anilinium and of $-NH^+$ in pyridinium ions. The data for benzoic acids and phenols form a part of our earlier publication[5]. The *pK* values in water were obtained by extrapolation of the linear plot of *pK* versus mol fraction of dioxane; the *pK* (W) values thus obtained, exhibit a good agreement with the reported values[4,12].

Estimtion of ρ*-values*

The plots of ΔpK ($= pK$ unsubstituted $- pK$ substituted, i.e. $pK_u - pK_s$) against σ were drawn to obtain ρ values. Values of σ were taken from the consolidated table compiled by Shorter[13]. For substitutents which involve cross-conjugation σ^n values were used. The plots were linear for each of the series and the correlation coefficient of each

Table 1 — *pK* Values (±0.01 to 0.04) of Substituted Organic Compounds

Temp. = 303 ± 0.1 K; μ = 0.1 *M* ($NaClO_4$)

Substituent	% Dioxane (v/v)					
	0	10	20	40	60	80
(A) Benzoic acid series						
Nil	4.20	4.45	4.73	5.67	7.12	9.22
−*m* Cl	3.82	4.05	4.40	5.30	6.63	8.75
−*p* Cl	3.98	4.15	4.49	5.28	6.66	8.89
−*m* Br	3.85	4.12	4.66	5.51	6.78	8.42
−*m* I	3.82	3.90	4.19	5.11	6.61	8.28
−*p* I	3.75	4.15	4.39	5.37	6.95	8.98
−*m* NO_2	3.40	3.70	3.90	4.64	6.02	8.12
−*p* NO_2	3.33	3.55	3.74	4.66	5.99	8.15
−*m* NH_2	4.65	4.80	5.23	5.96	7.15	9.19
−*p* NH_2	4.93	5.15	5.51	6.44	7.90	10.21
(B) Phenol series						
Nil	10.02	10.70	10.96	11.90	12.36	14.70
−*m* Cl	9.14	9.40	9.67	10.43	11.67	13.56
−*p* Cl	9.46	9.58	9.75	10.61	11.51	13.64
−*m* NO_2	8.38	8.55	8.82	9.14	10.60	12.35
−*p* NO_2	7.18	7.25	7.33	8.09	9.03	10.86
−*m* NH_2	9.87	10.25	10.54	11.43	12.64	14.70
−*p* NH_2	10.30	10.72	11.12	11.85	13.67	15.27
−*m* OH	9.54	9.90	10.06	10.86	12.31	14.31
(C) Salicyclic acid series						
Nil	3.12	3.25	3.37	4.17	5.12	7.42
−4 Cl	2.90	3.10	3.37	3.80	4.76	7.04
−5 Cl	2.69	2.90	3.16	3.71	4.56	6.99
−5 Br	2.70	2.92	3.37	3.86	4.67	6.99
−4 I	2.83	3.00	3.22	3.77	4.96	7.16
−5 I	2.75	2.88	3.19	3.56	4.67	6.45
−5 OH	2.97	3.20	3.51	4.07	5.09	7.35
−5 NO_2	2.30	2.45	2.73	3.00	4.02	6.01
(D) Aniline series						
Nil	4.54	4.50	4.47	4.46	4.45	5.12
−*m* Cl	3.29	3.35	3.36	3.45	4.08	4.70
−*p* Cl	3.78	3.93	3.98	4.10	4.51	5.04
−*p* Br	3.74	3.50	3.59	4.05	4.54	4.82
−*m* OH	4.37	3.93	4.05	4.37	4.75	5.18
−*p* OH	5.50	5.52	5.50	5.52	5.80	7.17
−*m* CH_3	4.56	4.66	4.65	4.85	5.25	5.85
−*p* CH_3	4.94	4.80	4.76	4.80	5.12	6.24
−*p* OC_2H_5	5.25	5.31	5.32	5.41	5.48	6.69
−*m* OC_2H_5	4.13	4.08	4.08	4.17	4.28	4.69
−*p* OCH_3	5.29	5.23	5.19	5.17	5.48	5.73
(E) Pyridine series						
Nil	5.33	5.06	5.11	4.66	4.69	5.94
−*m* NH_2	5.98	6.02	5.94	5.85	5.97	7.38
−*p* NH_2	8.82	8.61	8.48	8.14	8.50	9.84
−*p* OH	4.82	4.80	4.87	4.87	5.08	6.39
−*p* DMA	5.11	5.14	5.06	4.99	5.18	6.50
−*m* C_2H_5	5.47	5.51	5.42	5.19	5.20	6.40
−*p* C_2H_5	5.77	5.81	5.75	5.51	5.43	6.67
−*m* CH_3	6.00	5.71	5.31	5.14	5.17	6.19
−*p* CH_3	6.17	5.92	5.68	5.39	5.50	6.61

plot was between 0.996 and 0.999. The ρ-values thus derived are given in Table 2.

The ρ-values increase with increase in the mol fraction of dioxane from 0.0 to 0.4. At dioxane mol fraction >0.4, a reversal in this order is seen for benzoic acid and salicyclic acid series and constancy for anilinium ion. The plots of ρ against 1/D or the mol fraction of dioxane do not exhibit a linear relationship over the entire range of composition. Decrease in dielectric constant should normally lead to increase in ρ-value due to change in the overall dielectric constant of the medium and/or due to specific solvation effect. If the ring solvation of the parent acid is unaffected in the substituted compounds, then, the plot of $pK(S)_s/pK(W)_s$ against $pK(S)_u/pK(W)_u$ should be linear with a unit slope[14]. Such plots were linear for $-CH_3$, ethyl and bromo substituted compounds but nonlinear for the $-NO_2$ and $-NH_2$ compounds. The deviation of the points from unit slope plot was greater at dioxane mol fraction of 0.24.

Application of Born equation

The ionization equilibria for the different series in mixed aqueous-solvents can be examined by the Born equation[15]

$$pK(S)-pK(W)=121.6\,(1/D-0.0128)\,(1/r_{A^-}+1/r_{H^+}) \quad \ldots(1)$$

In Eq. (1) $K(S)$ and $K(W)$ are the ionization constants of a neutral acid in a solvent mixture (S) and in water (W) respectively; D is the dielectric constant of the solvent mixture (S) and r_{A^-} and r_{H^+} represent the radii of the acid anion and the proton respectively. The radius of phenoxide and benzoate anions are assumed to be similar. The radius ($r_{A^-}=3.31$ Å) of the phenoxide ion has been obtained from the volume (91.6 cm^3) of the ion[16]. It was assumed that the molecule and its ion occupy an approximately equal spherical cavity in solution. r_{H^+} was taken equal to 0.80 Å (ref. 17).

The variation of $pK(S)-pK(W)$ against 1/D predicted by Eq. (1) was compared with the experimental data for benzoic acid, phenol and salicyclic acid and their substituted derivatives. The experimental points almost coincided with the theoretical line up to 40% of dioxane. Thereafter, these showed deviations which increased with the increase in dioxane content. All the experimental points taken together exhibit a curvature and do not confirm to the linear dependence required by the born equation[15]. The curved nature of these plots indicates the failure of the Born equation to take local variations in dielectric constant into account[17,18].

The non-applicability of this equation and the non-linearity of the plots is ascribed to the nonlinear nature of the free energy function for the transfer of proton from water to water-dioxane mixtures[19].

Variation of ρ with D

The values of $\Delta\rho(=\rho_S-\rho_W)$ were obtained for the five series and were averaged (Table 3). The standard deviations in 10, 20 and 40% dioxane-water mixtures are within the limits of uncertainties of these values, and are beyond the limits for 60% and 80% dioxane-water mixture. The Δρ for 90% was not averaged as the three values exhibited wide divergence. The almost constancy of Δρ for 10, 20 or 40% dioxan-water mixtures, for all the five series is worth noting because the ionization processes are different. The processes are ionogenic for phenol and benzoic acid series and isoelectric for pyridinium and anilinium ions.

Δρ varies linearly with 1/D (Fig. 1) except the one corresponding to 80% dioxane-water mixture

Table 2—ρ-Values of Pyridinium and Anilinium Ions, Salicyclic Acids, Benzoic Acids and Phenols in Various Dioxane-Water Medium at 303 ± 0.1 K

% Dioxane (v/v)	Dielectric constant	Mol fraction of dioxane	ρ-Values				
			Pyridinium ion	Anilinium ion	Salicylic acid	Benzoic acid	Phenol
0	78.54	0.00	5.29	2.94	1.05	1.00	2.23
			5.26*	2.93*		1.00*	2.26*
10	69.69	0.02	5.38	2.98	1.09	1.05	2.30
20	62.50	0.04	5.44	3.03	1.13	1.07	2.36
40	42.35	0.12	5.55	3.19	1.28	1.30	2.52
60	25.15	0.24	5.80	3.46	1.46	1.42	2.83
80	10.14	0.45	6.01	4.68	1.58	1.68	3.12
90	5.62	0.64		4.69	1.53	1.29	

*Literature values

Table 3 — $\Delta\rho(\pm 0.03)$ $(=\rho_W - \rho_S)$ Values of Pyridinium Ion, Salicylic Acids, Benzoic Acids and Phenols Series in Dioxane-Water Mixtures

% Dioxane (v/v)	Δρ					Average Δρ
	Pyridinium ion	Anilinium ion	Salicylic acid	Benzoic acid	Phenol	
10	0.09	0.04	0.04	0.05	0.07	0.06 ± 0.02
20	0.15	0.09	0.08	0.07	0.13	0.104 ± 0.03
40	0.26	0.25	0.23	0.30	0.29	0.266 ± 0.03
60	0.51	0.52	0.41	0.42	0.60	0.492 ± 0.07
80	0.72	0.74	0.53	0.68	0.89	0.705 ± 0.138
90	—	0.75	0.48	0.29	—	—

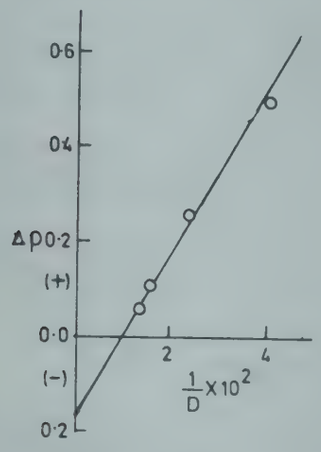

Fig. 1 — Variation of Δρ with 1/D, in water-dioxan mixtures

(correlation coefficient = 0.9992). The relationship between Δρ and 1/D obtained by the method of least squares is given by Eq. (2)

$$\Delta\rho = 19.34\,(1/D) - 0.201 \quad \ldots (2)$$

The utility and the scope of Eq. (2) was ascertained as follows:

(i) *pK* values for *m*- and *p*-substituted $-CH_3$, $-Cl$, $-Br$ and $-OCH_3$ anilinium ions were experimentally derived in alcohol-water mixtures. The data were utilized to get $\rho_{expt.}$ $\rho_{calc.}$ was obtained from Eq. (2) and compared with $\rho_{expt.}$. A satisfactory agreement was noted (Table 4).

(ii) Values of ρ_{calc} from Eq. (2) were compared with the literature ρ values for phenol, 4-nitrophenol and benzoic acid. A fairly satisfactory agreement is observed (Table 5) for all the mixtures, except the three, wherein the percentage of organic component is high.

(iii) The Hammett equation for the water medium (W) and solvent mixture (S) can be written separately (Eqs 3 and 4)

$$pK(W)_s = pK(W)_u - \rho_W\sigma \quad \ldots (3)$$

$$pK(S)_s = pK(S)_u - \rho_S\sigma \quad \ldots (4)$$

where s and u stand for substituted and unsubstituted derivatives respectively. Combining Eqs (3) and (4) we get

$$pK(S)_s = \frac{\rho_S}{\rho_W}\{pK(W)_s - pK(W)_u\} + pK(S)_u \quad \ldots (5)$$

The magnitude of ρ_S for any solvent mixture with a known dielectric constant can be derived from Eq. (2). Values of $pK(W)_u$ and $pK(W)_s$ for

Table 4 — Hammett's ρ for Substituted Anilinium Ions in Different Alcohol-Water Mixtures at 303 ± 0.1 K

Alcohol	Dielectric constant	ρ-values	
		Obs.	Calc. from Eq. (2)
Methanol	74.1	2.98	2.99
Ethanol	59.0	3.03	3.07
Methanol	41.0	3.18	3.21
Ethanol	41.0	3.19	3.21
n-propanol	41.0	3.19	3.21

Table 5 — Comparison of ρ_{calc} from Eq. (2) with $\rho_{lit.}$

Medium	Dielectric constant	ρ-Values	
		Literature (refs 20-25)	Calc.
	Benzoic acid		
50% methanol	54.9	1.09	1.15
Pure methanol	31.5	1.54	1.41*
70% ethanol	38.0	1.74	1.31*
50% methanol	54.9	1.24	1.15
	4-Substituted phenols		
10% methanol	74.1	2.29	2.29
40% methanol	59.6	2.45	2.38
50% methanol	54.9	2.46	2.38
60% methanol	50.1	2.48	2.42
80% methanol	40.0	2.42	2.51
90% methanol	35.7	2.36	2.57*
	Phenol		
Butanol-water	70.0	2.34	2.31

Table 6—Comparison of *pK* Values Observed by Other Workers with the Ones Calculated by the JAK Equation

	Ethanol		
4-t-butylpyridine	40	4.86	4.98
3-CH_3-aniline	50	4.09	4.09
3,5-dimethylaniline	50	4.61	4.59
	Methanol		
4-Nitrophenol	10	7.18	7.18
	20	7.31	7.28
	30	7.44	7.50
	40	7.57	7.63
	50	7.72	7.78
	60	7.91	7.94
	70	8.14	8.14
	80	8.47	8.36
	90	9.07	8.80
4-Methylphenol	20	10.57	10.58
	30	10.81	10.82
	40	11.01	11.06
	50	11.19	11.26
	60	11.34	11.38

common organic acids are available in the literature[12]. The $pK(S)_s$ for any substituted compound in any solvent mixture, therefore, can be obtained from Eq. (5), provided $pK(S)_u$ is known. $pK(S)_s$ values thus obtained for substituted anilines and phenols are given in Table 6. The agreement between the calculated and the literature values is fairly close for all the solvent mixtures, except those having higher percentage (>70%) of organic component. Equation (2) therefore seems to be capable of predicting *pK* values of an organic acid in a solvent mixture where the organic part is not rich.

In aquo organic solvent mixture the two components differ in their solvating power. Hence activity of water is a principal deciding factor for *pK*.

The linear variation of *pK* with the mol fraction of organic component in aquo organic solvent mixture requires that the water activity be proportional to the mol fraction of water in the solvent mixture. The plots of log a_w versus mol fraction of water for the three binary solvent mixtures are shown in Fig. 2. For each mixture, the points corresponding to mixtures having mol fraction of water greater than 0.6 only, fall on a straight line.

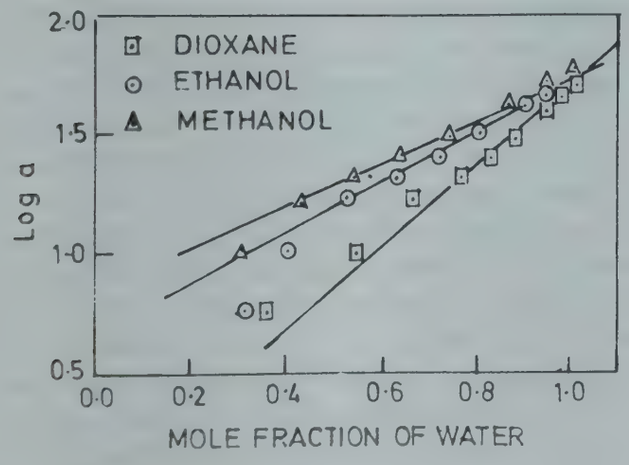

Fig. 2—Plot of log a_w against mol fraction of the water in mixed aqueous solvents

It seems, therefore, that the dielectric constant of a medium as well as the mol fraction of water, are the two factors responsible for the dissociation equilibria. This clearly accounts for the limited linearity in *pK* versus 1/D plots and the limited validity of Eq. (2).

References

1 Hine J, *Structural effects on equilibria in organic chemistry* (Wiley Interscience, New York) 1975.

2 Hammett L P, *J Am chem Soc*, **59** (1937) 96.

3 Hammett L P, *Trans Faraday Soc*, **34** (1938) 156.

4 Hepler L G, *Solute solvent interactions*, edited by J F Coetzee & C D Ritchie (Marcel Dekker, New York) 1969.

5 Jahagirdar D V, Deshpande R G & Shelke D N, *J chem Soc Perkin II*, (1977) 1513.

6 Belcher R & Nutten A J, *Quantitative inorganic analysis* (Butterworth, London), 1960, 177.

7 Kielland J, *J Am chem Soc*, **59** (1937) 1675.

8 Van Uitert L G & Haas C G, *J Am chem Soc*, **75** (1953) 451.

9 Van Uitert L G & Fernelius W C, *J Am chem Soc*, **76** (1954) 5887.

10 Martell A E & Calvin M, *Chemistry of metal chelate compounds*, (Prentice Hall, New York) 1962.

11 Irving H & Rossotti H, *J chem Soc*, (1954) 2904.

12 Sillen L G & Martell A E, *Stability constants*, Special Publication No. 17 and 23 (The Chemical Society, London) 1964 and 1971.

13 Shorter J, *Correlation analysis in organic chemistry*—an introduction to linear free-energy relationships, (Clarendon Press, Oxford) 1973, 17.

14 Kondo Y, Matsui T & Takura N, *Bull chem Soc, Japan*, **42** (1969) 1037.

15 Born M, *Z Physik*, **1** (1920) 45.

16 Rochester C H & Rossall B, *Trans Faraday Soc*, **65** (1969) 992.

17 Sager E E, Robinson R A & Bates R G, *J Res Natl Bur Stand*, **A68** (1964) 305.

18 Woodhead M, Paabo M, Robinson R A & Bates R G, *J Res Natl Bur Stand*, **A69** (1965) 243.

19 Julliard J, *Bull Soc Chim France*, (1968) 1894.

20 Jaffe H H, *Chem Rev*, **53** (1953) 191.

21 Grunwald E & Berkowitz B J, *J Am chem Soc*, **73** (1951) 4939.

22 Rochester C H & Parsons G H, *Trans Faraday Soc*, (1974) 1058.

23 Hopkins H P & Ali S Z, *J Am chem Soc*, **99** (1977) 2069.

24 Hopkins H P, Jahagirdar D V, Moulik S P, Webb H M, Davidson W R & Pedley M C, *J Am chem Soc*, **106** (1980) 4341.

25 Patai S, *Chemistry of the amino groups* (Interscience) 1968, 191.

Indian Journal of Chemistry
Vol. 27A, July 1988, pp. 606-608

A Structural Reinvestigation of the Reported Anhydride† from *o*-$HO_2As(C_6H_4CO_2H)_2$: Novel Spirobicyclic & Tricyclic Acyloxy(carboxy)arsorane Structures

SWARN S PARMAR*, HARVEEN K SALUJA & HARINDAR K BATHLA
Department of Chemistry, Guru Nanak Dev University, Amritsar 143 005

Received 20 *August* 1987; *revised and accepted* 23 *November* 1987

A detailed examination of the IR, TG, DTG, DTA and acid equivalent data shows that the attempt to prepare *o*-$HO_2As(C_6H_4CO_2H)_2$ (3a) did not yield its anhydride (4a) as claimed [*J chem Soc*, 1924, 2025] but its impure isomer, monohydrate of (4a), which has been characterised now as the first novel tricyclic acyloxy(carboxy)arsorane (3b) in solid phase. The compound (4a) has now been prepared for the first time by the dehydration of (3b) and is shown to exist as intermolecularly H-bonded spirobicyclic acyloxy(carboxy)arsorane (4b).

In our earlier communications[1,2] we have shown that *o*-carboxyphenylarsonous acid (1a)[3,4] and *o*-carboxyphenylarsonic acid (2a)[3,5] actually exist as benzoxarsole monohydrates (1b) and (2b) respectively. We now report the results of a reinvestigation into the characterization of the anhydride (4a) reported to be isolated during an unsuccessful attempt to prepare *o*-$HO_2As(C_6H_4CO_2H)_2$ (3a)[3].

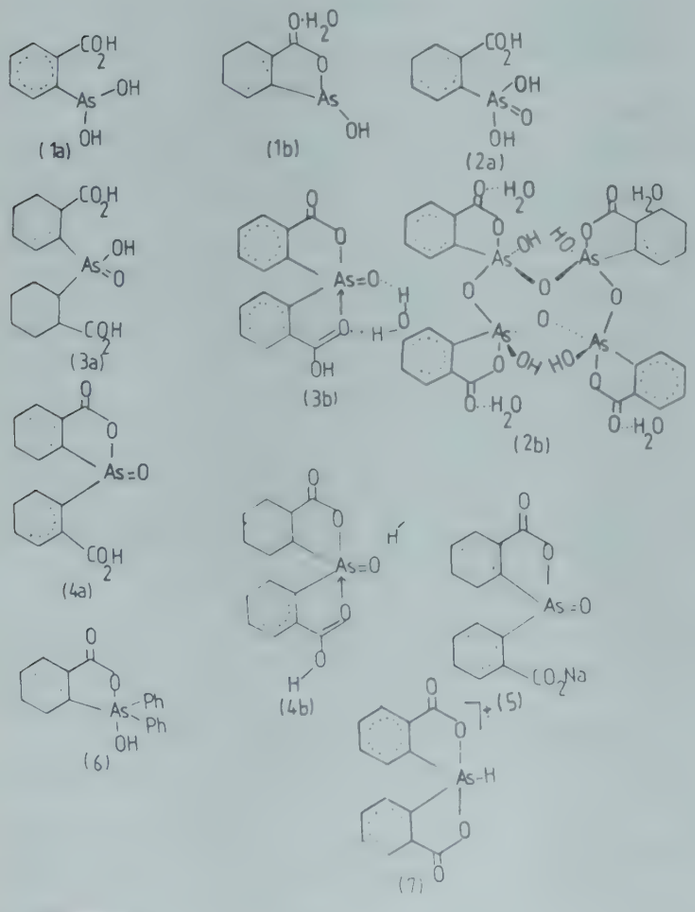

†1-Oxy-1-(*o*-carboxyphenyl)-3H-2, 1-benzoxarsol-3-one.

Materials and Methods

Commercially available chemicals were used without purification. The benzoxarsole monohydrate (1b) earlier known as *o*-carboxyphenylarsonous acid or *o*-benzoarsenious oxide was prepared by the literature method[3].

Infrared spectra (4000-200 cm^{-1}) were recorded in KBr pellets/CH_2Cl_2 on a PYE-UNICAM SP3-300 spectrophotometer. ^1H NMR spectra were recorded on a Jeol JNM-PMX 60SI NMR spectrometer using TMS as internal standard. Mass spectra were recorded on Jeol-JMS-01SG-2 instrument at CDRI, Lucknow. The thermal analysis of (3a) and (4a) were carried out on an STA 780 thermobalance.

Preparation of 1-*oxy*-1-(*o*-*carboxyphenyl*)-3*H*-2, 1-*benzoxarsol*-3-*one monohydrate* (3*b*)

The reported outline[3] for the preparation of (4a) has been developed into the following procedure.

A solution of anthranillic acid (9g) in a mixture of hydrochloric acid (13 cm^3) and water (72 cm^3) was diazotized with a saturated solution of $NaNO_2$ (5g) at -5°C. Sodium *o*-benzarsenite solution was prepared by dissolving (1b) in a freshly prepared hot solution of NaOH (2g) in distilled water (34 cm^3) and to it a saturated solution of $CuSO_4.5H_2O$ (0.2 g) was added. The diazotized solution was added to this *o*-benzarsenite solution in small portions at 0°C with constant stirring which was continued for 10 min after the complete addition. Reaction mixture was heated at 60°C for 2h, cooled and acidified with dilute hydrochloric acid. The resulting brown solid was filtered and crystallized first from MeOH and then from boiling water. A pure white compound obtained after a few crystallizations from water, melted at 254-5°C (the reported[3] m.p.). Acid equivalent 308 (found) and 305, 312 (re-

ported[3]). Further repeated crystallizations from water could improve the m.p. upto 282-3°C. Acid equivalent 346.7 (found) and 350.0 (reqd.); I.R. (cm^{-1}) (KBr) 3535w, 3420w, 3080w, 3020vw, 2350vw, 1705ssh, 1685s, 1580w, 1460m, 1335s, 1280s, 1250s, 1170w, 1125m, 1050w, 970w, 842m, 810vw, 780w, 752s, 725vw, 680m, 570vw, 480m, 400m, 320s, 300w; ^{1}H NMR (DMSO)δ7.8 (8H, m, ArH); mass: m/z 350(M^+, n.o.), 316($M^+ - H_2O - O$), 288(316 − CO), 244(288 − CO_2), 243(244-H), 228(244 − O), 227(228 − H), 196(316 − C_6H_4: − CO_2), 195(196 − H), 181($C_6H_5COC_6H_4^+$), 152(196-CO_2), 151(195—CO_2), 139(195—C_2O_2), 105(196—AsO), 91(AsO^+).

Preparation of 1-*oxy*-1-*o*-*carboxyphenyl*)−3*H*−2, 1-*benzoxarsole*-3-*one* (4*a*)/(4*b*):

A solution of [(3b), (0.2g)] in TFA (10 cm^3) was refluxed for 4h and the excess solvent was removed by vacuum distillation. A gum was obtained which solidified after keeping *in vacuo* for 2hr. The crude compound thus obtained was recrystallized from dry benzene m.p. 282-3°C. The dehydration of (3b) to (4a)/(4b) can also be achieved by refluxing in benzene, treatment with anhydrous $AlCl_3$ in CH_2Cl_2 or heating at 110°C. Acid equivalent: 330.5 (found), 332.0 (reqd.); ^{1}H NMR (DMSO): δ7.83 ppm (8H, m, ArH); IR (cm^{-1}) (KBr): 3115vw, 3080vw, 2370vw, 1740s, 1685s, 1580w, 1450m, 1320m, 1285m, 1285w, 1270m, 1230m, 1160sh, 1130w, 1108w, 1040m, 1018w, 970vw, 842s, 800w, 770w, 745m, 715w, 675s, 470s, 392s, 320w, 270vw; the mass spectrum is identical with that of (3b).

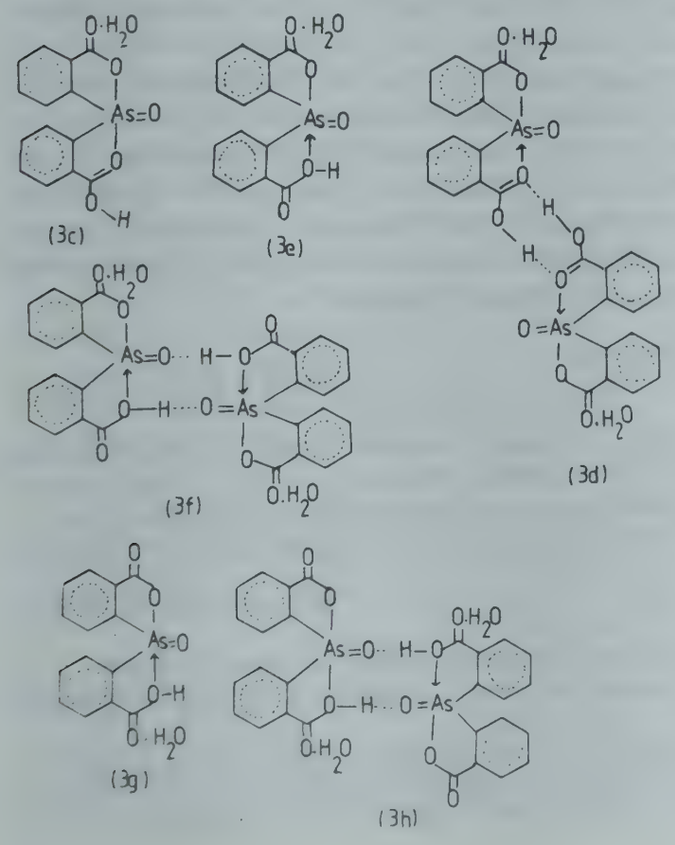

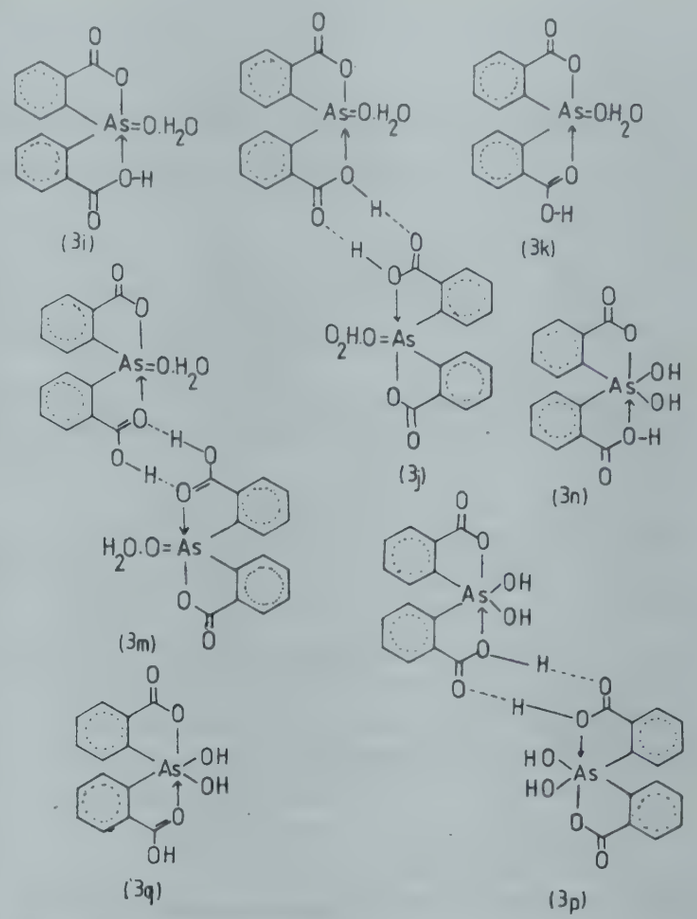

Preparation of Monosodium salt (5)

A solution of the compound [(3b), (0.2 g)] in MeOH (10 cm^3) was titrated against a saturated NaOH solution using phenolphthalein as indicator. The solid salt formed in solution was separated azeotropically m.p. 300°C; IR cm^{-1} (KBr) 3500b, 3085w, 2400vw, 2360vw, 1975vw, 1670bs, 1590s, 1460m, 1420m, 1340m, 1290m, 1260m, 1150m, 1130m, 1055m, 890s, 845m, 812w, 752s, 720w, 690m, 575vw, 480m, 395m, 258w.

Results and Discussion

The improvement in the melting point from 255 to 282-3°C and in the acid equivalent value from 308 to 346.7 on further recrystallizations from water proves that the compound (m.p. 255, acid equivalent 308) considered by Aeschlimann and McCleland[3] to be the anhydride (4a) is actually the contaminated form of its monohydrate [m.p. 282-3°C, acid equivalent 346.7 (Reqd 350)]. The anhydride (4a) has now been obtained for the first time by the treatment of the monohydrate with TFA/$AlCl_3$, refluxing in C_6H_6 or heating it at 110°C and has the expected acid equivalent value (Found 330.5, Reqd 332). The presence of water in the monohydrate is also confirmed by its TG curve which shows the loss of one water molecule

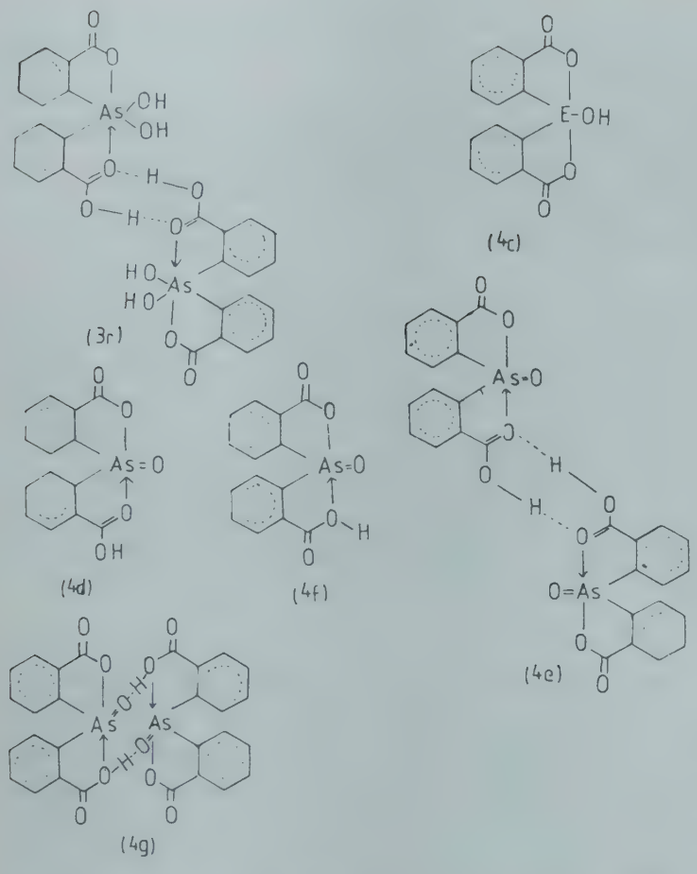

(Found 5%, Reqd 5.14%) between 80 and 107°C. This change is associated with the appearance of DTG and endothermic DTA peaks at 94°C. The anhydrous intermediate is stable upto 204°C and then loses half water molecule upto 284°C (DTG and endothermic DTA peaks at 258°C). The thermal analytical data of the anhydride (4a) show, as expected, the loss of only half water molecule at 204-284°C.

The appearance of two bands at 1705-45 and 1685 cm^{-1} in the $\nu C=O$ region in the solid state IR spectra of (4a) and its monohydrate suggests the presence of two types[a] of carbonyl groups but the absence of $\nu As=O$ (800-900 cm^{-1})[b], δOH (900-950 cm^{-1}) and νOH (2500-2700 cm^{-1}) bands[2] indicates the absence of the As = O[c] and dimeric CO_2H[d] groups. The high energy C = O band is missing in the spectrum of their monosodium salt (5) which contains only one $\nu C=O$ band at 1675 cm^{-1}. Thus, the band present at 1675-85 cm^{-1} in all the three spectra may be attributed to $\nu C=O$ of benzoxarsole ring[6]. The second $\nu C=O$ band present only in the spectra of the first two compounds may be ascribed to the monomeric CO_2H group. This assignment is supported by the appearance of ν_{OH} band at 3100 and 3545 cm^{-1} in the spectra of (4a) and its monohydrate respectively. The lowering of $\nu_{C=O}$ value from 1785 cm^{-1} (in $PhCO_2H$ monomer)[7] to 1745 cm^{-1}[e] in the spectrum of (4a) may be explained in terms of its solid state structure (4b) which contains intramolecular coordination of the carbonyl oxygen to arsenic(V). The further lowering of this $\nu_{C=O}$ value to 1705 cm^{-1}[f] in the spectrum of the monohydrate may be attributed to the simultaneous H-bonding of the carbonyl oxygen with the water molecule which is also H-bonded to the As = O oxygen in (3b). The absence of $\nu_{As=O}$ band and the presence of $\nu_{OH}(As-OH)$[g] band[8,9] at 2370 and 2350 cm^{-1} in the spectra of (4a) and its monohydrate respectively as well as the appearance of $\nu_{OH}(H_2O)$ band at 3420 cm^{-1} in the latter spectrum and its absence in the former are also consistent with the proposed solid phase structures (4b) and (3b).

As expected for structures (3b) and (4b), their PMR(DMSO) spectra are almost identical but all the aromatic protons appear as a single multiple at δ7.80 and 7.83 ppm respectively (cf ^1H NMR spectrum of (6)[9]. The molecular ion peak is not observed in the mass spectra of (3b) and (4b) which are identical and contain the highest m/z peak at 316 that may be explained in terms of the formation of a stable spirobicyclic diacyloxy arsorane (7) ion corresponding to $(M^+ - H_2O - O)$ and $(M^+ - O)$ ions respectively.

It can, therefore, be concluded that the attempt to prepare (3a) by Aeschlimann and McCleland[3] did not yield its anhydride (4a) as claimed but its impure isomer, monohydrate of (4a), which has been now purified and found to exist as the first novel tricyclic acyloxy (carboxy) arsorane structure (3b). The dehydration of the monohydrate (3b) yields the anhydride (4a) which exists as the first spirobicyclic acyloxy(carboxy)arsorane (4b). Thus, the anhydride (4a) and its monohydrate (3b) have been isolated for the first time during this reinvestigation.

[a]Rules out (3a) and (4c), [b]$\nu_{As=O}$ band at 890 cm^{-1} in (5); two bands at 800 and 845 cm^{-1} appear in each of the spectra of (3b), (4b) and (5). [c]Rules out (3c), (3d), (3g), (4a), (4d) and)4f). [d]Rules out (3d), (3j), (3m), (3p), (3r) and (4e).

[e]Rules out (4f) and (4g) for which $\nu_{C=O}$ is expected at 1785 cm^{-1}. [f]Rules out (3g), (3h), (3k) and (3i) since for the first three the band is expected at ~ 1740 cm^{-1} and for the last one at 1785 cm^{-1}. [g]Favours (3a), (3n), (3p), (3q) and (3r) but all of these fail to explain the observed acid equivalent value.

References

1 Parmar S S, Basra T S, Malhotra R M & Sandhu S S, Indian J Chem, **19A** (1980) 886.
2 Parmar S S, Basra T S, Bhasin H K, Jain A & Sandhu S S, *Indian J Chem*, **20A** (1981) 669.
3 Aeschlimann J A & McCleland M P, *J chem Soc*, (1924) 2025.
4 Pushkarna S K, Pannu M S & Parmar S S, *Indian J Chem*, **13** (1975) 195.
5 Barclay G A & Nyholm R S, *J Proc Roy Soc, New South Wales*, **81** (1947) 77.
6 Braunholtz J T & Mann F G, *J chem Soc*, (1957) 3285.
7 Taylor M D, Carter C P & Wynter C I, *J inorg nucl Chem*, **30** (1968) 1503.
8 Ferguson G & Macaulay E W, *Chem Commun*, (1968) 1288.
9 Bathala H K, Parmar S S, Saluja H K, Slawin A M Z & Williams D J, *J chem Soc Chem Commun*, (1987) 685.

Indian Journal of Chemistry
Vol. 27A, July 1988, pp. 609-612

Chlorothionitrene Complexes of Molybdenum: Part 1—Synthesis, Characterization & Reactivity of Mo(VI) Complexes

JYOTI SETH, MINU GUPTA & UMESH AGARWALA*
Department of Chemistry, Indian Institute of Technology, Kanpur 208 016

Received 24 *September* 1987; *revised and accepted* 23 *November* 1987

Chlorothionitrene complexes of Mo(VI) having 2,2′-bipyridine and 1,10-phenanthroline as coligands have been synthesized by reactions of Mo(II) carbonyl complexes with trithiazyl trichloride. The complexes have been characterized by microanalytical, electronic, vibrational and EPR spectral data.

Although considerable advances have been made in transition metal nitrosyl chemistry[1], only a few papers describing the isolated and well characterized analogous thionitrosyls have appeared in the literature[2-5]. Among several reagents used for thionitrosylation reactions, the behaviour of NSCl has been found to be intriguing and nature of the resulting S—N species attached to the metal center under different experimental conditions is hard to predict[6-12]. Among the various possible modes of bonding, the mode wherein NSCl is coordinated to the metal center as thionitrene group is supported by the works of many groups[7-10]. During our probe into the reactions of $(NSCl)_3$ with Mo(II) carbonyl derivatives, an interesting reaction was noted wherein the products showed the presence of NSCl bonded to the molybdenum as thionitrene group. The results of these studies are described herein.

Materials and Methods

All chemicals used were of reagent grade or comparable purity. Molybdenum hexacarbonyl was a gift sample from the Climax Molybdenum Company, USA. Molybdenum pentachloride, 2, 2′-bipyridine and 1,10-phenanthroline (all from Aldrich Chemicals, USA) were used as such. Sephadex LH-20 was purchased from the Sigma Chemical Co.

The starting materials, $[Mo(CO)_3(L-L)X_2]$[(L−L) = bipyridine or *o*-phenanthroline; $X_2 = I_2$ or Br_2], $[Mo(NSCl)Cl_4]_2$ and trithiazyl trichloride ($S_3N_3Cl_3$) were prepared by the literature methods[7,13,14]. The solvents were dried by the known procedures[15] and degassed just prior to use. All experiments were performed under N_2 blanket.

(a) *Reactions of* $S_3N_3Cl_3$ *with* $[Mo(CO)_3(L-L)X_2]$ [$(L-L$ = 2, 2′-*bipyridine*, 1, 10-*phenanthroline*; $X_2 = I_2$ *or* Br_2]

A solution of trithiazyl trichloride (0.03 mmol) in dichloromethane (10 ml) was added to a stirred solution of $[Mo(CO)_3(L-L)X_2]$ (0.2 mmol) in dichloromethane (15 ml). Gas evolution occurred. The reaction mixture was stirred for 1 hr and upon concentration under reduced pressure to near dryness *in vacuo* a green brown residue (compound-I) was obtained. It was washed with a little benzene, thoroughly with pet-ether and recrystallized from dichloromethane-pet ether and dried *in vacuo.*

The product (I) was further purified on a column (25 cm × 2.5 cm) of Sephadex LH-20. Elution with dichloromethane at a rate of ~2 ml/min afforded greenish brown band which moved as a single band throughout the column. The eluate was concentrated to about 10 ml under reduced pressure and the concentrate kept at 0°C for a few days whereupon micro-sized brown crystals of I were deposited on the walls of the container. These were collected before the solution was fully concentrated, and washed successively with a little benzene, pet ether and dried *in vacuo.*

The same compound (I) was also obtained as a powdery greenish brown solid from the concentrate of the eluate by precipitating with light pet ether. It was washed thoroughly with benzene, pet ether and dried *in vacuo* (yield, 40%).

Attempts to purify the compounds on silica gel or alumina column failed because of their decomposition on the column. In both the cases a brown insoluble band was formed on top of the column which did not move with any solvent.

(b) *Reactions of* 2,2′-*bipyridine and* 1,10-*phenanthroline with* $[Mo(NSCl)Cl_4]_2$

A stirred suspension of $[Mo(NSCl)Cl_4]_2$ (0.1 mmol) in dichloromethane (15 ml) was treated with stoichiometric amount of the base and stirring was continued for about 1 hr. The solution was filtered and on the addition of light pet ether to the greenish brown filtrate a solid compound was precipitated, which was collected and washed with excess of benzene. The

precipitate was further freed from traces of impurities by passing its CH_2Cl_2 solution through Sephadex LH-20 column, and the eluate was treated as described in (a) above. The compound, thus obtained, was found to have the same composition as prepared in (a), viz. $[Mo(NSCl)Cl_4(L-L)]$ (yield, 60%).

(c) *Thermal decomposition of* $Mo(NSCl)Cl_3X'(L-L)(X' = Cl\ or\ Br)$

Accurately weighed $[Mo(NSCl)Cl_3X'(L-L)]$ (100 mg) was heated at 220° for 4 hr in a two-necked closed round bottom flask (25 ml capacity) having inlet and outlet tubes. Through the inlet tube a slow continuous stream of nitrogen gas was allowed to flow and the ensuing gases from the outlet tube were dissolved in water. After gas evolution had practically ceased, the water containing the dissolved gaseous products was analysed for sulphur and chloride. The colour of the left-over compound in the flask was changed to maroon.

In another experiment a known weight of $[Mo(NSCl)Cl_3X'(L-L)]$ was taken on a small watch glass, heated to 220° for 4 hr in an oven, cooled and subsequently weighed. The mass loss on heating corresponded to an atom of sulfur and two chlorine atoms per molecule of complex. The mass loss corresponded to the amount of sulfur and chloride found in water of the above experiment.

Physical and spectral measurements

General information concerning instrumentation and analyses of the complexes is described in a previous paper[16]. ESR spectra in dichloromethane at room and the liquid nitrogen temperatures and X-ray powder patterns of the complexes were recorded using Century series 109E Line EPR spectrophotometer and 150-Debye Flex 2002 diffractometer, respectively.

Results and Discussion

The reaction of $S_3N_3Cl_3$ with $[Mo(CO)_3(L-L)X_2]$ in dichloromethane proceeds rapidly to yield complexes of the type $[Mo(NSCl)Cl_3X'(L-L)]$ (cf. Table 1). These complexes are highly soluble in $POCl_3$ producing red coloured solutions which on concentration give moisture-sensitive products possibly $[Mo(NSCl)Cl_3X'(L-L)]$, $POCl_3$. The compounds are also soluble in halosubstituted organic solvents yielding solutions from which original complexes can again be precipitated by adding petroleum ether. The complexes are decomposed on treatment with methanol.

The compounds are not very stable at room temperature decomposing slowly to a maroon products. These can, however, be preserved at low temperature (~ 0°C) for a few days. On thermolysis, they lose mass corresponding to about one mol of SCl_2 per mol of the complex. It is further corroborated by the analyses of hydrolysed gaseous products which correspond to approximately one mol of sulphur and a little more than two mol of halide per mol of the complex. It appears that (i) the compounds on heating lose initially a molecule of SCl from the coordinated NSCl group followed by the loss of another chloride ion in order to keep the charge balance and (ii) Mo(VI) during decomposition process gets partially reduced to Mo(V) to yield polymeric nitrido complexes of molybdenum with the evolution of chlorine[18]. Similar observations have been reported earlier for other thionitrene complexes[7].

The IR spectra of the complexes exhibit three bands of moderate intensity in the region 900-1000 cm^{-1}, assigned to NSCl moiety bonded as thionitrene group ($=N=S-Cl$)[7,10,17]. The earlier works[7-9] on thionitrene complexes report only one band in this region. The splitting could possibly be attributed to interaction of thionitrene group with other coordinated ligands. Similar splitting has also been observed in complexes having $POCl_3$ as coligand[7]. These bands do not appear in the IR spectra of the maroon products obtained on decomposition. The intense band at 940 cm^{-} in the maroon products is assigned to $\nu_{Mo\equiv N}$. Though the $\nu_{Mo\equiv N}$ appears slightly in the lower wavenumber region as compared to the one usually found in most of the nitrido complexes (~ 1000 cm^{-1}), the lowering may possibly be caused by partial reduction of Mo(VI) to Mo(V) at elevated temperatures[18,19]. In the absence of single crystal X-ray structure data and in the light of their insolubility in any solvent, the IR diagnostic criterion for the presence of $Mo\equiv N$ bond in +5 oxidation state in these complexes has only a limited value. The presence of Mo(V) species in these complexes is however corroborated by their magnetic properties and the ESR spectral data discussed later.

The electronic spectra of the complexes exhibit fairly strong ligand to metal charge transfer bands characteristic of Mo(VI) compounds[20]. Besides, the intraligand bands of the coligands (bipyridine or *o*-phenanthroline, ~ 300 nm), the compounds display bands at 250, 375 and 500 nm (cf. Table 1). The 250 nm band can conveniently be assigned to $\pi(X) \rightarrow Mo(VI)$ CT transition[21]. The 500 nm band is highly unsymmetrical and is sometimes found to be split. The 375 nm band along with one of the components of the 500 nm band is attributed to π(diimine) $\rightarrow$ Mo(VI) CT transition[21]. The second component of the unsymmetrical 500 nm band could probably arise due to CT to the metal involving thionitrene group. In general, the CT band of the type $\pi(\text{diimine}) \rightarrow M(t_{2g})$ show marked solvatochromism[21]. Preliminary sol-

Table 1—Analytical Data, Colour, Melting Points Thermal Decomposition Data and Electronic Spectral Data of Compounds

Sl. No.	Compound, colour*, m.p.	Found (calc)%						Thermal decomposition			Electronic spectra λ_{max} (nm)
		C	H	N	S	X	Mo	Mass (% loss)	S	X	
I	$[Mo(NSCl)Cl_4(Bipy)]$	25.1	1.7	8.7	6.4	37.4	19.4	22.8	6.3	14.6	250, 320, 380, 476,
	G, 220 (d)	(25.3)	(1.6)	(8.8)	(6.7)	(37.1)	(20.1)	(21.6)	(6.7)	(14.9)	510
II	$[Mo(NSCl)Cl_3Br(Bipy)]$	23.1	1.7	8.4	5.7	41.7	17.9	20.9	5.2	13.8	240, 318, 390, 476,
	GB, 230 (d)	(23.0)	(1.5)	(8.0)	(6.1)	(42.6)	(18.4)	(19.7)	(6.1)	(13.6)	515
III	$[Mo(NSCl)Cl_4(o\text{-phen})]$	29.4	2.1	7.9	5.8	36.2	20.0	22.1	5.8	14.8	240, 300, 370, 475,
	G, 220 (d)	(28.8)	(1.6)	(8.4)	(6.4)	(35.4)	(19.2)	(20.6)	(6.4)	(14.2)	510
IV	$[Mo(NSCl)Cl_3Br(o\text{-phen})]$	26.8	2.1	8.2	6.2	39.7	16.8	20.2	5.2	13.6	250, 300, 385, 475
	GB, 220 (d)	(26.4)	(1.4)	(7.9)	(5.9)	(40.8)	17.6)	(18.9)	(5.9)	(13.0)	520
V	$[Mo(N)Cl_3(Bipy)]_n^{\dagger}$	33.8	1.8	11.9	1.5	26.8	26.3				
	M,	(32.1)	(2.1)	(11.2)	—	(28.8)	(25.7)				
VI	$[Mo(N)Cl_2Br(Bipy)]_n^{\dagger}$	29.9	2.5	10.4	1.6	32.4	24.8				
	M,	(28.7)	(1.9)	(10.0)	—	(36.1)	(22.9)				
VII	$[Mo(N)Cl_3(o\text{-phen})]_n^{\dagger}$	37.7	2.8	11.4	1.8	23.1	26.8				
	M,	(36.2)	(2.0)	(10.6)	—	(26.9)	(24.2)				
VIII	$[Mo(N)Cl_2Br(o\text{-phen})]_n^{\dagger}$	34.2	2.4	10.8	1.2	32.0	23.1				
	M,	(32.6)	(1.8)	(9.5)	—	(34.1)	(21.7)				

* G = green, GB = greenish brown, M = maroon.

† The analyses of these compounds do not exactly match the calculated values, possibly because of mixing of the reduction products.

vent dependent studies indicate similar behaviour of one of the components of 500 nm band. We have tentatively utilized this as a criterion for differentiating the CT bands listed in Table 1.

All the compounds $[Mo(NSCl)Cl_3X'(L-L)]$ are diamagnetic at room temperature indicating that metal is present in the highest oxidation state (d^0-configuration). The absence of any signal in the ESR spectra of the complexes at room and liquid nitrogen temperatures confirmed their diamagnetic behaviour.

The maroon products obtained on thermal decomposition exhibit partial paramagnetism and their magnetic moments fall in the range of 1.1 to 1.2 B.M. The latter range is lower than the one expected for a d^1-system suggesting partial reduction of Mo(VI) during decomposition of thionitrene complexes. The presence of Mo(V) in the decomposition product was further confirmed by the powder ESR spectra of the maroon compounds which showed typical spectra. The values of g_1, g_2, g_3 and $\langle g \rangle$ were calculated. For $[MoNCl_3bipy]$, $g_1 = 1.9698$, $g_2 = 1.9455$, $g_3 = 1.9096$ $\langle g \rangle = 1.94$; and for $[MoNCl_3o\text{-phen}]$, $g_1 = 1.9873$, $g_2 = 1.9315$, $g_3 = 1.8901$, $\langle g \rangle = 1.9367$.

The striking and conclusive evidence for establishing the proposed formulation of the complexes described herein and their characterisations has been obtained by carrying out reactions of diimines (bipyridine and *o*-phenanthroline) with coordinatively unsaturated $[Mo(NSCl)Cl_4]_2$ complex, assuming no change in the nature of NSCl bonding during the course of reactions, viz. Mo = N = S − Cl type. This type of bonding in $[Mo(NSCl)Cl_4]_2$ complexes has been proved by single crystal X-ray studies[7]. The identical nature of the complexes thus prepared and the ones described earlier (chemical analyses, chemical and spectral behaviour and X-ray powder patterns) has been taken as a conclusive evidence for the same type of NSCl bonding in both the complexes. With this presumption along with other evidence it has been concluded that NSCl in the complexes is bonded as a thionitrene group, viz. Mo = N = S − Cl.

Acknowledgement

One of the authors (Ms J Seth) thanks the CSIR, New Delhi, for the award of a senior research fellowship. The authors acknowledge Dr. George A. Trigdinos, Climax Molybdenum Co., USA, for the kind supply of molybdenum hexacarbonyl.

References

1 Johnson B F G & McCleverty T A, *Prog Inorg Chem*, **7** (1966) 27; Connelly N G, *Inorg chim Acta Rev*, **6** (1977) 47.

2 Pandey K K & Agarwala U C, *Z anorg allg chem*, **461** (1980) 231.

3 Pandey K K, Raju D M K, Nigam H L & Agarwala U C, *Proc Indian Natl Sci Acad*, **48** (1982) 16.

4 Roesky W H & Pandey K K, *Adv Inorg Chem Radiochem*, **26** (1982) 337.

5 Kelly P F & Woollins J D, *Polyhedron*, **5** (1986) 607.

6 Chivers T & Edelmann F, *Polyhedron*, **5** (1986) 1667.

7 Kynast U & Dehnicke K, *Z anorg allg Chem*, **502** (1982) 29.

8 Ulrich K, Muller U & Dehnicke K, *Z anorg allg Chem*, **508** (1984) 26.

9 Kynast U, Klingelhofer P, Muller U & Dehnicke K, *Z anorg allg Chem*, **515** (1984) 61.
10 Seth J, Gupta M & Agarwala U C, *Bull Chem Soc Japan*, (In press).
11 (a) Eicher J, Klingelhofer P, Muller U & Dehnicke K, *Z anorg allg Chem*, **514** (1984) 79; (b) Kynast U, Conradi E, Muller U & Dehnicke K, *Z Naturforsch*, **39b** (1984) 1680.
12 Wadle H, Conradi E, Muller U & Dehnicke K, *Z Naturforsch*, **41b** (1986) 429 and references therein.
13 Stiddard M H B, *J chem Soc (A)*, (1966) 317.
14 Magiure K D, Smith J J & Jolly W L, *Chemy Ind*, **39** (1963) 334.
15 Vogel A I, *A text book of practical organic chemistry*, (Longmans Green London) (1980) pp. 264.
16 Rao K M, Mishra L & Agarwala U C, *Polyhedron*, **5** (1986) 1491.
17 Muller U, Klingelhofer P, Kynast U & Dehnicke K, *Z anorg allg Chem*, **520** (1985) 18.
18 Kruger K & Dehnicke K, *Z Naturforsch*, **34b** (1979) 1343.
19 Chatt J & Dilworth J R, *Chem Commun* (1984) 517.
20 Larson M L & Moore W F, *Inorg Chem*, **5** (1966) 801.
21 Lever A B P, *Inorganic electronic spectroscopy* (Elsevier, New York) 1984 pp. 227.

Indian Journal of Chemistry
Vol. 27A, July 1988, pp. 613-616

Ternary Complexes of Copper(II) with Malonic Acid & O,O; O,N & N,N Donor Ligands

G VENKAT NARAYANA, S J SWAMY & P LINGAIAH*
Department of Chemistry, Kakatiya University, Warangal 506 009

Received 1 *June* 1987; *revised* 11 *August* 1987; *accepted* 19 *October* 1987

The formation constants of the ternary complexes of Cu(II) with malonic acid (O,O donor ligand) as a primary ligand and oxalic acid, maleic acid, fumaric acid, succinic acid, phthalic acid, salicylic acid, pyrocatechol (O,O donor ligands); *o*-aminophenol, 8-quinolinol (O,N donor ligands); and 2,2′-bipyridyl and ethylenediamine (N,N donor ligands) as secondary ligands have been evaluated *p*H-metrically at 25°C and $\mu = 0.1M$ (KNO_3). The value of $\Delta \log K$ ($\log K^{MA}_{MAL} - \log K^{M}_{ML}$) is more when the coordination occurs via N,N donor ligands and it is less for the O,O donor ligands. For the O,N donor ligands, the value is midway between those observed for pure O,O and N,N donor ligands.

Sigel and coworkers[1-4] and Bhattacharya and coworkers[5-7] have observed that in the case of ternary complexes of N,N donor ligands like 2,2′-bipyridyl and 1,10-phenanthroline as primary ligands the Δ log K values are positive if secondary ligands are O,O donors, negative if the secondary ligands are N,N donors and midway between the two if the secondary ligands are N,O donors. In the absence of a similar type of study with O,O donor ligands, we thought it worthwhile to undertake the present investigation involving O,O donor ligand as primary ligand and O,O; O,N and N,N donor ligands as secondary ligands. In the present paper the stability constants of the ternary complexes of copper(II) with malonic acid as the primary ligand and oxalic acid (OA), maleic acid (MA), fumaric acid (FA), succinic acid (ScA), phthalic acid (PhA), salicylic acid (SA), pyrocatechol (PC) (O,O donor ligands); *o*-aminophenol (*o*-AP), 8-quinolinol (8-HQ) (O,N donor ligands); and 2,2′-bipyridyl (bipy), ethylenediamine (en) (N,N donor ligands) as secondary ligands, evaluated *p*H-metrically at 25° and $\mu = 0.1M$ (KNO_3) are reported.

Materials and Methods

All the chemicals used were of AR grade. The ligands were recrystallized or distilled before use and their purity was checked by TLC and melting point or boiling point determinations. Copper(II) solution was prepared by dissolving required amount of cupric nitrate in CO_2-free doubly distilled water and standardized by the literature method[8]. All the ligand solutions were prepared in doubly distilled water except the solution of 8-HQ, which was prepared in 1% ethanol.

An Elico digital *p*H-meter model LI-120 with glass and calomel electrode assembly (accuracy ± 0.01 *p*H unit) was used for *p*H measurements. It was standardized against standard buffers of *p*H 4.00 and 9.20 before each titration. The following sets of solutions were titrated against carbonate-free $0.2M$ NaOH at 25° and $\mu = 0.1M$ (KNO_3): (i) HNO_3 ($4 \times 10^{-3}M$); (ii) i + ligand A ($2 \times 10^{-3}M$); (iii) ii + Cu(II) ($2 \times 10^{-3}M$); (iv) i + ligand L ($2 \times 10^{-3}M$); (v) iv + Cu(II) ($2 \times 10^{-3}M$); and (vi) iii + ligand L ($2 \times 10^{-3}M$).

Results and Discussion

In all the systems it was observed that the *p*H of precipitation of MAL complexes was much higher than that of binary systems (MA and ML). Further evidence for mixed ligand complexes was provided by the deviation of mixed ligand titration curve from the composite curve. The latter curve was drawn theoretically by the graphical addition of 1 : 1 ML/MA curve to the titration curve of the free ligand A/L.

From the tiration curves it was observed that the interaction of the two ligands with the central metal ion in different systems occurred in three different ways: (i) The ligands PC, *o*-AP, bipy, en and Maln interact with the metal ion in step-wise manner: $M + A \rightleftharpoons MA$; $MA + L \rightleftharpoons MAL$; $M + L \rightleftharpoons ML$; $ML + A \rightleftharpoons MAL$; (ii) the ligands SA, 8-HQ and Maln interact simultaneously with the metal ion to give a ternary complex: $M + A + L \rightleftharpoons MAL$; and (iii) the ligands OA, MA, FA, ScA, PhA and Maln react with the metal ion to form binary complexes which disproportionate to give the ternary complex: $M + A \rightleftharpoons MA$; $M + L \rightleftharpoons ML$; $MA + ML \rightleftharpoons MAL + M$.

Table 1—Formation Constants of Ternary Complexes (Malonic Acid (A)-Cu(II)-Ligand (L) Complexes)

[$\mu = 0.1M$ (KNO_3); log $K^{M}_{MA} = 4.83$; log $K^{MA}_{MA_2} = 3.28$; and temp. = 25°C]

Ligand (L)	log K^{M}_{ML}	log $K^{ML}_{ML_2}$	log β_{MAL}	Δ log K	log X
Oxalic acid	4.28	3.97	8.54	−0.57	0.72
Maleic acid	4.02	2.82	9.39	0.54	3.83
Succinic acid	3.23	—	8.16	0.10	—
Fumaric acid	3.19	—	6.28	−1.74	—
Phthalic acid	3.49	2.59	9.16	0.84	4.13
Salicylic acid	10.83	8.05	16.40	0.74	5.81
Pyrocatechol	11.28	8.62	16.74	0.63	5.48
o-Aminophenol	7.81	6.92	13.51	0.87	4.18
8-Quinolinol	12.85	10.86	18.99	1.31	6.16
2,2′-Bipyridyl	8.00	5.60	14.61	1.78	7.51
Ethylenediamine	10.31	8.60	15.30	0.16	3.58

The formation constants of the ternary complexes have been evaluated by different methods[9,10] depending upon the nature of the interaction between the metal ion and ligands, and the values are given in Table 1, along with those of the binary systems.

The stability constants of ternary complexes are characterized by the difference in stability constants, i.e. Δ log K, which is given by Eq. (1), and the disproportionation constant log X which is given by Eq. (3), the equilibrium being represented by Eq. (2).

$$\Delta \log K = (\log K^{MA}_{MAL} - \log K^{M}_{ML}) = (\log K^{ML}_{MLA} - \log K^{M}_{MA}) \quad \ldots (1)$$

$$MA_2 + ML_2 \rightleftharpoons 2MAL; \quad X = \frac{(MAL)^2}{(MA_2)(ML_2)} \quad \ldots (2)$$

$$\log X = 2 \log \beta_{MAL} - (\log \beta_{MA_2} + \log \beta_{ML_2}) \quad \ldots (3)$$

The values expected for Δ log K and log X, from statistical arguments[11] are −0.3 to −0.9 and 0.6, respectively. Higher values of Δ log K and log X indicate that the ternary complex formation is favoured over the binary ones.

The data presented in Table 1 show that the experimental Δ log K and log X values are greater than the statistical ones, indicating that apart from the statistical factors the stability of the ternary complexes is also governed by other factors like ring size of chelate, neutralization of charge in the ternary complex formation and formation of π-bonds. The last point is important for achieving a large stability of the ternary complex. The Δ log K values in the case of terna· complexes, CuAL, where L coordinates either through N,N or O,N atoms are positive. The Δ log K values are more positive for N,N ligands whereas in the case of O,O ligands the Δ log K values are less positive or small negative. This can be explained based on the metal-ligand interactions and electron repulsions.

It is observed that in the ternary complex of Cu(II)-Maln-bipy, bipy first interacts with the metal ion to form $(Cu\text{-bipy})^{2+}$. The ligand Maln then interacts with this complex to give the ternary complex. The greater stability of the bipy ternary complex is because of Cu → bipy π-interaction, and hence the electron density on the metal ion is reduced and effective electronegativity of $(Cu\text{-bipy})^{2+}$ is almost the same as that of Cu(II). Thus the σ-bonding tendency of Maln to combine with $(Cu\text{-bipy})^{2+}$ is not significantly lowered, consequently the Δ log K is more positive. No such π-interactions are expected with en. Hence, a small positive Δ log K value observed in its ternary complex may be due to the formation of neutral ternary complex and a five- and six-membered chelate rings in the ternary complex. The log X values also follow the same trend.

The Δ log K values are less positive in ternary complexes with O,N donors. The Δ log K of 8-HQ binary complex is less than that of the bipy ternary complex. This is due to the fact that the π-interactions are less with 8-HQ as it contains only one tertiary nitrogen as compared to two in bipy. The Δ log K is large for 8-HQ ternary complex than that for *o*-AP complex. This is due to greater π-interaction between metal and 8-quinolinol in comparison to that in *o*-AP (nitrogen atom being primary in *o*-AP while tertiary in 8-HQ). The log X values also parallel to Δ log K values.

The lesser magnitude of positive Δ log K values with O,O donor ligands is due to the fact that no π-interactions are possible in these ligands. The greater values of Δ log K with PhA, SA and PC may be due to the presence of an aromatic ring. The order of stabilities in the case of aromatic O,O donor ligands is: PhA > SA > PC. This order may be explained as follows: The mixed ligand chelate is formed by the simultaneous replacement of water molecules from the coordination sphere of Cu(II) ion with the formation of four Cu – O bonds. Since the carboxylate oxygen is not directly bound to the benzene nucleus, it therefore, adjusts stereochemically more easily than the phenolate oxygen which is directly attached to the benzene nucleus. Greater strain in Cu – O bond is, therefore, expected in the latter case. The coulombic repulsion between the end oxygens will be more when both O,O donor atoms are phenolic oxygens (due to higher electronegativity) than when they are carboxylic oxygens. Thus, the Δ log K should be higher when L coordinates through two carboxylate oxygens (PhA) than the two phenolate oxygens (PC). An intermediate value is obtained when L is SA, which contains one carboxylate and one phenolate oxygen.

The data in Table 1 also show that the log X values are not in accordance with the Δ log K values. This trend may be explained as follows: Generally for the systems to which Eqs. (3) and (4) are valid, the contribution to log X is more,

$$\log X = (\log K^{MA}_{MAL} - \log K^{ML}_{ML_2}) + (\log K^{ML}_{MAL} - \log K^{MA}_{MA_2}) \quad \ldots (4)$$

if the difference between the stepwise stability constants, log K_1 and log K_2, is more. Since the difference between the log K_1 and log K_2 values of Cu(II)-PhA system is small and those of SA and PC are more, the log X value for PhA is less and for SA and PC complexes it is more.

The stability order with respect to the aliphatic dicarboxylic acids is: MA > ScA > OA > FA. The higher stabilities of maleic (MA) and succinic (ScA) acid complexes, eventhough maleate or succinate ions form seven-membered rings in the ternary complex in contrast to a five-membered ring by oxalate, may be due to the fact that the strain involved in the Cu(II)-Maln-OA chelate may be more than in Cu(II)-Maln-ScA due to the greater repulsion between O,O of Maln and of OA. Similar observations have been recorded by Mali[12] and Kapoor[13]. They observed that Zn(II)-citric-oxalic acid and Zn(II)-NTA-oxalic acid complexes are less stable than the corresponding malonic acid and succinic acid complexes. The higher stability of maleic acid complex is due to the presence of double bond in the ligand which increases the stability of the complex due to exocylic conjugation. The furmaric acid, due to its *trans*-geometry may impart greater strain during chelate formation, so it forms less stable ternary complex.

Further, the stability of these complexes may also be explained in terms of electron repulsion. In the formation of binary complexes there is electron repulsion between the metal ion *d*-electrons and lone pair of electrons present on the coordinating atom of the ligand. However, in the case of ternary complexes of bipy, due to the back donation of electrons through π-bonding, the electron density on Cu(II) is reduced, hence the repulsion between the metal *d*-π-electrons and the additional lone pair of electrons over the second ligand in the ternary complex is less. There is no extra lone pair present on π-bonding nitrogen atom and hence this effect is not felt in N,N donor ligands. In O,N donor ligands, there are lone pairs of electrons over oxygen. The repulsion between oxygen atom of O,N ligands and that of O,O of Maln takes place and the Δ log K is decreased. In the case of L, coordinating through O,O atoms there are lone pair of electrons on both the ligands, so greater repulsion is possible, which further decreases the Δ log K values.

From the foregoing results it can be concluded that the O,O donor ligands form more stable ternary complexes with N,N donor ligands than with O,O donor ligands. The stability of mixed O,N donor ligands is midway between those of pure O,O and N,N donor ligands.

Acknowledgement

One of the authors (GVN) thanks the CSIR, New Delhi, for the award of a research fellowship.

References

1 Beck M T, *Chemistry of complex equilibria* (Van Nostrand, New York) 1970, 174.
2 Griesser R & Sigel H, *Inorg Chem*, **9** (1970) 1238.
3 Walker F A, Sigel H & Mc Cormick D B, *Inorg Chem*, **11** (1972) 2756.
4 Huber P R, Griesser R, Prijs B & Sigel H, *European J Biochem*, **10** (1969) 238.
5 Chidambaram M V & Bhattacharya P K, *J inorg nucl Chem*, **32** (1970) 3271.
6 Doraswamy Uma & Bhattacharya P K, *Indian J Chem*, **13** (1975) 1069.

7 Patel J P, Patel V K K & Bhattacharya P K, *Indian J Chem*, **21** (1982) 590.
8 Schwazenbach G, *Complexometric titrations* (Interscience, New York), 1957, 77.
9 Miss Parikh P L & Bhattacharya P K, *Indian J Chem*, **12** (1974) 402.
10 Ramamoorthy S & Santappa M, *J inorg nucl Chem*, **33** (1971) 1775.
11 Sigel H, *Angew Chem (Intn Edn)*, **14** (1975) 394.
12 Mali B D & Sen D N, *Indian J Chem*, **20A** (1981) 695.
13 Kapoor K, Kumari V, Sharma P C & Chaturvedi G K, *J Indian Chem Soc*, **54** (1977) 685.

Indian Journal of Chemistry
Vol. 27A, July 1988, pp. 617-621

Synthesis & Structural Studies of Oxovanadium(IV), Manganese(II), Iron(II), Cobalt(II), Nickel(II) & Copper(II) Complexes with New Tridentate Schiff Bases having ONO & ONN Donor Systems

(Miss) L NALANDA SHARADA & M C GANORKAR*
Department of Chemistry, Osmania University, Hyderabad 500007

Received 12 *May* 1987; *revised* 18 *September* 1987; *rerevrised and accepted* 11 *December* 1987

Two new schiff bases have been synthesized by the condensation 6-chloro-4-hydroxy-3-acetylcoumarin with *o*-aminophenol (Cl-HACAP) and 2,6-diaminopyridine (Cl-HACDPy). Complexes of oxovanadium(IV), manganese(II), iron(II), nickel(II) and copper(II) with Cl-HACAP and Cl-HACDPy have been prepared. Molar conductance measurements indicate that the complexes are non-electrolytic in nature. The analytical data show that the metal to ligand ratio in all the complexes is 1:1. The complexes are characterized on the basis of analytical data, conductivity measurements, TG analysis, magnetic moment measurements and spectral data. The IR data show that the ligands act as tridentate ONO and ONN donor systems.

Although transition metal complexes of 6-chloro-4-hydroxy-3-acetylcoumarin are known[1], comparatively much less work has been done on the transition metal complexes of the schiff bases derived from it. Hence we thought it of interest to prepare schiff bases of 6-chloro-4-hydroxy-3-acetylcoumarin with two different amines, i.e., *o*-aminophenol and 2,6-diaminopyridine, and study their complexing behaviour with oxovanadium(IV), manganese(II), iron(II), cobalt(II), nickel(II) and copper(II).

Materials and Methods

All the chemicals used were of AR quality. 2,6-Diaminopyridine (Riedel), malonic acid (Riedel), nitrobenzene (Wilson Lab), *p*-chlorophenol (E. Merck) and aluminium chloride (Ranbaxy) were used in the preparation of ligands.

The schiff bases were prepared by refluxing 6-chloro-4-hydroxy-3-acetylcoumarin with *o*-aminophenol (1:1, in ethanol) and 2,6-diaminopyridine (1:1, in methanol) for one hour when the two ligands were obtained as colourless solids. Their purity was checked by TLC and m.p. determination: Cl-HACAP (m.p. 230 ± 2°C), Cl-HACDPy (m.p. 200-5°C).

The metal chelates of Cl-HACAP were synthesized by refluxing ethanolic solutions of respective metal chlorides (0.01 mol) and the ligand (0.01 mol) for about 2-3 hr and keeping the reaction mixtures overnight. The metal chelates of Cl-HACDPy were synthesized by refluxing the methanolic solutions of respective metal chlorides (0.01 mol) and the ligand (0.01 mol) for about an hour. The respective metal chelates that separated out were filtered, washed successively with hot solvent followed by pet. ether (60-80°) and dried *in vacuo*. In the case of oxovanadium(IV) and Fe(II) complexes, vanadyl sulphate and aqueous ethanolic solution of ferrous ammonium sulphate were used.

The complexes were analysed for metal contents employing standard procedures after destroying the organic matter with a mixture of nitric and hydrochloric acids. Sulphur and chlorides were estimated as $BaSO_4$ and AgCl respectively[2]. Nitrogen was determined by microanalysis.

Electrical conductances of 1×10^{-3} *M* solutions of all complexes in DMF were measured by conductivity meter model D_1-909 (Digism electronics) and digital direct reading conductivity meter 304 (Systronics). The thermogravimetric analysis was carried out on a manually operated thermobalance, with the heating rate of 5° per minute. The magnetic susceptibilities of the complexes were determined by Gouy method using $Hg[Co(NCS)_4]$ as the calibrant and the experimental magnetic susceptibilities were corrected for diamagnetism[3]. Electronic spectra were recorded in nujol mull at room temperature on UV-visible spectrophotometer DMR-21 and ESR spectra were recorded on a JEOL-JES-F3X spectrometer. The infrared spectra of the ligand and the complexes were recorded in KBr on a Perkin-Elmer spectrophotometer model 627.

Results and Discussion

All the complexes reported here are coloured and stable towards air and moisture. Most of them are insoluble in common organic solvents

Table 1 – Analytical Data of Complexes of Cl-HACAP & Cl-HACDPy

Ligand/Complex	Found (Calc) %				
	Metal	C	H	N	Cl
Cl-HACAP	–	60.00	3.55	4.25	10.92
$C_{17}H_{12}O_4NCl$		(62.29)	(3.05)	(4.27)	(10.84)
VO(II)-[Cl-HACAP]	12.95	51.82	2.60	3.58	9.21
($V C_{17}H_{10}O_5NCl$)	(12.91)	(51.72)	(2.53)	(3.54)	(9.00)
Mn(II)-[Cl-HACAP.2H_2O]	13.20	48.80	3.40	3.40	8.50
($Mn C_{17}H_{14}O_6NCl$)	(13.13)	(48.75)	(3.34)	(3.34)	(8.48)
Fe(II)-[Cl-HACAP.2H_2O]	13.35	48.70	3.25	3.34	8.50
($Fe C_{17}H_{14}O_6NCl$)	(13.31)	(48.65)	(3.33)	(3.33)	(8.46)
Co(II)-[Cl-HACAP.2H_2O]	14.00	48.30	3.35	3.35	8.42
($Co C_{17}H_{14}O_6NCl$)	(13.95)	(48.29)	(3.31)	(3.31)	(8.40)
Ni(II)-[Cl-HACAP.2H_2O]	14.00	48.32	3.46	3.46	8.40
($Ni C_{17}H_{14}O_6NCl$)	(13.90)	(48.30)	(3.31)	(3.31)	(8.78)
Cu(II)-[Cl-HACAP]	16.30	52.30	3.60	3.45	9.12
($Cu C_{17}H_{10}O_4NCl$)	(16.25)	(52.17)	(2.55)	(3.58)	(9.07)
Cl-HACDPy	–	58.00	3.62	12.39	10.75
$C_{16}H_{12}O_3N_3Cl$		(58.4)	(3.640)	(12.74)	(10.769)
VO(II)-[Cl-HACDPy]	10.25	38.90	2.50	8.49	7.09
($V C_{16}H_{13}O_8N_3ClS$)*	(10.32)	(38.93)	(2.633)	(8.509)	(7.192)
Mn(II)-[Cl-HACDPy]	12.595	44.12	2.95	9.40	16.1
($Mn C_{16}H_{13}O_4N_3Cl_2$)	(12.598)	(44.06)	(2.981)	(9.63)	(16.052)
Fe(II)-[Cl-HACDPy]	10.50	37.18	2.92	8.12	6.79
($Fe C_{16}H_{15}O_9N_3ClS$)*	(10.81)	(37.2)	(2.904)	(8.1319)	(6.873)
Co(II)-[Cl-HACDPy]	13.32	43.58	2.92	9.52	15.85
($Co C_{16}H_{13}O_4N_3Cl_2$)	(13.39)	(43.66)	(2.954)	(9.544)	(15.90)
Ni(II)-[Cl-HACDPy]	13.32	43.58	2.58	9.52	15.50
($Ni C_{16}H_{13}O_4N_3Cl_2$)	(13.34)	(43.68)	(2.95)	(9.549)	(15.91)
Cu(II)-[Cl-HACDPy]	13.72	41.52	3.22	9.12	15.25
($Cu C_{16}H_{15}O_5N_3Cl_2$)	(13.73)	(41.50)	(3.242)	(9.078)	(15.1)

*Satisfactory S analysis was also obtained.

and sparingly soluble in DMF, dioxane and DMSO.

The conductance values of 1×10^{-3} *M* solutions of all the complexes in DMF (2.1-10.1 mhos cm^2 mol^{-1}), show their non-electrolytic behaviour.

The analytical data of the ligands and complexes are given in Table 1 which show that the metal to ligand ratio in all the complexes is 1:1.

TG and DT analyses were carried out to confirm the presence of coordinated water in the complexes of Cl-HACAP. The mass loss was found to be equivalent to two moles of water in the case of Mn(II), Fe(II), Co(II) and Ni(II) complexes and it was a two-step process. Two endothermic peaks in each case have been obtained. [Mn(II) at 145° and 160°C; Fe(II) at 140° and 165°C; Co(II) at 130°C and 170°C; and Ni(II) at 135°C and 165°C].

In the case of Cl-HACDPy complexes the thermogravimetric analysis shows that Cu(II) and Fe(II) complexes have two moles of coordinated water while Mn(II), oxovanadium(IV), Co(II) and Ni(II) complexes have only one mole of water.

Both, Cl-HACAP and Cl-HACDPy can exhibit tautomeric forms (I-IV).

The ligands Cl-HACAP and Cl-HACDPy may exist in equilibrium mixtures of lactone and chromone forms or may prefer only one of the forms depending upon the energy difference amongst these tautomeric forms.

The IR spectrum of Cl-HACAP shows a strong broad band in the region 3050-3300 cm^{-1} assignable to inter- and intra-molecular hydrogen-bonded νOH[4]. Three intense bands observed at 1670, 1590, 1460 cm^{-1} are assigned to νC=O (chromone), νC=N and νC−O respectively. The IR band for νC=O in chromone form generally appears in the range 1650-1670 cm^{-1} while νC=O of lactone form appears in the range 1700-1720 cm^{-1}. Since the ligand shows the band at 1670 cm^{-1}, it is concluded that the ligand in the solid state has chromone structure. In the complexes, the behaviour of the ligand is somewhat different. In oxovanadium(IV) and Cu(II) complexes it is present in the lactone form and in the rest of the complexes it is present in the chro-

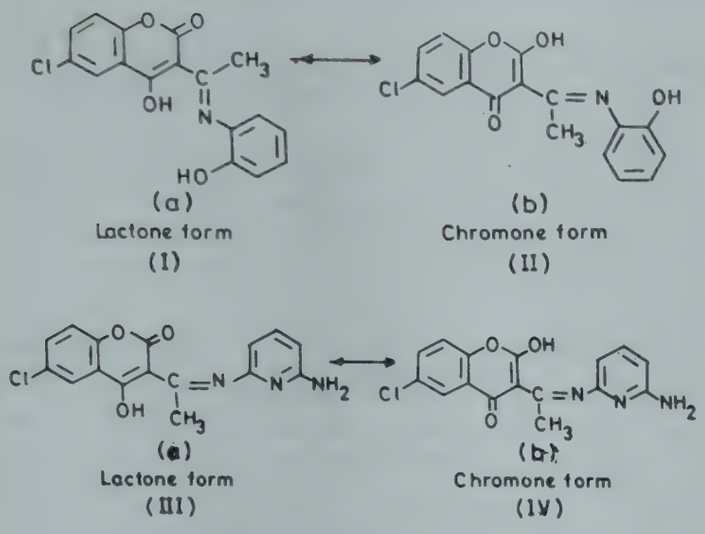

mone form. In the spectra of the complexes the absence of a broad band at 3050-3300 cm^{-1} indicates the cleavage of the hydrogen bond, deprotonation of the phenolic oxygen, and its coordination to the metal ion. The spectra of Mn(II), Fe(II), Co(II) and Ni(II) complexes show a broad absorption in the region 3320-3400 cm^{-1} which indicates the presence of coordinated water[5] the presence of which is also confirmed by TG analysis. In the case of oxovanadium(IV) and Cu(II) complexes no such band is observed indicating the absence of coordinated water. A strong band at 1460 cm^{-1} assigned to $\nu C-O$ in the free ligand, is resolved into two peaks in the complexes. The lower energy band is assigned to $\nu C-O$ of coumarin moiety while the higher energy one is attributed to $\nu C-O$ of benzene moiety[6]. Both the bands occur at higher frequencies compared to $\nu C-O$ in the free ligand. This indicates participation of both the phenolic oxygens in coordination subsequent to deprotonation[7,8]. As the shift in case of $\nu C-O$ on benzene moiety is high (~ 40 cm^{-1}) it is assumed that the oxygen of this group acts as a bridging centre[9]. The positive shift in $\nu C=N$ (15-20 cm^{-1}) in complexes confirms the participation of the azomethine nitrogen in complex formation[10,11]. A new band in oxovanadium(IV) complex at 900 cm^{-1} is attributed to $\nu V=O$[12]. The extra bands around 580 and 460 cm^{-1} are assigned to $\nu M-N$ and $\nu M-O$ modes respectively[13,5]. The changes in the IR spectra of the complexes indicate the formation of metal chelates.

A broad absorption is observed at 3050-3300 cm^{-1} in the IR spectrum of the ligand Cl-HACDPy which is assigned to inter and intra-molecular hydrogen bonded νOH vibration. The bands due to $\nu_{as}NH_2$ and ν_sNH_2 could not be pinpointed. These might have been overlapped with the broad absorption. Intense bands at 1720, 1610, 1430 cm^{-1} are assignable to $\nu C=O$ (lactone), $\nu C=N$[14] of azomethine and $\nu C-O$[6] (phenolic) respectively. The bands between 1570 and 1420 cm^{-1} are ascribed to $\nu C=N$ (ring) and $\nu C=C$ of pyridine ring[9] respectively[15,16]. In the IR spectra of all the complexes a broad band is observed in the region 3150-3500 cm^{-1} whis is assigned to overlapping of the bands due to νNH_2 and coordinated water. The presence of coordinated water is confirmed by TG and DT analysis and by the presence of new peaks at 820-840 cm^{-1} in the complexes. The absence of strong band in the region of 3500-3600 and appearance of a new peak at about 1440-1460 cm^{-1}, assignable to $\nu C-O$ (phenolic), indicate cleavage of the hydrogen bonding, deprotonation of hydroxyl group and subsequent coordination of oxygen with metal ion. The downward shift in $\nu C=N$ (10-15 cm^{-1}) shows the participation of nitrogen of azomethine group in complexation[17,18]. There is a downward shift (35-45 cm^{-1}) in $\nu C=O$ (lactone) in the complexes of Mn(II), Co(II) and Ni(II) which favours the participation of oxygen of $\nu C=O$ (lactone) forming polymeric species[19,20]. In rest of the complexes there is no change in $\nu C=O$ (lactone). Considerable changes have been noticed in the bands in the range 1560-1430 cm^{-1} which are consistent with the participation of nitrogen of the pyridine ring in coordination[18]. A new peak at 900 cm^{-1} is assigned to $\nu V=O$[5]. The presence of $M-O$ and $M-N$ bonding is confirmed by new peaks observed in the region 600-400 cm^{-1} (ref. 21). The presence of chloride was confirmed by analytical data.

From the IR data it has been concluded that Cl-HACDPy behaves as a monobasic tridentate ligand, coordinating to metal ions through the deprotonated phenolic oxygen, the azomethine nitrogen and the nitrogen of pyridine ring.

The observed magnetic moment of oxovanadium(IV)-[Cl-HACAP] complex is 1.5 B.M. The low magnetic moment may be attributed to antiferromagnetic coupling of spin[22]. The electronic spectrum of this complex exhibits two bands at 12048 and 26315 cm^{-1} which may be assigned to the transitions $^2b_2 \rightarrow {}^2e$ and $^2b_2 \rightarrow {}^2a_1$ respectively in square-pyramidal geometry. The oxovanadium(IV)-[Cl-HACDPy.SO_4] complex possesses room temperature magnetic moment value of 1.79 B.M. Its electronic spectrum exhibits two bands at 14285 and 16000 cm^{-1} which are assigned to the transitions $b_2 \rightarrow e$ and $b_2 \rightarrow a$, respectively in a distorted octahedral geometry[23].

The room temperature magnetic moment of Mn(II)-[Cl-HACAP.$2H_2O$] complex is 4.57 B.M.

The observed moment is low compared to spin-only value (5.92 B.M.) for high-spin Mn(II) complexes. This may be due to the presence of very small amount of Mn(III) species[24] and strong metal-metal interaction in the complexes. The Mn(II) complex displayed very weak absorption bands and it was difficult to assign them to definite transitions. The Mn(II)[Cl-HACDPy.Cl.H_2O] complex shows the magnetic moment of 5.86 B.M. which is slightly low when compared to spin-only value of 5.92 B.M. The low value may be due to the presence of Mn(III) species or spin-exchange in the solid phase[24]. Its electronic spectrum exhibits several weak absorption in the range 12200-25000 cm^{-1}. A polymeric octahedral structure is proposed for Mn(II) complex.

The observed room temperature magnetic moment of Fe(II)-[Cl-HACAP.$2H_2O$] complex is 4.97 B.M. which is low compared to the expected magnetic moment[25]. The low value may suggest strong metal-metal interaction. The visible spectrum of Fe(II) complex exhibits a broad band at 13000 cm^{-1} assignable to $^5T_{2g} \rightarrow {}^5E_g$ transition[26]. The magnetic moment of Fe(II)-[Cl-HACDPy.$2H_2O.SO_4$] was found to be 5.24 B.M. which is well within the range of high-spin octahedral Fe(II) complexes[27]. Fe(II) complex shows a very weak absorption at 12275 cm^{-1} which may be assigned to the transition $^5T_{2g} \rightarrow {}^5E_g$ under octahedral geometry[26].

The Co(II)-[Cl-HACAP.$2H_2O$] complex possesses a magnetic moment value of 4.5 B.M. which is in agreement with the value required for three unpaired electrons. Its electronic spectrum shows three bands at 8510, 18510 and 21276 cm^{-1} which may be assigned to the transitions $^4T_{1g} \rightarrow {}^4T_{2g}$ (F), $^4T_{1g}$ $(F) \rightarrow {}^4A_{2g}$ (F), $^4T_{1g}$ $(F) \rightarrow {}^4T_{1g}$ (P) respectively. The positions of the observed bands agree with those of the other reported Co(II) octahedral complexes. The Co(II)-[Cl-HACDPy.Cl.H_2O] complex exhibits magnetic moment of 4.24 B.M. suggesting high-spin octahedral configuration[27]. This Co(II) complex shows two main bands at 25640 and 18500 cm^{-1} which are assignable to the transitions $^4T_{1g}$ $(F) \rightarrow {}^4T_{2g}$ (F) and $^4T_{1g}$ $(F) \rightarrow {}^4T_{2g}$ (P) respectively in a high-spin octahedral configuration[28].

The observed room temperature magnetic moment of Ni(II)-[Cl-HACAP.$2H_2O$] complex is 2.605 B.M., close to the value required for octahedral structure. Its electronic spectrum shows three bands at 9523, 16000 and 26315 cm^{-1} which can be assigned to the transitions $^3A_{2g}$ $(F) \rightarrow {}^3T_{2g}$ (F), $^3A_{2g}$ $(F) \rightarrow {}^3T_{1g}$ (F) and $^3A_{2g}$ $(F) \rightarrow {}^3T_{1g}$ (P) respectively[26]. The observed magnetic moment value of Ni(II)-[Cl-HACDPyCl.H_2O] complex is 2.8 B.M. and its electronic spectrum shows three characteristic bands at 10526, 17540 and 27770 cm^{-1} which are suggestive of octahedral geometry. The three bands are assigned to $^3A_{2g}$ $(F) \rightarrow {}^3T_{2g}$ (F), $^3A_{2g}$ $(F) \rightarrow {}^3T_{1g}$ (F) and $^3A_{2g}$ $(F) \rightarrow {}^3T_{1g}$ (P) transitions respectively[28].

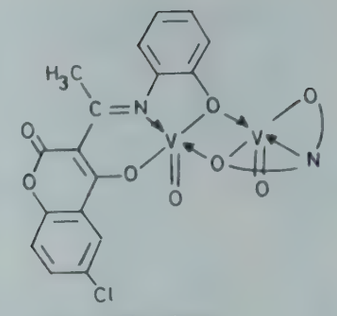

Lactone structure

(V)

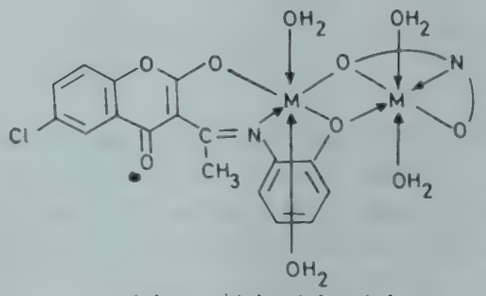

(b) M=Mn(II),Fe(II),Co(II) and Ni(II)(Chromone structure)

(VI)

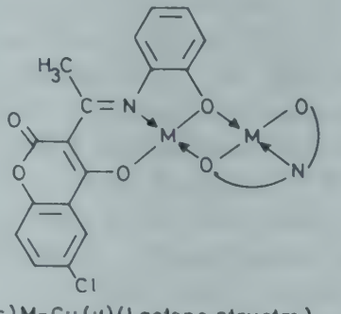

(c) M=Cu(II)(Lactone structre)

(VII)

The room temperature magnetic moment of Cu(II)-[Cl-HACAP] complex is 1.6 B.M. The low value of magnetic moment may be due to the metal-metal interactions due to the presence of bridging structure. The electronic spectrum of Cu(II) complex displays three bands at 13700, 14925 and 19420 cm^{-1} which can be assigned to the transitions $^2B_{1g} \rightarrow {}^2B_{2g}$, $^2B_{1g} \rightarrow {}^2A_{1g}$ and $^2B_{1g} \rightarrow {}^2E_g$ respectively under the square-planar geometry. The Cu(II)-[Cl-HACDPy.Cl.$2H_2O$] complex possesses a magnetic moment value of 1.8 B.M. which is well within the range of octahdral complexes[27,29]. Its electronic spectrum exhibits a broad band at 13000-17000 cm^{-1} which is assignable to the $^2E_g \rightarrow {}^2T_{2g}$ transition in octahe-

dral geometry. The broadness of the band is due to the Jahn-Teller distortion operative for the d^9 configuration. A distorted octahedral geometry has been tentatively assigned. The ESR spectra of oxovanadium(IV) and Cu(II) complexes of Cl-HACAP show sharp bands corresponding to the g_{av} value of 1.9650 and 2.068 which is resultant of $g_{\parallel}$ and $g_{\perp}$. The g_{av} values of the corrsponding complexes with Cl-HACDPy are 1.9894[30] and 2.0634[31] respectively which are in agreement with the values required for one unpaired electron.

On the basis of analytical data, conductivity data, magnetic susceptibility measurements, TG and DT analysis and spectral data, structures V-VII are proposed for the present complexes.

Acknowledgement

One of the authors (LNS) is thankful to the CSIR, New Delhi, for the award of Junior and Senior Research Fellowships.

References

1 Manku G S, Bhatt A N & Jain B D, *Anal chim Acta*, **52** (1975) 958.
2 A I Vogel, *A text book of quantitative inorganic analysis*, *3rd Edn* (*Longman Green, London*), 1961, *pp.* 496, 486, 533, 523, 527 *and* 529.
3 *Figgis B N & Lewis J, Modern coordination chemistry*, edited by J Lewis & R G Wilkins (Interscience, New York) 1960, 403.
4 Dutta R L & Ray R K, *J Indian chem Soc*, **60** (1983) 185.
5 Nakamoto K, *Infrared spectra of inorganic and coordination compounds* (*Wiley, Interscience, New York*) 1970, 163, 173, 159, 214.
6 *Dyer John R, Applications of absorption spectroscopy of organic compounds* (Prentice Hall, New Delhi) 1984.
7 Biradar N S, Mahale V B & Havinale B R, *Curr Sci*, **45(1)** (1976) 6.
8 Biradar N S, Raythatha R H & Mahale V B, *Curr Sci*, **45(4)** (1976) 124.
9 Syamal A & Kale K S, *Indian J Chem*, **19A** (1980) 225.
10 Patel M N & Patel M M, *Indian J Chem*, **20A** (1981) 628.
11 Agarwal R C, Singh N K & Singh R P, *Inorg chim Acta*, **32** (1979) 187.
12 Suniti Kumar, Bhasin K K, Kapila V P & Mahajan R K, *Indian J Chem*, **23A** (1984) 200.
13 Narang K K & Agarwal A, *Inorg chim Acta*, **9** (1974) 137.
14 Kovacic J E, *Spectrochim Acta*, **23A** (1967) 183.
15 Colthup N B & Daly L H, *Introduction to infrared and Raman spectroscopy* (Academic Press, New York) 1964, 233.
16 Silverstein Robert M & Bassler G Clayton, *Spectrometric identification of organic compounds* (John Wiley, New York), 1981.
17 Okawa H, Tokki T, Horaka N, Mutoy & Kida S, *Bull chem Soc* (*Japan*), **46** (1973) 1462.
18 Shah N R & Shah J R, *Indian J Chem*, **21A** (1982) 176.
19 Ryzhenko L M, Khidekal M L & Shebal Dove, *Izv Akad Nauk, SSSR Ser Khim*, **6** (1974) 1418.
20 Prabhakaran C P & Patel C C, *J inorg nucl Chem*, **34** (1972) 3485.
21 Daga Kailash, Sharma Shobha, *Indian J Chem*, **25A** (1986) 782.
22 Syamal A, Bari M A & Niazi, *Indian J Chem*, **23** (1984) 164.
23 Srivastava R S, Yadav L D S, Khare R K & Srivastava A K, *Indian J Chem*, **20A** (1981) 516.
24 Holm R H, Everett (Jr) G W & Chakravorty A, *Progr inorg Chem*, **7** (1966) 120.
25 Jorgensen C K, *Adv chem Phys*, **5** (1963) 33.
26 Cotton F A & Wilkinson G, *Advanced inorganic chemistry*, (Wiley Eastern, New Delhi), 1976, 862.
27 Figgis B N & Lewis J, *Prog inorg Chem*, **6** (1964) 37, 67, 157, 185, 210.
28 Lever A B P, *Inorganic electronic spectroscopy* (Elsevier Amsterdam) 1968, 333, 343, 355, 356.
29 Lewis J & Wilkins R G, *Modern coordination chemistry* (Interscience, New York) 1967.
30 Mathew M, Cacty A J & Palenii G J, *J Am chem Soc*, **92** (1970) 3197.
31 Goodman B A & Roynor J B, *Advances in inorganic and nuclear chemistry*, Vol. 13, edited by H J Emeles & A G Sharpe (Academic Press, New York) 1970, 316.

Indian Journal of Chemistry
Vol. 27A, July 1988, pp. 622-625

Molecular Complex Formation of Thiosalicylic Acid with *n*-Propanol

M M SELEIM, MAGDA S SALEH, H SEDAIRA & K A IDRISS*
Chemistry Department, Faculty of Science, Assiut University, Assiut, Egypt

Received 14 *July* 1987; *revised and accepted* 9 *December* 1987

The formation of 1:1 molecular complex of thiosalicylic acid (TSA) with *n*-propanol has been studied spectrophotometrically. The formation constants (K_f), free energy changes (ΔG) and molar absorptivities of the TSA-*n*-propanol molecular complex in cyclohexane, CCl_4 and $CHCl_3$ as solvents have been determined. K_f values vary with solvent in the order: cyclohexane > CCl_4 > $CHCl_3$. The oscillator strength (f) for the bonded molecules is greater than that for free molecules, indicating enhanced interaction between the lone pair of electrons on the oxygen atom of the carboxyl OH in TSA molecule and the ring π-electrons, presumably due to an intermolecular (O – H...O) bond formation. The electronic absorption spectra of TSA in different two-component solvents are also discussed.

The most obvious specific solute-solvent interactions occur via H-bonding solute to solvent and produce, in protic solvents, anomalous band shift giving deviation from the predictions of the dielectric theory. Solvents capable of acting as electron donors or acceptors are expected to show similar behaviour, particularly in respect of charge transfer (CT) transitions where competitive donor-acceptor interaction by the solvent will modify the ground and excited state electron distribution. In this paper, the effect of molecular complex formation between thiosalicylic acid (TSA) and *n*-propanol via an intermolecular H-bonding has been examined and characterized employing UV spectroscopy. The formation constants and H-bonding energy have been determined from the spectral measurements in mixed solvents and the observed spectral shifts and intensity changes are discussed.

Materials and Methods

Thiosalicylic acid used was of BDH (pure) grade. Spectrograde (E Merck) CCl_4, $CHCl_3$ and cyclohexane, after purification, were purged with oxygen-free dry nitrogen immediately before use. Spectrograde *n*-propanol was obtained from E Merck.

Stock solution (10^{-3} *M*) of TSA was prepared accurately, and working solutions were obtained from it by accurate dilution. The absorption spectra were recorded at 20°C ± 0.1°C on a Unicam SP 8000 spectrophotometer using 1 cm matched stoppered quartz cells.

Results and Discussion

The absorption spectra of TSA in organic solvents of varying polarities indicate that both λ_{max} and ε are influenced by the nature of the solvent used (Fig. 1). The linear variation of absorbance with solute concentration in *n*-propanol confirms that solute-solute interaction is of minor import-

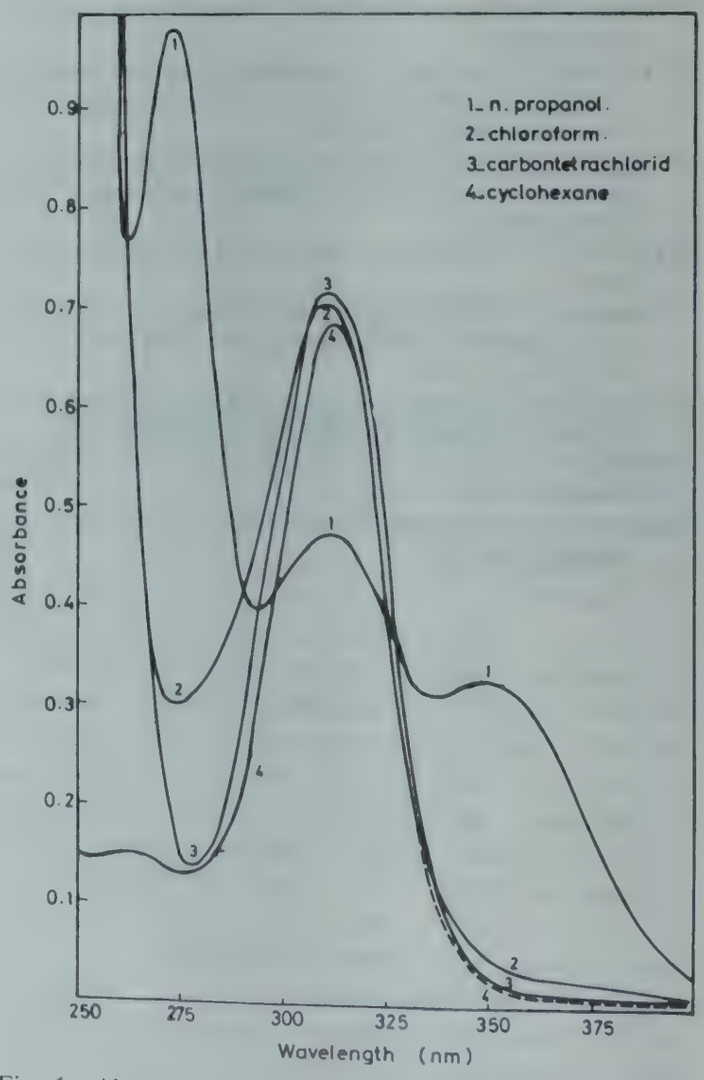

Fig. 1 – Absorption spectra of thiosalicylic acid in organic solvents of varying polarities [(1) *n*-propanol; (2) chloroform; (3) CCl_4 and (4) cyclohexane].

ance in this solvent. The UV spectrum of TSA in *n*-propanol exhibits peaks at 235, 270, 310 and 350 nm. The 235 nm band corresponds to π-π^* transition of the aromatic ring. The large molar absorptivity, the red shift observed when solvent polarity is increased and the disappearance of the band in nonpolar solvents suggest that the band at 270 nm is due to a CT transition within the benzene moiety. The band at 350 nm is tentatively assigned as intramolecular CT band, the transition being between the oxygen of the carboxyl OH and the ring π-electrons. The most interesting effects of changing the solvent are observed for the CT band. The neutral form of TSA is expected to predominate in nonpolar solvents. Although for salicylic acid the anionic form is present only to a small extent in any solvent, the greater acidity of the mercapto group causes the anionic form of TSA to become more prevalent in polar solvents. Hydrogen bonding solvents are also likely to affect the formation of the anionic species of TSA.

The carboxyl group can be strongly H-bonded in both proton donor and proton acceptor solvents. Thus, H-bonding solvents such as *n*-propanol tend to stabilize the monoanionic form of TSA more than the neutral molecules. Therefore in nonpolar solvents, the neutral TSA species will predominate and as the polarity or the H-bonding strength of the solvent increases, the equilibrium will be shifted toward the anionic form.

The 350 nm band, not having an analogue in benzoic acid spectrum has been identified as a CT transition in thiosalicylate anion. The rapid decrease in the absorbance of CT band with decrease in solvent polarity can be ascribed to the decrease in the concentration of anionic form of TSA.

Thiosalicylic acid (TSA) can readily interact with *n*-propanol, a proton acceptor solvent, leaving a residual negative charge on the oxygen of the carboxyl OH (see structure I). Accordingly, the intramolecular CT is enhanced leading to a red shift of the CT band in this solvent.

It is to be noted that the resonance energy of the carboxyl group must be partially overcome on complexation with *n*-propanol. As a result it is possible that the intramolecular hydrogen bond in TSA is actually somewhat strengthened owing to stabilization of the structure (I), rather than weakened by conjugation of the carboxyl group to *n*-propanol. The addition of two *n*-propanol molecules, one to the carboxyl OH and another to SH group of one TSA molecule is more or less excluded on electrostatic ground.

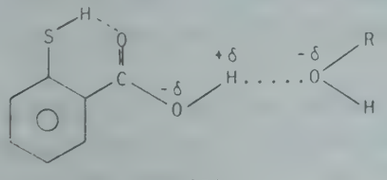

(I)

The formation of TSA-*n*-propanol molecular complex was investigated by studying the spectral behaviour in mixed solvents. A set of absorption spectra were measured taking the three-component systems, viz. TSA-*n*-propanol and the nonpolar solvent. The concentration of *n*-propanol was increased in steps from 0.35 to 13.5 *M*. In every case, a mixture of *n*-propanol and the nonpolar solvent in which the concentration of *n*-propanol was identical to that in the sample solution was taken as the reference.

Such spectra in mixed solvents show a regular decrease in absorbance of 350 nm band and its shift to shorter wavelength with increase in the proportion of the nonpolar component. The red shift of 350 nm band with increase in *n*-propanol concentration denotes an increase in solvation energy in the excited state. Accordingly, the molecules in the excited state are present in a cage of dipoles which are more oriented than in the pure low polarity solvent[2,3]. According to Pimentel[4], the observed red shift can be explained by an increase in the strength of H-bond between solute and solvent on the addition of *n*-propanol. The increase of H-bond strength would be higher for the excited state than that for the ground state.

To investigate the effect of dielectric constant of the medium on the band shift ($\Delta\bar{\nu}$), the relation of Gati and Szalay (see Eq. 1) was applied

$$\Delta\bar{\nu} = (a-b)\left(\frac{\eta^2-1}{2\eta^2+1}\right) + b\frac{(D-1)}{(D+1)} \qquad \ldots (1)$$

in which a and b are constants and η is the refractive index of the medium. The plots of $\Delta\bar{\nu}$ as a function of $(D-1)/(D+1)$ in all systems investigated are nonlinear indicating that the band shift is governed by other factors besides the dielectric constant of the medium. These factors include solute-solvent interaction via intermolecular H-bond leading to the formation of a TSA-*n*-propanol molecular complex. The intensity change of the CT band in two-component solvents is accompanied by the development of a new band at the longer wavelength side. A clear isosbestic point is observed which indicates the existence of an equilibrium between the bonded and free molecules. Oscillator strength for the transitions of both the

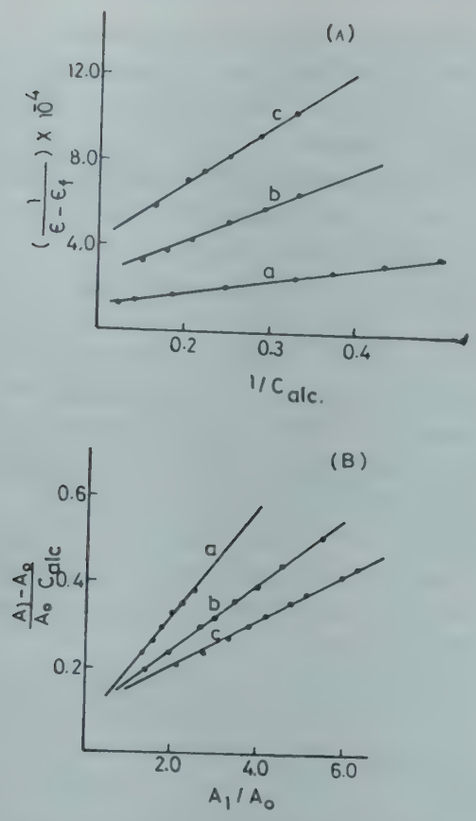

Fig. 2 – Determination of K_f of TSA-*n*-propanol molecular complex in chloroform (a), carbon tetrachloride (b) and cyclohexane (c) as solvents.

free and bonded species were determined using the familiar relation (2)

$$f = 5.32 \times 10^{-9}/\varepsilon d\nu \quad \ldots (2)$$

The oscillator strength for H-bonded molecules (f_b) is always greater than that for free molecules (f_f), which means an enhanced interaction between the lone pair electrons on the oxygen atom of the OH group in TSA molecule and the ring π-electrons presumably due to an intermolecular (O – H....O) bond formation.

Formation constant of the TSA-n-propanol molecular complex

The formation constant (K_f) of the TSA-*n*-propanol molecular complex was determined from the spectral behaviour in mixed solvents using the following methods:

Method (i): Using Eq. (3)[5]:

$$1/(\varepsilon - \varepsilon_f) = [1/K_f(\varepsilon_b - \varepsilon_f)](1/C_{alc.}) + [1/\varepsilon_b - \varepsilon_f] \quad \ldots (3)$$

In Eq. (3) ε_f and ε_b are the molar extinction coefficients of free and H-bonded molecules respectively, and ε that of a solution in which alcohol concentration was $C_{alc.}$. All the extinction coefficients are with reference to a given wavelength. On extrapolating the linear plot of $1/(\varepsilon - \varepsilon_f)$ versus $1/C_{alc.}$ to the point where $1/(\varepsilon - \varepsilon_f) = 0$, K_f was obtained as $K_f = -1/C_{alc.}$ (Fig. 2A). According to Eq. (3) the extinction coefficient (ε_b) of the H-bonded species is given by the relation (4)

$$\varepsilon_b = \varepsilon + (\varepsilon - \varepsilon_f/KC_{alc.}) \quad \ldots (4)$$

The constancy of the K_f values over several wavelengths supports the existence of a 1:1 complex in solution.

Method (ii): In this method Eq. (5) was applied[6].

$$\log\frac{A - A_0}{A_{max} - A} = n\log C_{alc.} - \log K_f \quad \ldots (5)$$

In Eq. (5) A, A_0 and A_{max} are the absorbances in mixed, inert and proton acceptor solvents, respectively. The plot of $\log (A - A_0)/(A_{max} - A)$ versus $\log C_{alc.}$ is linear with a slope (n), the number of propanol molecules of about unity. Log K_f is equal to value of $\log C_{alc.}$ at which $\log A - A_0/A_{max} - A = 0$.

Method (iii): In this method Eq. (6)[7] was applied.

$$(A_1 - A_0)/A_0C_{alc.} = k_f\varepsilon_1/\varepsilon_0 - KA_1/A_0 \quad \ldots (6)$$

In Eq. (6) A_1 and A_0 are the absorbances at a given wavelength in mixed solvent and inert solvent respectively, and ε_0 and ε_1 are molar extinction coefficients of the solute and complex species.According to Eq. (6), the plot of $(A_1 - A_0)/A_0C_{alc.}$ against A_1/A_0 should be linear, with slope = K and intercept = $K\varepsilon_1/\varepsilon_0$ (Fig. 2B). The mean value of K_f in all systems investigated and the corresponding ΔG values are given in Table 1.

For each binary solvent system, the data near the CT-band maximum are consistent with the existence of a single 1:1 (TSA-*n*-propanol) complex.

Table 1 – Average Value of K_f and ΔG fr TSA-*n*-Propanol Complex at 20°C ± 0.1°C in Different Solvents

System	log K_f	K_f ($cm^3\ mol^{-1}$)	ΔG ($KJ\ mol^{-1}$)
n-Propanol-cyclohexane	1.275	18.84	−7.150
n-Propanol-CCl_4	1.130	13.49	−6.334
n-Propanol-$CHCl_3$	0.934	8.58	−5.234

Table 2 – Maximum Molar Absorptivities and Wavelengths of Band Maximum for TSA-*n*-Propanol Complex in Different Solvents

System	$10^4\varepsilon_{max}$	λ_{max} (nm)
n-Propanol-cyclohexane	0.90	350
n-Propanol-CCl_4	0.95	354
n-Propanol-$CHCl_3$	1.60	352

The constancy of K_f values for a given binary system at different wavelengths supports the existence of a 1:1 complex in solution[8].

For the donor-acceptor-solvent ternary systems under investigation nonpolar solvent component drastically affects the computed K_f values (Table 1). Competitive donor solvent complexes in $CHCl_3$, and possibly in CCl_4, can block the donor orbital and thus reduce the value of the formation constant in these solvents. The molar absorptivity of the assumed 1:1 complex near the absorption maxima is approximately constant (cf Table 2).

For the systems studied in the present investigation, the wavelengths of maximum absorption for TSA-*n*-propanol complex vary with solvent in the order: cyclohexane $< CHCl_3 < CCl_4$. Some authors[9,10] have reported similar behaviour for various complexes. The results cannot be explained in terms of average solvent properties alone, but they can be interpreted by the supposition that the formation of one isomeric complex is favoured by the structure of the solvent.

References

1 Suppan P, *J chem Soc (A)*, (1968) 3125.
2 Bayless N S & Macrae E G, *J phys Chem*, **56** (1954) 1002.
3 Macrae E G, *J phys Chem*, **61** (1957) 562.
4 Pimentel G C, *J Am chem Soc*, **79** (1957) 3323.
5 Baba H & Suzuki S, *J chem Phys*, **35** (1961) 1118.
6 Issa R M, Ghoneim M M, Idriss K A & Harfoush A, *A Phys Chem (Neue Folge)*, **94** (1975) 135.
7 El-Ezaby M S, Salem T M, Zewail A H & Issa R M, *J chem Soc (B)*, (1970) 1293.
8 Johnston G D & Bowen R E, *J Am chem Soc*, **87** (1965) 1955.
9 Foster R, *J chem Soc*, (1960) 1075.
10 Bhattacharya R, *J chem Phys*, **30** (1959) 1367.

Indian Journal of Chemistry
Vol. 27A, July 1988, pp. 626-628

Notes

Statistical Entropy of Adsorption of *n*-Alkanes

MOOL C GUPTA* & VIJAY G MAHAJAN†
Chemistry Department, Nagpur University, Nagpur 440010.

Received 27 *February* 1987; *revised* 6 *November* 1987; *rerevised and accepted* 27 *December* 1987

Entropy of adsorption of *n*-alkanes has been calculated using statistical models of adsorption of gases on to solid surfaces. It is found that when the temperature difference between the boiling point of *n*-alkane and the temperature at which chromatographic adsorption takes place is large, adsorption can be explained by mobile adsorption model and when the difference is small, adsorption can be accounted by localized adsorption model.

Molecular statistical investigations have been carried out mostly for adsorption of monoatomic and quasi-monoatomic molecules, but have seldom been used in the study of the adsorption of polyatomic molecules[1-3]. Kiselev *et al.*[4] used statistical method for estimating change in entropy and heat capacity for adsorption of hydrocarbons on to graphitized thermal carbon black at zero surface coverage at different temperatures. However, the experimental entropy of adsorption has been determined by measuring chromatographic retention volume at different temperatures[5-7]. In this note change in entropy of chromatographic adsorption is calculated theoretically on the basis of statistical models. The values are compared with those obtained experimentally for adsorption of *n*-alkanes on chemisorb P-nickel catalyst adsorbent at different temperatures by measuring retention volume[5-7] in order to get an insight into the nature of mechanism of the adsorption process in chromatographic adsorption. However, many workers have suggested that the magnitude of heat evolved during adsorption usually indicates the nature of the adsorption on surfaces[8-10].

Calculations

If the adsorption of *n*-alkanes at high temperatures is viewed as the equilibrium gas phase ⇌ adsorbed phase, the molar entropy change would be given by the difference between the molar entropy of the gas in adsorbed phase (S^{ad}) and gas phase (S^{g}). The former is the sum of two terms (i) the molar thermal entropy, S^{ther}, and (ii) the configurational entropy, S^{conf}, of ideal surface state, which for monolayer adsorption is related to surface coverage[11,12] and for nearly half surface coverage it is negligible. S^{ther} and S^{g} can be calculated by using statistical models of adsorption[5].

The gas molecules in adsorbed phase are confined to adsorption sites. On adsorption, in terms of the localized model, molecules lose all their translational degrees of freedom, which are replaced by vibrational motion. However in the mobile model, molecules are free to diffuse over the surface as a two-dimensional gas and the translational motion perpendicular to surface is replaced by vibrational motion. Adsorbed molecules also lose some of their rotational degrees of freedom as evidenced by the study of the shape of IR bands and sticking coefficient at surfaces[13-16]. However, the IR spectroscopy of physically adsorbed molecules suggests[17] that there is only a slight shift in the vibrational frequencies on adsorption. Therefore, vibrational entropy in gas and adsorbed phases may be taken as same.

Thus, the molar entropy change on adsorption, ΔS^{ad}, will be given by Eq. 1,

$$\Delta S^{ad} = S_{tr}^{ther} - S_{tr}^{g} + \Delta S_{rot} \quad \ldots (1)$$

where S_{tr}^{ther} and S_{tr}^{g} are translational entropy in adsorbed phase and gas phase respectively. For mobile adsorption (in which molecules freely diffuse over the surface as two-dimensional gas), Eq. 1 becomes,

$$\Delta S_{mobile}^{ad} = S_{tr}^{ther}(\text{2-dimensional gas}) - S_{tr}^{g} + \Delta S_{rot} \quad \ldots (2)$$

$$\Delta S_{loc}^{ad} = -S_{tr}^{g} + \Delta S_{rot} \quad \ldots (3)$$

whereas, for localized adsorption (losing all translational degrees of freedom) Eq. 1 can be written as,

The translational entropy can be calculated from the knowledge of the translational partition function[18].

By substituting the constants the translational entropy in adsorbed phase is given as,

$$S_{tr}^{ther}(\text{2-dimensional gas}) = R \ln (M.T.\sigma_m) + 275.3\ JK^{-1}\ mol^{-1} \quad \ldots (5)$$

and for gas phase it will be,

$$S_{tr}^{g} = R \ln (M^{3/2}.T^{5/2}) - 9.685\ JK^{-1}\ mol^{-1} \quad \ldots (6)$$

†Present address: Department of Chemistry, Jijamata College of Science, Buldhana, Maharastra.

Table 1 – Physical Constants Used in Computation of Entropy Change

Alkane	Boiling Point K	Heat of adsorption*		Heat of fusion** ΔH_m ($J g^{-1}$)	Co-area $\sigma_m \times 10^{15}$ (m^2)	Entropy of fusion ($J mol^{-1} K^{-1}$)
		ΔH ($kJ mol^{-1}$)	Temp. range (°C)			
n-Pentane	309.46	7.40	200.360	116.58	3.55	56.66
n-Hexane	342.16	10.78	200-360	151.61	3.87	73.53
n-Heptane	371.56	21.00	200-260			
		8.20	280-360	141.20	4.18	77.58
n-Octane	398.86	57.85	200-260			
		11.87	280-360	180.62	4.49	95.27
n-Nonane	423.66	60.65	200-260			
		12.58	280-360	120.51	4.78	70.43
n-Decane	447.16	—	—	202.06	5.07	118.21
2,4-Dimethyl pentane	353.66	17.64	200-260			
		7.90	280-360	64.58	4.30	51.82

*Obtained from ln v_g vs. 1/T plot by Mathur *et al.*, adsorbent chemisorb-P-nickel catalyst (private communication).

**West R C, *Hand book of chemistry & physics*, 59th Edn. (McGraw-Hill, N.Y.) 1978-79 p. 724.

where σ_m is the area of molecule and can be calculated from liquid density data, ρ, by[10] Eq. 7,

$$\sigma_m = 3.464\,(M/4\sqrt{2}.N.\rho)^{2/3} \quad \ldots (7)$$

The rotational entropy change, ΔS_{rot}, may be estimated by the loss of some rotational degrees of freedom in gas-condensed liquid equilibrium as shown by Rastogi *et al*[19]. This entropy change is equal to $\Delta H_m/T$, where ΔH_m is the enthalpy change on melting and T is the melting point.

Thus, from Eqs (2)-(7) and data in Table 1, entropy change values for chromatographic adsorption of *n*-alkanes are calculated and are summarised in Table 2. In each case 1st and 2nd columns contain values calculated from Eqs (2) and (3) respectively. The experimental values are listed in column 3 as reported by Mathur *et al.*[6] and have been determined by measuring retention volume, v_g, at different temperatures and using the relation $-\Delta G^{ad} = RT\ ln\ v_g$, where $-\Delta G^{ad}$ is the free energy change on adsorption.

It is observed from Table 2 that the values of entropy change for *n*-pentane, *n*-hexane and 2,4-dimethylpentane are in good agreement with those calculated on the basis of mobile adsorption model using Eq. (2). The values for *n*-heptane and *n*-nonane in the temperature range 200-260°C are in agreement with those calculated using Eq. (3), while at higher temperatures the values are in agreement with those calculated using Eq. (2). This behaviour can be related to the difference in their boiling points and the temperature at which the adsorption is carried out. When this difference is large, mobile adsorption is favoured and when it is small localized adsorption in favoured. Though both kinds of adsorption seem to be physical adsorptions, Mathur *et al.*[7] have suggested that the former is chemisorption and the latter is physical adsorption on the basis of heat of adsorption values.

The calculated values for *n*-octane and *n*-decane show only the trend and are not in good agreement with the experimental values. The enthalpy of fusion (hence the entropy of fusion) for these even number carbon atom alkanes is abnormally high as compared to that for other homologues containing odd number carbon atoms. In case of such alkanes it has been suggested[20] that terminal methyl groups are *trans* to each other whereas they are *cis* to each other in odd number carbon atom alkanes. It appears that the alkanes with odd number carbon atoms do not align as closely in crystal lattice as those with even number carbon atoms. Further, Weber *et al.*[21] have suggested that in *n*-octane like fluids, large amount of alignment and straightening of chain is induced by large surfaces. Also $-\Delta S^{ad}$ increases with temperature which may be due to decrease in surface coverage with increase in temperature.

Thus, in chromatographic adsorption of *n*-alkanes at different temperatures both mobile and localized physical adsorptions take place and the transition temperature is 260°C. However, the essential difference between the two is that in the case of former the molecule is not associated with

Table 2 – Entropy Change on Chromatographic Adsorption of *n*-Alkanes at Different Temperatures

Temp. (°C)	*n*-Pentane $-\Delta S^{ad}$ (J K^{-1} mol^{-1})			*n*-Hexane $-\Delta S^{ad}$ (J K^{-1} mol^{-1})			*n*-Heptane $-\Delta S^{ad}$ (J K^{-1} mol^{-1})			*n*-Octane $-\Delta S^{ad}$ (J K^{-1} mol^{-1})		
	Eq (2)	Eq (3)	Exp.	Eq (2)	Eq (3)	Exp.	Eq (2)	Eq (3)	Exp.	Eq (2)	Eq (3)	Exp.
200	27.5	113.0	9.90	12.7	100.4	17.77	8.6	98.2	36.7	−9.1	82.1	108.84
220	28.2	113.0	9.90	13.2	101.3	19.1	9.1	99.0	37.0	−9.0	83.0	108.2
240	28.5	114.7	11.85	13.7	102.1	17.86	8.6	99.9	36.9	−8.2	83.8	107.64
260	29.0	115.5	11.72	14.1	102.9	18.03	10.1	100.7	36.96	−7.7	84.6	105.6
280	28.4	116.3	11.58	14.6	102.6	17.68	10.5	101.5	13.62	−7.2	85.3	18.91
300	29.9	117.7	12.05	15.0	104.4	18.02	11.0	102.2	13.29	−6.8	86.0	19.3
320	30.3	117.7	11.75	15.5	105.1	17.40	11.4	102.9	12.05	−6.4	86.7	19.14
340	30.7	118.4	13.10	15.9	105.8	17.97	11.8	103.6	13.12	−6.1	87.5	19.2
360	31.1	119.1	12.0	16.3	106.4	17.13	12.2	104.3	13.27	−5.6	88.2	19.1

	n-Nonane			*n*-Decane			2,4-Dimethylpentane		
	Eq (2)	Eq (3)	Exp.	Eq (2)	Eq (3)	Exp.	Eq (2)	Eq (3)	Exp.
200	15.6	108.4	110.56	−32.2	62.0	–	34.11	123.9	31.50
220	15.6	109.3	110.56	−31.7	62.9	–	34.6	124.8	31.5
240	16.7	110.1	110.87	−31.2	63.8	–	35.1	125.7	31.2
260	16.7	110.7	109.93	−30.7	64.5	–	35.6	126.5	31.21
280	17.6	111.7	109.93	−30.2	65.5	–	36.1	127.2	31.81
300	18.1	112.4	20.11	−29.8	65.9	–	36.9	127.9	12.14
320	18.5	113.1	20.60	−29.2	66.7	–	37.3	129.4	12.77
340	18.9	113.8	20.28	−29.0	67.4	–	37.7	130.0	12.49

any particular site and so is indistinguishable from any other of its kind, and the whole area is available for adsorption. Hence, the concept of the number of ways in which a molecule can be adsorbed on the total available sites is questionable, but it has been assumed for mathematical simplicity. Further, Eqs (2) and (3) have been deduced by considering molecules to be independent in both gas and adsorbed phases. It may be reasonable in gas phase (because of low pressure), but intermolecular forces would be expected to play a role in adsorbed phase because of close proximity of molecules. However, in localized adsorption, molecules are separated by a potential field and the magnitude of the intermolecular forces may be negligible.

The molecular interactions in the adsorbed phase between molecules occupying adjacent sites may be followed using an interaction parameter, w, as in the case of Bragg-William approximation[18]. This may predict a critical value of w/kT above which a homogeneous adsorbed layer is unstable. This kind of transition has been observed to occur above 260°C in the case of *n*-heptane, *n*-octane, *n*-nonane and 2,4-dimethylpentane.

References

1 Pashkus D P & Afreimovitch A J, *J chromatography*, **58** (1971) 55.

2 Lal M & Spenser D, *Trans Faraday Soc II*, **70** (1974) 910.

3 Vidat-Madjar C & Guiochon G, *Advances in chromatography*, Vol. 13 (Marcell Dekkar, N.Y.) 1975.

4 Kiselev A V & Pashkus D P, *Trans Faraday Soc II*, **72** (1976) 950.

5 Adamson A W, *Physical chemistry of surfaces*, 2nd Edn (Interscience, N.Y.) 1967, Ch. 12 & 13.

6 Mathur D S, Choubey U D & Sinha A, *J chromatography*, **99** (1974) 231.

7 Mathur D S, Choubey U D & Sinha A, *Fertilizer Tech*, **14** (1977) 265.

8 Di Corcia A & Liberti A, *Trans Faraday Soc*, **66** (1970) 967.

9 Casanova C, De Paz M, Dondi M G, Klein M L & Scoles G, *Discuss Faraday Soc*, **40** (1965) 188.

10 Atkinson D & Curthoys G, *J chem Educ*, **56** (1979) 802.

11 Takaisi T, Yusa A & Amakasua F, *Trans Faraday Soc I*, **67** (1971) 3565.

12 Kembell C & Riedeal E K, *Proc Roy Soc* (*London*), **A87** (1946) 53.

13 Blyholde G & Richardson E A, *J phys Chem*, **66** (1962) 2597.

14 Shepperd N & Yates D J C, *Proc Roy Soc* (*London*), **A238** (1956) 69.

15 Gupta M C & Sonepure R I, *Indian J Chem*, **26A** (1987) 250.

16 Eyring H, Henderson D, Stover B J & Eyring E M, *Statistical mechanics & dynamics*, 2nd Edn (Wiley Interscience, N.Y.) 1982.

17 Falmen M & Yates D J C, *J phys Chem*, **63** (1959) 187.

18 Hill T L, *An Introduction to statistical thermodynamics*, (Addison-Wesley Reading, Massachusette) 1962, Ch. 14.

19 Rastogi R P & Girdhar H L, *Indian J Chem*, **2** (1964) 469.

20 Drewster R Q & McEwan W E, *Organic chemistry*, 3rd Asian Edn (Prentice-Hall, N.Y.) 1961, 40.

21 Weber T A & Halfand T, *J chem Phys*, **72** (1980) 4014.

Indian Journal of Chemistry
Vol. 27A, July 1988, pp. 629-631

Physico-chemical Studies in Mixed Solvents: Part III—Conductances of Lithium, Sodium & Potassium Perchlorates in Diethylformamide-Water Mixtures

S P JAUHAR*, P S GURAYA & S P NARULA
Department of Chemistry, Panjab University, Chandigarh 160 014

Received 9 *January* 1987; *revised* 14 *September* 1987; *accepted* 1 *December* 1987

Conductances of $LiClO_4$, $NaClO_4$ and $KClO_4$ have been measured in diethylformamide (DEF)-water mixtures containing 4.26, 10.61, 21.07, 41.58 and 100.0 mol % DEF in the electrolyte concentration range $7.223\text{-}59.157 \times 10^{-4}$ mol dm^{-3} at 25°C. The data have been analysed by Fuoss-Onsager-Skinner equation and Fuoss-Hsia equation as expanded by Fernandez and Prini. The limiting molar conductance for a given electrolyte in DFF-water mixtures decreases sharply with the increase in DEF content upto 30-35 mol % DEF and there-after it gradually increases. All the three salts show associated nature in DEF-water mixtures.

In our earlier studies[1,2], we have reported conductances and transference numbers of some electrolytes in diethylformamide (DEF). In order to understand the behaviour of the electrolytes in terms of change from dipolar aprotic solvent (DEF) to dipolar protic solvent (H_2O), presently we have measured the conductances of a few alkali metal perchlorates in DEF-water mixtures at 25° ± 0.01°C and the data have been analysed by Fuoss-Onsager-Skinner (F-O-S) equation and Fuoss-Hsia equation as expanded by Fernandez and Prini.

DEF (Fluke AG) (sp. conductance 2.6×10^{-7} ohm^{-1} cm^{-1}; density, 0.9015 g ml^{-1}; and viscosity, 0.01142P) and conductivity water (sp. cond. $4\text{-}6 \times 10^{-7}$ ohm^{-1} cm^{-1}) were used. All DEF-water mixtures were prepared by weight and converted into mol % DEF. Perchlorates of lithium, sodium and potassium were purified as reported earlier[3].

Conductances[1], densities[4] (experimental accuracy = ± 0.0001 g ml^{-1}) and viscosities[4] (accuracy = ± 0.002 cP) were measured as reported. The dielectric constants of DEF-water mixtures were taken from literature[5] while their densities and viscosities were experimentally determined.

All measurements were carried out at 25 ± 0.01°C. The transfer of materials was done quickly in order to avoid long exposure to moisture.

Conductances of lithium, sodium and potassium perchlorates were measured in DEF-water mixtures containing 4.26, 10.61, 21.07 and 41.58 mol % DEF in the electrolyte concentration range of $7.223\text{-}59.157 \times 10^{-4}$ mol dm^{-3} at 25°C. The experimental data were analysed by the Fuoss-Onsager-Skinner equation[6] as described previously[7].

Analysis of the data (Table 1) reveals that except for pure DEF, the association constants of the electrolytes in different binary mixtures are positive, indicating their associated nature. For pure DEF, the association constants are negative, indicating unassociated nature of the electrolytes. The values for these salts in water are taken from literature[8].

The conductance data have also been treated[9] by using Fuoss-Hsia-Fernandez-Prini (FHFP) equations (1-3) obtained by expanding[10-12] the Fuoss-Hsia expression[13], where the symbols have their usual meanings.

$$\Lambda = \gamma[\Lambda_0 - S(C\gamma)^{1/2} + EC\gamma \log C\gamma + JC\gamma + J_{3/2}(C\gamma)^{3/2}] \quad \ldots (1)$$

$$K_A = \frac{1-\gamma}{\gamma^2 C f_{\pm}^2} \quad \ldots (2)$$

$$\ln f_{\pm} = -\frac{A(C\gamma)^{1/2}}{1 + BR(C\gamma)^{1/2}} \quad \ldots (3)$$

The distance parameters in Eq. (1), i.e. J and $J_{3/2}$ have been taken as equal to Bjerrum critical distance, $q = Z^2e^2/2DkT$. The expressions for J and $J_{3/2}$ used here are those given by Fernandez-Prini[10]. Under these conditions, conductance depends upon two parameters, Λ_0 and K_A which are adjusted by least squares method to fit the experimental data. The values of Λ_0 and K_A obtained by this method are also included in Table 1.

The analysis of the data by the above equations reveals that the association constants for the electrolytes in most of the binary solvent mixtures are positive, indicating their associated nature. Limiting molar conductances (Λ_0) of $LiClO_4$, $NaClO_4$ and $KClO_4$ in DEF-water mixtures of varying compositions decrease initially with increase in % DEF in water and then increase gradually. The minima in Λ_0 of these salts have been observed in DEF-water mixtures containing 30-35 mol % DEF. The minima in Λ_0 versus composition plots are not at the same composition as viscosity maxi-

Table 1—Limiting Molar Conductances (Λ_0) and Association Constants (K_A) of Some 1:1 Electrolytes in Different DEF-water Mixtures at 25°C

Mol % DEF	Fuoss-Onsager-Skinner			Fuoss-Hsia-Fernandez-Prini		
	Λ_0	K_A	$\sigma\Lambda$	Λ_0	K_A	$\sigma\Lambda$
			$LiClO_4$			
0.00	106.69	—	—	—	—	—
4.26	71.62 ± 0.1	134.0 ± 6.9	0.03	71.64 ± 0.02	137.1 ± 0.4	0.02
10.61	40.39 ± 0.05	94.5 ± 4.4	0.01	40.41 ± 0.01	98.0 ± 0.3	0.01
21.07	35.45 ± 0.03	186.8 ± 3.5	0.01	35.49 ± 0.01	195.6 ± 0.3	0.01
41.58	31.01 ± 0.03	59.8 ± 2.6	0.01	31.04 ± 0.01	70.2 ± 0.3	0.01
100.00	49.18 ± 0.10	24.1 ± 3.6	0.04	48.46 ± 0.03	28.0 ± 1.3	0.06
			$NaClO_4$			
0.00	118.11	—	—	—	—	—
4.26	75.80 ± 0.12	72.5 ± 5.8	0.04	75.86 ± 0.04	77.0 ± 0.4	0.03
10.61	48.53 ± 0.03	71.5 ± 2.3	0.01	48.56 ± 0.01	75.6 ± 0.2	0.01
21.07	40.33 ± 0.02	106.2 ± 1.2	0.01	40.40 ± 0.01	114.9 ± 0.2	0.01
41.58	31.40 ± 0.03	55.1 ± 2.6	0.01	31.46 ± 0.01	68.0 ± 0.3	0.01
100.00	54.47 ± 0.02	—	0.04	54.25 ± 0.03	17.7 ± 0.4	0.03
			$KClO_4$			
0.00	141.52	—	—	—	—	—
4.26	101.90 ± 0.02	73.6 ± 0.6	0.01	101.90 ± 0.01	74.2 ± 0.1	0.01
10.61	55.88 ± 0.04	71.1 ± 2.6	0.02	55.90 ± 0.01	74.2 ± 0.2	0.01
21.07	44.73 ± 0.01	70.1 ± 0.6	0.01	44.80 ± 0.01	77.7 ± 0.2	0.01
41.58	38.02 ± 0.05	40.0 ± 3.2	0.02	38.08 ± 0.02	51.7 ± 0.3	0.02
100.00	55.92 ± 0.04	—	0.01	56.25 ± 0.03	43.4 ± 0.6	0.02

Table 2—Walden Products ($\Lambda_0\eta_0$) and Relative Walden Products [$(\Lambda_0\eta_0)_r = \Lambda_0\eta_0/(\Lambda_0\eta_0)_{H_2O}$] of Some 1:1 Electrolytes in DEF-water Mixtures at 25°C

Electrolyte		Mol % DEF					
		Water	4.26	10.61	21.07	41.58	10.0
$LiClO_4$	$(\Lambda_0\eta_0)$	0.953	1.158	1.024	1.116	0.856	0.560
	$(\Lambda_0\eta_0)_r$	—	1.21	1.07	1.17	0.90	0.59
$NaClO_4$	$(\Lambda_0\eta_0)$	1.055	1.226	1.230	1.270	0.867	0.620
	$(\Lambda_0\eta_0)_r$	—	1.16	1.17	1.20	0.82	0.59
$KClO_4$	$(\Lambda_0\eta_0)$	1.265	1.648	1.417	1.408	1.050	0.637
	$(\Lambda_0\eta_0)_r$	—	1.30	1.12	1.11	0.83	0.50

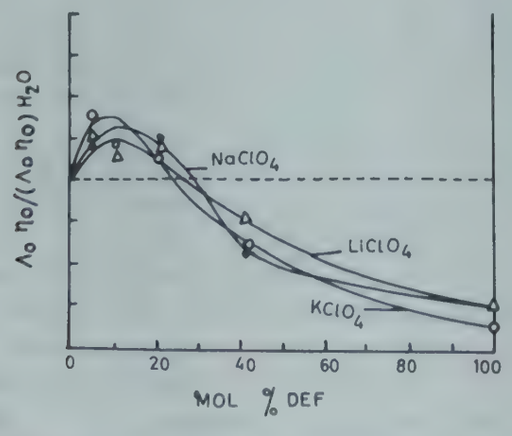

Fig. 1—Variation of relative Walden product, $[\Lambda_0\eta_0/(\Lambda_0\eta_0)_{H_2O}]$ of electrolytes with solvent composition in DEF-water mixtures

ma (25 mol % DEF) reported for DEF-water mixtures in the absence of any electrolyte. Similar observations have also been noted for some electrolytes in other mixed solvents[7,14,15], and this may be attributed to the selective solvation of ions besides the solvodynamic viscous force. In all the solvent compositions, the limiting molar conductances decrease in the order $KClO_4 > NaClO_4 > LiClO_4$ in accord with the decreasing solvation of cations (anion, ClO_4^- being same) and increase in ionic radii.

To have better understanding[16,17] of the nature of solutions, limiting Walden products of the salts in mixed solvents relative to their values in pure

water $[\Lambda_0\eta_0/(\Lambda_0\eta_0)_{H_2O}]$ have been calculated and are recorded in Table 2. Variation of $[\Lambda_0\eta_0/(\Lambda_0\eta_0)_{H_2O}]$ with solvent composition (Fig. 1) pass through a maxima at about 10 mol % DEF for all the perchlorates. Such maxima have also been observed[7,14,16–18] in other solvents. Kay *et al.*[16–18] have explained the height of these maxima in terms of structure breaking power and dehydration of the ions upon addition of second solvent. In the present binary mixtures, the heights of maxima decrease in the order $KClO_4 > NaClO_4 > LiClO_4$, in accord with the structure breaking power of the cations. In the solvent compositions 30-35 mol % DEF, the Walden products for these electrolytes are almost similar to those in pure water. Beyond 35 mol % DEF, the monotonic decrease in Walden products may be due to progressive solvation of ions. It seems that, in DEF-rich region, the cations are selectively solvated by DEF. Since the size of the DEF molecule is fairly large, the solvation of cations leads to large solvodynamic entities which seem to lower the value of $\Lambda_0\eta_0$.

References

1 Jauhar S P, Guraya P S, Chauhan K S & Narula S P, *Indian J Chem*, **19A** (1980) 850.

2 Jauhar S P, Guraya P S, Chauhan K S & Narula S P, *Indian J Chem*, **20A** (1981) 606.

3 Paul R C, Banait J S & Narula S P, *Z phys Chem (NF)*, **94** (1975) 199.

4 Jauhar S P, Banait J S, Guraya P S & Narula S P, *Indian J Chem*, **19A** (1980) 797.

5 Rohdewald P & Moldner M, *J phys Chem*, **77** (1973) 373.

6 Fuoss R M, Onsager L & Skinner J F, *J phys Chem*, **69** (1965) 2581.

7 Narula S P, Guraya P S, Jauhar S P & Delesalle G, *Indian J Chem*, **20A** (1981) 129.

8 Harned H S & Owen B B, *The physical chemistry of electrolyte solutions* (Reinhold, New York) 1959.

9 Justice J C, *Electrochim Acta*, **16** (1971) 701.

10 Fernandez-Prini R, *Trans Faraday Soc*, **65** (1969) 3311.

11 Justice J C, Bury R & Treiner C, *J chem Phys Biol* (France), **65** (1968) 1708.

12 Justice J C, *J chim Phys Biol (France)*, **66** (1969) 1193.

13 Fuoss R M & Hsia K L, *Proc Natl Acad Sci* (USA), **57** (1967) 1550 & **58** (1968) 1918.

14 Singh D, Bahadur L & Ramanamurti M V, *J soln Chem*, **6** (1977) 703.

15 Bahadur L & Ramanamurti M V, *J chem Soc Faraday Trans* 1, (1980) 1409.

16 Kay R L & Broadwater T L, *Electrochim Acta*, **16** (1971) 667.

17 Kay R L, Cunningham G P & Evans D F, *Hydrogen bonded solvent systems*, edited by A. Covington & P Jones (Taylor and Francis, London) 1968, pp. 249.

18 Broadwater T L & Kay R L, *J phys Chem*, **74** (1970) 3802.

Indian Journal of Chemistry
Vol. 27A, July 1988, pp. 632-634

Kinetics of Ru(III)-catalysed & Uncatalysed Oxidation of Chloroacetic Acids by N-Bromosuccinimide in Aqueous Solution

P SAROJA & SUSHAMA KANDLIKAR*

Department of Chemistry, Nizam College (Osmania University), Hyderabad 500 001

Received 5 *June* 1987; *revised* 17 *September* 1987; *accepted* 17 *November* 1987

The title reaction, studied in the presence of mercuric acetate and sulphuric acid is first order in [NBS] both in the presence and absence of catalyst Ru(III). However, the order in [substrate] in the absence of Ru(III), is unity which changes to fractional order in its presence. Increase in $[H^+]$ retards the reaction rate. The order of reactivities of the three acetic acids is: trichloroacetic acid > dichloroacetic acid > monochloroacetic acid. Individual rate constants (k), formation constants (K_1) of the complexes of chloroacetic acids and the catalyst and corresponding thermodynamic parameters have been evaluated and a suitable mechanism involving the unprotonated NBS as the reactive species has been suggested.

N-Bromosuccinimide (NBS) has been extensively used as an oxidant in the study of kinetics and mechanism of oxidation of both organic and inorganic substrates. Similar work does not appear to have been carried out employing monochloroacetic acid (MCA), dichloroacetic acid (DCA) and trichloroacetic acid (TCA) as substrates and hence the title investigation.

All the chemicals used were either BDH or E. Merck (AR) samples. The solution of $RuCl_3$ (Johnson-Matthey) was standardised by the method given by Houriuchi and Ichiyyo[1]. Purified acetic acid was used. Solution of NBS was always prepared afresh and standardised iodometrically[2]. All the reactions were carried out in reaction flasks blackened from outside. The reaction was followed by the method described earlier[3].

The results can be summarised as follows:

(i) The reaction mixture containing chloroacetic acid (5×10^{-2} mol dm^{-3}), H_2SO_4 (5×10^{-3} mol dm^{-3}), and $Hg(OAc)_2$ (2×10^{-2} mol dm^{-3}) was mixed with large excess of [NBS] and kept for 36 hr at 30°C. The unutilised NBS was estimated iodometrically till a constant value was obtained. This stoichiometric run indicated that 1 mol of NBS reacted with 1 mol of chloroacetic acid to afford 1 mol of formaldehyde (characterised as usual) in the case of MCA and DCA and 1 mol of formic acid in the case of TCA.

(ii) Under the experimental conditions [NBS] ≪ [S] (where S = substrate) and in the presence and absence of Ru(III) the plots of log $a/(a-x)$ versus time were linear passing through the origin indicating the order in [NBS] to be unity for both the catalysed and uncatalysed systems.

(iii) The rate increased with increase in [S]. The plot of log (rate) versus log [S] in the absence of Ru(III) was linear with unit slope indicating first order dependence in [S].

(iv) At fixed [Ru(III)], the rate of oxidation increased considerably but order in [S] changed from unity to fractional, viz. 0.6, 0.5 and 0.4 in the case of MCA, DCA and TCA respectively.

(v) The reaction rate increased with increase in [Ru(III)] and order in [Ru(III)] was fractional, when the gross rate V_g was considered. However, when the uncatalysed rates V_u were deducted from gross rates V_g the order in [Ru(III)] was unity as revealed by the linear plot of log $V_c (= V_g - V_u)$ versus log [Ru(III)].

(vi) A four-fold change (0.02 to 0.08 mol dm^{-3}) in mercuric acetate concentration had negligible effect on the rate of oxidation.

(vii) Added succinimide in the concentration range of 0.02 to 0.1 mol dm^{-3} had a negligible retarding effect.

(viii) Addition of salts, like $NaClO_4$ and $KHSO_4$ etc. did not have much effect on the rate of reaction.

(ix) The rates of reactions were retarded by increase in $[H^+]$ at constant ionic strength ($NaClO_4$) in the presence as well as in the absence of Ru(III) catalyst. As a typical case the data for NBS – TCA system are given in Table 1.

(x) The reaction rates decreased with increase in percentage of acetic acid in the solvent medium. For

Table 1—Effect of Variation of $[H^+]$ on Rate of Oxidation of Chloroacetic Acids

10^3 [NBS] = 5.00 mol dm^{-3}; 10^2 [$Hg(OAc)_2$] = 2.00 mol dm^{-3}; 10^2 [TCA] = 5.00 mol dm^{-3}; $1/k'$ values are given in parentheses

10^2 $[H^+]$ mol dm^{-3}	10^7 V mol dm^{-3} s^{-1}		
	T = 303 K	T = 313 K	T = 323 K
0.1	2.08 (2.40)	3.75 (1.33)	6.25 (0.80)
0.5	1.67 (3.00)	3.33 (1.50)	5.83 (0.86)
2.5	1.45 (3.45)	2.92 (1.71)	5.00 (1.00)
5.0	1.25 (4.00)	2.50 (2.00)	4.58 (1.09)
10.0	0.83 (6.00)	1.67 (3.00)	3.33 (1.50)
20.0	0.63 (8.00)	1.25 (4.00)	2.50 (2.00)
K (dm^3 mol^{-1})	10.36	9.31	8.75

Table 2—Kinetic and Thermodynamic Parameters for Uncatalysed and Catalysed Reactions

Substrate	$k'' \times 10^4$ (mol^{-1} dm^3 s^{-1}) 303 K	E_a (kJ mol^{-1})	$\Delta G\ddagger$ (kJ mol^{-1})	$-\Delta S^\ddagger$ (JK^{-1} mol^{-1})
	Uncatalysed reaction			
MCA	1.67	68.9	96.3	98.7
DCA	2.50	57.5	95.1	132.5
TCA	6.66	46.0	92.2	161.1
	*Catalysed reaction**			
	k dm^3 mol^{-1} s^{-1}			
MCA	6.57	26.8	69.5	149.2
DCA	8.76	23.0	68.8	159.4
TCA	17.00	17.2	67.1	172.9

*Values of K_1 (dm^3 mol^{-1}) are found to be 8.00, 9.24 and 10.3 at 303 K for MCA, DCA and TCA respectively.

example, under the conditions $[NBS] = 5.0 \times 10^{-3}$ mol dm^{-3}, $[TCA] = 5.0 \times 10^{-2}$ mol dm^{-3}, $[Hg(OAc)_2] = 2.0 \times 10^{-2}$ mol dm^{-3}, $[H^+] = 5.0 \times 10^{-3}$ mol dm^{-3} and temp. = 303 K, 10^7 rate decreased from 3.3 to 0.8 mol dm^{-3} s^{-1} in the absence of catalyst and from 4.16 to 1.67 mol dm^{-3} s^{-1} in the presence of 2.0×10^{-5} mol dm^{-3} of Ru(III) when percentage (v/v) of acetic acid was increased from 10 to 80.

The reaction was carried out at three different temperatures in the range of 300 to 325 K and the thermodynamic parameters have been computed using Arrhenius equation (Table 2).

Uncatalysed reaction

The rate of reaction decreased with increase in $[H^+]$ (Table 1). This may be explained by assuming an equilibrium between unprotonated and protonated NBS ($NBS + H^+ \rightleftharpoons N^+BSH$) and that unprotonated species is the reactive one.

The observed first order dependence in [NBS] as well as in [S] in the uncatalysed reaction is suggestive of a mechanism shown in Scheme 1 (taking MCA as a typical example).

Scheme 1 leads to the rate law (1),

$$-\frac{d[NBS]}{dt} = \frac{k''[NBS][S]}{1 + K[H^+]} \quad \ldots (1)$$

which is in complete accord with the observations. Equation (1) may be written as

$$-\frac{d[NBS]}{dt} \times \frac{1}{[NBS]} = k' = \frac{k''[S]}{1 + K[H^+]} \quad \ldots (2)$$

Taking reciprocal of Eq. (2) we get

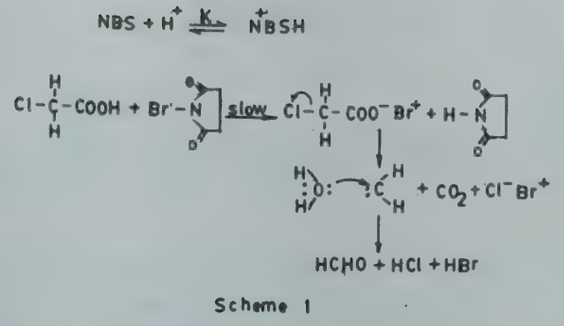

Scheme 1

$$\frac{1}{k'} = \frac{1}{k''[S]} + \frac{K[H^+]}{k''[S]}$$

When $1/k'$ was plotted against $[H^+]$ at different temperatures the plots were linear; k'' values were calculated from the intercepts and when these values were substituted in the values of slope the different equilibrium constants (K) were evaluated (Table 1). These K values decreased with increase in temperature indicating that the protonation of NBS is exothermic in nature.

In order to find out the nature of reactive species, the solvent effect was studied with varying acetic acid content in the solvent. The reaction rate decreased with decrease in dielectric constant i.e. with the increase in acetic acid content, showing a dipole-dipole type of reaction in agreement with the Kirkwood's theory[4].

Catalysed reaction

First order dependence in [NBS] and fractional order in [S] and [Ru(III)], and the ability of platinum group metals to form complexes with organic substrates and highly enhanced rates substantiate formation of Ru(III)−S complex (Scheme 2) which slowly reacts with NBS in the rate-determining step to give products.

$$NBS + H^+ \overset{K}{\rightleftharpoons} N^+BSH$$

$$Ru(III) + S \overset{K_1}{\rightleftharpoons} [Ru(III) - S]\text{complex}$$

$$[Ru(III) - S] + NBS \xrightarrow[\text{slow}]{k} [Ru(V) - S]$$

$$[Ru(V) - S] \xrightarrow{\text{fast}} HCHO + HBr + Ru(III) + NH(CH_2CO)_2 + HCl$$

Scheme 2

Scheme 2 leads to rate law (3)

$$-\frac{d[NBS]}{dt} = k[NBS][\text{complex}] \quad \ldots (3)$$

$$-\frac{d[\text{NBS}]}{dt} = \frac{kK_1[\text{NBS}][\text{S}][\text{Ru(III)}]}{\{1+K_1[\text{S}]\}\{1+K[\text{H}^+]\}}$$

$$-\frac{d[\text{NBS}]}{dt} \times \frac{1}{[\text{NBS}]} = k' = \frac{kK_1[\text{S}][\text{Ru(III)}]}{\{1+K_1[\text{S}]\}\{1+K[\text{H}^+]\}} \quad \ldots (4)$$

where k' is the observed pseudo-first order rate constant, k the bimolecular rate constant for the slow step and K_1 the formation constant. Equation (3) explains all the experimental observations obtained. Taking reciprocal of Eq. (4) we get

$$\frac{1}{k'} = \frac{1}{[\text{S}]}\left\{\frac{1+K[\text{H}^+]}{kK_1[\text{Ru(III)}]}\right\} + \frac{1+K[\text{H}^+]}{k[\text{Ru(III)}]} \quad \ldots . (5)$$

It is clear from Eq. (5) that the plot of $1/k'$ versus $1/[\text{S}]$ at fixed [Ru(III)] should be linear; such Michaelis-Menten reciprocal plots were obtained for all the three acetic acids studied with an intercept on the $1/k'$ axis confirming the derived rate law. From the values of the intercept and slope and the values of K obtained from the unctalysed reaction (Table 1) the bimolecular rate constants (k) and the formation constants (K_1) were evaluated at different temperatures (Table 2).

The rates of oxidation of different acetic acids for both uncatalysed and catalysed reactions followed the order; TCA> DCA> MCA. It was observed that the formation constant (K_1) decreased with increase in temperature indicating that the reaction between Ru(III) and the chloroacetic acid is exothermic in nature. This is also indicated by the ΔH values corresponding to the formation constants. From the results in Tables 1 and 2 it is clear that both $\Delta H^{\ddagger}$ and $\Delta S^{\ddagger}$ are important in controlling the rates of reaction, though the enthalpy factor seems to be predominating. This point was also verified by calculating the isokinetic temperature[5] (β) which was found to be 360 K for catalysed and 400 K for uncatalysed reactions. These are well above the temperature range (303 to 323 K) employed in the work. Constancy of calculated $\Delta G^{\ddagger}$ for catalysed and uncatalysed systems indicates that an identical mechanism is operative for all the three acids.

The authors are thankful to Prof T Navaneeth Rao, and Prof B Sethuram for encouragement and useful discussions.

References

1 Houriuchi Y & Ichiyyo O, *Chem Abstr*, **72** (1970) 50624.
2 Mathur N K & Narang C K, The determination of organic compounds with N-bromosuccinimide, (Academic Press, New York) 1975.
3 Sushama Kandlikar, Sethuram B & Navaneeth Rao T, *Indian J Chem*, **17A** (1979) 264.
4 Kirkwood K G, *J chem Phys*, **2** (1934) 351.
5 Leffler J E, *J org Chem*, (1955) 1202.

Indian Journal of Chemistry
Vol. 27A, July 1988, pp. 635-636

Polyesters of Dimer Acid & Ethylene Glycol†

U D N BAJPAI*, S HINGORANI, A JAIN, H P TIWARI‡ & S K NEMA§

Department of Post Graduate Studies and Research in Chemistry, Rani Durgavati Vishwavidyalaya Jabalpur 482 001

Received 21 *July* 1987; *revised* 17 *November* 1987; *accepted* 10 *December* 1987

The polyesterification reaction between dimer acid (DA) and ethylene glycol (EG) under different experimental conditions has been studied in order to obtain the optimum conditions for synthesizing poly(ethylene glycol) dimerate plasticizers having molecular weights in range of 1000 to 3000. The effects of molar ratio and catalyst concentration on the course of reaction, acidity number, the molecular weight and the intrinsic viscosity of the resultant polyester have been investigated.

Bifunctional esterification necessarily leads to low molecular weight (< 10,000), linear, saturated polyesters, which are useful as plasticizers. Polyester plasticizers are normally prepared by a diol-dicarboxylic acid condensation. Many workers have reported the preparation of polyesters with glycols and unsaturated dibasic acids[1–3]. Herein we report the synthesis of a plasticizing polyester obtained by the polyesterification reaction between dimer acid[4] (DA) (I) and ethylene glycol (EG) and the effects of varying catalyst concentrations and molar ratios between DA and EG on the rate of the reaction.

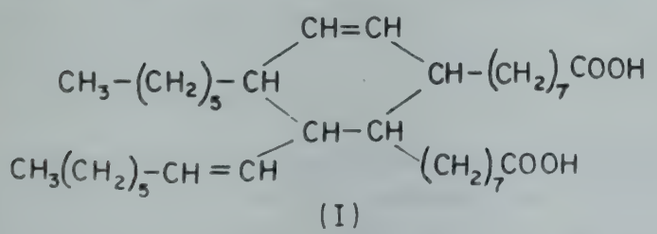

(I)

All the chemicals used were of AR grade. The dimer acid 1010, a gift from Vikram Sarabhai Space Centre, Trivandrum, was used as such. It had the composition: 98% dimer acid + 2% trimer acid and was a dimer of ricinoleic acid. Alcoholic KOH solution (0.1 *N*) was standardised by titrating against 0.1 *N* potassium hydrogen phthalate.

A reaction mixture containing the calculated amount of DA, EG and *p*-toluenesulphonic acid catalyst, if required, was kept at 160° ± 0.1°C under oxygen-free N_2 atmosphere. After fixed intervals of time aliquots (0.2 g each) of hot resin were withdrawn for acid group determination. This reaction was continued for 5 hr. The polyester obtained was a viscous liquid of dark brown colour.

Increase in molecular weight during the course of polyesterification reaction was studied by end group analysis[5] at fixed time intervals. Intrinsic viscosity of the polymer was determined by noting the efflux time of the pure solvent (benzene) and of the polymer solution through a capillary tube viscometer at 28°C. The specific viscosity at polyester concentration of 0.4g/100 ml of benzene was calculated and this was considered as intrinsic viscosity[6].

Different molar ratios, viz. 1:1, 1:1.1, 1:1.2, 1:1.3, 1:1.4, 1:1.5 (DA:EG) were tested, keeping other parameters constant. Polyesters of molecular weights in the range of 1000 to 3000 were obtained from the runs employing excess of EG, which thus behaves like a monofunctional reactant, a molecular weight regulator usually employed in polyesterification reaction. It is observed that as the reaction proceeds, the acidity number decreases in a regular manner becoming constant as the reaction reaches towards completion. The plot of acidity number against time is the same for the polymeric material obtained at molar ratios upto 1:1.3. When higher concentration of EG is used, i.e. at molar ratios 1:1.4 and 1:1.5 excess EG restricts the formation of a homogeneous mixture.

The molecular weight increases gradually with time. The reactants with molar ratios upto 1:1.3 (DA:EG) give polyesters having molecular weights in the range of 1000 to 3000. Increase in the concentration of EG decreases the molecular weights of the resulting polyesters. This may be due to the fact that excess of EG in the system restricts the formation of homogeneous mixture and thus inhibits the normal process of polyesterification. When molecular weight was plotted against time linear plots were obtained.

The effect of varying catalyst concentration (*p*-toluenesulphonic acid) on the rate of reaction was studied, under the following conditions: DA/EG ratio of 1:1.3; temp = 160°C ± 0.1°C. This polyesterification reaction was studied using 0.025, 0.075, 0.10 and 0.25g % of the catalyst. Reaction time decreased considerably in the presence of catalyst. The

---

†Paper presented at the Annual Convention of Chemists held at Ravishankar University, Raipur, 1985.

‡Department of Chemistry, University of Allahabad, Allahabad.

§Vikram Sarabhai Space Centre, Trivandrum.

rate of the reaction increased with increase in [catalyst] the increase being very rapid for the reaction mixture containing 0.1 g % catalyst. The molecular weight of the resulting polyester was also found to increase with increase in [catalyst]. The polyester of desired molecular weight was obtained in the catalyst concentration range of 0.075 to 0.10 g %.

Molar ratios of DA/EG were varied from 1:1 to 1:1.4, keeping the [catalyst] fixed at 0.075 g % and other parameters constant. The acid number was found to decrease with time in all the runs. The molecular weight of the resulting polyester was found to increase with time, its value being dependent on the amount of EG used. Polyester of desired molecular weight was obtained when molar ratio of 1:1.3 (DA:EG) was used. It is observed that the intrinsic viscosity increases with time of the reaction. However, the magnitude of increase is very small in the absence of the catalyst. Nevertheless in the presence of catalyst (0.075 g %) increase in intrinsic viscosity was significant evidently due to increase in molecular weight of polyester.

References

1 Carothers, *U S Patent*, **2** (1939) 174, 619.
2 Bradley T F & Johnston W B, *Ind engng Chem*, **32** (1940) 802; **33** (1941) 86.
3 Cowan J C & Wheeler D H, *J Am chem Soc*, **66** (1944) 84-88.
4 Kumar V G, Venkatachalam S & Rao K V C, *J polymer Sci*, **22** (1984) 2319-2323.
5 Schulz G V & Schon K G, *Z phys Chemie* (*Frankfurt*), **2** (1954) 197.
6 IUPAC Report on Nomenclature in the field of polymers, *J polymer Sci*, **8** (1952) 257.

Indian Journal of Chemistry
Vol. 27A, July 1988, pp. 637-639

Transition Metal Complexes of Hydrazones

R L DUTTA* & KUNTALA DE

Department of Chemistry, The University of Burdwan, Burdwan 713 104

Received 14 *August* 1987; *revised and accepted* 6 *November* 1987

Complexes of Ni(II), Co(II), Cu(II), Mn(II), Zn(II), and Hg(II) chlorides and dioxovanadium(V) with 2-benzoylpyridine isonicotinoylhydrazone and 2-benzoylpyridine quinaldinoylhydrazone have been synthesised and characterised on the basis of analytical, magnetic moment, electronic spectral and infrared spectral data. In a few cases thermal analyses have been carried out to confirm the presence of coordinated aquo groups. Both the ligands have been found to function as neutral tridentate (N,N,O) donors in the isolated complexes.

In continuation of our earlier work[1–3] on complexes of 2-benzoylpyridine benzoylhydrazone (LH) and 2-benzoylpyridine salicyloylhydrazone ($L'H_2$), we report in this note coordination complexes of 2-benzoylpyridine isonicotinoylhydrazone (L″H) (1) and 2-benzoylpyridine quinaldinoylhydrazone (L‴H) (2).

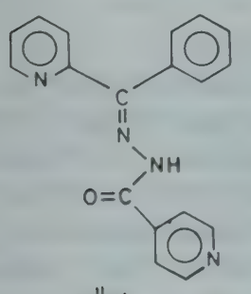

(L″H)

(1)

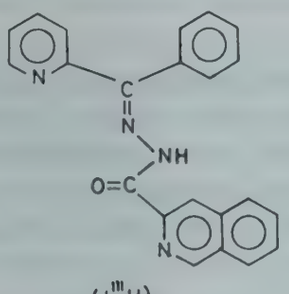

(L‴H)

(2)

2-Benzoylpyridine was obtained from M/s Sigma Chemicals. Isonicotinic acid hydrazide was a BDH product. Quinaldinoylhydrazide was prepared following the standard procedure[4]. The condensation of 2-benzoylpyridine with the above two hydrazines has been reported in our earlier communication[3]. $[VO(acac)_2]$ was prepared by following the standard procedure[5].

Synthesis of complexes

The appropriate ligand and the anhydrous metal chlorides (in 1:1 mole ratio) were dissolved in minimum volume of ethanol and refluxed for 2 hr. The separated crystals were filtered, washed with ethanol and dried over silica gel. Further refluxing of the filtrate did not yield any product. For preparing $[Ni(L''H)SO_4]H_2O$, $NiSO_4.7H_2O$ was dissolved in methanol and then reacted with (L″H). The dioxovanadium(V) complex of (L″H) was obtained by ref luxing a mixture of $[V(O)(acac)_2]$ and ligand in methanol for 3 hr. On cooling, a yellow compound separated, which was collected, washed with cold alcohol and dried.

$[Ni(L''H)SO_4]H_2O$ (0.3 g) was suspended in rectified spirit (10 ml). 2,2′-Bipyridyl (0.12 g) was added to it and was heated on a steam bath for 5 min and cooled in a refrigerator over night. Pink crystals of $[Ni(L''H)(bipy)]SO_4,6H_2O$ were filtered, washed with ice cooled alcohol and dried over silica gel.

The IR spectra were recorded at CDRI, Lucknow and IACS, Calcutta. The electronic spectra were re corded in mull at IISC, Bangalore. Magnetic susceptibilities were determined by Gouy method using $CuSO_4.5H_2O$ as the standard. Diamagnetic corrections were applied using Pascal's data[6]. Conductances of 10^{-3} *M* solutions of the complexes in methanol were measured with the help of a Philips conductivity bridge. Thermolysis curves were obtained at IACS, Calcutta using a Shimadzu DT-30 Thermal Analyser in nitrogen atmosphere (heating rate = 20°C/min). The purity of the samples was checked through elemental analyses (metal, C, H, N and anion). The analytical data are shown in Table 1.

Reaction between a given metal chloride and excess of ligand (L″H or L‴H) produces complex of the type $[M(L''H)/(L'''H)Cl_2]$ or $[M(L'''H)Cl_2,H_2O]$. Under similar conditions in the presence of $NiCl_2$, the ligands (LH) and $(L'H_2)$ get deprotonated and produce complexes $[Ni(L)_2]$ and $[Ni(L'H)_2]$ respectively[1]. That the ligands are present in the keto form is indicated by a small shift[7] ($\Delta\nu$ = 10-20 cm^{-1}) of $\nu C=O$ of the ligands at 1690 and 1685 cm^{-1} respectively. $\nu C=N$ of the free ligands (1600 cm^{-1}) shows a small downward shift ($\sim$10 cm^{-1}) in the complexes.

A mass loss of 3.5% over the range 220-270°C for $[Ni(L'''H)Cl_2H_2O]$ corresponds to the loss of coordinated H_2O (calc. 3.6%). The sample shows two-step decomposition to give NiO at 530°C (% loss found, 85.2 and calc. 85.1; % NiO found, 14.8; calc. 14.9). For $[Ni(L''H)Cl_2].H_2O$ water is lost over the temperature range 70-150°C (found, % H_2O, 3.6 and calc. % H_2O, 4.0). The anhydrous compound is stable upto 270°C and then gives a product which is stable over 350 to 400°C. This stage approximates to the loss of one coordinated chlorine

Table 1—Characterisation Data of Complexes

Compounds*	Colour	Found (calc.) %					$\mu_{eff.}$
		M	N	C	H	Cl/SO_4	
$[Ni(L''H)Cl_2]H_2O$	Yellow	13.1 (13.05)	12.6 (12.45)	47.47 (48.03)	3.58 (3.55)	15.9 (15.78)	3.09
$[Ni(L''H)SO_4]H_2O$	Yellow	12.33 (12.36)	11.85 (11.79)	44.90 (45.5)	4.12 (3.37)	20.0 (20.2)	3.0
$[Co(L''H)Cl_2]$	Red	13.8 (13.63)	12.88 (12.96)	48.91 (50.0)	3.50 (3.24)	16.5 (16.43)	5.02
$[Mn(L''H)Cl_2]$	Orange	12.78 (12.83)	13.10 (13.08)	49.75 (50.47)	3.6 (3.27)	16.48 (16.59)	5.9
$[VO_2(L''H)OH]$	Yellow	13.35 (12.67)	13.98 (13.93)	54.5 (53.13)	3.55 (3.73)	—	0
$[Zn(L''H)Cl_2]$	Yellow	15.24 (14.91)	12.79 (12.77)	49.48 (49.27)	3.38 (3.19)	16.27 (16.2)	—
$[Hg(L''H)Cl_2]$	Yellow	34.8 (34.97)	9.85 (9.76)	—	—	12.5 (12.37)	—
$[Ni(L''H)(bipy)]SO_4,6H_2O$	Pink	8.26 (8.14)	11.8 (11.65)	—	—	13.24 (13.32)	2.95
$[Co(L''H)Cl_2(H_2O)]$	Green	11.86 (11.78)	11.26 (11.20)	52.84 (52.81)	3.13 (3.2)	14.25 (14.2)	5.0
$[Ni(L''H)Cl_2(H_2O)]$	Yellow	11.9 (11.74)	11.4 (11.2)	52.81 (52.83)	3.4 (3.6)	14.3 (14.2)	3.18
$[Mn(L''H)Cl_2]$	Yellow	11.3 (11.5)	11.5 (11.7)	56.0 (55.23)	4.0 (3.34)	14.75 (14.85)	5.8
$[Hg(L''H)Cl_2]$	Faint yellow	32.35 (32.16)	9.0 (8.98)	—	—	11.3 (11.38)	—
$[Cu(L''H)Cl_2(H_2O)]$	Black	12.88 (12.58)	11.37 (11.1)	52.0 (52.3)	3.17 (3.56)	14.27 (14.07)	1.84

*Do not melt even up to 200°C

in the form of HCl (% loss from $[Ni(L''H)Cl_2]H_2O$ to $[Ni(L'')Cl]$, 14.3; calc. 12.12). Both the samples show paramagnetic moments (3.09 & 3.18 B.M.) indicating pseudo-octahedral structure. A ligand-oxygen bridged dimeric structure with the chlorines at *trans* positions is indicated for $[Ni(L''H)Cl_2].H_2O$. The far IR spectrum of the ligand shows a shoulder at 240 cm^{-1} and a sharp peak of medium intensity at 250 cm^{-1}. The complex $[Ni(L''H)Cl_2].H_2O$ shows a shoulder at 240 cm^{-1} and a broad intense absorption band centred at 250 cm^{-1}. This enhancement of absorption is suggestive of *trans* $Ni\text{-}Cl_2$ species. Complexes of the type *trans*-$[Ni\text{-}Cl_2(Py)_4]$ show[8] one νNi-Cl.

The $\nu_2 : \nu_1$ ratios for the two nickel complexes are around 1.5 supporting pseudo-octahedral stereochemistry[9] $[Ni(L''H)Cl_2]H_2O$: 9.56, 14.95, 25.0 kK; $[Ni(L''H)Cl_2,H_2O]$: 9.95, 14.22, 26.31 kK). The three electronic transitions may be assigned as $^3A_{2g} \rightarrow {}^3T_{2g}(\nu_1)$; $^3A_{2g} \rightarrow {}^3T_{1g}(\nu_2)$ and $^3A_{2g} \rightarrow {}^3T_{1g}(P)(\nu_3)$. Expectedly, the 10 *Dq* values (ν_1 of the complexes) are far lower than 10 *Dq* values[1] of $[Ni(L)_2]$ (12.1 kK) and $[Ni(L'H)_2]$ (11.3 kK)[1].

The compl x $[Ni(L''H)SO_4]H_2O$ easily loses the lattice bound water. $\nu C=O$ is shifted from 1690 to 1630 cm^{-1} with the shoulders at 1670 and 1685 cm^{-1}. The $\nu C=N$ shifts from 1580 to 1575 cm^{-1}. The sharp peaks of the ligand at 1000, 1070, 1085, 1110, 1140, 1160, 1180 cm^{-1} are replaced by a broad intense absorption observed from 1040 to 1200 cm^{-1} with peaks around 1050, 1100, 1150, 1180 and 1200 cm^{-1}. A multiply coordinated sulphato group[10] is strongly indicated. Its magnetic moment (3.01 B.M.) indicates six coordination. A bidentate coordination of the sulphato group and attainment of six coordination around nickel(II) are possible in a ligand oxygenbridged dimeric structure, the three donor atoms (N,N,O) of the ligand occupying a face of an octahedron.

The light pink $[Ni(L''H)(bipy)]SO_4,6H_2O$ has a magnetic moment of 2.95 B.M. indicating pseudo-octahedral geometry. Its molar conductance in aqueous medium ($\Lambda_M = 236$ ohm^{-1} cm^2mol^{-1}; $MgSO_4$[11] : 266 $ohm^{-1}cm^2mol^{-1}$) indicates uncoordinated sulphate ion in solution. In methanol, strong ion pair formation is observed ($\Lambda_M = 94$ ohm^{-1} cm^2 mol^{-1}). Its IR spectrum in KBr matrix reveals a strong band at 1120 cm^{-1} confirming the presence of sulphate ion outside the coordination zone[10]. This

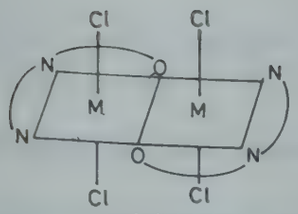

(3)

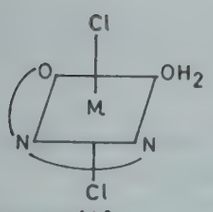

(4)

complex substantiates that a ligand oxygen bridged dimeric structure prevails.

The Co(II) complexes, $[Co(L''H)Cl_2]$ and $[Co(L''H)Cl_2(H_2O)]$ indicate significant solvolysis in methanol ($\Lambda_M = 48$ and 168 ohm^{-1} cm^2mol^{-1}). $\nu C=O$ of (L''H) shifts from 1690 to 1670 cm^{-1} while that of (L''H) shifts from 1685 to 1655 cm^{-1}, thus indicating keto form of the hydrazone ligands in the complexes. $[Co(L''H)Cl_2(H_2O)]$ loses 3.7% in mass in the range 220-280°C (calc. for one H_2O, 3.6%). The corresponding DTA curve reveals an endothermic peak within the above temperature range. Both the Co(II) complexes are paramagnetic ($\mu \sim 5.0$ B.M.) strongly favouring six coordinate geometry[12]. Since the ligand at most can function as a tridentate (N,N,O) donor the complex $[Co(L''H)Cl_2]$ is likely to be a ligand oxygen-bridged dimer with chlorines at *trans* positions (**3**) (one strong band at 240 cm^{-1} in the far IR). Highly intensified absorption at 240 cm^{-1} for both $[Ni(L''H)Cl_2(H_2O)]$ and $[Co(L''H)Cl_2(H_2O)]$ indicates *trans* disposition of the coordinated chlorides (**4**).

The nujol mull electronic spectrum of $[Co(L''H)Cl_2]$ is not well resolved, whereas that of $[Co(L''H)Cl_2(H_2O)]$ shows bands at 10.2, 15.77, 18.15 (sh) and 23.09 kK. The 10.2 and 23.09 kK bands may be assigned to $^4T_{1g} \rightarrow {}^4T_{2g}(\nu_1)$ and $^4T_{1g} \rightarrow {}^4T_{1g}(P)(\nu_3)$ transition. An approximate value of 12.7 kK as 10 *Dq* is indicated.

$[Cu(L''H)Cl_2(H_2O)]$ shows a mass loss of 3.9% over the temperature range 190-280°C (calc. loss for one H_2O, 3.56%). The sample decomposes completely around 680°C to give CuO. $\nu C=O$ shifts downwards by 15 cm^{-1}. Magnetic moment is normal (1.84 B.M.). A broad band centred around 16.4 kK is also usual[13].

The Mn(II) complexes are similar in composition and magnetic moments $[Mn(L''H)Cl_2]$, 5.9 B.M.; $[Mn(L''H)Cl_2]$, 5.8 B.M.). The lowering of $\nu C=O$ indicates keto form of the hydrazone ligand. Ligand oxygen-bridged dimeric structures are likely. $\nu C=O$ of (L''H) shows a small shift (5 cm^{-1}) in the diamagnetic complex $[VO_2(OH)(L''H)]$. ν_{as} and ν_s modes of the *cis* VO_2 group appear at 970 and 885 cm^{-1} {cf. $(NH_4)_3[VO_2(C_2O_4)_2]2H_2O$}[14].

References

1 Dutta R L & Hossain Md M, *Indian J Chem*, **23A** (1984) 30.
2 Seth S & Chakraborty S, *Acta Crystallogr*, **C40** (1984) 1530.
3 Dutta R L & De K, *Indian J Chem*, (in press). IC-5370.
4 Cook A H, Heilbron I M & Steger L, *J chem Soc*, (1943) 413.
5 Moeller T, *Inorganic synthesis*, Vol 5 (McGraw-Hill, New York) 1957, 113.
6 Dutta R L & Syamal A, *Elements of magnetochemistry* (S Chand Co, New Delhi) 1982, 9.
7 Dutta R L & Sarkar A K, *J inorg nucl Chem*, **43** (1981) 57.
8 Clark R J H & Williams C S, *Inorg Chem*, **4** (1965) 350.
9 Sacconi L, *Transition metal chemistry*, Vol 4 (Marcell Dekker, New York) 1968, 199.
10 Nakamoto K & Mc Carthy P J, *Spectroscopy & structure of metal chelate compounds* (John Wiley, New York) 1963, 269.
11 Conway B E, *Electrochemical data* (Elsevier, Amsterdam) 1952, 145.
12 Carlin R L, *Transition metal chemistry*, Vol 1 (Marcel Dekker, New York) 1965, 21.
13 Cotton F A & Wilkinson G W, *Advanced inorganic chemistry*, 3rd Ed (Wiley Eastern, New Delhi) 1972, 916.
14 Satyanarayana D N & Patel C C, *Bull chem Soc Japan*, **37** (1964) 1736.

Indian Journal of Chemistry
Vol. 27A, July 1988, pp. 640-642

Synthesis & Characterisation of Some Bimetallic Derivatives of Dioxouranium(VI) Dialkyldithiophosphates $[UO_2(dtp)_2]$

(Mrs) P R SHUKLA* & S K SRIVASTAVA
Chemistry Department, Lucknow University, Lucknow 226 007

Received 11 *May* 1987; *revised* 14 *September* 1987; *rerevised and accepted* 23 *November* 1987

Several new $UO_2(dtp)_2$ complexes and their bimetallic derivatives with Hg(II), Cd(II) and Ag(I) acceptors have been prepared. The structures of the complexes have been determined through various physicochemical studies. In bimetallic derivatives, coordination from one of the sulphur atoms of $UO_2(dtp)_2$ to the soft metal acceptors is concluded.

In recent years, metal[1,2] and organometal[3,4] dithiophosphates have attracted much attention, but only a single report has appeared on the corresponding oxometal derivatives[5]. This note reports the synthesis and characterisation of some new dioxouranium(VI) dithiophosphates and their adducts with some soft acceptors such as Hg(II), Cd(II) and Ag(I). This study, for the first time reports coordination from the lone pair of the sulphur atom of dithiophosphates, initially bonded to dioxouranium moiety in the parent compounds.

Dioxouranium(VI) acetate (BDH) was converted to $UO_2(OH)_2$ by interaction with aqueous ammonium hydroxide. Phosphorus pentasulphide (BDH), alcohols, 2,2-dimethoxypropane/ and triethyl orthoformate (all Aldrich) were distilled/recrystallised before use. The solvents were purified by standard methods. All reactions were carried out in an atmosphere of dry nitrogen.

Preparation of dioxouranium(VI) bis(dialkyldithiophosphates)

The title compounds were prepared by the insertion of P_4S_{10} between dioxouranium(VI) hydroxide and alcohols using 2,2-dimethoxypropane or triethyl orthoformate as the solvent according to following equation,

$$2UO_2(OH)_2 + P_4S_{10} + 8ROH \rightarrow 2UO_2[S(S)P(OR)_2]_2 + 4H_2O + 2H_2S$$

(R = as in Table 1)

In a representative experiment, to a mixture of freshly prepared dioxouranium(VI) hydroxide (10 mmol) and P_4S_{10} (5 mmol) suspended in 2,2-dimethoxypropane (50 ml) was added slowly methanol (40 mmol) with constant stirring, over a period of 4 hr. The mixture was refluxed when P_4S_{10} went into solution. Dioxouranium(VI) bis(dimethyldithiophosphate) was separated either by keeping in a deep freeze or by the addition of excess of hexane. The product was washed with hexane-ether mixture and dried *in vacuo* over P_4O_{10}.

Identical products were obtained by the reaction of dioxouranium(VI) acetate with sodium salt of dimethyldithiophosphoric acid in methanol at room temperature.

Reaction of dioxouranium(VI) bis(dimethyldithiophosphates) with Hg(II), Cd(II) and Ag(I) salts

In a typical experiment, a mixture of a solution of dioxouranium(VI) bis(dimethyldithiophosphate) (10 mmol) in methanol and $HgCl_2$ (25 mmol) in acetone was stirred at room temperature for about 4 hr. The precipitated product was filtered, washed with acetone/methanol several times and finally with diethyl ether. The product was dried *in vacuo* over P_4O_{10}.

Table 1—Analytical Data of Dioxouranium Bis(Dialkyldithiophosphates)

Dithiophosphate (m.p., °C)	Yield† (%)	Found % (Calc.)			
		U	C	H	S
$UO_2[S(S)P(OCH_3)_2]_2$ (>240)	88	40.6 (40.7)	8.2 (8.4)	2.0 (2.0)	21.8 (21.9)
$UO_2[S(S)P(OC_2H_5)_2]_2$ (198(d))	86	37.1 (37.1)	15.0 (15.0)	3.1 (3.1)	19.9 (20.0)
$UO_2[S(S)P(OC_3H_7^i)_2]_2$ (196(d))	90	34.1 (34.1)	20.6 (20.7)	4.0 (4.0)	18.2 (18.4)
$UO_2[S(S)P(OC_3H_7^n)_2]_2$ (>240)	85	34.1 (34.2)	20.6 (20.7)	3.9 (4.0)	18.3 (18.4)
$UO_2[S(S)P(OC_4H_9^n)_2]_2$ (205(d))	84	31.6 (31.6)	25.5 (25.5)	4.7 (4.8)	17.2 (17.0)

†Through insertion reaction.

Table 2—Analytical Data of Molecular Adducts of Dioxouranium Bis(Dimethyldithiophosphates) $2M'X_2$ or 2 MX

Adduct (m.p., °C)	Found % (Calc.)					
	U	Metal Hg/Ag/Cd	C	H	N	S
$UO_2[S(S)P(OCH_3)_2]_2.2HgCl_2$ (>240)	21.1 (21.1)	35.4 (35.5)	4.2 (4.2)	1.0 (1.0	—	11.3 (11.4)
$UO_2[S(S)P(OCH_3)_2]_2.2Hg(SCN)_2$ (195(d))	19.5 (19.6)	32.8 (32.9)	7.8 (7.9)	0.9 (1.0)	4.5 (4.6)	21.0 (21.0)
$UO_2[S(S)P(OCH_3)_2]_2.2CdCl_2$ (>240)	28.3 (28.3)	26.6 (26.8)	5.6 (5.7)	1.4 (1.4)	—	15.2 (15.2)
$UO_2[S(S)P(OCH_3)_2]_2.2AgSCN$ (200(d))	25.9 (26.0)	23.4 (23.6)	7.8 (7.8)	1.4 (1.5)	3.0 (3.0)	20.8 (21.0)
$UO_2[S(S)P(OCH_3)_2]_2.2Hg(OCOCF_3)_2$ (171(d))	16.5 (16.6)	27.8 (27.8)	×	×	×	8.8 (8.9)
$UO_2[S(S)P(OCH_3)_2]_2.2Hg(OClO_3)_2$ (†)	17.1 (17.2)	28.8 (28.9)	×	×	×	9.2 (9.3)
$UO_2[S(S)P(OCH_3)_2]_2 2AgOClO_3$ (†)	23.8 (28.8)	21.5 (21.6)	×	×	×	12.7 (12.8)
$UO_2[S(S)P(OCH_3)_2]_2.2AgOCOCF_3$ (190(d))	23.1 (23.2)	21.0 (21.0)	×	×	×	12.4 (12.5)

†Explodes before melting. ×Due to explosive character or presence or fluorine, analysis of C, H, N was not possible.

Similar adducts were prepared using $Hg(SCN)_2$, $Hg(OCOCF_3)_2$, $Hg(ClO_4)_2$, $CdCl_2$, AgSCN, $Ag(ClO_4)$, $AgOCOCF_3$ as acceptors (Table 2).

Metal contents and sulphur were determined by the reported methods[6]. Semi-micro estimation of C, H and N and recording of infrared spectra in the range 4000-200 cm^{-1} were carried out at CDRI, Lucknow. The molar conductance values were measured at room temperature by a Phillip's magic eye conductivity bridge model PR9500 using a diptype conductivity cell. Magnetic susceptibilities were determined at room temperature by Gouy's method.

The elemental analyses (Table 1) indicate 1:2 (metal: dithiophosphate) stoichiometry for the complexes. The compounds are yellow-green solids, soluble in common organic solvents. The conductance data in DMSO (10-20 ohm cm mol^{-1}) and acetonitrile (70-90 ohm cm mol^{-1}) show their non-electrolytic nature though in the latter solvent considerable dissociation seems to occur. Magnetic measurements indicate that the complexes are diamagnetic.

In the IR spectrum of dioxouranium(VI) bis-(dimethyldithiophosphate), a strong band occurring in the region 680 ± 2 cm^{-1} has been assigned to $\nu P=S$. It suggests chelating behaviour of dithiophosphate groups[4,7]. Two absorptions around 1020 ± 20 and 752 ± 3 cm^{-1} are assigned to $(P)-O-C$ and $P-O-(C)$ stretching modes respectively[8]. Two absorptions assigned to $\nu U=O$ at 920 ± 5 and 800 ± 4 cm^{-1} clearly indicate the presence of a linear UO_2 moiety[9]. Conclusive evidence of sulphur to metal bonding is provided by an absorption appearing at 378 ± 2 cm^{-1} assigned to $\nu(U-S)$ mode[10]. Structure(I) may be proposed for dioxouranium(VI) bis-(dialkyldithiophosphates) in the solid state.

(I)

In the IR spectra of molecular adducts, dioxouranium(VI) bis(dimethyldithiophosphates).$2M'X_2$ or 2MX(M'=Hg, Cd; M=Ag; X=Cl, SCN, ClO_4, $OCOCF_3$) two strong absorptions located at 610 and 530 cm^{-1} are assigned to $\nu(P=S)$ and $\nu(P-S)$. These indicate the presence of unidentate dialkyldithiophosphate groups. This observation was supported by the shift of $\nu(P)-O-C$ and $\nu P-O-(C)$ to higher wavenumbers (1045 ± 5 and 840 ± 2 cm^{-1} respectively). Due to formation of a new coordination bond considerable electron drift from R takes place resulting in increase in bond orders of C–O and P–O.

The dioxouranium(VI) associated modes of vibration remain unaltered in the adducts. Stretching absorptions due to Hg-S, Cd-S, and Ag-S could not be identified since they lie beyond the recording range of the instrument employed. The thiocyanate group is S-bonded since $\nu C \equiv N$, $\nu C=S$ and δNCS appear at 2060, 730 and 460 cm^{-1} respectively[11]. The trifluoroacetate groups are unidentate[12] since $\nu_{as}OCO$ and $\nu_{sy}OCO$ appear at 1690 and 1430 cm^{-1}, re-

spectively, with $\Delta\nu OCO = 260\ cm^{-1}$. The perchlorate group is unidentately coordinated as $\nu_s Cl-O$, $\nu_s ClO_3$, $\delta_{as} ClO$, $\delta_s ClO_3$ and $\delta_{as} ClO_3$ are located at 910, 1040, 1130, 690 and 620 cm^{-1} respectively[13].

It is thus concluded that one of the sulphur atoms of the dialkyldithiophosphate groups in $UO_2(dtp)_2$ is coordinated to the soft metal atom giving rising to molecular adducts. On the basis of above evidence, structure(II) may be proposed for dioxouranium(VI) bis(dimethyldithiophosphates). $2MX_2$ or 2 MX.

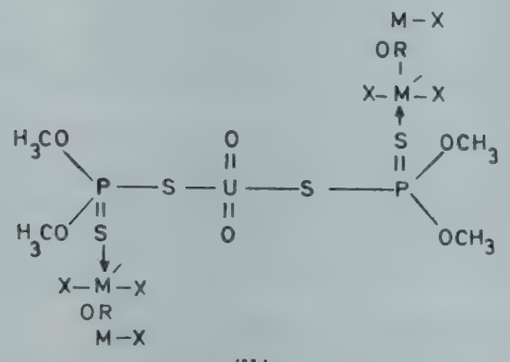

(II)

In the adducts, Hg(II) and Cd(II) are tricoordinated[14] and Ag(I) possesses a coordination number of two[15].

The authors are thankful to Prof. T N Srivastava (Retd. Emeritus Scientist, CSIR) for valuable suggestions. Financial assistance from UGC is gratefully acknowledged.

References

1 Tkachov V V & Alovmyan L O, *Koord Khim*, **8** (1982) 215.
2 Ohki Y, Nakamura M, Suzuki T, Nagai K, Shimoi M & Ouchi A, *Bull chem Soc Japan*, **58** (1985) 1953.
3 Lefforts J L, Molloy K C, Zuckerman J J, Haiduc I, Guta C & Ruse D, *Inorg Chem*, **19** (1980) 2861.
4 Singh B P, Srivastava G & Mehrotra R C, *Synth React inorg met org Chem*, **13** (1983) 963.
5 Edelblut E A & Wetworth R A D, *Inorg Chem*, **19** (1982) 2006.
6 Vogel A I, *A text-book of quantitative inorganic analysis* (Longman, London).
7 Thomas L C, *Interpretations of the infrared spectra of organophosphorus compounds* (Hyden, London).
8 Corbridge D E C, *Topics Phosphorus Chem*, **6** (1969) 235.
9 Dix A H, Diesveld J W & Vanderlinden J G M, *Inorg chim Acta*, **L51** (1977) 24.
10 Bradley D C & Gitlitz M H, *J chem Soc (A)* (1969) 1152.
11 Norbury A H, *Adv inorg Chem radio Chem*, **17** (1975) 31.
12 Garner C D & Hughes B, *Adv inorg Chem radio Chem*, **17** (1975) 1.
13 Hathway B J & Under Hill A E, *J chem Soc*, (1961) 3091.
14 Allman T & Goel R G, *Can J Chem*, **62** (1984) 615.
15 Das R N & Ramannarao D V, *Indian J Chem*, **11** (1973) 603.

Indian Journal of Chemistry
Vol. 27A, July 1988, pp. 643-644

Potentiometric Studies on Some Bivalent Metal Complexes of 2-Hydroxy-1-naphthaldehyde Monosemicarbazone (HNAS)

SAHADEV, R K SHARMA & S K SINDHWANI*
Department of Chemistry, University of Delhi, Delhi 110 007

Received 16 *July* 1987; *revised* 22 *September* 1987; *accepted* 8 *December* 1987

The proton-ligand stability constants of 2-hydroxy-1-naphthaldehyde monosemicarbazone and metal-ligand stability constants of its complexes with Mg^{2+}, Mn^{2+}, Cd^{2+}, Pb^{2+}, Zn^{2+}, Co^{2+}, Ni^{2+}, Cu^{2+} and UO_2^{2+} have been determined potentiometrically at different ionic strengths in 75% (v/v) aqueous dioxan medium. The method of Bjerrum and Calvin as modified by Irving and Rossotti has been used to find out the values of $\bar{n}$ and *pL*. The stability constants have been calculated on IBM 360 FORTRAN IV computer using the weighted least squares method. The values of $S_{min} = \chi^2$ have also been calculated. The order of stability constants is found to be: $UO_2^{2+} > Cu^{2+} > Ni^{2+} > Co^{2+} > Zn^{2+} > Pb^{2+} > Cd^{2+} > Mn^{2+} > Mg^{2+}$. The other thermodynamic parameters and ligand field stabilization energies have been calculated from the stability constants.

The semicarbazones and thiosemicarbazones of certain aldehydes and ketones have significant antimicrobial activities[1-5]. Domagk *et al.*[6] reported for the first time the antitubercular activities of metal thiosemicarbazones and semicarbazones. The activity of semicarbazones is thought to be due to their strong chelation with trace metal ions present in biological systems.

As a part of a study undertaken in our laboratories on the stabilities of metal complexes of biologically active ligands, we report here the stabilities of the complexes of some bivalent metal ions with 2-hydroxy-1-naphthaldehyde monosemicarbazone (HNAS) at various ionic strengths in 75% (v/v) aqueous dioxan medium.

A digital *p*H meter (ECIL, model *p*H 5651) in conjunction with a glass electrode (0-14 *p*H range) was used for *p*H measurements. All the measurements were made at a constant temperature using an MLW (FRG) (NBE type) thermostat. An IBM 360 FORTRAN IV computer was used for most of the calculations.

Preparation of ligand

2-Hydroxy-1-naphthaldehyde (1.038 g) was dissolved in the minimum amount of ethanol and an aqueous solution containing equal amounts of semicarbazide hydrochloride (0.672 g) and anhydrous sodium acetate was added to it. The mixture was refluxed for 2 hr, filtered (if necessary) and cooled in ice. The semicarbazone was precipitated by adding dilute hydrochloric acid and recrystallized from ethanol. 2-Hydroxy-1-naphthaldehyde monosemicarbazone (HNAS) solution was prepared in 75% (v/v) aqueous dioxan medium. The decomposition point of the ligand (HNAS) is 214°C. The purity of the ligand was checked by TLC, elemental analyses, IR and NMR spectra. The solutions of bivalent metal ions were standardised by conventional methods. Me_4NOH (TMAH) (E Merck, AG Darmstadt) in 75% aqueous dioxan was used as the titrant. The solution was standardised with oxalic acid. $HClO_4$ was standardised with prestandardised Na_2CO_3 and diluted to the required strength (0.05 mol l^{-1}) with doubly distilled water. Sodium perchlorate (E Merck, AG Darmstadt) was used to maintain the ionic strength constant for different sets. Dioxan (Merck) was purified before use.

Investigations were carried out at different ionic strengths (0.1, 0.05, 0.025 and 0.01 mol l^{-1}). *p*H correction factor and volume correction factor were applied for getting accurate values of stability constants. For each set of experiments, the final volume was made up to 20 cm^3, maintaining 75% aqueous dioxan medium. Each set was titrated against 0.05 *M* TMAH in 75% aqueous dioxan. Requisite amount of $NaClO_4$ was added to maintain the ionic strength at 0.1, 0.05, 0.025 and 0.01 *M*. These titrations were carried out in a closed double walled container in an atmosphere of nitrogen, which was presaturated with 75% aqueous dioxan.

Values of $\bar{n}_H$ were calculated at various *p*H values from the above titration curves. The values of $\log \bar{n}_H/1-\bar{n}_H$ versus *p*H gave linear plots having intercept equal to pK_a (ligand dissociation constant) and slopes equal to unity. From the titration curves of solutions, $\bar{n}$ values of the metal complexes were determined at various *p*H values. From pK_a and $\bar{n}$ values at different *p*H values, the corresponding values of *pL* were calculated. The $\bar{n}$ and *pL* data were subjected to the weighted least squares method developed by Sullivan *et al.*[10] on an IBM 360 FORTRAN IV computer to get β_n values. The weighted least square treatment determined the set of β_n values which make the function U

$$U = \sum_{n=0}^{N} (y - x - nz)\,\beta_n x^n$$

Table 1 – Stability Constants of Bivalent Metal Complexes of 2-Hydroxy-1-naphthaldehyde Monosemicarbazone

[Ionic strength = 0.1 *M* $NaClO_4$; temp. = 20 ± 0.5°C]

Metal ion/ ligand	Weighted least squares method			
	$\log K_1$	$\log K_2$	$\log \beta_2$	S_{min}
H^+	10.45	—	—	—
Mg^{2+}	3.22	3.03	6.25	0.0051
Mn^{2+}	5.03	4.17	9.20	0.0341
Cd^{2+}	5.65	4.23	9.88	0.0302
Pb^{2+}	6.05	5.80	11.85	0.0548
Zn^{2+}	7.82	6.43	14.25	0.0190
Co^{2+}	8.60	7.58	16.18	0.0097
Ni^{2+}	8.93	7.99	16.92	0.2232
Cu^{2+}	9.10	8.24	17.34	0.2512
UO_2^{2+}	9.98	9.36	19.34	0.1163

nearest to zero, by minimizing S

$$S = \sum_{i=1}^{1} W_i U^2 (x_i y_i z_i)$$

with respect to variation in β_n. S_{min} has the same statistical distribution as χ^2 with K degrees of freedom and the weight defined in accordance with Sullivan *et al.*[11]. S_{min} can be equated to χ^2.

The order of stability constants of the metal complexes with HNAS is: $UO_2^{2+} > Cu^{2+} > Ni^{2+} > Co^{2+} > Zn^{2+} > Pb^{2+} > Cd^{2+} > Mn^{2+} > Mg^{2+}$. The order is in good agreement with the order found by Mellor and Maley[12] and Irving and Williams[13,14]. In all the systems, the values of $\log K_1$ are greater than $\log K_2$ values. The $\log K_1$, $\log K_2$, $\log \beta_2$ and S_{min} values at different ionic strengths are given in Table 1. All the complexes appear to be high spin.

Finally, in view of the very low (5.0×10^{-4} *M*) concentration of metal ions used in the titration, it has been assumed that the possibility of formation of polynuclear complex is negligible. In the present studies, it has been observed that the value of dissociation constant (pK_a) of the ligand (HNAS) and stability constant decreases with increasing ionic strength of the medium, which is in agreement with Debye-Huckel equation[15]. The thermodynamic stability constants were obtained by extrapolating the linear plot of $\log K_1$ versus $\sqrt{\mu}$ to zero ionic strength.

The ligand field stabilization energy, 'δH' and E_r (Mn – Zn) values have been calculated according to the method of George and McClure and listed in Table 2. The orders of enthalpies, free energies and ligand field stabilization energies

Table 2 – Er(Mn – Zn) and δH Values for Complexes of HNAS

Parameters	Metal ions				
	Mn^{2+}	Co^{2+}	Ni^{2+}	Cu^{2+}	Zn^{2+}
$\log K_1^\circ$	5.95	9.28	9.33	10.45	8.02
ΔG	7.98	12.44	12.51	14.01	10.75
ΔG_r	—	4.46	4.53	6.03	2.77
ΔH_H	—	43.00	62.00	63.00	47.00
ΔH_L	—	47.46	66.53	69.03	49.77
$[(n\text{-}5)/5]E_r$	—	19.91	29.86	39.82	—
δH	—	27.55	36.67	29.21	—

ΔG = Free energy change = 2.303 *RT* $\log K_1^\circ$, where *R*, T and K_1° have usual significance and temp. = 293K.
ΔG_r = Change in heat content for the formation of the complex in solution.
ΔH_H = Heat of hydration of metal ion.
ΔH_L = Heat of complexation referred to metal ion in gaseous and ligand in solution state.
n = Number of electrons in 3*d* orbital.
$[(n\text{-}5)/5]E_r$ = Lattice energy difference for Zn^{2+} and Mn^{2+} complexes.
δH = Thermodynamic stabilization energy.
$\log K_1^\circ$ = Value employed for the above calculations, have been obtained by extrapolating the $\log K_1$ versus $\sqrt{\mu}$ (linear) to zero ionic strength.

'δH' have been found to be: Mn < Co < Ni < Cu > Zn; Mn < Co < Ni < Cu > Zn and Co < Ni > Cu respectively.

References

1 Barreet P A, *Nature*, **206** (1965) 1340.
2 Doamaral J R, Blanz E J & French F A, *J mednl Chem*, **12** (1969) 21.
3 Bauer D J, Vincent L St, Kempe C H & Downe A W, *Lancet*, **2** (1963) 494.
4 Petering H G, Buskirk H H & Underwood G E, *Cancer Res*, **64** (1964) 367.
5 Orlova N N, Aksevova V A, Selidovkin D A, Bogdanova Z N S & Pershin G N, *Russ pharm Toxical*, (1968) 348.
6 Domagk G, Behnisch R, Mietzsch F & Schmidt H, *Naturwissenschaften*, **33** (1946) 315.
7 Bjerrum J, *Metal amino formation of aqueous solution* (Hasse, Copenhagen), 1941, 298.
8 Calvin M & Wilson K W, *J Am chem Soc*, **67** (1945) 2003.
9 Irving H M & Rossotti H S, *J chem Soc*, (1954) 2904.
10 Sullivan J C, Rydberg J & Miller W F, *Acta chem scand*, **13** (1959) 2023.
11 Sullivan J C, Rydberg J & Miller W F, *Acta chem scand*, **13** (1959) 2059.
12 Mellor D P & Maley L, *Nature*, **159** (1947) 370.
13 Irving H & Williams R J P, *Nature*, **162** (1948) 746.
14 Irving H M & Williams R J P, *Analyst*, **77** (1952) 813.
15 Nasanen R & Ekman A, *Acta chem scand*, **6** (1952) 1389.

Indian Journal of Chemistry
Vol. 27A, July 1988, pp. 645-647

Stability Constants of Cobalt(II) Complexes with Some Thiols

E M KHAIRY, N A DARWISH, A L EL–ANSARY* & O E SHERIF

Chemistry Department, Faculty of Science, Cairo Univerity, Cairo, Egypt

Received 25 *November* 1985; *revised* 29 *September* 1986; *rerevised and accepted* 11 *December* 1987

Cobalt(II) forms violet coloured complexes with thiophenol (Ia), *p*-toluenethiol (Ib), *p*-nitrothiophenol (Ic) and *p*-chlorothiophenol (Id), in isopropanol. All the ligands form 1:1 and 1:4 (M:L) complexes; stable 1:2 complex is detected only with thiol Ib. The stepwise stability constants have been calculated using various methods. The solid complexes have been also prepared and characterised by elemental analysis, TGA and IR spectroscopy.

The synthesis and properties of metal complexes of S-containing ligands, such as thioketones, thiols and thiocarboxylic acids, were reviewed by Ohnchi[1]. Kumar *et al.*[2] showed by spectrophotometric studies that Co(II) and thiosalicylic acid form a dark-brown 1:3 complex which is stable in the *p*H range 3-11.5. Monothiolates of cobalt were studied by Ospanov[3], who reported formation of a 1:2 (Co:ligand) complex in acid medium and a 1:4 species in neutral to slightly alkaline media.

The present investigation comprises the preparation and spectrophotometric investigation of Co(II) complexes with thiophenol (Ia), *p*-toluenethiol (Ib), *p*-nitrothiophenol (Ic), and *p*-chlorothiophenol (Id).

All the chemicals used were of AR grade. A stock solution of $Co(ClO_4)_2.6H_2O$ was prepared and standardised by titrating with EDTA[4]. Solutions of all the thiols were invariably freshly prepared before each experiment.

The molecular compositions of the stable complexes detected in solution were confirmed by several experimental techniques[5-9]. The overall and stepwise formation constants of the complexes were evaluated by applying the mole ratio method and the method of corresponding solutions[10].

Spectrophotometric studies of the complexes formed in solution were conducted using Pye-Unicam SP 1750 and Carl-Zeiss spectrophotometers.

The solid complexes were prepared by adding different proportions of metal ion to ligand (1:1 to 1:6), both being dissolved in isopropanol. The products, which separated out after being left overnight in contact with the mother liquor, were filtered, thoroughly washed with ethanol and ether, and then dried *in vacuo*. The precipitated complexes were analysed for C, H, N, Cl and S using microanalytical methods. The percentage of Co(II) was also determined by EDTA titration[4].

The IR spectra of the thiols and the separated solid complexes were scanned in the 400-4000 cm^{-1} range using a Pye Unicam SP 1100 infrared spectrophotometer, applying the KBr disc technique.

The results of spectrophotometric studies in solution indicate no significant effect of *p*H within the range 4.0-10.5 on the absorbance of Co(II) complexes with most of the above thiols. However, the maximum absorption of Co(II)-Ib complex is observed at *p*H 6.0. It was also found that the process of complex formation comes to completion after a time period of 30-60 min. This may be taken as an indication of a rather slow ligand substitution process.

Stability constants of complexes

The stability constants of the complex species obtained in solution were calculated by graphical and

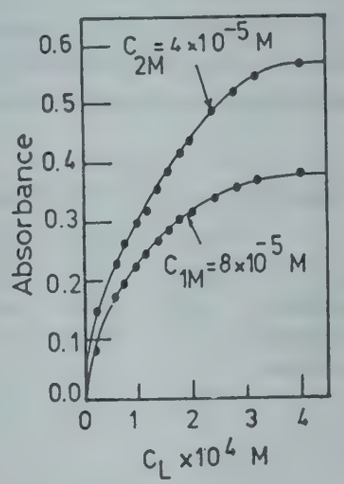

Fig. 1—Absorbance-C_L plot for Co(II)-thiophenol complexes using the corresponding solutions method

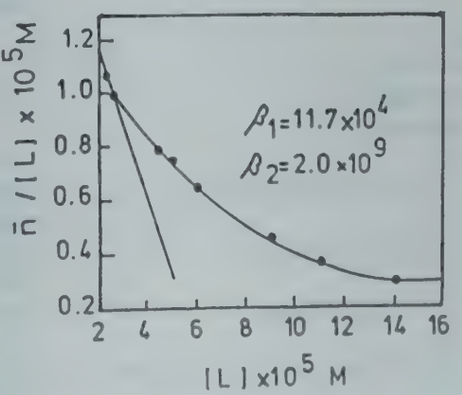

Fig. 2—Application of Olerup method to Co(II)-thiophenol complexes

computational techniques[10-15]. Grabaric *et al.*[10] have used the spectrophotometeric results obtained by the corresponding solutions method to calculate the formation constants of Ni(II)-2-hydroxybutyrate complexes. Their method as modified by Khairy *et al.*[16] was applied in this work. The absorbance-ligand concentration curves of the corresponding solutions are shown in Fig. (1). From the curves, the formation function n and the free ligand concentration [L] were calculated, whereby $n/[L]$ values were obtained and plotted against [L] (Fig. 2). By extrapolation to [L] = zero, the value of K_1 (β_1) could be determined.

The results are listed in Table 1. There is a good correlation between the stability constants and the basicity constants of the thiolato ligands. The log β values increase as the pK_a values increase. This relation was also observed while correlating Hammett (σ) constants and is indicative of the fair competition between the metal ion and proton of the thiol molecule.

The analytical data of the solid complexes (Table 2) reveal the formation of 1:1 and 1:4 complexes in the case of Ia, 1:2 complex in the case of Ib, and 1:4 complexes withIc and Id.

The assignment of the main bands in the IR spectra of free thiols and their Co(II) complexes are given in Table 2. The S-H stretching band located at 2600-2550 cm^{-1} (ref. 17) in free thiols is lowered to 2300-2400 cm^{-1} indicating coordination through the thiol S-atom. The coordination is also confirmed by a similar shift of the C-S stretching vibration, e.g. in case of thiophenol the band shifts from 730 to 685 cm^{-1}. In all complexes, a broad band observed in the range 3340-3640 cm^{-1} is attributed to νOH of the coordinated isopropanol molecule[17]. This confirms the participation of alcohol (solvent) molecules in the coordination sphere of some complexes. On the other hand, a broad band appears in the spectra of some complexes around 3400 cm^{-1}, which is attributed to νOH of water, confirming its presence in the complex separated.

The molar conductance values of the solid complexes in DMF (0.001 *M*) reveal that Co-Ib, Co-Ic and Co-Id are non electrolytes while that of Co-Ia (85.8 mho cm^2/mol) indicates the ionic nature of perchlorate ions.

Thermogravimetric analysis of the solid complexes was obtained using Du Pont 1090 TGA. The results shown in Table 3 are in good agreement with the proposed formulae. It is clear that the water molecules are coordinated more tightly than isopropanol.

References

1 Ohnchi Akira, *Kagakv Naryoiki*, **25** (1971) 487.

Table 1—Stability Constants of Co(II)-Thiol Complexes

	$\log \beta_1$	$\log \beta_2$	$\log \beta_3$	$\log \beta_4$
Co(II)-Thiophenol	4.99	4.7	13.93	18.46
Co(II)-*p*-Toluenethiol	5.23	9.88	14.13	18.44
Co(II)-*p*-Nitrothiophenol	5.22	9.45	13.53	17.81
Co(II)-*p*-Chlorothiophenol	8.3	7.77	11.78	16.32

Table 3—Thermogravimetric Data of Co(II)-Thiol Complexes

Complex	130-140°C*		160-180°C†	
	Calc.	Found	Calc.	Found
Co-Ia (1:1)	28.34	27.9	8.50	8.20
(1:4)	—	—	6.75	6.95
Co-Ib (1:2)	28.24	28.10	—	—
Co-Ic (1:4)	7.94	7.83	2.38	2.41
Co-Id (1:4)	15.89	15.65	—	—

* Loss of C_3H_7OH, † loss of H_2O

Table 2—Analytical and IR Data of the Complexes

Ligand/complex	C% Calc. (found)	H% Calc. (found)	S% Calc. (found)	νSH cm^{-1}	νC—S cm^{-1}	νOH cm^{-1}
Thiophenol (Ia)				2570(s)	730(s)	(Ia)
p-Toluenethiol (Ib)				2580(s)	730(s)	
p-Nitrothiophenol (Ic)				2560(s)	680(s)	
p-Chlorothiophenol (Id)				2580(s)	740(s)	
Co(II)-Ia (1:1)	34.0	5.9	7.6			3640-3340(b)
$Co(C_6H_5S)(C_3H_7OH)_2(H_2O)_2ClO_4$	(34.9)	(5.7)	(7.8)			
Co(II)-Ia (1:4)	54.04	4.88	24.02	2320(v.w)		3300-3660(b)
$Co(C_6H_5SH)_2(C_6H_5S)_2(H_2O)_2$	(54.00)	(4.80)	(24.20)			
Co(II)-Ib (1:2)	55.4	5.13	19.69			3320-2600(b)
$Co(CH_3C_6H_4S)_2(C_3H_7OH)_2$	(55.5)	(5.00)	(19.60)			
Co(II)-Ic (1:4)	42.92	3.71	16.96	2340(v.w)		3640-3380(b)
$Co(NO_2C_6H_4S)_2(NO_2C_6H_4SH)_2(C_3H_7OH)H_2O$	(42.70)	(3.70)	(16.60)			
Co(II)-Id (1:4)	47.69	4.50	16.96	2400(v.w)		3400-3620(v.w)
$Co(ClC_6H_4S)_2(ClC_6H_4SH)_2(C_3H_7OH)_2$	(48.00)	(4.30)	(7.30)			

2 Kumar A N, Nigam H L & Katyal M, *J Prakt Chem*, **33** (1966) 160.
3 Ospanov Kh K, Fedosov S N, Songina O A & Sarmurzina R G, *Izv Akad Nauk Kaz SSR Ser Khim*, **22** (1972) 4.
4 Welcher F J, *The analytical uses of ethylenediaminetetraacetic acid* (D Von Norstand, New Jersy) 1965, 234.
5 Yoe J H & Jones A L, *Ind Eng Chem Anal Edn*, **16** (1944) 11.
6 Harvey A E & Manning D L, *J Am chem Soc*, **72** (1950) 4488.
7 Vosburgh W C & Cooper G R, *J Am chem Soc*, **63** (1941) 437.
8 Bent H E & French C L, *J Am chem Soc*, **63** (1941) 658.
9 Asmus E L, *Z anal Chem*, **178** (1960) 104.
10 Grabaric B, Piljac I & Filipovic I, *Anal Chem*, **45** (1973) 1932.
11 Olerup H, *Svensk Kem Tidskr*, **85** (1943) 324.
12 Rossotti F J C & Rossotti H S, *Acta chem scand*, **9** (1956) 1166.
13 Rossotti F J C & Rossotti H S, *The determination of stability constants* (McGraw Hill, New York) 1961, 108.
14 Bjerrum J, *Metal amine formation in aqueous solution* (Hasse, Copenhagen), 1941.
15 Leden I, *Z phys chem*, (*Leipzig*), *A*, **188** (1941) 160.
16 Khairy E M, Shoukry A F & Ahmed J U, *Egypt J Chem*, **25** (1982) 545.
17 Rao C N R, *Chemical applications of infrared spectroscopy* (Academic Press, London) 1963, 297, 611.

Indian Journal of Chemistry
Vol. 27A, July 1988, pp. 648-649

Phthalhydrazidylazoacetylacetone as a Chemiluminescent Complexometric Indicator

K KRISHNAKUTTY & N THANKARAJAN*
Department of Chemistry, University of Calicut, Kerala 673635

Received 24 *August* 1987; *revised and accepted* 19 *November* 1987

Phthalhydrazidylazoacetylacetone has been shown to be a suitable chemiluminescent indicator in EDTA titration of Mn(II), Ni(II), Cu(II), Zn(II), Cd(II), Ca(II) and Mg(II). Applicability of the indicator in highly coloured solutions has also been demonstrated.

Phthalhydrazidylazoacetylacetone (PHA) has been reported as an efficient chemiluminescent (CL) indicator in acid-base titrations[1]. This note reports the use of PHA as a CL indicator in complexometric titrations with EDTA. The added advantage of PHA is its applicability even in highly coloured solutions.

In alkaline medium, oxidation of PHA by hydrogen peroxide is attended[2] by a weak CL emission at 475 nm. However, in the presence of heavy metal ions which catalyse decomposition of hydrogen peroxide, the CL emission is quite intense. Complexones like EDTA can, however, effectively deprive the heavy metal ions of their catalytic effect, by sequestering them. Thus, when a solution of a catalytic metal ion, admixed with the indicator solution, is titrated in alkaline medium against standard EDTA containing hydrogen peroxide, the end point is marked by the abrupt attenuation of the bright CL emission. If titration is carried out in the reverse direction, the CL emission intensifies suddenly at the end point. Although many azo compounds have been used as indicators in chelatometric titrations, this is the first report of use of an azo compound as a CL indicator in such titrations[3].

The indicator solution was prepared by dissolving PHA (10 mg) in ethanol (50 ml), and diluting to 100 ml with water.

In a typical titration, the metal salt solution (10 ml) containing ammonia buffer (5 ml, *p*H 10) and the indicator (five drops) was titrated against standard 0.01 *M* EDTA solution, which was 0.001% with respect to hydrogen peroxide. Mixing was effected by a magnetic stirrer. At the end point, an excess drop of the titrant produced a sudden change from intense Cl to a dull glow. Although a semi-darkened room is preferable for detection of end point, titrations can be carried out even in daylight by placing the titration flask in a cardboard box with an observation hole on one side. This method was used for the direct determination of copper(II), nickel(II), zinc(II), cadmium(II) and manganese(II).

Table 1 – Results of Estimations

Analyte metal	Metal content (mg) in 10 ml of metal salt solution			
	Theoretical	Standard method	CL method	
			Without g.v.	With g.v.
Manganese	5.50	5.49	5.51	5.51
Nickel	5.79	5.82	5.78	5.80
Copper	6.51	6.48	6.55	6.54
Zinc	6.59	6.55	6.58	6.61
Cadmium	11.28	11.26	11.31	11.30
Magnesium	2.44	2.43	2.42	2.42
Calcium	4.05	4.02	3.98	4.01

g.v. = gentian violet.

Results obtained presently and those of complexometric titrations using metallochromic indicators are given in Table 1. In all cases blank titrations were carried out. Variation of results observed was less than ± 0.02 mg in replicate determinations of the various metal ions. Concentrations of these divalent metal ions as low as 10^{-4} *M* could thus be determined.

Calcium and magnesium ions are ineffective in catalysing decomposition of hydrogen peroxide, and hence do not cause intense CL with the indicator. These ions were, therefore, determined indirectly as follows: To a buffered solution (*p*H 10) of calcium or magnesium ion, a known excess of EDTA, indicator (five drops) and hydrogen peroxide (five drops, 0.01%) were added, and the unreacted EDTA back titrated against standard copper(II) salt solution. At the end point the feeble glow of the solution suddenly became brilliant. Results of these determinations are also included in Table 1. Determination of the total content of calcium and magnesium in hard water yielded accurate results by this method.

To test the efficiency of the CL indicator in highly coloured solutions, titrations using the indicator were carried out in the presence of gentian violet (0.003%). These results are also included in Table 1. Heavy metal ions which catalyse the decomposition of hydrogen peroxide evidently interfere in these determinations. However, with suitable masking agents the selectivity of the method can be increased so that it becomes viable in the analyses of metal ions in a variety of matrices.

References

1 Thankarajan N & Krishnankutty K, *Talanta*, **34** (1987) 507.

2 Thankarajan N, Krishnankutty K & Srinivasan T K K, *J. Indian chem Soc*, **63** (1986) 977.

3 Bishop E, *Indicators* (Pergamon Press, New York) 1972.

Indian Journal of Chemistry
Vol. 27A, July 1988, pp. 650-651

Extractive Photometric Determination of Palladium(II) with 4-Nitrosoresorcinol in Presence of Pyridine & Some of Its Methyl Substituted Derivatives

A SARKAR, T K THOKDAR, P K PARIA* & S K MAJUMDAR

Department of Chemistry, North Bengal University, Darjeeling 734 430

Received 18 *June* 1987; *revised* 14 *September* 1987; *accepted* 11 *December* 1987

An extractive photometric method is proposed for the determination of Pd(II) using 4-nitrosoresorcinol and pyridine/substituted pyridines. The mixed-ligand complexes of palladium(II) with 4-nitrosoresorcinol and pyridine/its methyl derivatives are extractable into chloroform and obey Beer's law. The molar absorptivities of the complexes are $(2.6\text{-}3.5) \times 10^4$ l mol^{-1} cm^{-1} at λ_{max} 395-400 nm and Sandell's sensitivities are 0.003-0.004 μg Pd(II)/cm^2. The influence of foreign ions is studied.

The use of pyridine-thiocyanate for extractive-photometric determination of various metals is well established[1–6]. 4-Nitrosoresorcinol reacts with cobalt(II) and palladium(II) to form red complexes which are insoluble in chloroform. The reaction was used for detection and determination of the metals[7,8] in aqueous solution by colour comparison. In the present note we report the extractive photometric determination of Pd(II) with 4-nitrosoresorcinol in presence of pyridine and some of its methyl substituted derivatives like α-picoline, β-picoline, γ-picoline and 2,4,6-collidine, extractable into chloroform under optimum conditions.

The absorbance measurements were made with a Shimadzu PR 1 spectrophotometer equipped with stoppered quartz cells of 10 mm path length. An ECL 5651 digital *p*H meter was used for *p*H measurements.

Palladium chloride (Johnson & Matthey) (1 g) was dissolved in hot conc. HCl (1 ml) and diluted to 250 ml with distilled water followed by standardisation with dimethylglyoxime[9]. A working solution (210.5 μg Pd/ml) was prepared by dilution. Chloroform(E Merck), pyridine (BDH), α-picoline (Riedel), β-picoline, γ-picoline (BDH), (Fluka) and 2,4,6-collidine (BDH) were distilled before use.

4-Nitrosoresorcinol was prepared according to γ-picoline the known procedure[10]. The light yellow crystalline solid, which was formed, was filtered off and recrystallized from dilute ethanol. The reagent in the solid state is very unstable, but its ethanolic solution is stable.

General procedure

An aliquot of sample solution was mixed with 0.2 ml of 1% ethanolic solution of 4-nitrosoresorcinol followed by addition of (0.5 ml, 100%) pyridine/α-picoline/β-picoline/γ-picoline/2,4,6-collidine. The *p*H of the solution was adjusted to 2 with KCl-HCl buffer. The volume of the aqueous phase was maintained at 10 ml. The solution was then equilibrated with 10 ml of chloroform in a separating funnel for 1 min. The two layers were allowed to settle. The separated organic layer was shaken with anhydrous sodium sulphate to remove any moisture. Finally the absorbance of the organic extract was measured at the corresponding absorption maxima (Table 1) against a palladium-free reagent blank. The amount of palladium(II) was determined from a previously prepared calibration curve.

The extraction of palladium complexes was investigated in the *p*H range 0-11. Chloroform extracts showed maximum and steady absorbance when the extractions were carried out in the *p*H range 1-8. When the extraction was repeated with the same aqueous phase, the organic extract virtually showed no absorbance. The aqueous phase, after extraction, was also tested for palladium by an independent method. This indicated a complete and quantitative extraction of palladium in this *p*H range.

The spectra of the mixed-ligand complexes were scanned in the wave-length region 300-600 nm against the corresponding reagent blanks. The Pd(II)-complexes showed absorption maxima at 395-400 nm. As the reagent blanks showed some absorbances in the aforesaid wave-length region, all the analytical measurements were carried out against the respective reagent blanks. Figure 1 shows the spectrum of pd(II)-4-nitrosoresorcinol-γ-picoline system and the corresponding reagent blank. The optimum concentration of the reagents for the purpose of quantitative extraction of the complexes was ascertained by extracting palladium(II) at various concentrations of 4-nitrosoresorcinol and pyridine bases. Extraction was found to be quantitative when 0.2 ml of 1% ethanolic solution of 4-nitrosoresorcinol and 0.5 ml of pyridine/α-picoline/β-picoline/γ-picoline/2,4,6-collidine were used. Under these optimum conditions 84.2 μg of Pd(II) was found to be quantitatively extracted. The higher concentrations of the reagents had no adverse effects on the extraction.

The quantitative extraction of palladium occurred in a single operation when the layers were shaken

Table 1—Details of Extractive Methods

Parameter	Base employed				
	Pyridine	α-picoline	β-picoline	γ-picoline	2,4,6-collidine
λ_{max} (nm)	395	400	395	395	400,410*
Molar absorptivity ($l\,mol^{-1}cm^{-1}$)	3.28×10^4	2.68×10^4	3.44×10^4	3.52×10^4	3.47×10^4
Sandell's sensitivity ($\mu g/cm^2$)	0.0032	0.0039	0.0030	0.0029	0.0031

*shoulder

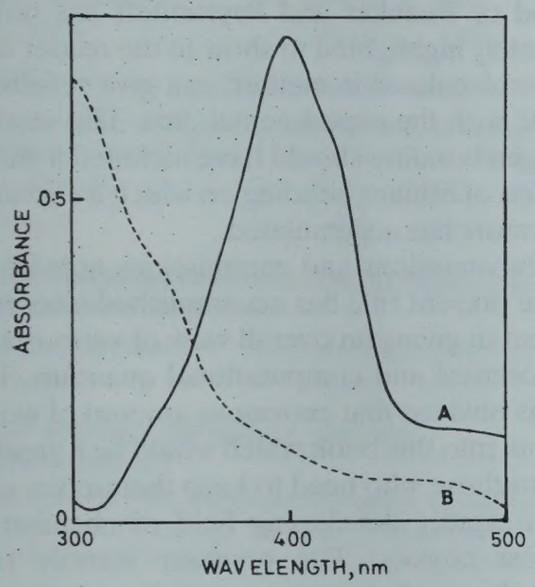

Fig. 1—Absorbance spectra of (A) Pd(11)-4-nitrosoresorcinol-γ-picoline complex (4.2 ppm Pd) and (B) reagent blank

for 1 min. Chloroform extracts, obtained after the recommended procedure, showed a steady absorbance for at least 12 hr.

In all the cases Beer's law was found to be valid over the concentration range 1-20 ppm of palladium. The corresponding molar absorptivities of the complexes (on the basis of palladium content) and respective Sandell's sensitivities were calculated and are presented in Table 1.

Effect of diverse ions

In order to study the effects of diverse ions on the extraction behaviour, palladium was extracted and determined according to the general procedure in presence of the respective foreign ions. Deviation of not more than ± 3% from the expected absorbance was taken as the standard tolerance limit. In practice all the pyridine bases i.e., pyridine/α-picoline/β-picoline/γ-picoline/2,4,6-collidine showed similar behaviour regarding interferences.

Palladium(II) (84.2 μg) can be determined without interference in presence of 50-60 fold excess of Ni(II), Cd(II), Hg(II), Zn(II), V(V), Pt(IV), Rh(III), Mn(II) and Be(II). The system tolerated 20-25-fold excess of Mo(VI), Zr(IV), U(VI), La(III), Al(III), Tl(I), Pb(II) and Cr(III). 10-fold excess of Fe(III) and Cu(II) could be tolerated in presence of ammonium bifluoride and citrate respectively. High results were obtained in presence of Co(III).

Among the anions tested, 100-fold excess of borate, phosphate, bromide, iodide, phthalate, acetate, tartrate, citrate, fluoride, ascorbate, oxalate did not interfere. 30-Fold excess of EDTA did not have any effect. Thiocyanate and thiosulphate interfere seriously. More than 100-fold excess of chloride, nitrate and sulphate was found to be harmless.

With γ-picoline the precision and accuracy of the proposed method was tested by analyzing solutions containing a known amount of Pd(II) following the recommended procedure. The average of six determinations of 84.2 μg Pd was found to be 83.4 μg with the relative mean deviation of ± 1%.

References

1 Chattopadhyay P & Majumdar S K, *Indian J Chem*, **22A** (1983) 91.

2 Forsythe J H W, Magee R J & Wilson C L, *Talanta*, **1** (1958) 249.

3 Moeller T & Zogg R E, *Analyt Chem*, **22** (1950) 612.

4 Yatirajan V & Arya S P, *Talanta*, **22** (1975) 861.

5 Ayres G H & Scroggie I E, *Analyt chim Acta*, **26** (1962) 470.

6 Deshmukh G S & Tatwawadi S Y, *J scient ind Res*, **20B** (1961) 506.

7 Overholser L G & Yoe J H, *Ind Engng Chem Anal Ed*, **15** (1943) 310; *Chem Abstr*, **37** (1943) 3691.

8 Takaki S & Nagase Y, *J Phar Soc Japan*, **58** (1938) 324.

9 Vogel A I, *A textbook of quantitative inorganic analysis* (ELBS, London) 1962.

10 Welcher F J, *Organic analytical reagents*, Vol 3 (Van Nostrand, Princeton) 1962.

Indian Journal of Chemistry
Vol. 27A, July 1988, p. 652

BOOK REVIEWS

Applied Quantum Chemistry by G Naray-Szabo, P R Surjan & J G Angyan (D. Reidel Publishing Company, P.O. Box 989,3300, A Z Dordrecht, Netherlands), 1987, pp. 489 + xiv, Price $ 129.00.

This title gives an excellent overview of the present status of nonrelativistic quantum chemistry. It deals essentially with the molecular orbital (MO) theory and its applications to molecules and supermolecules. The subject matter of the book is spread over four chapters. Various models and methods of quantum chemistry are described in Chapter 1 using the traditional first quantizatioin formalism. The computational methods are discussed in the order: Ab initio theory, NDO-based and other semi-empirical theories and qualitative MO theory. The transformational freedom of the Hartree-Fock method has been discussed at great length. The chemical bond is described in Chapter 2 where emphasis has been laid on its local character and transferability. Chapter 3 is devoted to molecular structure. Various quantum chemical methods for the calculation of geometry, conformation, excited and ionized states, electrical and magnetic properties etc. of molecules are discussed in this chapter. Chemical reactions are described in Chapter 4. A number of representative tables comparing theoretically calculated values with the experimental data are included. Thus, an experimentalist or a theoretical chemist can easily scan the data himself and decide whether theory can provide sufficiently accurate results for his purpose. A list containing about 1500 general references and another list containing about 200 selected recent (1984-1986) references are included as the background source material. The relevant experimental methods are also indicated at appropriate places.

There are a few typographical errors. This is probably not unusual for a book of this length (490 pages). Relativistic quantum chemistry, density functional theory and many-body theories are practically excluded from consideration. A few pages could have been devoted especially to the first two topics. The tremendous potentiality of the MRD-CI method of Buenker and Peyrimhoff has not been adequately highlighted to show to the reader that for small molecules this method can give results comparable with the experimental data. The section on hydrogen bonding should have included a short description of lithium bonding on which a vast amount of literature has accumulated.

A few omissions and commissions notwithstanding, the present title has accomplished a commendable feat in giving an overall view of various aspects of theoretical and computational quantum chemistry. It is obvious that enormous amount of work has been put into this book which would be a great timesaver to those who need to keep themselves abreast of this rapidly developing field of chemistry and chemical physics. The reviewer warmly recommends this book to every practising quantum chemist and molecular physicist and to those who are seriously contemplating to work in theoretical chemistry. A book of this type needs frequent updating and a good background of quantum chemistry is required in order to have a clear grasp of its subject matter.

A B Sannigrahi
Department of Chemistry
Indian Institute of Technology
Kharagpur 721 302

CSIR SCIENTIFIC PERIODICALS

JOURNAL OF SCIENTIFIC & INDUSTRIAL RESEARCH (Monthly)

With a fine record of over 45 years' service to the scientific community, this journal has grown into India's leading general science periodical. Intended to fulfil the responsibility of helping the research workers to keep themselves abreast of current developments in various fields of science and technology the journal carries editorial features highlighting important scientific events in India and abroad, articles on science policy and management of science review articles on topics of current research interest, technical reports on international and national conferences, reviews of scientific and technical publications, and notes on major advances in various fields.

Annual Subscription	Rs 200.00	$ 70.00	£ 45.00
Single copy	20.00	7.00	4.50

INDIAN JOURNAL OF CHEMISTRY (Monthly)

Section A: Started in the year 1963, the journal is devoted to papers in Inorganic, Physical, Theoretical and Analytical Chemistry.

Annual Subscription	Rs 300.00	$100.00	£ 70.00
Single copy	30.00	10.00	7.00

Section B: This journal is devoted to papers in Organic Chemistry, including Medicinal Chemistry.

Annual Subscription	Rs 300.00	$100.00	£ 70.00
Single copy	30.00	10.00	7.00

INDIAN JOURNAL OF PURE & APPLIED PHYSICS (Monthly)

Started in the year 1963, this journal is devoted to original research communications (full papers and short communications) in all conventional branches of physics (except radio and space physics).

Annual Subscription	Rs 250.00	$ 85.00	£ 55.00
Single copy	25.00	8.50	5.50

INDIAN JOURNAL OF RADIO & SPACE PHYSICS (Bimonthly)

The journal, which is being published beginning from March 1972, is intended to serve as a medium for the publication of the growing research output in various areas of radio and space physics, such as ionospheric propagation, magnetosphere, radio and radar astronomy, physics and chemistry of the ionosphere; neutral atmosphere; airglow, winds and motion in the upper atmosphere; stratosphere-mesosphere coupling, ionosphere-magnetosphere coupling; solar-terrestrial relationship, etc.

Annual Subscription	Rs 125.00	$ 42.00	£ 28.00
Single copy	25.00	8.50	5.50

INDIAN JOURNAL OF TECHNOLOGY (INCLUDING ENGINEERING) (Monthly)

This journal publishes papers reporting results of original research of applied nature pertaining to unit operations, heat and mass transfer, products, processes, instruments and appliances, etc. The journal is of special interest to research workers in departments of applied sciences in universities, institutes of higher technology, commodity research laboratories, industrial cooperative research institutes, and industrial research laboratories.

Annual Subscription	Rs 250.00	$ 85.00	£ 55.00
Single copy	25.00	8.50	5.50

INDIAN JOURNAL OF EXPERIMENTAL BIOLOGY (Monthly)

This journal, devoted to the publication of research communications in the fields of experimental botany, zoology, microbiology, pharmacology, endocrinology, nutrition, etc., is the only one in India with such a wide coverage and scope.

Annual Subscription	Rs 250.00	$ 85.00	£ 55.00
Single copy	25.00	8.50	5.50

INDIAN JOURNAL OF BIOCHEMISTRY & BIOPHYSICS (Bimonthly)

This journal, published in association with the Society of Biological Chemists (India), Bangalore, is the only research journal in India devoted exclusively to original research communications in biochemistry and biophysics.

Annual Subscription	Rs 125.00	$ 42.00	£ 28.00
Single copy	25.00	8.50	5.50

INDIAN JOURNAL OF MARINE SCIENCES (Quarterly)

Commencing publication from June 1972, this journal is devoted to research communications (full papers and short communications) pertaining to various facets of marine research, viz. biological, physical, geological and chemical oceanography.

Annual Subscription	Rs 125.00	$ 42.00	£ 28.00
Single copy	35.00	12.00	8.00

RESEARCH AND INDUSTRY (Quarterly)

Intended to serve as a link between science and industry, this journal is addressed primarily to technologists, engineers, executives and others in industry and trade. It publishes informative original articles containing practical details of processes and products devoted in India, which show promise of ready utilization, and technical digests on new processes, products, instruments and testing methods which are of interest to industry Developments in Indian industry are regularly reported.

Annual Subscription	Rs 125.00	$ 42.00	£ 28.00
Single copy	35.00	12.00	8.00

INDIAN JOURNAL OF TEXTILE RESEARCH (Quarterly)

Commencing publication from March 1976, this journal is devoted to the publication of papers reporting results of fundamental and applied researches in the field of textiles.

Annual Subscription	Rs 125.00	$ 42.00	£ 28.00
Single copy	35.00	12.00	8.00

MEDICINAL & AROMATIC PLANTS ABSTRACTS (Bimonthly)

Carries informative abstracts of scientific papers published in important Indian and foreign journals relating to different aspects of medicinal and aromatic plants. Each issue contains about 350 abstracts with a subject index.

Annual Subscription	Rs 225.00	$ 75.00	£ 50.00
Single copy	45.00	15.00	10.00

CURRENT LITERATURE ON SCIENCE OF SCIENCE (Monthly)

Carries abstracts, digests, book reviews, news & notes and R&D statistics with emphasis on problems of S&T in developing countries, it also covers the areas of science policy, R&D planning and management, technology transfer, technology assessment and science and society.

Annual Subscription	Rs 100.00	$ 30.00	£ 12.00
Single copy	10.00	3.00	1.20

Please contact

SENIOR SALES AND DISTRIBUTION OFFICER
PUBLICATIONS & INFORMATION DIRECTORATE, CSIR
Hillside Road, New Delhi 110012

RN 7090/63

CSIR PUBLICATIONS

WEALTH OF INDIA

An encyclopaedia of the economic products and Industrial resources of India issued in two series

RAW MATERIALS SERIES – Contains articles on plant, animal and mineral resources.

	Rs.	$	£
Vol. I(A) (Revised)	300.00	94.00	74.00
Vol. I (A-B)	120.00	60.00	26.00
Vol. II (C)	143.00	66.00	34.00
Vol. III (D-E)	158.00	64.00	40.00
Vol. IV (F-G)	98.00	54.00	24.00
Supplement (Fish & Fisheries)	84.00	32.00	21.00
Vol. V (H-K)	171.00	68.00	42.00
Vol. VI (L-M)	135.00	68.00	30.00
Supplement (Livestock including Poultry)	153.00	68.00	39.00
Vol. VII (N-Pe)	150.00	60.00	38.00
Vol. VIII (Ph-Re)	129.00	64.00	28.00
Vol. IX (Rh-Se)	156.00	70.00	38.00
Vol. X (Sp-W)	338.00	150.00	85.00
Vol. XI (X-Z)	223.00	77.00	44.00

INDUSTRIAL PRODUCTS SERIES – Deals with major, Small-Scale and Cottage Industries

Part I (A-B)	87.00	40.00	22.00
Part II (C)	111.00	48.00	28.00
Part III (D-E)	150.00	67.00	39.00
Part IV (F-H)	189.00	84.00	48.00
Part V (I-L)	135.00	46.00	34.00
Part VI (M-Pi)	42.00	16.00	5.60
Part VII (Pl-Sh)	90.00	36.00	12.00
Part VIII (Si-Ti)	99.00	54.00	20.00
Part IX (To-Z)	120.00	68.00	24.00

BHARAT KI SAMPADA (Hindi Edition of Wealth of India, Raw Materials):

Vol. I (अ-औ)	57.00	32.00	13.00
Vol. II (क)	54.00	30.00	12.00
Vol. III (ख-न)	54.00	30.00	12.00
Vol. IV (प)	125.00	68.00	32.00
Vol. V (फ-मेरे)	90.00	44.00	20.00
Vol. VI (मेल-रू)	120.00	54.00	26.00
Vol. VII (रे-वाटा)	203.00	80.00	50.00
Vol. VIII (वाय-सीसे)	300.00	80.00	50.00
Livestock (Kukkut Palan)	51.00	30.00	12.00
Fish & Fisheries (Matsya aur Matsyaki)	74.00	42.00	10.00
A Dictionary of Generic & Specific Names of Plants & Animals Useful to Man	45.00	22.00	10.00

Please Contact :

SENIOR SALES & DISTRIBUTION OFFICER
PUBLICATIONS & INFORMATION
DIRECTORATE, CSIR
HILLSIDE ROAD, NEW DELHI - 110012

OTHER PUBLICATIONS

	Rs.	$	£
The Useful Plants of India	192.00	64.00	48.00
A Dictionary of the Flowering Plants in India by H. Santapau & A.N. Henry	63.00	28.00	16.00
Glossary of Indian Medicinal plants by R.N. Chopra, S.L. Nayar & I.C. Chopra	93.00	32.00	20.00
Supplement to Glossary of Indian Medicinal Plants by R.N. Chopra, I.C. Chopra & B.S. Verma	51.00	18.00	12.00
The Flora of Delhi by J.K. Maheshwari	42.00	16.00	5.50
Illustrations to the Flora of Delhi by J.K. Maheshwari	105.00	44.00	26.00
Herbaceous Flora of Dehra Dun by C.R. Babu	216.00	120.00	44.00
Gnetum by P. Maheshwari & Vimla Vasil	30.00	12.00	4.00
Marsilea by K.M. Gupta	62.00	27.00	16.00
Aquatic Angiosperms	30.00	12.00	4.00
Indian Fossil Pteridophytes by K.R. Surange	99.00	44.00	25.00
Cedrus by P. Maheshwari & Chhaya Biswas	63.00	28.00	16.00
Proteaceae by C. Venkata Rao	108.00	48.00	27.00
Pinus by P. Maheshwari & R.N. Konar	45.00	22.00	16.00
Loranthaceae by B.M. Johri & S.P. Bhatnagar	83.00	37.00	21.00
Abies & Picea by K.A. Chowdhury	21.00	12.00	4.20
Indian Thysanoptera by T.N. Ananthakrishnan	39.00	16.00	5.20
The Millipede Thyropygus by G. Krishnan	18.00	7.00	2.40
Indian Sardines by R.V. Nair	33.00	14.00	4.40
Drug Addiction with special Reference to India by R.N. Chopra & I.C. Chopra	19.00	7.00	2.40
Diosgenin & other Steroid Drug Precursors by L.V. Asolkar & Y.R. Chandha	54.00	26.00	12.00
Cholera Bacteriophages by Dr. Sachimohan Mukerjee	45.00	20.00	12.00
Cottonseed Chemistry & Technology by K.S. Murti & K.T. Achaya	116.00	64.00	26.00
Corrosion Map of India	27.00		3.60
Rural Development and Technology: A Status Report-cum-Biblio-graphy by PR Bose and V.N. Vashist	150.00	76.00	34.00
Termite Problems in India	14.00	6.00	1.80
Research & Development Management	38.00	20.00	
Proceedings of the Seminar on Primary Communications in Science & Technology in India by R.N. Sharma & S. Seetharama	78.00	35.00	68.00

Packing and Postage Extra

Printed & Published by Shri S.S. Saksena, Editor, Publications & Information Directorate (PID) Hillside Road, New Delhi 110012, at PID Photocomposition-cum-Printing Unit

Regd No. D(C)-1018